

TERRESTRIAL CARBON DYNAMICS OF SOUTHERN UNITED STATES IN
RESPONSE TO CHANGES IN CLIMATE, ATMOSPHERE, AND
LAND-USE/LAND COVER FROM 1895 TO 2005

Except where reference is made to work of others, the work described in this dissertation is my own or was done in collaboration with my advisory committee. This dissertation does not include proprietary or classified information.

Chi Zhang

Certificate of Approval:

Graeme Lockaby
Professor
Forestry and Wildlife
Sciences

Hanqin Tian, Chair
Alumni Professor
Forestry and Wildlife
Sciences

Art Chappelka
Professor
Forestry and Wildlife
Sciences

Joe F. Pittman
Interim Dean
Graduate School

TERRESTRIAL CARBON DYNAMICS OF SOUTHERN UNITED STATES IN
RESPONSE TO CHANGES IN CLIMATE, ATMOSPHERE, AND
LAND-USE/LAND COVER FROM 1895 TO 2005

Chi Zhang

A Dissertation

Submitted to

the Graduate Faculty of

Auburn University

in Partial Fulfillment of the

Requirements for the

Degree of

Doctor of Philosophy

Auburn, Alabama
May 10, 2008

TERRESTRIAL CARBON DYNAMICS OF SOUTHERN UNITED STATES IN
RESPONSE TO CHANGES IN CLIMATE, ATMOSPHERE, AND
LAND-USE/LAND COVER FROM 1895 TO 2005

Chi Zhang

Permission is granted to Auburn University to make copies of this dissertation at its
discretion upon request of individuals or institutions and at their expense.
The author reserves all publication rights

Signature of Author

Date of Graduation

DESSERTATION ABSTRACT

TERRESTRIAL CARBON DYNAMICS OF SOUTHERN UNITED STATES IN
RESPONSE TO CHANGES IN CLIMATE, ATMOSPHERE, AND
LAND-USE/LAND COVER FROM 1895 TO 2005

Chi Zhang

Doctor of Philosophy, May 10, 2008
(M.S., Wuhan Institute of Botany, Chinese Academy of Sciences, 1999)
(B.S., Wuhan University, 1996)

248 Typed Pages

Directed by Hanqin Tian

Historical human activities and environmental changes have strongly modified the global carbon cycle, which can lead to both an energy shortage and environmental problems such as global warming due to elevated atmospheric CO₂. North American terrestrial ecosystems, especially in the Southern United States (SUS) were suggested to be important carbon sinks. In this dissertation a dynamic land ecosystem model (DLEM) was applied to assess the carbon storage of SUS terrestrial ecosystems, and to study the ecosystems' responses to historical climate change, atmospheric change (i.e. elevated CO₂, elevated nitrogen deposition, and elevated tropospheric ozone stress), and land-use change (cropland conversion, urbanization, and reforestation). First, a series of landscape-level case studies were conducted on three different types of Southern terrestrial ecosystems: the natural ecosystem of Great Smoky Mountain National Park

(GRSM), the semi-natural ecosystem along a rural-urban gradient in west Georgia, and urban ecosystems in SUS. Results from these studies suggested that the undisturbed Southern forest ecosystem has potential to store large amounts of carbon (as high as 15.9 kg m⁻² in GRSM) which is very sensitive to disturbances, especially changes in land use. Historical cropland conversion has resulted in significant carbon emissions in SUS, while the vast cropland abandonment since the mid-20th century has made many regions in the SUS net carbon sinks. The impacts of urbanization on SUS carbon balance became more and more important since the 1970s. A high resolution spatial database throughout thirteen Southern states was developed as a model input to study the regional carbon balance of SUS in response to multiple stresses in the past 110 years. The model output suggests that the total terrestrial ecosystem carbon (TOTEC) storage of the SUS is about 20.26 P g C (1 P = 10¹⁵), 55% of which is stored in soil, 39% in plant biomass, and about 7% in litter pools. Forests account for 84% of the ecosystem carbon storage in SUS. Our model estimation, which is comparable to the results of other studies, indicated that since 1950, the terrestrial ecosystem of SUS was a carbon sink of 46.4 T g C / year. Before 1950, however, the region had acted as a net carbon source of 1.56 P g C since 1895. Historical land-use change, elevated CO₂ and elevated atmospheric nitrogen deposition were among the most important factors controlling the Southern carbon balance. Temporal patterns were generally controlled by the impacts of historical land-use change, while the long-term CO₂ and nitrogen fertilization effects due to atmospheric change enhanced the carbon sequestration capacity of Southern ecosystems. All the environmental factors together resulted in a net carbon sink of about 0.9 P g C in SUS from 1895 to 2005.

ACKNOWLEDGEMENTS

First of all, I want to thank Dr. Hanqin Tian, my major professor. His scientific philosophy and his insights in our research field not only inspired me in my doctoral study but also will become precious fortunes for my future academic career. My achievements in the five years' doctoral study could not be possible without his instructions, his directions, and his patience. I was fortunate to have Dr. Graeme Lockaby and Dr. Art Chappelka to be my academic committee members. Their instructions and suggestions were very valuable to me in conducting my PhD projects.

I also thank Ms. Shufen Pan who not only provided me many good suggestions on how to prepare for my academic career, but also offered help both in school and off campus. I thank all the group members who worked together to develop the model I used in this study. I thank Dr. Mingliang Liu for his kindly support in my research. Furthermore, I thank Wei Ren, Hua Chen, Diane Styers, Guangsheng Chen and Yuhang Wang for their contribution on Chapter 3, and Erik B. Schilling and John Stanturf for their contribution on Chapter 4. I want to express my heartily thanks to Ms. Patti Staudenmaier who gave me so much help during my studies in Auburn University.

Finally, and most importantly, I want to thank my family, my wife, my mother and father. I owe them so much that there are no words to express my gratitudes. Without the self-sacrifice of my wife, Hua Shao, I could not be able to pursue the PhD degree in Auburn. They give me so much and ask for nothing. I shall dedicate this dissertation to them.

Style manual or journal used:

ECOSYSTEMS

Computer software used:

ArcGIS ®

ERDAS IMAGINE ®

Borland C++ ®

Intel C++ Compiler ®

Microsoft

Excel ®

Word ®

Powerpoint ®

TABLE OF CONTENTS

LIST OF TABLES.....	xi
LIST OF FIGURES.....	xiii
CHAPTER 1 INTRODUCTION	1
1. Objectives.....	4
2. Approaches.....	5
3. Dissertation Structure	11
CHAPTER 2 LITERATURE REVIEW.....	13
1. Carbon, energy and global warming.....	13
2. Carbon sinks in terrestrial ecosystem.....	15
3. The causes of the carbon sink in the terrestrial biosphere.....	18
4. The ecosystem complexity and model simulation approach.....	20
5. Ecosystem models and their application in ecology research.....	22
CHAPTER 3 CASE STUDY I – Impacts of climatic and atmospheric changes on carbon dynamics in the Great Smoky Mountains National Park.....	24
Abstract.....	24
1. Introduction.....	25
2. Methods.....	28
3. Results and Discussion.....	40

4. Conclusions.....	55
CHAPTER 4 CASE STUDY II –	
Effects of Forest Regrowth and Urbanization on Ecosystem Carbon Storage in a Rural-Urban Gradient in the Southeastern United States.....	57
Abstract.....	57
1. Introduction.....	58
2. Method and data.....	60
3. Results and discussion.....	72
CHAPTER 5 CASE STUDY III –	
Impacts of urbanization on carbon balance of the Southern United States from 1865 to 2002.....	85
Abstract.....	85
1. Introduction.....	86
2. Dataset and research methods.....	89
3. Results and analysis.....	105
4. Discussion.....	111
5. Conclusion.....	121
CHAPTER 6 REGIONAL STUDY –	
Carbon Storage of Southern United States and Its Responses to Multiple Stresses from 1895 to 2005.....	122
Abstract.....	122
1. Introduction.....	123
2. Research Method.....	126

3. Results and analysis.....	147
4. Limitation, improvements, and future research needs.....	197
5. Conclusion.....	199
CHAPTER 7 GENERAL CONCLUSION.....	200
REFERENCES.....	203
APPENDIX I. MODEL VALIDATION.....	227

LIST OF TABLES

Table C3.1 Description of the seven simulation scenarios in the case study of the Great Smoky Mountain National Park (GRSM).....	39
Table C3.2 Overall change in Great Smoky Mountain National Park forest carbon density from 1971 to 2001.....	45
Table C4.1 Error matrix of the land-use classification.....	66
Table C4.2 Land cover change between 1974 and 2002.....	72
Table C4.3 Carbon density in three West Georgia counties (1974 – 2002).....	78
Table C5.1 The input dataset in the case study three.....	94
Table C5.2 Parameters for Dynamic Land Ecosystem Model urban processes.....	103
Table C5.3 The productivity and carbon storage of the Southern US (SUS) urban and developed regions as simulated by Dynamic Land Ecosystem Model.....	106
Table C5.4 Comparison of the productivity, carbon density and carbon storage of managed and unmanaged urban lawn.....	109
Table C5.5 Comparison of our estimates of the city of Atlanta against other studies	112
Table C5.6 Comparison of the mean carbon densities for each of the 13 Southern states as estimated by Dynamic Land Ecosystem Model against the estimates of Pouyat et al. (2006).....	115
Table C6.1.1 The simulation design to investigate the impacts of multiple stresses on the Southern US carbon dynamic from 1865 to 2005.....	129
Table C6.1.2 The input dataset required by Dynamic Land Ecosystem Model in the Southern US regional study.....	130
Table C6.2.1 Estimated carbon storage of the Southern United States.....	148
Table C6.2.2 The estimated carbon density of the Southern United States (unit:	

10 ¹⁵ g C).....	149
Table C6.2.3 Carbon storage of different land cover types in the thirteen southern states (unit: T g C; 1 T = 10 ¹²) in 2005.....	154
Table C6.2.4 Comparison of model-simulated vegetation carbon density (g C/m ²) of each state against the estimate based on forest inventory data.....	155
Table C6.2.5 Comparison of model- simulated soil carbon density (g SOC/m ²) from 1987 and 1997 against the state-by-state estimate based on the forest inventory analysis dataset (FIA) (Birdsey and Lewis 2002).....	156
Table C6.2.6 Estimated total ecosystem carbon storage (TOTEC) of the Southern United States in 1895, 1950, 1980, and 2005.....	161
Table C6.2.7 Comparison of model-derived SUS carbon sequestration rate against the estimates from other regional studies.....	162

LIST OF FIGURES

Figure C1.1 Diagram of the Integrative Approach to Address Large-Scale Issue (Tian et al., 2008).....	7
Figure C1.2 Project design. DLEM: dynamic land model (Tian et al., 2005). TEM: terrestrial ecosystem model (Tian et al., 2003). The color of arrows indicates the type of environmental changes considered in the study. The black arrow indicates multiple stresses.....	10
Figure C3.1 Location of study region (Welch et al., 2002). Great Smoky Mountains National Park (GRSM) is located along the North Carolina–Tennessee border in the southeastern United States in the southern part of the Appalachian Mountains. Elevation ranges from approximately 250 m along the outside boundary of the Park up to more than 2000 m in the center of the park. Climate records from more than two hundred climate stations (black dots) were used to generate the climate datasets for the simulation.....	29
Figure C3.2 The distribution of major vegetation types in Great Smoky Mountains National Park (late 1980s) (a) Original 100 meter resolution vegetation map developed by MacKenzie (1993) and (b) the $1 \times 1 \text{ km}^2$ resolution 4-category vegetation map aggregated from map (a) by us to drive the model.....	30
Figure C3.3 Dynamic Land Ecosystem Model (DLEM). The DLEM (Tian et al., 2005) is a process-based model which couples biophysical processes (energy balance), biogeochemical processes (water cycles, carbon cycles, nitrogen cycles, and trace gases (NO_x , CH_4)-related processes), community dynamics (plant distribution and succession), and disturbances (land conversion, agriculture management, forest management, and other disturbances such as fire, pest etc.) into one integral system. DLEM can simulate the complex interactions of multiple stresses such as climate change, elevated CO_2 , tropospheric O_3 , N deposition, human disturbance, and natural disturbances.....	32
Figure C3.4 The temporal and average spatial pattern of temperature and precipitation in GRSM: (a) Temporal variation of yearly average temperature from 1971 to 2001, (b) Temporal variation of annual total precipitation from 1971 to 2001, (c) Spatial pattern of average daily temperature during study period, (d) Spatial pattern of average annual precipitation during study period.	42
Figure C3.5 The interannual, intraannual, and seasonal pattern of tropospheric O_3	

(AOT40, ppb-hr) in GRSM: (a) Interannual variation of average AOT40 from 1971 to 2001, (b) Intraannual variation of AOT40, (c) Spatial pattern of AOT40 in December, (d) Spatial pattern of AOT40 in July. The AOT40 increases with altitude.....	43
Figure C3.6 Changes in great smoky mountain carbon pools (unit: T g; 1 T g = 10 ¹² g) from 1971 to 2001. VEGC denotes vegetation carbon pool; SOC denotes soil carbon pool; LTRC denotes litter C pool; TOTC denotes total carbon storage. Scenarios: CLMCO2 = climate + CO2 effect; CLMO3 = climate + O3 effect; CLMCO2O3 = combination of climate + CO2 + O3 effect.....	47
Figure C3.7 The spatial pattern of the GRSM C pool (a) C storage in 1971 (b) C storage in 2001 (c) C storage changes from 1971 to 2001.....	50
Figure C3.8 Transient responses of net primary productivity (NPP) and carbon storage to multiple environmental stresses. Scenarios under comparison: CLM = climate only; O3 = O3 only; CO2 = CO2 only, CLMCO2O3 = combination effects of climate, O3, and CO2. (a) Effect of climate; CO2-fertilization, and O3 damage on NPP; (b) Cumulative carbon storage from each of the factors in (a).....	52
Figure C4.1 Location and population growth of the west Georgia (West GA) research site. Dot size in the West GA county maps (right) shows the population growth (number of people/km ²) from 1974 to 2002 (US Census Bureau, http://www.census.gov/). From 1974 to 2002, population density of Muscogee County increased 41 people per km ² ; Population density of Harris County increased 9 people per km ² ; Population density of Meriwether County increased 2 people per km ² . The three counties, from the southwest to the northeast, form an urban-rural gradient.....	62
Figure C4.2 Land-cover change in the three counties of west Georgia from mid-1970s to early 2000s.(a) Land-cover map in 1974; (b) Land-cover change (LCC) from 1974 to 2002; (c) Land-cover map in 2002.....	75
Figure C4.3 Land-cover change in the three counties of west Georgia during 29 years (1974-2002).....	76
Figure C4.4 Net carbon exchange between the atmosphere and terrestrial ecosystems in the three west GA counties from 1974 to 2002.....	79
Figure C4.5 Contribution of different land conversion to net carbon exchange (g/m ²) between terrestrial ecosystems and the atmosphere in the study area as estimated by TEM. Positive NCE means carbon sink, negative NCE means carbon source.....	82
Figure C5.1 The boundary of the Southern US (SUS) and the location of its urban /developed regions (in red).....	91

Figure C5.2 The spatial pattern (a) and temporal pattern (b) of land-use change of SUS between 1865 and 2002.....	101
Figure C5.3 Diagram of urban-submodel. PPT: precipitation (mm); TEMP: temperature (⁰ C); NDEP: N deposition (gN/m ²).....	102
Figure C5.4 The temporal pattern of (a) urban area, (b) urban ecosystem productivity, and (c) urban carbon storage from 1865 to 2002 in Southern US. VEGC: vegetation carbon; LTRC: litter carbon; SOC: soil organic carbon	107
Figure C5.5 Effects of the lawn managements on the (a) productivity and (b) carbon storage of Southern urban/developed regions	110
Figure C5.6 Changes in (a) soil organic carbon (SOC) and (b) total ecosystem carbon (TOTEC) due to urbanization in Southern US. The values are derived by comparing the size of contemporary urban carbon densities against pre-urbanization carbon pools.....	118
Figure C5.7 Impacts of urbanization on carbon balance of different SUS terrestrial ecosystems; (a) impacts of urbanization on the carbon density of different carbon pools. NCE is the net carbon exchange or net carbon balance of ecosystem due to urbanization, it equals to the change of total carbon storage during a certain period of time; (b) the temporal pattern of net carbon exchange due to urbanization.....	119
Figure C6.1.1 The boundary and potential vegetation (see Section 2.2) of the Southern US.....	127
Figure C6.1.2 Spatial pattern of the mean daily temperature of Southern US from 1895 to 2005.....	133
Figure C6.1.3 Temporal pattern of mean daily temperature from 1895 to 2005.....	134
Figure C6.1.4 Spatial pattern of mean annual precipitation of Southern US from 1895 to 2005.....	134
Figure C6.1.5 Temporal pattern of annual precipitation from 1895 to 2005.....	135
Figure C6.1.6 Spatial pattern of tropospheric ozone, using average AOT40 in 1990 as an illustration.....	137
Figure C6.1.7 Temporal pattern of ozone input dataset.....	137
Figure C6.1.8 Annual mean ozone concentration records from 22 CASTNET stations in the study region showed that had continuous records of more than 5 years between 1995 and 2005.....	138

Figure C6.1.9 NH ₄ deposition in 2005 illustrated s an example.....	139
Figure C6.1.10 NO _y deposition in 2005 illustrated as an example. NO _y includes all oxidized forms of nitrogen other than N ₂ O.....	139
Figure C6.1.11 Total nitrogen deposition in 2005 illustrated as an example.....	140
Figure C6.1.12 Temporal patterns of nitrogen deposition from 1895 to 2005 based on the three period (1860, 1993, 2050) N deposition dataset of Dentener (2006).....	140
Figure C6.1.13 Changes in atmospheric CO ₂ from 1895 to 2005.....	141
Figure C6.1.14 Spatial pattern of nitrogen fertilizer map from 2000 as an illustration	143
Figure C6.1.15 Temporal pattern of nitrogen fertilization from 1945 to 2001.....	143
Figure C6.1.16 Spatial patterns of land-use change from 1865 to 2005.....	144
Figure C6.1.17 Temporal patterns of land-use change from 1895 to 2005.....	145
Figure C6.1.18, Impervious surface map of the Southern US in 2005.....	146
Figure C6.1.19 The distribution of urban lawn in the Southern US in 2005.....	147
Figure C6.2.1 Total ecosystem carbon density of the Southern US in 2005 as estimated by our model	150
Figure C6.2.2 Ecosystem carbon storage in different land cover types of the Southern US in 2005 as estimated by our model.....	151
Figure C6.2.3 The ecosystem carbon density of different land cover types in the Southern US in 2005 as estimated by our model.....	152
Figure C6.2.4 Trends in carbon dynamics in the southern United States from 1895 to 2005 as estimated by our model.....	159
Figure C6.2.5 Carbon storage of 13 southern states in 1895, 1950, and 2005, respectively as estimated by our model.....	159
Figure C6.2.6 Spatial distribution of carbon sinks and sources in the Southern US during 1895 – 2005 as estimated by our model.....	160
Figure C6.2.7 Comparisons of carbon storages of different land-cover types in the Southern US in 1895, 1950, and 2005 as estimated by our model.....	163
Figure C6.3.1 The effects of air temperature (a) and precipitation (b) on the	

ecosystem productivity in SUS estimated by model simulation. (a) The pattern of NPP generally follows the fluctuation of annual precipitation. (b) The temperature seems negatively correlated with the pattern of NPP, implying the global warming may have vegetative impact on warm temperate ecosystems like the Southern US...	167
Figure C6.3.2 Changes in Southern US carbon storage in response to climate change from 1895-2005.....	168
Figure C6.3.3 Comparison of the carbon storage of the 13 southern states in 1895, 1955, and 2005. * Note: The unit of total Southern US ecosystem carbon storage is 10 P g	168
Figure C6.3.4 CO ₂ fertilization effect on the annual NPP of the Southern US (single factor scenario).....	170
Figure C6.3.5 Dynamics of Southern US carbon storage in response to elevated CO ₂ concentration	172
Figure C6.3.6 Carbon accumulation in ecosystems of the 13 southern states in response to the CO ₂ fertilization effect during the study period.....	173
Figure C6.3.7 The CO ₂ -induced carbon sequestration map of the Southern US.....	173
Figure C6.3.8 The response of land cover types to the elevated CO ₂ concentration in the Southern US from 1895 – 2005.....	174
Figure C6.3.9 Effects of ozone stress on the ecosystem NPP.....	175
Figure C6.3.10 Impact of ozone stress on the terrestrial carbon storage in SUS. (a) Spatial patterns of the ozone impact. (b) The impact on carbon storage of each state. (* The unit of total SUS ecosystem carbon storage is 10 T g C.).....	176
Figure C6.3.11 Impacts of elevated atmospheric N deposition on ecosystem productivity.....	178
Figure C6.3.12 Responses of different land cover types to the elevated atmospheric N deposition.....	179
Figure C6.3.13 The carbon sinks generated by elevated atmospheric nitrogen deposition in the 13 southern states. N Deposition Effect = ALLCOMBINE - CLMCO2O3LUC scenarios.....	180
Figure C6.3.14 Responses of different land cover types to N deposition in Southern US in 2005.....	180
Figure C6.3.15 The spatial pattern of N deposition induced C sink in Southern US	182

Figure C6.3.16 Comparison of forest area between this study and Forest Inventory and Analysis (FIA)–derived data (Woodbury et al. 2006).....	184
Figure C6.3.17 Land-use change in two periods: 1894 to 1940 & 1940 to 2005....	186
Figure C6.3.18 Net carbon exchange (NCE, see Chapter 4, Section 2.2 for detail explanation) of SUS ecosystems due to land-use change from 1895 to 2005 (based on the results of single factor scenario).....	188
Figure C6.3.19 Impacts of urbanization, cropland conversion, and cropland abandonment on the regional carbon balance from 1895 to 2005 presented as (a) annual carbon dynamic and (b) accumulated net carbon exchange. (Based on the results of single factor scenario).....	189
Figure C6.3.20 Comparisons of the intensity of carbon sequestration due to ecosystem restoration (cropland abandonment) and carbon emission due to human disturbances (cropland conversion and urbanization) in the Southern US from 1895 - 2005. (Based on the single factor scenario).....	191
Figure C6.3.21 The spatial distribution of carbon pools and sinks during two time periods: the land-use change resulted in large carbon loss from 1895 to 1950 and the cropland abandonment created carbon sinks in the Southern US from 1950-2005.....	192
Figure C6.3.22 Comparing the model simulated responses of ecosystem productivity to multiple environmental stresses in the Southern US from 1895 – 2005.....	194
Figure C6.3.23 Comparing the accumulated impacts of multiple stresses on SUS carbon storage Interaction = ALLCOMBINE – CLM – LUC – NDEP – CO2 – O3	196
Figure C7.1 Application of the integrative approach in southern US to study the impacts of multiple stresses on regional C dynamics.....	202
Figure A2.1 Comparison of the model simulated net ecosystem exchange (NEE) against measured site flux dataset in the (a) Duke forest and the (b) Walker Branch watershed.....	228
Figure A2.2 Comparisons of the modeled annual NPP against 138 field measurements in the Southern US region.....	229
Figure A2.3 Comparisons of the model estimated carbon density of thirteen Southern states against estimation based on forest inventory analysis (FIA) dataset (Birdsey and Lewis, 2003).....	230

CHAPTER 1

INTRODUCTION

The carbon cycle is the combination of many different physical, chemical and biological processes that transfer carbon between the major storage pools: the atmosphere, vegetation, soil, and water. Through photosynthesis, plants fix incident solar energy into the reduced form of carbon compounds, which not only provide the elemental backbone for a myriad of organic molecules that comprise living organisms and organic detritus, but also supply the energy that drives the complex ecological processes throughout the biosphere. This carbon cycle is intimately coupled with energy flow and has been responsible for the formation of coal, petroleum, and natural gas, the fossil fuels that are the primary sources of energy for our modern societies.

Human activities have profoundly changed the carbon cycle since the industrial revolution. Fossil combustion and vast deforestation have released large amounts of CO₂ into the atmosphere. Atmospheric concentration of CO₂ has increased by 31 percent (Intergovernmental Panel on Climate Change, IPCC, 2007, <http://www.ipcc.ch/>) during the last two centuries. At the same time, the global temperature appear to have increased in an unprecedented rate, which is generally believed mainly caused by the stronger heat insulating capability of the atmospheric CO₂, or so called “green house effect”. This rapid change of atmospheric composition and climate system could threaten the sustainability

of the earth's ecosystems and harm our economy.

Another threat to the economy is the depletion of our energy resources. Fossil fuels, currently our major energy source, are literally nonrenewable. As the energy consumption of developed countries keep increasing (e.g. US and Canada's energy consumption increased by 8-10% from 1990 to 2002) and globalization stimulates the rapid industrialization of developing countries, the world's fossil fuel reservoirs are diminishing more quickly than in previous decades (Strahan, 2007). The foreseeable global energy crisis, together with the environmental problems involved with fossil fuel combustion, force humans to look for clean and renewable energy sources. Biofuel, the technique of storing and harvesting solar energy into biomass provides a promising substitute. The United States Department of Agriculture's Forest Service (USDA FS) actively participates in a government-wide initiative aimed at promoting development and use of biobased products and bioenergy. Programs include research on enhancing opportunities to use forest biomass to produce energy and other value-added products; developing economical, environmentally acceptable woody cropping systems to produce energy and other value-added products; and exploring new processes to convert wood into ethanol (Perlack et al., 2005). A nation's potential biofuel storage is measured as the total biomass of its terrestrial ecosystems. This bio-energy supply will be related to the productivity and carbon sequestration rate of its terrestrial ecosystems.

Important negative feedbacks (in response to climate changes) have been observed in the global terrestrial ecosystems, which could both reduce atmospheric CO₂ accumulation

rate and enhance ecosystem biomass accumulation rate. Results from CO₂ enrichment experiments showed that elevated atmospheric CO₂ could stimulate plant growth, and enhance their biomass (i.e. biofuel) accumulation in terrestrial ecosystems (Norby et al., 2005). Furthermore, since the mid 1990s, the large scale forest regrowth in mid-latitude regions of the globe has increased ecosystem carbon storage (Fan et al., 1998). Evidence shows that over the last 10-20 years, nearly half of the CO₂ released by burning fossil fuels has been absorbed on land and in the oceans (IPCC, 2007), and increasing amounts of atmospheric CO₂ appears to be being absorbed by terrestrial vegetation (IGBP Terrestrial Carbon Working Group, 1998).

Both inventory dataset and model simulation results suggests that most of terrestrial carbon sinks are located in the North Hemisphere, where the terrestrial ecosystem of North America seems to uptake more carbon than the region of Eurasia-North Africa (Fan et al., 1998). The mid-latitude North America, i.e. the coterminous US, appears to be where the major North American carbon sinks located. Research results indicated that approximately 30% of fossil fuel emissions are offset by a sink of approximately 530 ± 265 million tons of carbon per year in the US (Pacala et al., 2007). There are large uncertainties in the magnitude and location of the North American carbon sinks. The mechanisms underlying this effect are also unclear. However, there appears to be general agreement that the vast forest regrowth on degraded cropland since the 2nd World War generated the largest carbon sink in the US (Houghton et al., 1999; Schimel et al., 2000; Pacala et al., 2001; Pacala et al., 2007). Other factors such as elevated CO₂ and nitrogen deposition could also stimulate a plant's carbon sequestration. Increased air temperature

may stimulate the productivity of plants, but it can also enhance the soil respiration rate, and thus the net effect of temperature on the ecosystem carbon storage is difficult to evaluate, and could vary from region to region or change through time.

The Southern US has the most productive terrestrial ecosystems in the US (Holland et al., 1999; Birdsey and Heath, 1995, 2003) and has experienced pervasive land-use change in the past two centuries (Wear, 2002). It includes 29% of the total forest area and 40% of the timberland area of the coterminous US and in mid-1990s provided about 59% of US timber harvest (Haynes, 2003). The high productivity of Southern forest plantations indicates that the region has the potency to be one of the largest sources of biofuel in the US. Due to the large scale reforestation since the mid-20th century, the Southern US terrestrial ecosystems were suggested to play an important role in the North American carbon sink (Woodbury et al., 2006). Compared to the studies in other part of US, research on the carbon dynamics of the South US, however, is still limited.

1. Objectives

In this study we conducted a comprehensive analysis of the Southern US carbon dynamics in response to multiple environmental stresses across multiple scales. Our regional study covers 13 states (Alabama, Arkansas, Florida, Georgia, Kentucky, Louisiana, Mississippi, North Carolina, Oklahoma, South Carolina, Tennessee, Texas, and Virginia) (Wear, 2002) with a high spatial resolution of 8 km × 8 km. The study period covers 110 years from 1895 to 2005. Specific objectives are:

- (1) estimate the total carbon storage and carbon balance of the 13 Southern states;
- (2) study the spatial and temporal patterns of historical carbon dynamics of the Southern US;
- (3) analyze the (individual and combined) impacts of climate change, atmospheric change (including effects of elevated CO₂, O₃, and nitrogen deposition), and land-use change (cropland conversion, cropland abandonment, and urbanization) on ecosystem productivity and carbon balance of Southern terrestrial ecosystems.

2. Approach

2.1. The integrative approach for studying large-scale patterns and processes of terrestrial ecosystem under changed environment

This study will be conducted using an integrative approach (Tian et al., 2008) to address the impacts of the climate change, atmospheric changes, and land-use changes on the carbon dynamics of the SUS terrestrial ecosystems. The complex structure and feedbacks of the terrestrial ecosystem make it difficult to estimate its responses to different environmental factors. Furthermore, environmental stresses usually do not operate independently, but rather interact to produce combined impacts on ecosystem functioning. The spatial heterogeneity of the terrestrial ecosystem adds another level of complexity to the system. Accurate predictions of these responses to multiple environmental stresses

(climate change, atmospheric change, and land-use change), therefore, depend on successful integration across a range of processes and time scales. The large number of possible combinations and long time periods over which they operate, however, make it nearly impossible to investigate the effects of multiple stresses on ecosystem C storage through controlled experiments (Ollinger et al., 2002). Integrated process-based ecosystem models, which include the physiological responses to atmospheric and climate changes was proved to be a powerful tool in such multiple stress studies especially over large regions (Tian 2002; Tian et al., 1998, 2003; Karnosky et al., 2005).

The approach of model simulation, nourished by improved knowledge of the fundamental mechanisms, from molecular systems to the planetary ecosystem, and supported by the rapidly developing technology from high speed computer systems to the high resolution remote sensing sources of global coverage, is now playing a more and more important role in solving complex large-scale environment problems. A rapidly increasing literature indicates that ecological modeling and simulation have become a theme in the study of many questions about changing environments at various scales from local to regional to global (see Chapter 2). Models play a crucial role in synthesizing a huge quantity of data, conducting cross-scale extrapolation, analyzing multiple-factor interactions, predicting large-scale environmental processes, and providing a dynamic constraint on uncertainties in a variety of issues related to complex processes, as well as heuristics clues for empirical studies. Also models offer important tools for governments and society to assess the consequences of current and forthcoming environmental problems and make appropriate policies and timely decisions which will protect the

welfare of humankind and reduce losses from environmental disasters. Ecological modeling and simulation, therefore, are essential for integrating and advancing our understanding of ecosystem complexity as well as solving environmental problems and managing our environment toward sustainability. Furthermore, the recent rapidly developed databases of field experiments, forest inventory, remote sensing observations, and climate records provide detailed field observations for model parameterization and validation, and can supply comprehensive inputs that made regional/global integrated simulation feasible.

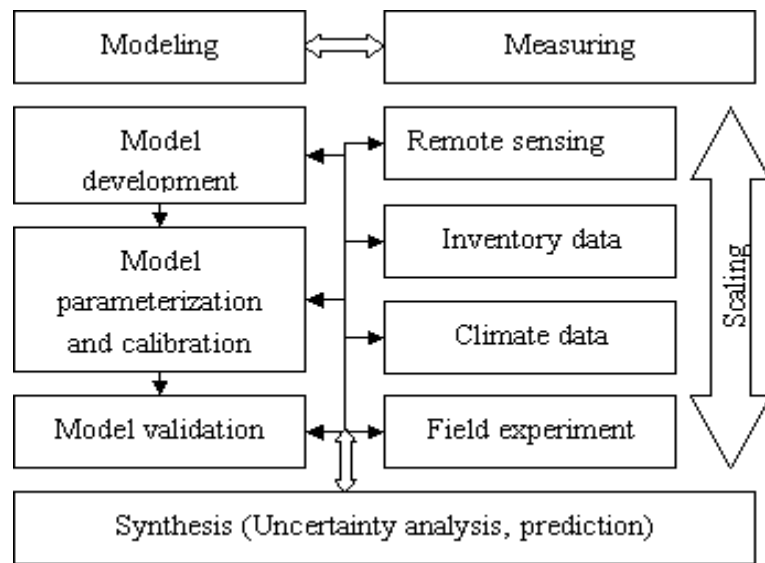


Figure C1.1 Diagram of the Integrative Approach to Address Large-Scale Issue (Tian et al. 2008)

In the integrative approach, the ecosystem model is first parameterized and validated with intensively studied site data. After the uncertainty of the model is assessed, simulations schemes are designed according to the research objectives and the model by a comprehensive collection of spatial datasets that are gathered from multiple-sources, usually across a wide range of scales. These field data are rescaled and converted according to the study objectives before being used as model inputs. The model outputs

include all kinds of variables that are of investigation interests. These outputs are usually first compared to the field observations for validation purpose before being used for regional assessments and predictions.

In this study remote sensing imageries, historical census records, and climate maps developed from climate records from thousands of climate stations were compiled and synthesized to generate the inputs (vegetation, land-use, atmosphere, and transient climate datasets) for the integrated process-based ecosystem models which were parameterized through literature review of intensive field studies. The simulation results were compared against field observations and the conclusions of other studies. Finally, the model predictions were formatted and analyzed to provide insight on the dynamics of carbon storage in SUS in response to the multiple stresses from 1895 to 2005.

2.2. Project design

Human disturbances were thought to be one of the most important factors that determined the spatial and temporal pattern of carbon storage in SUS (Wear, 2002). During the last two hundred years, human activities such as cropland-conversion and urbanization have modified the landscape of SUS, resulting in high spatial heterogeneity. According to the intensity of human disturbances, three types of landscapes were identified in the study region: natural ecosystems such as remote rural region or protected national parks, urban ecosystems that are dominated by human activities, and the intermediate type, for example rural-urban interfaces that are in the middle of transformation from rural to

urban ecosystems. Different landscape types usually have different land-cover composition, different carbon storage, and different responses to environmental stresses. In this project, before the comprehensive regional study, landscape-level case studies were conducted to evaluate the ecosystem productivity and carbon storage and their responses to the different environmental stresses that dominated the ecosystem processes of these three types of terrestrial ecosystems. In three case studies, we (1) evaluated the impacts of climate and atmospheric changes on the Great Smoky Mountain natural ecosystem, (2) studied the carbon dynamics across a rural-urban gradient in west Georgia due to land-use change, and (3) further investigate the carbon dynamics of the urban regions in the Southern US. (4) Finally, we developed a long-term high (spatial and temporal) resolution database for the entire Southern US and assessed carbon storage and historical carbon balance of the study region by applying a highly integrated biogeochemical model (Figure C1.2).

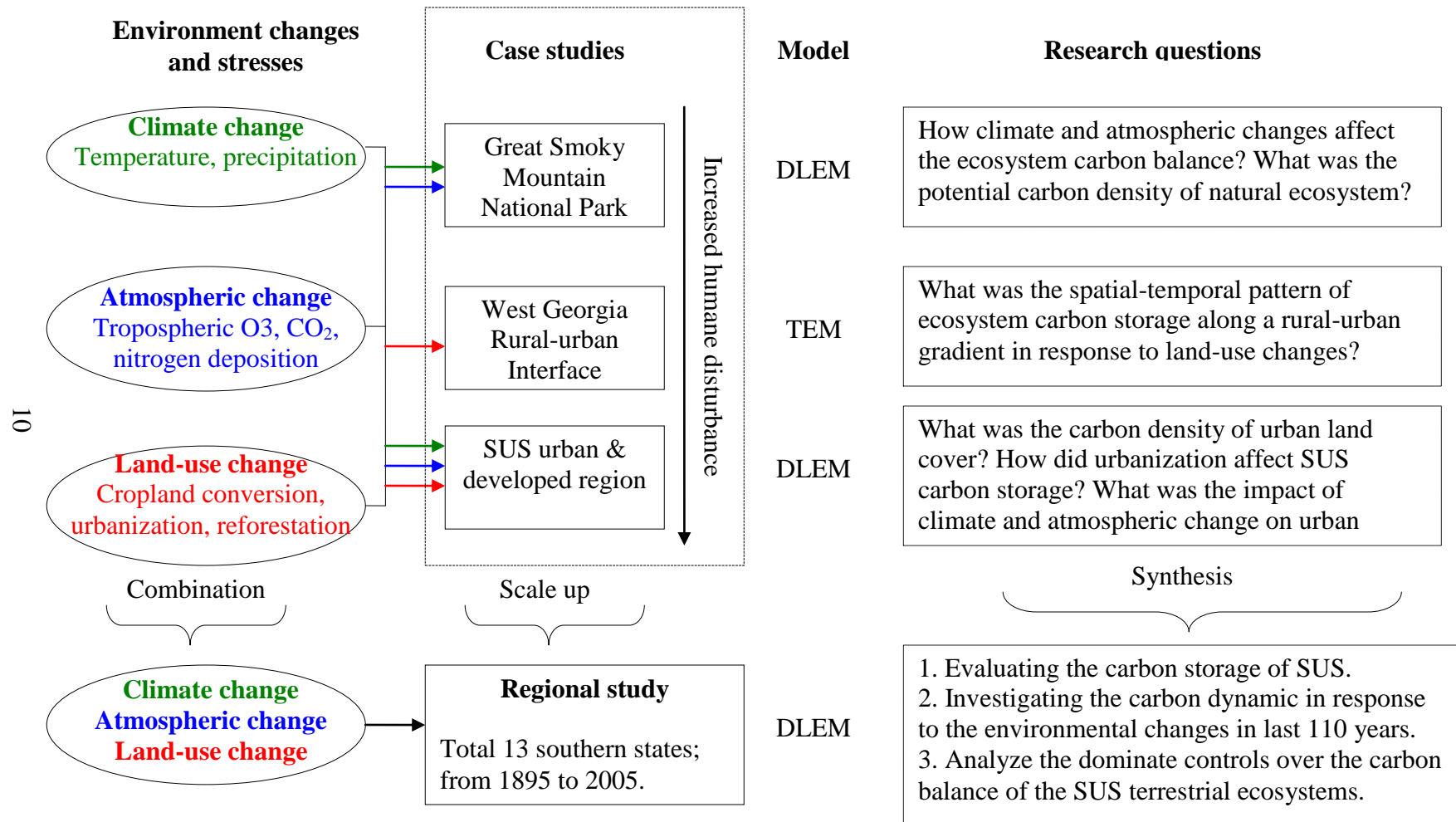


Figure C1.2 Project design. DLEM: dynamic land ecosystem model (Tian et al., 2005). TEM: terrestrial ecosystem model (Tian et al., 2003). Colors indicate different types of environmental changes considered in the studies. The black arrow indicates multiple stresses.

3. Dissertation Structure

Chapter 1 presents an introduction of the background, research questions, study problems, study objectives, and approaches adopted in this study.

Chapter 2 provides a detailed literature review on the past and current progress in assessing the magnitude and location of ecosystem carbon sinks, and the factors that control the terrestrial carbon dynamic.

Chapter 3-5 includes three case studies at the landscape-level: (1) the impacts of global environmental changes on the natural ecosystem (Great Smoky Mountains), (2) a semi-natural ecosystem (across a rural-urban gradient of three west Georgia counties), and (3) a human dominated urban ecosystems in the Southern US.

Chapter 6 describes a regional study in the Southern US. This study was generated and compiled from a long-term high resolution spatial dataset for the 13 Southern US states, which were used to drive the process based biogeochemical model to assess the carbon balance and analyze the carbon dynamics of Southern US terrestrial ecosystems in response to the changed environmental stresses from 1895 to 2005. An assessment of the magnitude of carbon pools for each of the 13 Southern states is provided. Carbon pools of different ecosystem types in the study region were also compared and the current carbon sink in the Southern US was estimated and compared to our estimation against the results of other studies. Finally the impacts of different environmental factors and their

combination effects on the productivity and carbon dynamics of Southern ecosystems were analyzed one by one.

Chapter 7 summarizes the findings in this study and assessed the uncertainties and proposed future improvements.

CHAPTER 2

LITERATURE REVIEW

1. Carbon, energy and global warming

Carbon (C) is one of the most abundant elements in the solar system and provides the structural basis for life on Earth. Carbon dioxide (CO₂) not only affects the rate of key ecological processes such as photosynthesis but also strongly affects the heat insulating capability of the atmosphere. In reduced form, carbon provides the elemental backbone for a myriad of organic molecules that comprise living organisms and soil humus. The global carbon cycle is intimately coupled with energy flow that drives ecological processes on earth. The energy stored in fossil fuel, ancient soil organic carbon pools, also provides the largest energy source for human industry and economy (Cleveland et al., 2006). Two of the challenges humans face: upcoming potential energy crisis and global warming are related to carbon cycles.

Non-renewable fossil fuel reserves are depleting quickly. There are currently 98 oil producing countries in the world, of which 64 are thought to have passed their geologically imposed production peak, and of those, 60 are in terminal production decline, while human demands for energy keeps increasing. For every barrel of oil we discovered, we now consume three. (Strahan, 2007). Biofuel, the technique of storing and

harvesting solar energy into biomass provides a promising substitute for non-renewable fossil fuel. In fact, biomass is already the largest domestic source of renewable energy in the US, having supplied nearly 2.9 quadrillion BTU (quad) of energy in 2003. Biomass currently provides over 3% of the total energy consumption in the US. Being a renewable energy source, the storage of biofuel is the potential biomass of the terrestrial ecosystem, with the primary limitation of biofuel being the the productivity and carbon sequestration capacity of the terrestrial ecosystem. The forest and agricultural lands of US, for example, have the potential to produce more than 1.3 P g dry biomass per year – enough to produce biofuels to meet more than one-third of the current demand for transportation fuels in US (Perlack et al., 2005).

The climate change problem is also partly related to our current structure of energy consumption. The release of carbon dioxide from fossil-fuel combustion (Marland et al., 2002) and other human activities such as land-use change (Houghton and Hackler 2002) has caused a significant perturbation in the natural cycling of carbon between land, atmosphere and oceans. Since the industrial revolution, atmospheric concentrations of CO₂ have increased by 31 % (Intergovernmental Panel on Climate Change, IPCC 2007, <http://www.ipcc.ch/>). These high levels of CO₂ have the potential to lead to changes in the earth climate system, alter ecological balance through physiological effects on vegetation, and threaten biodiversity and sustainability of the earth's ecosystem.

Global average temperatures increased by 0.8 °C during the 20th century, with the rate of change (0.2 °C per decade) for the period since 1976 roughly three times that for the past

100 years as a whole (Hansen et al., 2006). Using a wide range of carbon cycle models and potential economic scenarios, the IPCC (Prentice et al., 2001) estimated that every 1 ppm (10^{-6}) rise in atmospheric CO₂ concentration could increase global mean temperatures by about 0.01 °C. The model projections of the IPCC predict that by 2100 atmospheric CO₂ concentrations will have risen from its current value of 380 ppm to between 500 and 1000 ppm and that global mean temperatures will rise by between 1.5 °C and 5.8 °C.

2. Carbon sinks in terrestrial ecosystem

Research indicates that the earth's ecosystems respond rapidly to the altered carbon cycle (IPCC, 2007). Over the last 10-20 years, more than half of the CO₂ released by burning fossil fuels has been absorbed on land and in the oceans. These uptake and storage processes, so called "carbon sinks", provide a negative feedback to the altered carbon cycle, and maintain the stabilities of the global ecosystem, atmosphere system and climate system (Pacala et al., 2007).

The potential of future carbon sinks, however, is still not clear. Carbon sequestration efficiency has been observed to change from year to year and decade to decade, due to a variety of mechanisms, only partly understood. Past studies on historical climate change indicate that if human disturbances on the global carbon cycle exceed the self-maintenance capacity of the its ecosystem, the earth's climate could become very unstable, with very significant temperature changes, going from a warm climate to an ice age (vice

versa) in as rapidly as a few decades (Petit et al., 1999). Assessing and understanding the impacts of human-induced environmental stresses such as atmospheric change, climate change, and land-use change on the global carbon balance are therefore, likely to be among the most pressing issues of the 21st century. One remarkable carbon allocation feature is that an increasing amount of atmospheric carbon dioxide appears to be being absorbed by terrestrial vegetation (IGBP Terrestrial Carbon Working Group, 1998).

The importance of the carbon sink due to the terrestrial biosphere is recognized from analysis of the global carbon budget, including improved estimates of the ocean carbon uptake, as well as data on $^{13}\text{CO}_2/^{12}\text{CO}_2$ isotopic ratios (Ciais et al., 1995) and from changes in the abundance of O_2 relative to N_2 (Rayner et al., 1999). An analysis of the global carbon budget of the 1990s suggests that the annual emissions through fossil fuel combustion (plus cement production which emitted about 0.12 P g C) and deforestation in tropics were about 6.4 ± 0.4 P g ($1 \text{ P} = 10^{15}$) and 1.7 ± 1.0 P g respectively, while the carbon flux from the atmosphere into the ocean was about 2.1 ± 0.5 P g. Therefore the net carbon sink in terrestrial ecosystem was inferred to be about 2.8 ± 1.2 P g (Malhi, 2002).

Forest inventory records (Goodale et al., 2002) and remote sensing (Nemani et al., 2003) of vegetation appear to confirm a significant land carbon sink in the Northern Hemisphere (Ciais et al., 1995). Fan et al. (1998) suggested that North America, especially the coterminous US (“south of 51 degrees north”), has the largest terrestrial carbon sink in the North Hemisphere. They reported an annual sink as large as 1.76 ± 0.5 P g ($1 \text{ P g} = 10^5 \text{ g}$) in terrestrial ecosystems of North America, large enough to

completely offset a continental emission source from fossil fuel of 1.6 Pg C per year. Other studies, both land- and atmosphere-based approaches, also yield the consistent conclusion that the US terrestrial ecosystem is a relatively stable net sink for carbon (Houghton et al., 1999; Pacala et al., 2001; Pacala et al., 2007). These studies indicated that forest regrowth from abandoned cropland might be the most important factor among the mechanisms generating the terrestrial carbon sink (Caspersen et al., 2000). Therefore, the carbon dynamic of the Southern US is especially important to the national carbon balance of the US because this region has the most productive terrestrial ecosystems in the US (Holland et al., 1999; Birdsey and Heath, 1995, 2003) and has experienced pervasive land-use change in the past two centuries (Wear, 2002).

Large scale forest regrowth in the South since the later half of last century could have sequestered a significant amount of carbon from the atmosphere (Delcourt and Harris, 1980; Han et al., 2007; Chen et al., 2006b; Woodbury et al., 2006). Based on forest inventory (FIA) data and historical land census data, Delcourt and Harris (1980) made a gross assessment of historical carbon dynamics in the Southeastern US in response to land-use change. They estimated that from 1750 to 1950, the region was a net source for carbon at an average rate of 0.13 Pg C per year. Since the 1960s, the SE US was estimated as a carbon sink of 0.07 Pg C per year. Using an empirical ecosystem model, Woodbury et al. (2006) studied the effects of afforestation and deforestation on carbon cycling in forest floor and soil from 1900 to 2050 in the Southern US. Their results matched with the findings of Delcourt and Harris (1980). They found that the SE US acted as a carbon source before mid of the 20th century, and then it turned into a net

carbon sink due to vast reforestation. Chen et al. (2006b), using simulation results of a process model, concluded that the size of carbon sink of the regrowth forest in this region was nearly 80% larger than the size of carbon source in cultivated land since 1990s.

3. The causes of the carbon sink in the terrestrial biosphere

What caused the carbon sink in the terrestrial biosphere? The simplest possibility is that forests are recovering from past disturbance and are changing in age structure. In the temperate regions of North America and Europe, there has been a substantial abandonment of agricultural land in the late 20th century (Houghton et al., 1999). It was estimated that land-use change in US accumulated 2 ± 2 P g C after 1945, largely as a result of fire suppression and forest growth on abandoned farmlands (Houghton et al., 1999). During the 1980s, the net flux of carbon attributable to land management offset 10 to 30 % of US fossil fuel emissions.

Another possible mechanism for a terrestrial carbon sink is that some human-induced agent of global change is causing an enhanced rate of forest growth or an expansion of forest area. One of the primary suspects is the elevated atmospheric CO₂ itself. The higher ambient CO₂ concentration is likely to stimulate plant photosynthesis (Field, 2001) and thus enhance the growth of vegetation (Cao and Woodward, 1998). The majority of laboratory studies of tree growth under high CO₂ concentrations have shown enhanced growth rates, with on average, a 60% increase in plant productivity for a doubling of atmospheric CO₂. This simulated plant growth due to high CO₂ concentration is called CO₂ fertilization effect (Long et al., 2004).

Nitrogen fertilization effect is another potential stimulator of vegetation growth. Nitrogen is the nutrient that most limits growth in the northern forest ecosystems (Schlesinger, 1997). In many regions, however, human activities have greatly increased the supply of nitrogen in terrestrial ecosystems, either through application of fertilizers (ammonium compounds and nitrates) or else through by-products of fossil-fuel or biomass combustion (nitrogen oxides). The nitrogen supply to the biosphere has increased from a pre-industrial value of 0.10 P g N per year to a current value of 0.24 P g N per year (Schlesinger, 1997). This enhanced supply is likely to have a number of consequences that are harmful to ecosystems, but one potential beneficial side effect may be a fertilization of tree growth, either on its own (Holland et al., 1997) or in combination with the CO₂ fertilization effect (Oren et al., 2001).

Finally, climatic change is also likely to affect vegetation carbon balance, although the direction of this effect is not clear. Warming trends have been most severe at high northern latitudes, where higher temperatures are likely to lengthen growing seasons, thus increasing plant productivity (Nemani et al., 2003). However, this warming may also accelerate decomposition of vast carbon reserves held in boreal forest and tundra soils, resulting in not only an accelerated turnover rate but no net accumulation (Hobbie and Chapin, 1998). In tropical ecosystems, changes in precipitation are likely to have a greater effect than temperature changes, affecting, for example, whether an area can support a tropical rain forest or a savannah (Melillo et al., 1993). However, the expected altered regional pattern of precipitation in the face of climate change is far from clear.

4. The ecosystem complexity and model simulation approach

Experiments and model simulations have been designed to study the mechanisms of a wide variety of factors on the terrestrial carbon sink (Schlesinger, 1997; Chapin et al., 2002). Large uncertainties, however, still exist due to the complex negative or positive feedbacks in the terrestrial ecosystem. Many environmental factors, like the increases in temperature and alterations in precipitation patterns have both positive and negative impacts on ecosystem carbon sequestration. Increased tropospheric ozone (O₃) pollution could inhibit both plant productivity and soil respiration (Adams et al., 1986; Chappelka and Samuelson, 1998).

Furthermore, environmental stresses usually do not operate independently, but rather often interact to produce combined impacts on ecosystem functioning. The ecosystems' responses to realistic combinations of global changes are not necessarily simple interactions of responses induced by individual factors (Norby and Luo, 2004). A plants' photosynthetic capacity in response to elevated atmospheric CO₂ can be modified by increasing temperatures, soil nutrient deficiency (Shaw et al., 2002), or troposphere O₃ pollution. Soil water stress, however, may be reduced by elevated atmospheric CO₂ concentration (Drake et al., 1997). Melillo et al. (2002) reported that global warming could enhance carbon sequestration in mid-latitude temperate forests through increased soil nitrogen mineralization rate. In arid regions, however, soil warming may reduce water availability, and exacerbate water deficiency (Melillo et al., 1993).

Therefore, to understand the impacts of global change on the terrestrial carbon sink, not only individual effects of multiple factors such as climate (Hanson et al., 2005), elevated CO₂ (Ellsworth, 1999; Loya et al., 2003), elevated nitrogen deposition (Holland et al., 1999), and O₃ stress (Chappelka et al., 1988) should be considered, but their interactions (Ollinger et al., 1997; Shaw et al., 2002; Boisvenue and Running, 2006) should also be investigated. Another major factor contributing to this complexity is the inherent heterogeneity of the landscape at spatial scales ranging from microns to thousands of kilometers. It has become clear from experience that no single experimental approach to elucidating terrestrial carbon cycling is sufficient to predict responses over all time and space scales. Approaches that focus on isolated subsets of environmental factors or entirely rely on empirical relationships within isolated subsets of terrestrial systems, however, can be incomplete or subject to misinterpretation.

Accurate predictions of ecosystem responses to suites of global change factors, therefore, depend on successful integration across a range of processes and time scales. The large number of possible combinations and long time periods over which they operate, however, make it nearly impossible to investigate the effects of multiple stresses on ecosystem carbon storage through controlled experiments (Ollinger et al., 2002). Integrated process-based ecosystem models, which include the physiological responses of ecosystems to atmospheric and climate changes can be quite useful in such multiple stress studies (Tian et al., 1998, 2003; Karnosky et al., 2005).

5. Ecosystem models and their application in ecology research

An ecosystem model is an abstraction and simplification of the ecosystem, made to aid the conceptualization and measurement of complex ecosystems and to predict the consequences of an action that would be expensive, difficult, or destructive to do in the real system (Haefner, 2005). Field experiments and observations provide the basis for ecosystem models. The models reflect our current understanding of the ecosystem structure and functioning and are required to be checked frequently against field-based results. However, unlike the traditional field studies which tend to isolate and control very small components of nature, the philosophy for ecosystem modeling is holism, or integration, which is necessary for the study of complex systems such as an ecosystem which involves many nonlinear interactions among multiple subsystems through long periods of time (Haefner, 2005).

Another advantage of ecosystem models are that they can be used to conduct “virtual experiments” that are impossible to be conducted in field due to dollar constraints, the large temporal or spatial scale or just unacceptable by the society (e.g. destructive experiments that will involve environmental problems). The global climate change study, for example, requires the investigation of the earth climate, hydrology, element, and biotic systems as the research object. It is of course impossible to conduct experiments on the whole earth system. Furthermore, global change is a slow process that involves many years. No experiments can cover such long time periods. Although the fossil records can provide some field evidence, (Lorius et al., 1990) such data are usually both scarce and

elusive, not being able to provide enough information for a comprehensive understanding of historical processes of global change. Ecosystem modeling, therefore, is the best choice in such large scale (both in time and space) research (Tian, 2002).

Process-based biogeochemical models have been widely used in assessment of global carbon storage (Melillo et al., 1993; VEMAP Members 1995) as well as regional carbon balance (Schimel et al., 2000; Tian et al., 1998, 2003; Chen et al., 2006a), or carbon dynamics in landscape scales (Kimball et al., 1997; Zhang et al., 2007). Process-based biogeochemical models have been used to estimate responses of terrestrial ecosystems to global change in the past (Kutzbach et al., 1996), current (Potter et al., 2006), and future scenarios (Cramer et al., 2001). Process-based models have been powerful tools to investigate the impacts of multiple environmental stresses such as climate (Tian et al., 1998), CO₂ fertilization, nitrogen deposition (McGuire et al., 1992), O₃ stress (Ren et al., 2007), and land-use change (McGuire et al., 2001; Chen et al., 2006b), and their interactions (e.g. Thornton et al., 2002; McGuire et al., 1997; Tian et al., 2003; Zhang et al., 2007).

CHAPTER 3
CASE STUDY I. –

Impacts of climatic and atmospheric changes on carbon dynamics in the
Great Smoky Mountains National Park

Abstract

An integrated land ecosystem model was used to estimate carbon (C) storage and to analyze the impacts of environmental changes on C dynamics from 1971 to 2001 in Great Smoky Mountains National Park (GRSM). Simulation results indicate that forests in GRSM have a C density as high as 15.9 kg m^{-2} , about twice the regional average. Total carbon storage in GRSM in 2001 was 62.2 T g ($\text{T} = 10^{12}$), 54% of which was in vegetation, the rest in the soil detritus pool. Higher precipitation and lower temperatures in the higher elevation forests result in larger total C pool sizes than in forests at lower elevations. During the study period, the CO_2 fertilization effect dominated O_3 and climatic stresses (temperature and precipitation), and the combination of these multiple factors resulted in net accumulation of 0.9 T g C in this ecosystem.

Keywords Carbon storage; Multiple stresses; Air pollution; O_3 ; Carbon dioxide

1. Introduction

Forests have been major carbon (C) sinks in the United States (US) during the 20th century (Turner et al., 1995). The balance of this C sink can be affected by global climatic and atmospheric changes, and global forest net primary productivity (NPP) has increased in the last 20 years due to changes in these factors (Boisvenue and Running, 2006). Many natural forests in the US are in Class I Wilderness areas. These areas are generally located in more remote regions and are protected by Federal regulations (Department of the Interior (DOI), 1982), and include 16 national parks and other protected, “near-natural” environments. These forests can store large amounts of C, and play an important role in the regional and global C balance. Global change effects that are primarily transmitted via the atmosphere are likely to be detectable in these protected mountainous-forested ecosystems, especially at high altitudes where the ecosystems are generally considered to be sensitive to climate change. These forested ecosystems, therefore, may serve as locations where the environmental impacts of climatic and atmospheric change can be studied directly. Furthermore, meteorological, hydrological, and forest types change strongly over relatively short distances in mountain regions. As a result, the ecosystem C storage and its responses to global change also differ dramatically along the altitudinal gradients. Therefore, the strong altitudinal gradients in mountainous environments provide unique and sometimes the best opportunities to analyze global change processes and their impacts on C dynamics of natural forests (Becker and Bugmann, 2001).

The most significant atmospheric change during the last two centuries is the rapid rise of atmospheric CO₂ concentration which has been suggested to result in global climate change. Studies showed that the increased atmospheric CO₂ concentration can enhance forest growth and C sequestration capacity (Tian et al., 2000), thus providing a negative feedback at the atmospheric level. The beneficial effect of CO₂ fertilization, however, could be offset by the damaging effects of other air pollutants such as tropospheric O₃ (Adams et al., 1986; Chappelka and Samuelson, 1998; Felzer et al., 2004). To understand the effects of global change on C dynamics of forests in national parks, the effects of CO₂ (Ellsworth, 1999; Loya et al., 2003), climate (Tian et al., 1998), O₃ (Chappelka et al., 1988; Pye, 1988; Chappelka and Chevone, 1992), and their interactions (Ollinger et al., 1997; Tian et al., 1999; 2000; Boisvenue and Running, 2006) should be investigated. Furthermore, the various responses of different plant functional types to these stressors are also important (Reich, 1987; Chappelka and Samuelson, 1998; Weinstein et al., 2001). The large number of possible combinations and long-term periods over which they operate, however, make it nearly impossible to investigate the effects of multiple stresses on ecosystem C storage through controlled experiments (Ollinger et al., 2002). Integrated process models, which include the physiological responses of ecosystems to atmospheric and climatic changes can be quite useful in such multiple stressor studies (Ollinger et al., 1997; 2002; Martin et al., 2001; Felzer et al., 2004; Hanson et al., 2005; Karnosky et al., 2005).

In this study, we use the Dynamic Land Ecosystem Model (DLEM), an integrated ecosystem process model (Tian et al., 2005) that couples major biogeochemical and

hydrological cycles to make daily and spatially-explicit estimates of carbon fluxes and pool sizes in Great Smoky Mountains National Park (GRSM) from 1971 to 2001. DLEM is able to address responses of terrestrial ecosystems to multiple stresses including changes in climate, atmospheric composition (CO_2 and O_3), land use, and natural disturbances. The GRSM represents forested ecosystems typical of the eastern mixed pine hardwood regions in the US (Whittaker, 1966), a region that has long been recognized as being strongly affected by elevated O_3 concentrations (Neufeld et al., 1992; Mueller, 1994; Chappelka and Samuelson, 1998; Weinstein et al., 2001). GRSM is located downwind of large urban and industrial areas that generate large amounts of air pollutants or their precursors (Christine et al., 1994). Many field studies have revealed that GRSM forest growth has been inhibited by O_3 pollution (Neufeld et al., 1992; Somers et al., 1998). Simulations have been conducted by Weinstein et al. (2001) to investigate the effect of O_3 stress on photosynthesis and succession of a forest community in the Twin Creeks area of GRSM. Comprehensive evaluation of the impacts of multiple climate and atmospheric stresses on ecosystem productivity and C storage of the whole GRSM region has not yet been attempted. The purpose of this study was to use a model simulating approach to estimate the changes in GRSM C storage from 1971 to 2001 and to analyze forest responses to climate change, CO_2 fertilization, tropospheric O_3 stress, and the interactions of these multiple stresses.

2. Methods

2.1. Study region

Great Smoky Mountains National Park, the largest Class I Wilderness area in the eastern US, was established along the border of western North Carolina and eastern Tennessee in 1934 to protect the 2079 km² continuous eastern mixed pine hardwood forests that consist of approximately 85% deciduous forest, 13% coniferous forest, and < 2% in heath bald (MacKenzie 1993, Figs. 1 & 2). Elevations in GRSM range from approximately 250 m along the outside boundary of the Park up to more than 2000 m in the center of the park (Fig.1). The broad ranges of elevations in GRSM contribute to a wide variety of climates (Shanks, 1954; Busing et al., 2005). The climate is humid and warm at lower elevations, cool and wet at higher elevations (Thorntwaite, 1948). Annual precipitation at lower elevations is around 1200 mm while can be as high as 2000 mm at higher altitudes, similar to some of the wettest regions in the US (Busing et al., 2005). Overall annual average temperatures range from 10 - 12 °C.

The boreal or alpine coniferous forests [spruce-fir (*Picea-Abies*)] are located above 1400 m (Figs. 1 & 2). Northern Hardwood Forests dominate middle to upper elevations from 1000 – 1500 meters in the park. Oak (*Quercus* spp.) is the major component in this region. Pine (*Pinus* spp.) forests grow within low-elevation regions, especially in the northwestern portion of the Park (Welch et al., 2002; Figure C3.2).

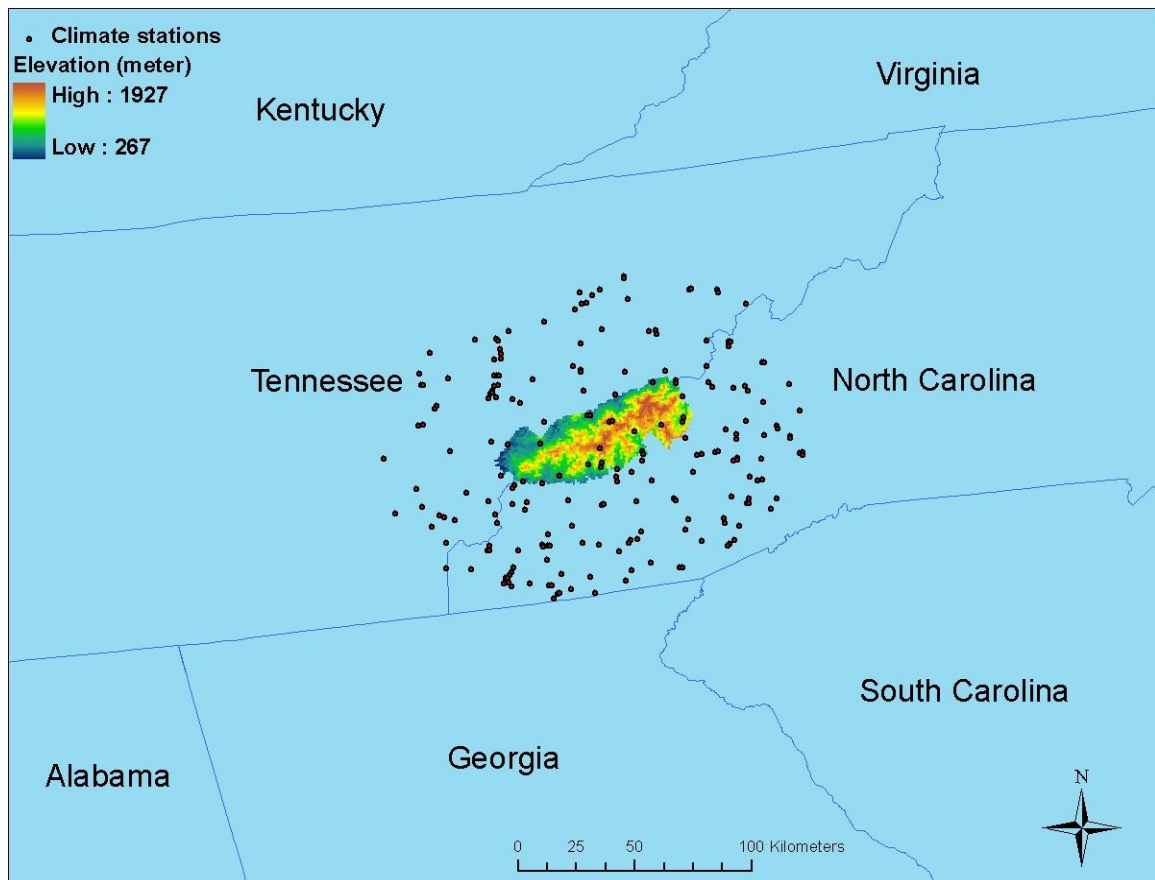


Figure C3.1 Location of study region (Welch et al., 2002). Great Smoky Mountains National Park (GRSM) is located along the North Carolina–Tennessee border in the southeastern United States in the southern part of the Appalachian Mountains. Elevation ranges from approximately 250 m along the outside boundary of the Park up to more than 2000 m in the center of the park. Climate records from more than two hundred climate stations (black dots) were used to generate the climate datasets for the simulation.

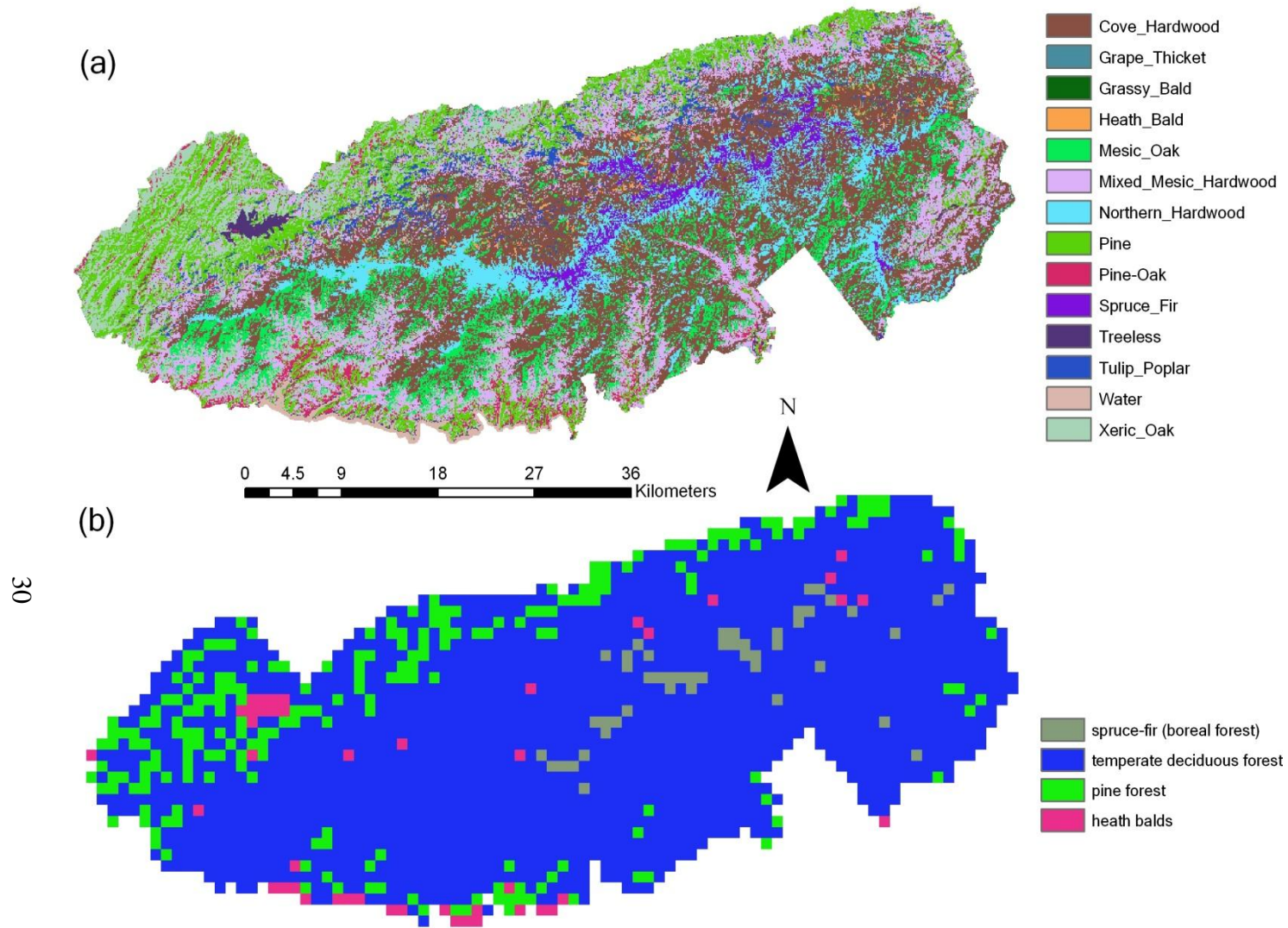


Figure C3.2 The distribution of major vegetation types in Great Smoky Mountains National Park (late 1980s) (a) Original 100 meter resolution vegetation map developed by MacKenzie (1993) and (b) the $1 \times 1 \text{ km}^2$ resolution 4-category vegetation map aggregated from map (a) by us to drive the model

O₃ exposures in GRSM are among the highest in the eastern US (Mueller, 1994; US EPA, 2001; DOI, 2002). The mean summer hourly O₃ concentration was about 51 ppb (Look Rock O₃ monitor site) to 55 ppb (Cove Mountain O₃ monitor site) during the 1980s and early 1990s (Mueller, 1994), while damage to vegetation was found to occur at levels as low as 50 ppb. On average, O₃ concentrations over the ridgetops of the park can be as high as or higher than in nearby cities, including Knoxville and Atlanta (DOI, 2002). The average O₃ concentration measured in the summer of 1989-1991 at the Hendersonville station in metropolitan Nashville, for example, was 6-12 ppb lower than the value measured at Great Smoky Mountain stations (Mueller, 1994). Data from the Clean Air Status and Trends Network (CASTNET) (<http://www.epa.gov/castnet/>) shows that the SUM06 index [calculated as the sum of hourly O₃ concentrations above 60 ppb summed over 12 hours (08:00 to 20:00) during a 3-month period] at the GRSM Look Rock O₃ monitoring station in the summer of 2001 was about 27 (ppb-hr). This value is higher than the 25 ppb-hr that US Environmental Protection Agency US EPA proposed as an alternative secondary standard (<http://www.epa.gov/castnet/>). O₃ pollution results in visible injury in GRSM vegetation (Neufeld et al., 1992). In a survey conducted in GRSM, Chappelka et al. (1997) reported 47% of the over 1600 black cherry (*Prunus Serotina*) examined showed visible foliar symptoms of O₃ injury.

2.2. The Dynamic Land Ecosystem Model (DLEM)

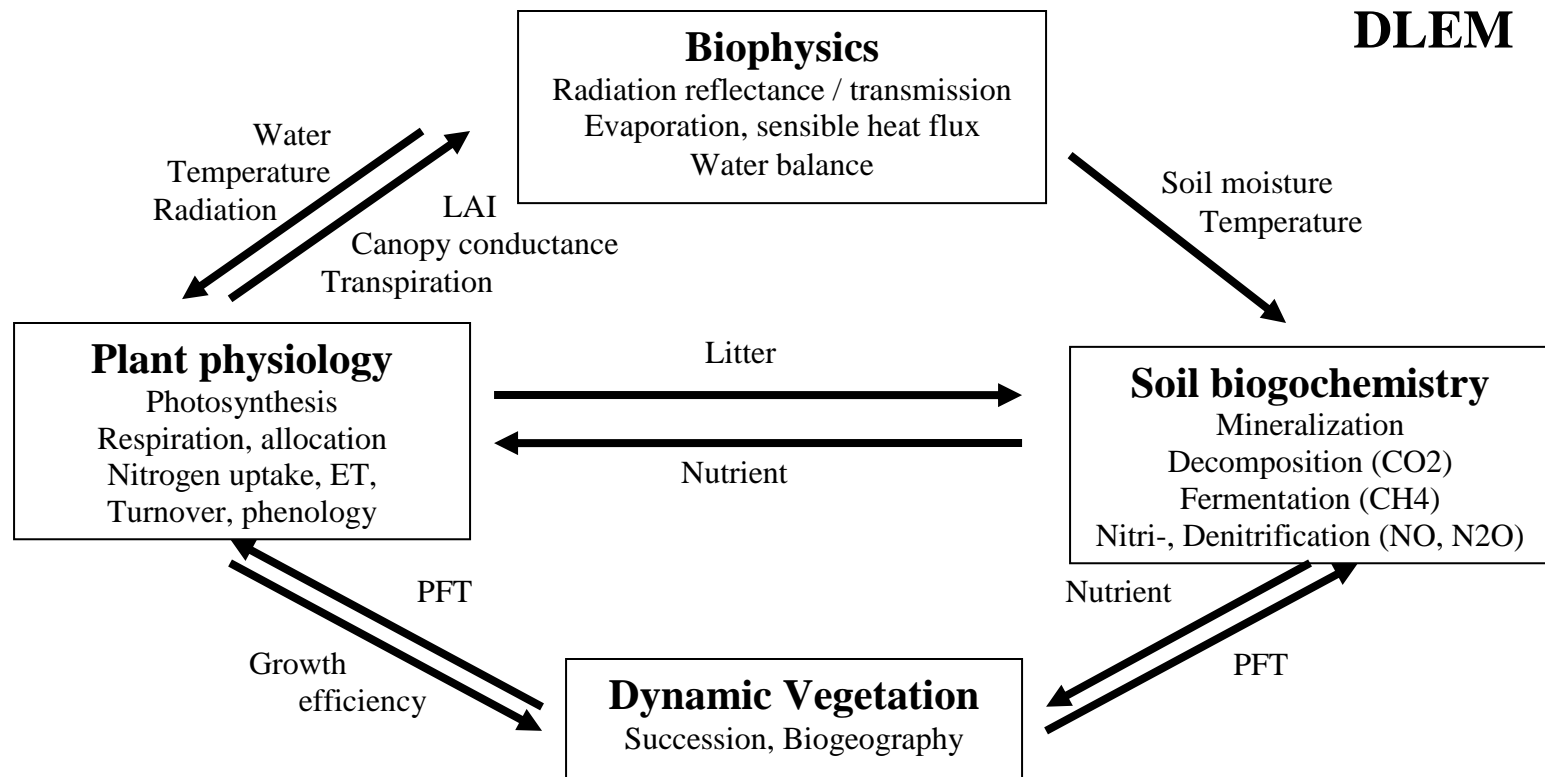


Figure C3.3 Dynamic Land Ecosystem Model (DLEM). The DLEM (Tian et al., 2005) is a process-based model which couples biophysical processes (energy balance), biogeochemical processes (water cycles, carbon cycles, nitrogen cycles, and trace gases (NO_x, CH₄)-related processes), community dynamics (plant distribution and succession), and disturbances (land conversion, agriculture management, forest management, and other disturbances such as fire, pest etc.) into one integral system. DLEM can simulate the complex interactions of multiple stresses such as climate change, elevated CO₂, tropospheric O₃, N deposition, human disturbance, and natural disturbances.

The DLEM (Tian et al., 2005; Chen et al., 2006a) is a process-based model which couples biophysical processes (energy balance), biogeochemical processes (water cycles, carbon cycles, nitrogen cycles, and trace gas (NO_x, CH₄)-related processes), community dynamics (plant distribution and succession), and disturbances (land conversion, agriculture management, forest management, and other disturbances such as fire, pests, etc.) into one integral model system (Figure C3.3). DLEM can simulate the complex interactions of multiple stresses such as climate change, elevated CO₂, tropospheric O₃, N deposition, human disturbance, and natural disturbances.

In DLEM, the carbon balance of vegetation is determined by photosynthetic rate, autotrophic respiration, litterfall (related to tissue turnover rate and leaf phenology), and plant mortality rate. Plants assimilate carbon by photosynthesis, and then use this carbon to compensate for the loss through maintenance respiration, tissue turnover, and reproduction. The photosynthesis submodel of DLEM estimates net C assimilation rate, leaf daytime maintenance respiration rate, and gross primary productivity (GPP, unit: g C m⁻² day⁻¹). The photosynthetic rate is first calculated at the leaf level. The results are then multiplied by the leaf area index to scale up to the canopy level (Tian et al., 2005). To simulate the detrimental effect of air pollution on ecosystem productivity, we developed the O₃ submodel based on the work of other researchers (Ollinger et al., 1997; Martin et al., 2001; Felzer et al., 2004), in which we simulate the direct effect of O₃ on photosynthesis.

The following equations and parameters were used in the model:

$$A = \min(w_j, w_c, w_e) \quad (1)$$

$$A' = A \times O_{3eff} \quad (2)$$

$$O_{3eff} = F(g_s, O_3, a) = 1 - a \times g_s \times O_3 \quad (3)$$

$$g_s = G(A') \quad (4)$$

$$g_c = g_s f(LAI, T_{min}, W, CO_2) \quad (5)$$

where w_j, w_c, w_e are the electron transport (or light)-limited, carboxylation-limited and export-limited rates respectively; A is the rate of photosynthesis; g_s is stomatal conductance and g_c is canopy conductance; LAI denotes leaf area index; T_{min} is the minimum temperature; and W is wind speed. O_{3eff} denotes the effects of O_3 on photosynthesis; a is the O_3 plant functional type-specific sensitivity coefficient (deciduous trees and heath bald: 2.6×10^{-6} ; coniferous trees: 0.7×10^{-6} ; Felzer et al., 2004). GPP is used to estimate net primary productivity (NPP) by subtracting the autotrophic respiration (R_A):

$$NPP = GPP - R_A \quad (6)$$

DLEM estimates the annual net carbon exchange (NCE) of the terrestrial ecosystem with the atmosphere using the following equation:

$$NCE = NPP - R_H - E_{NAD} - E_{AD} - E_P \quad (7)$$

where E_{NAD} is the magnitude of the carbon loss from a natural disturbance, E_{AD} is carbon loss during the conversion of natural ecosystems to agriculture, and E_P is the sum of carbon emission from the decomposition of products (Tian et al., 2003). Since GRSM is relatively undisturbed, E_{NAD} , E_P and E_{AD} are equal to 0. Therefore, NCE in GRSM is equal to net ecosystem production (NEP).

2.3. Input data

2.3.1. Base maps

Input base maps include: 1) elevation, slope, and aspect maps which are derived from the 7.5 minute USGS National Elevation Dataset (<http://edcnts12.cr.usgs.gov/ned/ned.html>); 2) soil datasets (pH, bulk density, depth to bedrock, soil texture represented as the percentage content of clay, sand, and silt) derived from the 1 km resolution digital general soil association map (STATSGO map) developed by the United States Department of Agriculture (USDA) Natural Resources Conservation, while the texture information of each map unit was estimated using the USDA soil texture triangle (Miller and White, 1998); and 3) a vegetation map (Figure C3.2b) for the late-1980s which was developed by MacKenzie (1993). MacKenzie developed this 100 meter resolution and 14 category vegetation type map of the GRSM based on satellite imageries. We aggregated these vegetation types into the deciduous, pine, spruce-fir, and heath types that were used

as our model input (Figure C3.2b). All of these input maps were aggregated into a 1×1 km resolution.

2.3.2. Generating daily climate dataset

The model simulation required 1 km resolution daily climate information (precipitation, maximum and minimum temperatures) in the study region. We generated the climate dataset from 1949 to 2001 based on climate data (Cooperative Summary of the Day, TD-3200 dataset, compiled by the National Climatic Data Center, <http://www.ncdc.noaa.gov/oa/ncdc.html>) from 216 stations that were located < 50 km from GRSM (Figure C3.1). We adopted the interpolation method developed by Thornton et al. (1997), with the following modifications:

- 1) Unlike the original approach that assesses the daily temperature lapse rate using least-squares regression technique, we used a fixed monthly lapse rate for minimum and maximum air temperatures, based on the study results of Busing et al. (2005) who used historical climate records of five GRSM stations of different elevations to analyze the elevation-climate pattern of GRSM.
- 2) We used the following empirical model to estimate the elevation-precipitation relationship of GRSM:

$$\text{PPT} = -0.0002 \times (\text{ELEV}^2 - \text{ELEV}_{\text{ref}}^2) + 0.9612 \times (\text{ELEV} - \text{ELEV}_{\text{ref}}) + \text{PPT}_{\text{ref}} \quad (8)$$

where PPT and PPT_{ref} are the predicted precipitation in the target grid and the precipitation of the climate station, respectively. $ELEV$ and $ELEV_{ref}$ are elevation of the grid and the climate station, respectively. The coefficients are derived based on the monthly precipitation and elevation relationship of GRSM reported by Busing et al. (2005). The R^2 for the regression fit was 0.98.

2.3.3. Atmospheric composition datasets

Standard IPCC CO_2 concentration history dataset (Enting et al., 1994) was used in this simulation. We did not consider the intra-annual CO_2 concentration change. The spatial pattern of atmospheric CO_2 concentration was assumed to be homogenous.

DLEM required a daily AOT40 input as the index of tropospheric O_3 stress. AOT40 is the accumulated dose over a threshold of 40 ppb during daylight hours (Felzer et al., 2004). In DLEM, we used an accumulation period of 30 days back-trajectory. To account for the effects of O_3 on terrestrial carbon dynamics, we developed a spatially explicit dataset of historical changes in the AOT40 index in GRSM. First, hourly O_3 data for five stations over 1988 to 2004 in the park were obtained from the National Park Service Air Resources Division (NPS, AQD, Lakewood, CO). These 5 stations are located across the park at various elevations including Cades Cove (564 m), Look Rock (793 m), Cove Mountain (1242 m), Purchase Knob (1500 m), and Clingmans Dome (2021 m). Due to limited hourly O_3 data for the Purchase Knob site, this location was

excluded from the development of the O₃ spatially explicit data set. The AOT40 index was calculated directly from the averaged hourly data for each site on a monthly basis. Second, we developed an AOT40 index regression model for each month using the calculated AOT40 index data. In these models, the AOT 40 index was the response variable while elevation was the only explanatory variable because O₃ concentration is correlated with elevation, *i.e.*, higher concentrations at higher elevations and greater exposure of forested ecosystems (Gilliam et al., 1989; 1995; Mueller, 1994; Chappelka et al., 1999). The regression model for each month was then interpolated to a 1 × 1 km² grid based on the elevation map. A linear interpolation method was used to interpolate the monthly AOT40 into a daily dataset which is required by DLEM. Using this method, we developed the AOT40 index transient data over the entire park for the period of 1988 to 2004. Prior to 1988, we used the AOT40 dataset developed by Felzer et al. (2004) which was modified by us so that the 1998 AOT40 matched our interpolated result.

2.4. Simulation Design

To address the objectives of the study we designed the following seven simulation scenarios for this study as described in Table C3.1. The last scenario (*i.e.*, CLMCO2O3) simulates the environmental change and carbon dynamics of GRSM ecosystems. We used it to assess the change of C storage of the system. We estimated the effects of climate, O₃, CO₂ factors, and their interactions respectively by analyzing the differences between CLMCO2O3 and CO2O3, between CLMCO2O3 and CLMO3, between CLMCO2O3 and CLMCO2, and between CLMCO2O3 and the sum of CLM, CO₂, and

O3. The CLM, CO2, and O3 scenarios estimate the general impacts of these single factors on the C dynamics of GRSM ecosystems. Besides identifying the impacts and interactions of different environmental factors, we also analyzed the responses of different vegetation types (pine forest, spruce-fir forest, deciduous forest, and heath bald) in GRSM to these environmental stresses.

Table C3.1 Description of the seven scenarios in this study

Scenarios	Description	Environmental Factors*		
		Climate change	CO ₂ fertilization	O ₃ stress
CLIMATE	Climate only	+	-	-
CO2	CO ₂ fertilization only	-	+	-
O3	O ₃ stress only	-	-	+
CLMCO2	Climate and CO ₂ combination	+	+	-
CLMO3	Climate and O ₃ combination	+	-	+
CO2O3	CO ₂ and O ₃ combination	-	+	+
CLMCO2O3	All environmental factors	+	+	+

* + indicates that transient effect of the environment factor is considered; - indicates that value of the environment factor is keep constant and its transient effect is not included in the simulation.

In this simulation, we first used the long-term climate normal data and pre-industrial CO₂ concentration data (288 ppm) as model inputs to run the model to the equilibrium state to build the simulation baseline for soil C pools and soil water pools. Then, for those scenarios involving transient climate we set up a spin-up run of 88 (22 × 4) years to

prevent any abnormal fluctuation due to the sudden switch from the equilibration state to the transient state. Only the climate data were allowed to vary in the spin run. Finally, we set up the simulation of each scenario described above. The 21-years simulation from 1949 to 1970 developed the historical background. Our analysis of simulation output focused on the period from 1971 to 2001.

3. Results and Discussion

3.1. Climatic change and the atmospheric change

Our climate data show no obvious trend of climate change in the GRSM occurred from 1971 to 2001, although an interannual fluctuation of temperature and precipitation was observed (Figure C3.4a). The average temperature was 11 °C. The most rapid interannual temperature rise (by 1.59 °C) took place during the years 1997-1998 when a strong El Niño occurred. The average precipitation was 1640 mm (Figure C3.4b). The largest increase in precipitation was observed during the years 1988-1989, a period when the strongest La Niña in the last two decades of the 20th century took place. According to our data set, the study region experienced a long-term drought from 1985 to 1988 when annual precipitation fell to 1277 mm in 1988, the driest year. We also found that spatial patterns of climate factors were closely related to elevation (Figs.4c, d). Precipitation in GRSM tended to increase with elevation (Figure C3.4d), while temperature declined with elevation with a lapse rate of about 2.9 to 5.6 °C km⁻¹ (Busing et al., 2005).

Our O₃ dataset shows that the annual average AOT40 increased from 1418 ppb-hr in 1971 to 3194 ppb-hr/30days in 2001. O₃ concentrations in GRSM fluctuated from season to season and from year to year. Figure C3.5a shows the interannual pattern of the AOT40 index from 1971 to 2001. O₃ concentrations increased linearly from 1418 ppb-hr in 1971 to 2216 ppb-hr in 1977. From 1977 to 1994, the AOT40 fluctuated around 2200 ppb-hr, and only increased slightly (8.7%) during the 18 years. In the late 1990s, O₃ stress in GRSM increased dramatically. The annual average AOT40 nearly doubled in four years from 1994 to 1998. After that, it dropped back quickly to 3194 ppb-hr in 2001.

Fig C3.5c and d show the spatial pattern of O₃ within the GRSM. O₃ concentrations are higher at the high elevation regions of GRSM (Mueller, 1994; Chappelka et al., 1999; DOI, 2002). CO₂ concentrations increased from 326.3 ppmv in 1971 to 371.0 ppmv in 2001 (Enting et al., 1994).

O₃ concentrations varied significantly from season to season (Figs. 5b, c, d). The AOT40 increased quickly in the spring, reached a first peak in May, and then dropped slightly in summer. In late summer, the AOT40 rose to a second peak, and then decreased linearly to September.

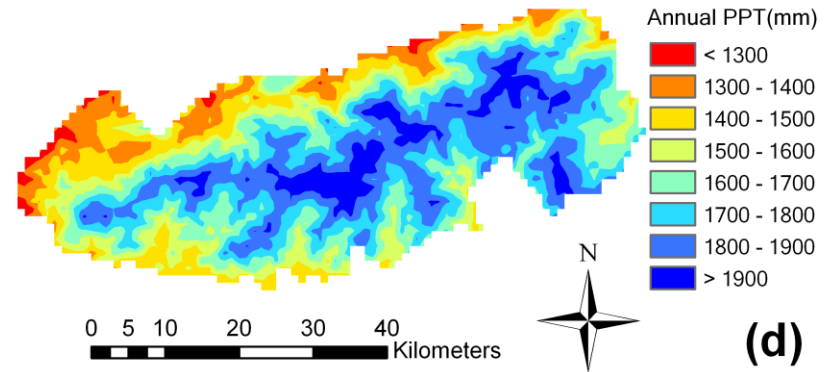
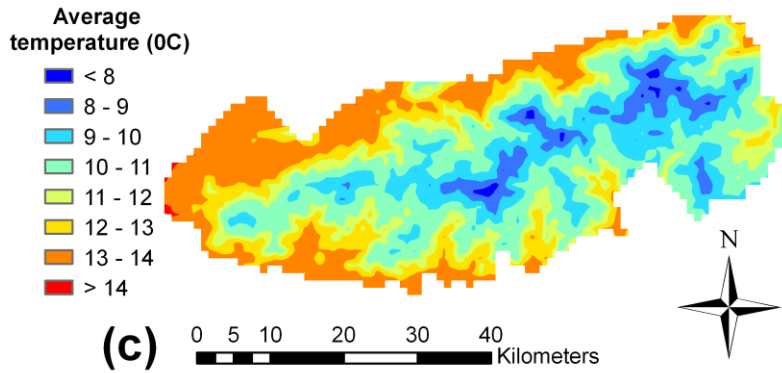
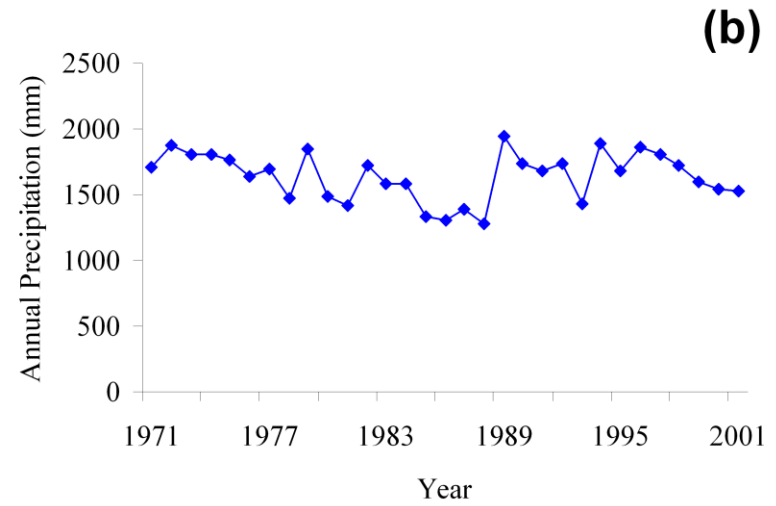
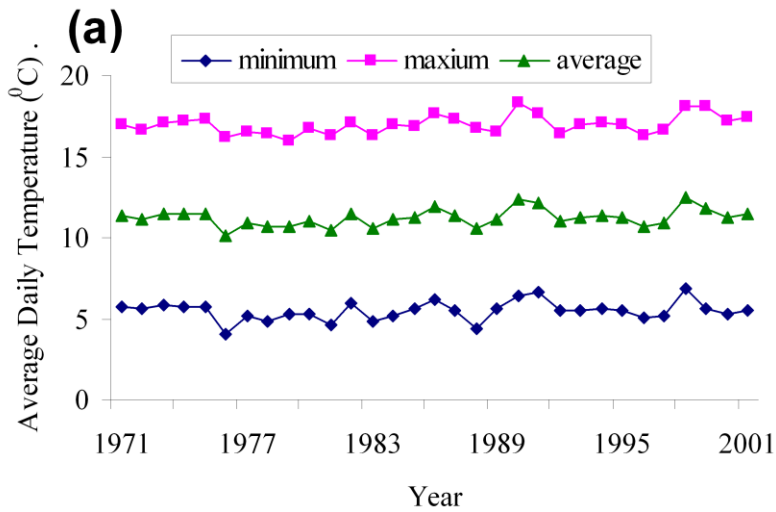


Figure C3.4 The temporal and average spatial pattern of temperature and precipitation in GRSM: (a) Temporal variation of yearly average temperature from 1971 to 2001, (b) Temporal variation of annual total precipitation from 1971 to 2001, (c) Spatial pattern of average daily temperature during study period, (d) Spatial pattern of average annual precipitation during study period.

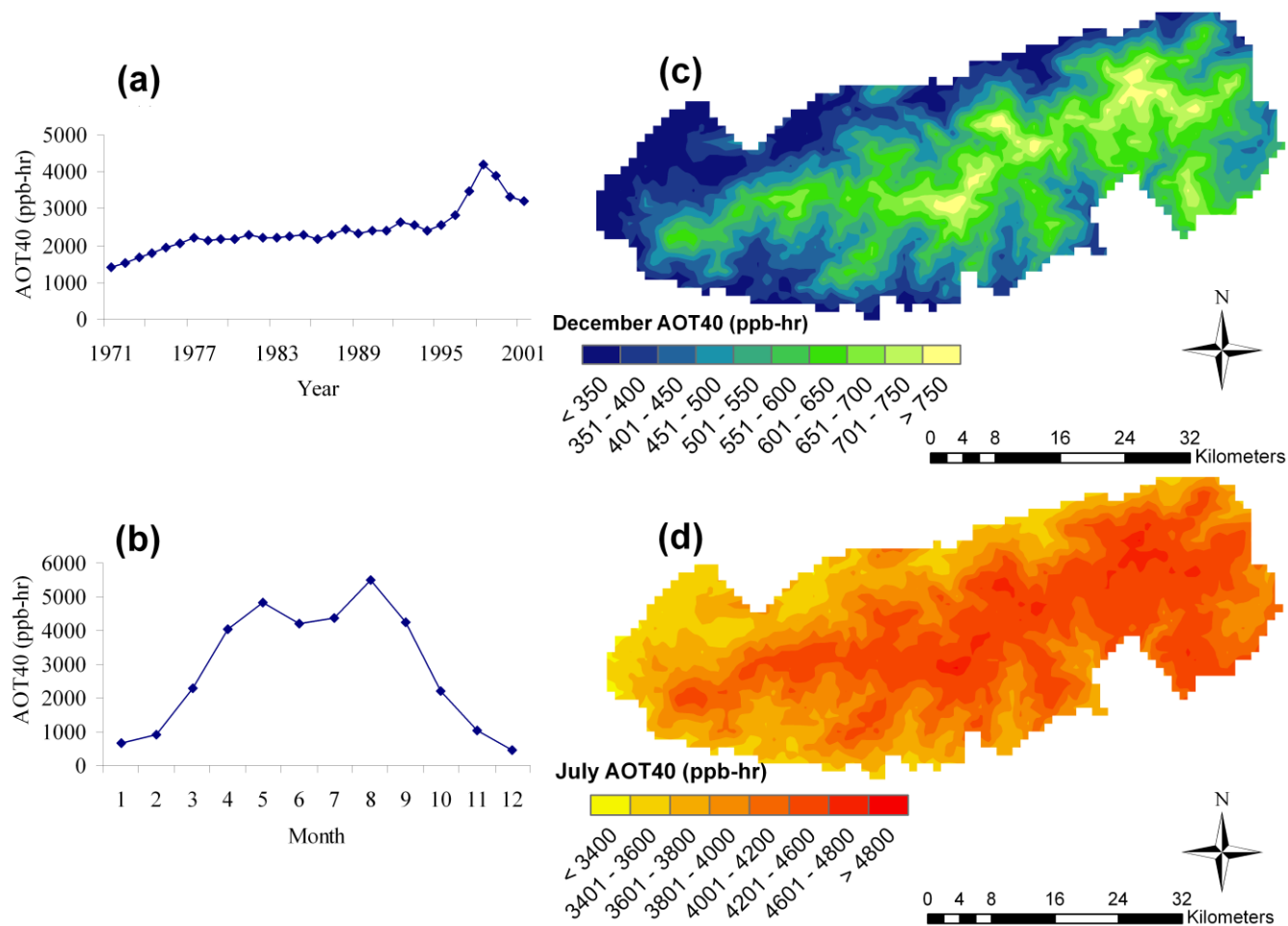


Figure C3.5 The interannual, intraannual, and seasonal pattern of tropospheric O₃ (AOT40, ppb-hr) in GRSM: (a) Interannual variation of average AOT40 from 1971 to 2001, (b) Intraannual variation of AOT40, (c) Spatial pattern of AOT40 in December, (d) Spatial pattern of AOT40 in July. The AOT40 increases with altitude.

3.2. Changes in carbon storage from 1971 to 2001

Our simulation result shows that from 1971 to 2001 the total C storage of GRSM increased slightly from 61.3 T g (1 T g = 10^{12} g) to 62.2 T g (calculated by multiplying the average total C (TOTC) density in Table C3.2 with area of GRSM). In 2001, about 54% of the C was stored in the living vegetation C pool (VEGC); about 44% was stored in the soil organic C pool (SOC). The rest of the C was stored in the litter C pool (LTRC). If the O₃ stress is not considered (CLMCO₂ scenario), however, the combined effects of climate and CO₂ fertilization together could have resulted in a 3% (or 1.8 T g) increase of total C storage during these 30 years. This suggests that O₃ stress could have reduced the C sequestration rate by 50% (about 0.9 T g) in GRSM. If the CO₂ fertilization effect is not considered (CLMO₃), the combination effects of climate and O₃ result in a 1.4 T g loss of C from 1971 to 2001. This means that the CO₂ fertilization effects may have contributed to about 2.3 T g C of sequestration in GRSM from 1971 to 2001.

Different vegetation types responded differently to O₃ in our model results. The TOTC of deciduous forests decreased by 2.5% from 1971 to 2001, while the TOTC of pine forests decreased by only 1.4% for the same period. In another study on a lower slope forest of the GRSM, current ambient levels of O₃ were predicted to accelerate forest succession by suppressing the growth of O₃ sensitive species (Weinstein et al., 2001).

Table C3.2 Overall change in Great Smoky Mountain National Park forest carbon density (gC / m²) from 1971 to 2001

		<u>CLMCO2O3</u>				<u>CLMCO2</u>				<u>CLMO3</u>			
		1971	2001	change	change (%)	1971	2001	change	change (%)	1971	2001	change	change (%)
VEGC	pine [@]	11782	11789	7	0.06	11786	11787	0	0.00	11649	11459	-190	-1.63
	spruce-fir	16266	16992	726	4.46	16352	17304	952	5.82	16031	15909	-121	-0.76
	deciduous	16475	16661	186	1.13	16596	17115	518	3.12	16235	15634	-601	-3.70
	heath bald	4734	4903	169	3.57	4750	4911	162	3.40	4761	4756	-6	-0.12
	average	15706	15884	179	1.14	15811	16276	464	2.94	15483	14951	-532	-3.44
SOC	pine	8981	9418	437	4.87	8989	9470	481	5.35	8845	8901	56	0.63
	spruce-fir	14413	14463	50	0.35	14417	14502	86	0.59	14574	14504	-70	-0.48
	deciduous	13420	13642	221	1.65	13440	13773	332	2.47	13564	13446	-118	-0.87
	heath bald	10681	10971	290	2.71	10694	11083	389	3.64	10423	10295	-128	-1.23
	average	12902	13144	242	1.88	12920	13264	344	2.66	13007	12908	-98	-0.76
LTRC	pine	958	983	25	2.58	964	1005	41	4.25	917	748	-169	-18.46
	spruce-fir	1396	1412	16	1.16	1382	1416	35	2.51	1443	1406	-37	-2.55
	deciduous	878	890	13	1.43	875	913	38	4.34	878	843	-34	-3.93
	heath bald	626	676	49	7.84	631	698	67	10.62	602	577	-25	-4.22
	average	893	908	15	1.65	891	930	39	4.36	889	840	-49	-5.51
TOTC	pine	21722	22190	468	2.16	21739	22261	522	2.40	21411	21108	-303	-1.41
	spruce-fir	32075	32867	792	2.47	32151	33223	1072	3.33	32048	31820	-228	-0.71
	deciduous	30773	31193	420	1.36	30912	31801	889	2.87	30677	29924	-753	-2.46
	heath bald	16041	16549	508	3.17	16074	16692	618	3.84	15787	15627	-160	-1.01
	average	29500	29936	435	1.48	29622	30469	847	2.86	29379	28700	-679	-2.31

@ Area of pine forest is 226 km²; area of deciduous forest is 1760 km²; area of spruce-fir alpine/boreal forest is 48 km²; area of heath bald is 45 km²; total area of GRSM is 2079 km².

The C density of GRSM forest ecosystems was high (Whittaker et al., 1974). Based on our results, in 2001, the spruce-fir boreal forests at higher elevations had an average VEGC density of 16 992 g C m⁻² (Table C3.2). This value agrees with Whittaker's (1966) estimate of 13 000 - 22 100 g VEGC m⁻² in GRSM spruce-fir forest biomass (by assuming a ratio of root to woody shoot dry biomass of 0.3, and a C to dry biomass ratio of 0.5). Our result shows that deciduous forests had an average C density of about 16.7 kg VEGC m⁻² in 2001. This value falls in the range of 8.4 - 39 kg VEGC m⁻² estimated by Whittaker (1966). Whittaker (1966) reported the pine-heath forest biomass to have 3.4 - 5.5 kg VEGC m⁻², and our estimation is about 4.9 kg VEGC m⁻². Our estimation of pine forest biomass is 11.8 kg VEGC m⁻², which also falls within the range of 8.4 - 12 kg VEGC m⁻² for pine forest biomass as estimated by Whittaker (1966). Our estimation of soil organic carbon (SOC) in GRSM was about 13 kg SOC m⁻² (Table C3.2), higher than the 11.2 kg C m⁻² reported by Miller et al. (2004), but close to Post's et al. (1982) estimation of 12.1 kg SOC m⁻² for overall cool, moist temperate forests. Daniels et al. (1987), however, found the SOC of a protected mesic southern Appalachian forest in North Carolina could be as high as 28 kg SOC m⁻².

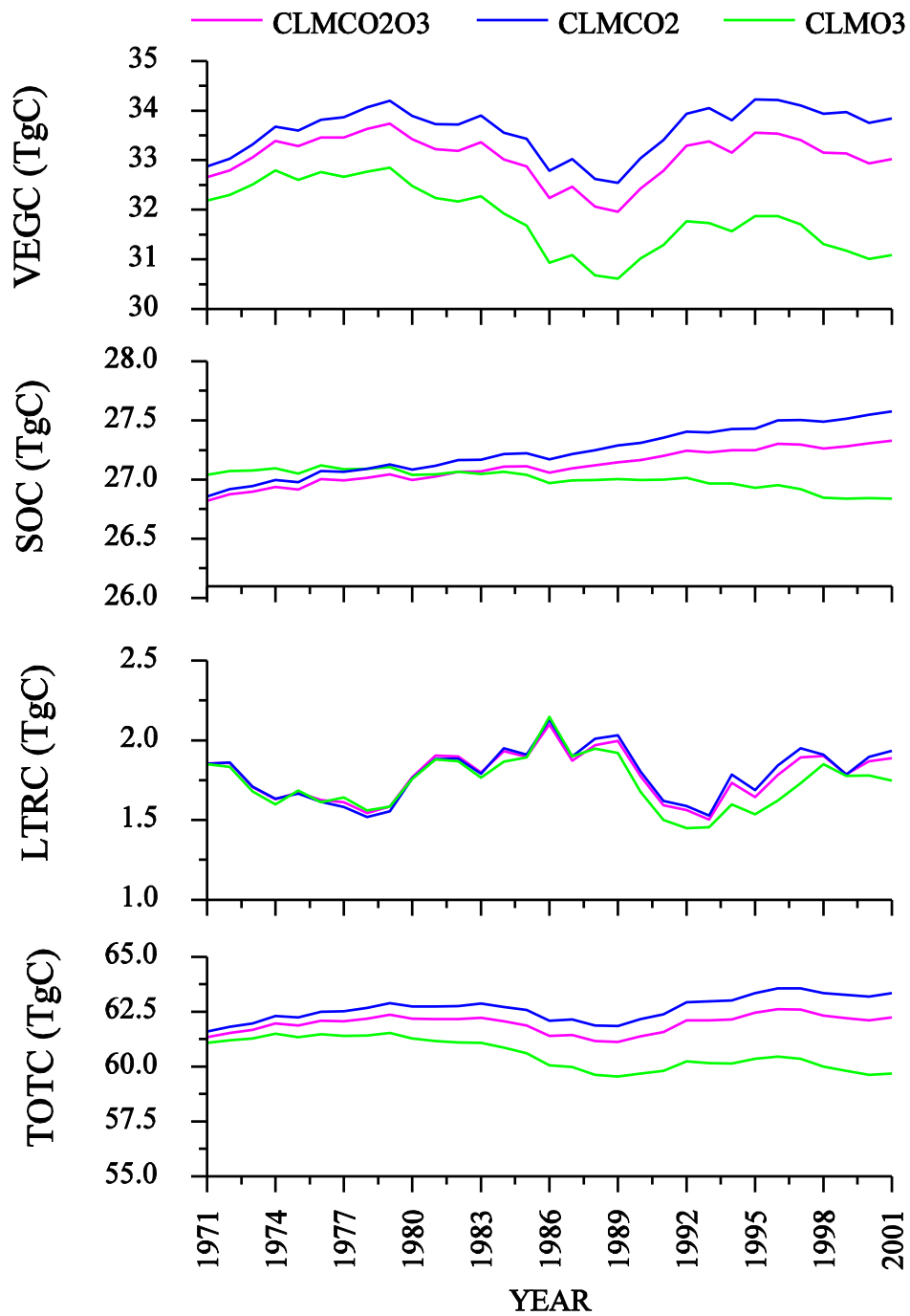


Figure C3.6 Changes in great smoky mountain carbon pools (unit: T g; 1 T g = 10^{12} g) from 1971 to 2001. VEGC denotes vegetation carbon pool; SOC denotes soil carbon pool; LTRC denotes litter C pool; TOTC denotes total carbon storage. Scenarios: CLMCO2 = climate + CO₂ effect; CLMO3 = climate + O₃ effect; CLMCO2O3 = combination of climate + CO₂ + O₃ effect.

Figure C3.6 shows the temporal pattern of C storage from 1971 to 2001. Since the SOC was relatively stable, the temporal pattern on total C dynamics was decided primarily by the change in the VEGC pool, which followed the general pattern of climate change, especially the interannual change in precipitation. The late 1980s drought (Figure C3.4b), for example, may have resulted in a loss of C storage in GRSM. The negative effect of O₃ stress and positive effect of CO₂ fertilization on ecosystem C sequestration become more and more evident through time and their combined effects resulted in a slight increase of C storage according to our analysis.

Figure C3.7 shows the spatial pattern of the GRSM C storage, and its net change from 1971 to 2001. Except for the scattered heath balds, the ecosystem total C storage generally increased with altitude. This pattern could be explained by the unique climate patterns of the GRSM. While the lower temperatures at the higher altitudes limited ecosystem C loss through respiration, the high precipitation enhanced plant C sequestration capacity (Figs. 4c, d). It seems that this climate effect dominated over the negative effect (on C sequestration) of high O₃ concentrations in high elevations (Figs. 5c, d). Our simulation results also indicate that the northern region of GRSM sequestered more C than the southern part of GRSM (Figure C3.7c). The low altitude and the mountain-top forests may store C, while some of the mid-altitude forests, especially those in the southwestern and southeastern regions, may lose small amounts of C in comparison with the magnitude of C sequestration during the simulation period. Our analysis shows that from 1971 to 2001, the average annual precipitation increase rate in the southeastern

and northeastern GRSM could be about 20% lower than the rate of increase for precipitation of the whole park. As the result, in these regions, C sequestration due to CO₂ fertilization and climate change could not compensate for the C loss due to increased O₃ exposures in the mid-latitudes (Figure C3.5).

According to our estimation, the average TOTC of GRSM could be as high as 30 kg C m⁻² in 2001, much higher than the regional average C density (McNulty et al., 1994). The average VEGC density was approximately 15.9 kg C m⁻². Whittaker (1966) reported that in GRSM “Cove forest biomasses are larger than any reported for either temperate or tropical forests”. The VEGC stored in undisturbed cove forests growing in GRSM valleys ranges from 25 to 30 kg C m⁻². The average VEGC and TOTC of North Carolina and Tennessee forests in 1997, as reported by Birdsey and Lewis (2003), were only 7.3 kg C m⁻² and 15.8 kg C m⁻², respectively, only half of the C density in GRSM. The total C pool size of the US is 37 210 T g, whereas the Southeastern US stores 5 280 T g, about 5269 g C m⁻², including both forested and non-forested land (Potter et al., 2006). Therefore, the C density of GRSM could be about 6 times that of the regional average value (McNulty et al., 1994; Potter et al., 2006). With such high C density, any climate change or atmospheric change could lead to significant amounts of C flux from GRSM. The analyses of impacts of climate change, CO₂ fertilization, and O₃ stress on C fluxes are, therefore, important for evaluating GRSM C dynamics in the past, its current C pool size, and its C sequestration capacity in the future.

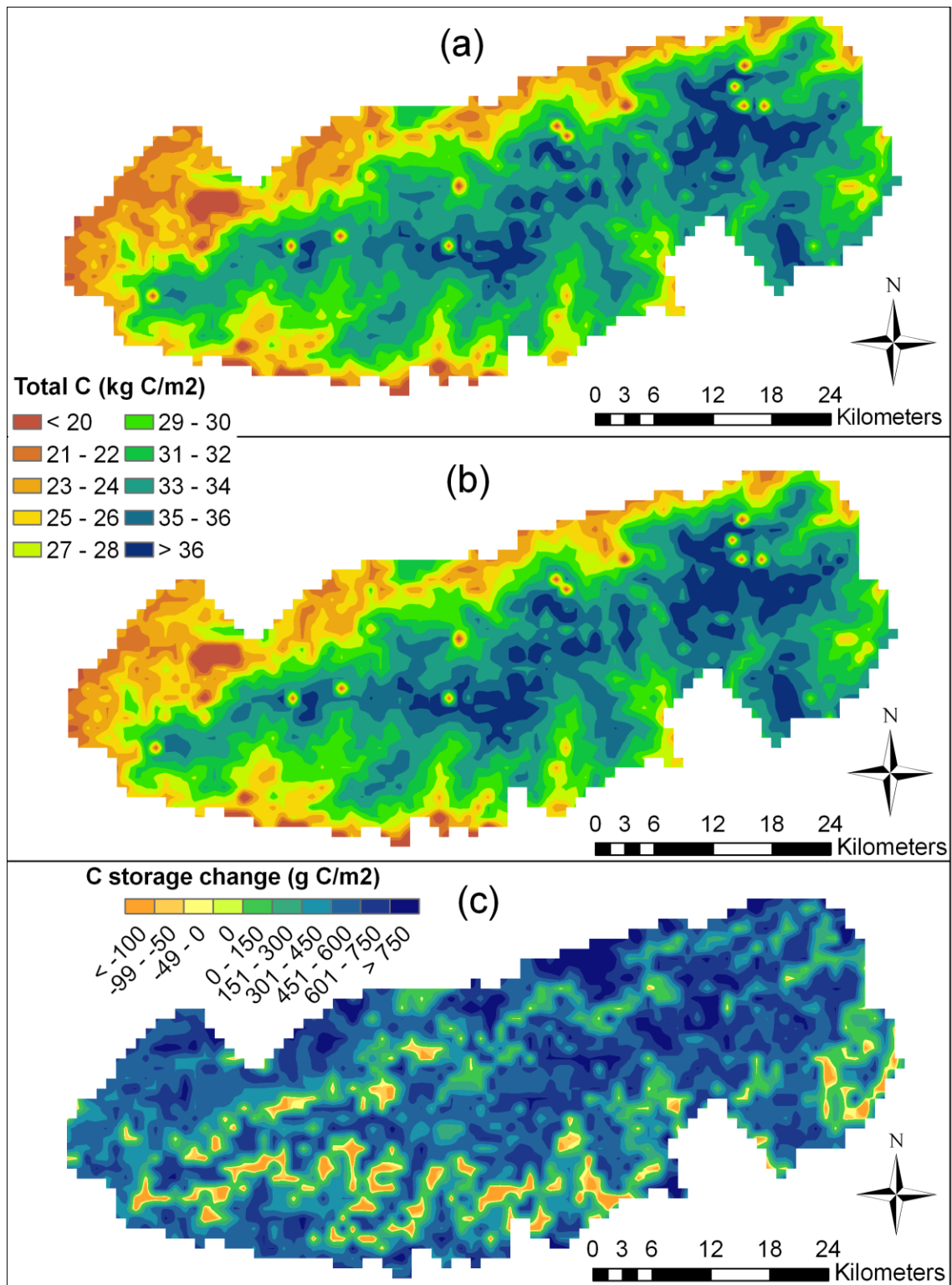


Figure C3.7 The spatial pattern of the GRSM C pool (a) C storage in 1971 (b) C storage in 2001 (c) C storage changes from 1971 to 2001.

3.3. Carbon fluxes

According to our simulation, the average annual net primary productivity (NPP) of GRSM was about 738 g C m^{-2} , close to the average of $700 - 840 \text{ g C m}^{-2}$, by assuming that the below-ground NPP to aboveground NPP ratio equals to 0.4 (Nadelhoffer et al., 1985); and C:dry biomass ratio equals 0.5 for well-stocked, mesic southern Appalachian forests reported by Whittaker (1966). The average annual NPP of spruce-fir and pine forests were about 642 g C m^{-2} and 715 g C m^{-2} , respectively. These estimations fall in the range of $514 - 980 \text{ g C m}^{-2}$ NPP for coniferous forests reported by Whittaker (1966). The average annual NPP of deciduous forests was about 748 g C m^{-2} , close to the average NPP (714 g C m^{-2}) of nine eastern deciduous forests reported by Whittaker (1974), and was within the range of GRSM deciduous forest NPP ($581 - 854 \text{ g C m}^{-2}$) reported by Busing et al. (1993).

Our simulation results indicate that the pattern of interannual variation of NPP in the CLMCO2O3 scenario was probably driven by climate variation (Figure C3.8a). The average annual NPP of the CLM, CO₂, and O₃ scenarios (Table C3.1; see Section 2.4) are 699 g C m^{-2} , 756 g C m^{-2} , and 675 g C m^{-2} , respectively. Their combined effect was 4% higher than their average value. There is evidence that elevated CO₂ concentrations cause partial stomatal closure, especially in C₃ plants, that survive solely on C₃ carbon fixation (Mott, 1988; Allen, 1990) and thus possibly reduce the stomatal uptake of O₃ (Paoletti and Grulke, 2005), although this mechanism may not work for all GRSM plant species, especially if injured by O₃ (Grulke et al., 2007).

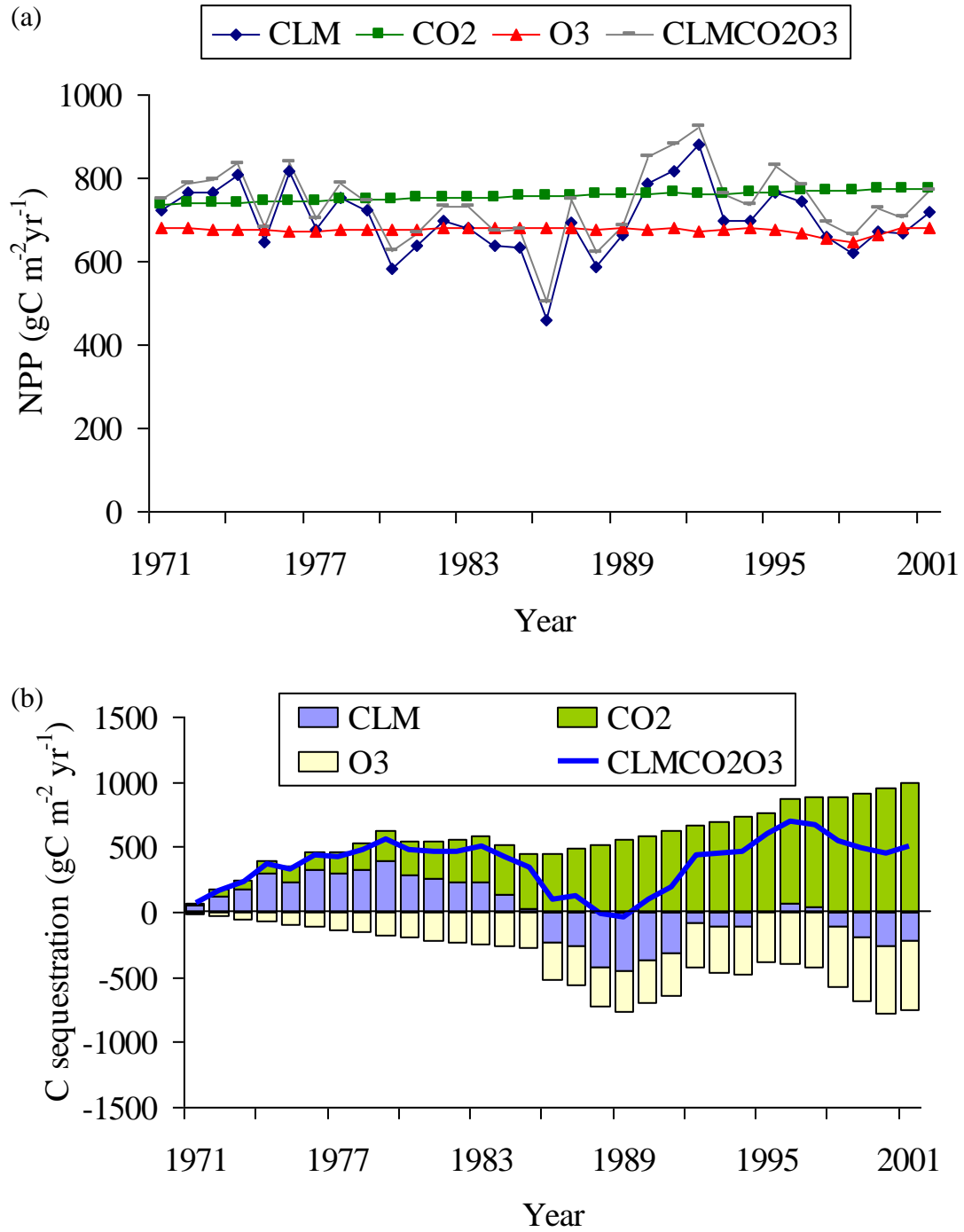


Figure C3.8 Transient responses of net primary productivity (NPP) and carbon storage to multiple environmental stresses. Scenarios under comparison: CLM = climate only; O₃ = O₃ only; CO₂ = CO₂ only, CLMCO₂O₃ = combination effects of climate, O₃, and CO₂. (a) Effect of climate; CO₂-fertilization, and O₃ damage on NPP; (b) Cumulative carbon storage from each of the factors in (a).

Cumulative carbon sequestration from climate change and atmospheric change is shown in Figure C3.8b. Unlike NPP, the temporal pattern of net C sequestration from 1971 to 2001 not only followed the fluctuations of climate change, but was also controlled by the cumulative effect of CO₂ fertilization, which constantly increased during the study period. Since the mid 1980s, the positive CO₂ fertilization effect on C sequestration might have dominated the O₃ stress and the negative effect of climate change, even though the C storage of the GRSM forest ecosystem decreased slightly in 1988 due to negative climate stress (Figure C3.8b).

3.4 Comparison of the simulation results with other studies

3.4.1. O₃ effect

Our results (Table C3.2) show that ambient O₃ stress could reduce GRSM vegetation biomass by approximately 2.5% (CLMCO2CO3 – CLMCO2). In a long-term field study with loblolly pine (*P. taeda*) in North Carolina, Shafer and Heagle (1989) found that the near-ambient O₃ concentrations (0.05 µl l⁻¹, seasonal 12-h mean) reduced the forest biomass by about 2-19%. Our results show that from 1971 to 2001, O₃ stress (CLMCO2O3 – CLMCO2) could reduce NPP by 3.1%. Based on a 6-year uncontrolled field study of mature loblolly pine growing in eastern Tennessee, McLaughlin and Downing (1995; 1996) reported that the forest productivity could be reduced by 0-15% (averaged 5%) due to the ambient O₃ stress. Teskey (1995) reviewed the literature for

southern coniferous forests, and concluded that the ambient O₃ could reduce forest productivity by 2-5%. Chappelka and Samuelson (1998) reviewed the ambient O₃ effects on forest trees of the eastern United States and suggested that the O₃ may reduce the growth of mature trees by about 2-9%.

Most of the field studies conducted were only short-term in nature. The majority of these studies focused on vegetation growth, but did not include the measurement of the soil C pool which is important for the estimation of the ecosystem carbon sequestration rate (or net carbon exchange, NCE). To validate our simulation, we also compared our results to other large-scale, long-term regional simulation studies conducted in the US. Ollinger et al. (1997) simulated the effects of O₃ using 64 O₃ monitoring sites across the northeastern US for the period 1987-1992, and found an annual NPP reduction of 3-16%. The results of a 300-year (1700-2000) simulation study in the same region (Ollinger et al., 2002) further suggested that the O₃ stress could have reduced NCE by about 46.7%. Felzer et al. (2004) used a monthly time-step terrestrial ecosystem model to estimate the effects of O₃ on NPP and NCE across the conterminous US, and estimated a mean 2.6-6.8% reduction for the annual NPP in response to historical O₃ levels during the late 1980s-early 1990s. Their results also suggested that O₃ exposure could have decreased US carbon sequestration by 49.3% (but did not consider agricultural management). These results agree with our estimation of a 3.1% reduction of NPP and 50% decline of carbon sequestration (see Section 3.2) due to O₃ stress in GRSM.

3.4.2. CO₂ fertilization effect

Our results suggest that during the 1971-2001 time period CO₂ fertilization (CLMCO2O3 – CLMO3) may have enhanced GRSM ecosystem productivity by about 8%. A comparison of the Free Air Enrichment Sites (FACE site) from their inception (Norby et al., 2005) showed a median increase of 23% in NPP across sites exposed to elevated CO₂ (550 ppm) in comparison with control sites (370 ppm). By assuming a linear interpolation of these FACE site results, Boisvenue and Running (2006) estimated that the CO₂ fertilization effect since 1950s could have increased global forest productivity by about 4%. Considering the acclimation of plants to rising CO₂ (Moore et al., 1999; El Maayar et al., 2006; de Graaff et al., 2006), however, the CO₂ fertilization effect in a lower concentration (e.g. the ambient atmospheric CO₂ concentration during the past 50 years) could be stronger than the effect observed in enrichment experiments (550 ppm). Therefore, we expect the actual enhancement on NPP due to rising CO₂ concentrations since 1950s could be higher than 4%, and be close to our estimation. Similarly, in a modeling study across the conterminous US, Felzer et al. (2004) estimated that the CO₂ fertilization effect could have resulted in a 6% increase in NPP from 1989 to 1993.

4. Conclusions

The carbon density of GRSM could be as high as 15.9 kg m⁻² in 2001, twice the regional (NC and TN) average C density. Although these forests are protected from land-conversion and catastrophic fire disturbances, the C storages in these forests are still

affected by climatic and atmospheric changes such as CO₂ fertilization and tropospheric O₃ pollution. The climatic and atmospheric environments of mountainous ecosystems also vary by elevation. The precipitation and O₃ concentrations of GRSM, for example, increase with elevation. The total C density may increase with altitude as a result of climate control along the altitudinal gradient (*i.e.*, high precipitation, which enhances forest growth and low temperatures, which inhibit respiration and decomposition). We estimated that O₃ has reduced C sequestration by about 0.9 T g C in GRSM, while the CO₂ fertilization effects contributed to a sequestration of about 2.3 T g C in GRSM from 1971 to 2001. The combined effects of climatic and atmospheric change during this 30-year period could have resulted in about a 0.9 T g C increase in the GRSM C pool. The average annual net primary productivity of GRSM was about 738 g C m⁻². The interactions among climatic and atmospheric factors enhanced the positive effects of CO₂ fertilization on GRSM C sequestration using modeled responses of stomatal conductance to elevated CO₂. Our simulation shows that the temporal pattern of NPP was controlled by the climate factors (temperature and moisture); while the temporal pattern of net C sequestration not only followed the fluctuations of climate change, but also was controlled by the cumulative effect of CO₂ fertilization, which was constantly rising during the study period. In the long run, the positive CO₂ fertilization effect on C sequestration dominated the O₃ stress and the negative effect of climate stresses.

CHAPTER 4

CASE STUDY II –

Effects of Forest Regrowth and Urbanization on Ecosystem Carbon Storage in a Rural-Urban Gradient in the Southeastern United States

Abstract

Forest regrowth after cropland abandonment and urban sprawl are two counteracting processes that have influenced carbon (C) sequestration in the southeastern United States in recent decades. In this study, we examined patterns of land use/land cover change and their effect on ecosystem C storage in three west Georgia counties (Muscookee, Harris, and Meriwether) that form a rural-urban gradient. Using time series Landsat imagery data including 1974, 1983 and 1991 and 2002, we estimate that from 1974 to 2002, urban land use for the area has increased more than 3.8 times (*i.e.* 184 km²). Most (63%) of new urban land uses were converted from forestland. Conversely, cropland and pasture area has decreased by over 59% (*i.e.* 380 km²), with most cropland area converted to forest. As a result, the net change in forest area was small over the past 29 years. Based on Landsat imagery and agricultural census records, moreover, we reconstructed an annual gridded data set of land-cover change for the three counties from 1850 to 2002. These data sets were then used as input to the Terrestrial Ecosystem Model (TEM) to simulate land use effects on C fluxes and storage for the study area. Simulated

results suggest that C uptake by forest regrowth ($\sim 23.0 \text{ g C/m}^2/\text{yr}$) was slightly larger than C released through the deforestation ($\sim 18.4 \text{ g C/m}^2/\text{yr}$) thus, making the three west Georgia counties a weak C sink. However, the relative importance of different deforestation processes in this area changed significantly through time. While agricultural deforestation was generally the most important C release process, the magnitude of C release induced by urbanization has increased over time. Since 1990, urbanization has accounted for 29% of total C loss from the study area. This study implies that balancing urban development and forest protection is critically important for carbon management and policy-making in the southeastern United States.

Keywords: Carbon storage, ecosystem model, deforestation, land use

1. Introduction

The terrestrial carbon (C) budget in North America and the underlying mechanisms remain uncertain (Fan et al., 1998; Bousquet et al., 2000; Wofsy and Harris, 2002). Increasing forestland area and rates of production have been proposed as important mechanisms for transferring C between land and the atmosphere (Houghton et al., 1999; Pacala et al., 2001; Goodale et al., 2002). While forest regrowth on abandoned agricultural land enhances carbon sequestration, deforestation and urban development lead to terrestrial C release to the atmosphere. However, the estimation of carbon source and sink induced by land-use change are still far from certain (Houghton 1999; Imhoff et al., 2000; Milesi et al., 2003; Tian et al., 2003). To better quantify the roles of

deforestation and forest regrowth on the regional carbon budget, it is essential to study landscapes where disturbance processes are rapid and pervasive (Turner et al., 1995). The purpose of this study is to characterize landscape changes along a rural-urban gradient in the southeastern United States, and to attribute effects of different land uses on C fluxes and storage in the terrestrial ecosystems of this area in the past three decades.

Since the middle of the last century, the Southeastern United States has undergone a long-term transition from agricultural land use to secondary mixed forests (Hart, 1980; Wear, 2002). Due to young stand ages, Turner et al. (1995) concluded that the Southeast and South-central regions of the US possessed the strongest biological C sinks. However, C emissions due to anthropogenic disturbances such as urbanization may essentially offset this sink. Recent analyses have indicated that trends in land development in the United States vary significantly by region (Alig et al., 2004) with the Southeast being characterized by rapid population growth and increasing urban land use. This is particularly evident in the Georgia Piedmont, where urbanization rate ranks among the highest in the Southeast region during the 1990s. A recent US Forest Service resource assessment (Wear, 2002) indicated that urbanization represents a primary threat to the Southeast forestland for the next 20 years. Furthermore, in this region, conversion of forestland into urban land uses is counterbalanced by a conversion of cropland into forests. Thus, extensive forest regrowth on abandoned agricultural land is thought to turn the Southeast into a carbon sink. However, increased rates of urban development in the region threaten forestland and can potentially reduce ecosystem productivity (Imhoff et al., 2000; Milesi et al., 2002), which could cause the Southeast to act as a carbon source.

Our challenge now is to accurately quantify the relative roles of forest regrowth and urbanization on net carbon balance in this area.

Our approach was to use a spatially-explicit process-based ecosystem model in conjunction with remotely sensed and agricultural census data to estimate annual sources and sinks of carbon across heterogeneous landscapes along an urbanization gradient. We selected three counties in the West Georgia Piedmont (Muscogee, Harris, and Meriwether), which formed an urban-rural land use gradient. We developed an annual gridded data set of land-use change for the three counties for the time period from 1850 to 2002 by using Landsat imagery data (1974, 1983, 1991, and 2002) and agricultural census record. This data set was then used as input for the Terrestrial Ecosystem Model (TEM) to simulate land use effects on C fluxes and storage for the area (McGuire et al., 2001; Tian et al., 2003). This study of the west Georgia area served as a pilot project for the extrapolation of our analyses into the entire Southeastern US.

2. Method and data

2.1. Study area

The study gradient ($85^{\circ}12'W/32^{\circ}22'N \sim 84^{\circ}29'W/33^{\circ}14'N$) was located to the northeast of Columbus, the third largest city in Georgia (Figure C4.1). These three lower Piedmont counties have undergone significant forest regrowth since the middle of the last century (Hart, 1980) as well as rapid population growth and related land development during the

1990s (U.S. Population by Region, 1990-2002, <http://www.census.gov/>). Development around Columbus is constrained by Fort Benning, a large military installation on the southeastern portion of Columbus and the Chattahoochee River to the west. Therefore, all expansion occurs in the remaining northeastern direction. The influence of Columbus on the surrounding landscape can be understood in terms of population statistics over the past decade for the 3 contiguous counties. Among the three west Georgia (West GA) counties, Muscogee County, within the Columbus city limits, had the highest population growth of 41 people per km² during the study period (1974 to 2002). Conversely, Meriwether County, furthest from the city, had the lowest population growth of 2 people per km², while Harris County, lying in between Muscogee and Meriwether counties, had a moderate population growth of 9 people per km² (<http://www.census.gov/>). Thus, these three counties form an urbanization gradient that can be used to study the effects of land-use change on the ecosystem C balance.

2.2 The model and simulation experiments

We used the Terrestrial Ecosystem Model (Tian et al., 1998, 1999, 2003; McGuire et al., 2001; Felzer et al., 2004) to simulate changes in C storage during three stages of disturbance: (1) conversion from natural vegetation to cultivation (cropland conversion), (2) production and harvest on cultivated land, and (3) abandonment of cultivated land (cropland abandonment). For a detailed discussion regarding the structure of the TEM model, please refer to Tian et al. (2003).

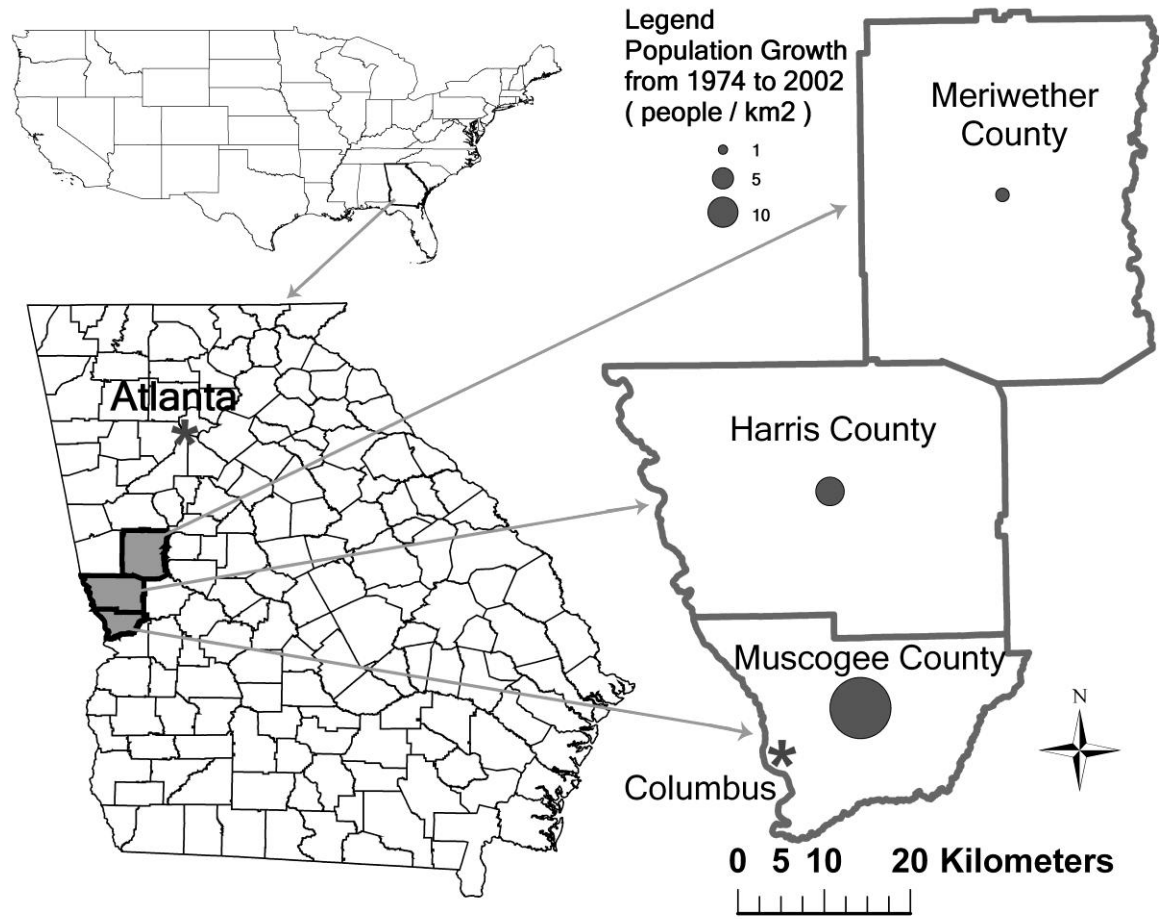


Figure C4.1 Location and population growth of the west Georgia (West GA) research site. Dot size in the West GA county maps (right) shows the population growth (number of people/km²) from 1974 to 2002 (US Census Bureau, <http://www.census.gov/>). From 1974 to 2002, population density of Muscogee County increased 41 people per km²; Population density of Harris County increased 9 people per km²; Population density of Meriwether County increased 2 people per km². The three counties, from the southwest to the northeast, form an urban-rural gradient.

Annual net carbon exchange (NCE) between the terrestrial biosphere and the atmosphere can be described by the equation:

$$\text{NCE} = \text{NPP} - \text{R}_H - \text{E}_{\text{NAD}} - \text{E}_{\text{AD}} - \text{E}_P \quad (1)$$

For this equation, NPP is net primary production, R_H is heterotrophic respiration, E_{NAD} represents emissions associated with non-anthropogenic disturbance, E_{AD} represents emissions from anthropogenic disturbances, and E_P represents the decomposition of products harvested from ecosystems for human use. We do not currently have the capability to simulate the C dynamics associated with E_{NAD} in this region, therefore, for this study, we estimate NCE by modifying Eq. (1) to:

$$\text{NCE} = \text{NPP} - \text{R}_H - \text{E}_{\text{AD}} - \text{E}_P \quad (2)$$

For regional extrapolations with TEM, we use spatially explicit data sets for vegetation, elevation, soil texture, mean monthly temperature, monthly precipitation, and mean monthly cloudiness (see *Section 2.4*). The input data sets were gridded at a resolution of 1 kilometer. In addition to the input data sets, TEM also requires soil- and vegetation-specific parameters assigned to a grid cell. Although many of the parameters in the model are defined from published information, some of the vegetation-specific parameters are determined by calibrating the model to the fluxes and pool sizes of intensively studied field sites. The data used to calibrate the model for different vegetation types are

documented in previous studies (Tian et al., 1999). To apply TEM to a transient scenario, it is first necessary to run the model to equilibrium with long-term baseline climatic data for the initial year of the simulation. Detailed documentation on the development, parameterization, and calibration of this dynamic version of TEM has also been previously published (Tian et al., 1999, 2003).

To focus on the effect of land-use changes, we used a constant climatic dataset – the average climate for the period from 1974 to 2002 and only allowed land cover to change over time in the simulation. We first ran the model to equilibrium with a natural vegetation map, which was derived from a contemporary land cover map with a substitution of cultivated and urban land by the potential vegetation types in the area. For the land use transient run, annual historical land use data between 1850 and 2002 were used as inputs. In this paper, however, our analysis was focused on three most recent decades (1974 to 2002), a period covered by Landsat imagery data. It is important to note, however, the following assumptions were made for urban land uses: (1) the intensive urban and transportation land type in the land cover maps (see following section) are impervious surfaces (Arnold and Gibbons 1996), and (2) the impervious surfaces has zero NPP and zero vegetation cover.

2.3. Development of gridded annual land-cover data sets

2.3.1. Land-cover classification based on Landsat imagery

Landsat images were collected for four years (1974, 1983, 1991, and 2002). We used a post-classification-comparison approach to derive land cover information from four

Landsat images for the area. To improve the consistency of the classification results, all the images were geo-registered to a 2003 orthophoto of the region (Lockaby et al., 2005). Then, water bodies were identified using supervised classification method (Jensen, 1996). Next, the water patches were masked out, and the rest of the pixels were classified using ISODATA unsupervised classification methods. A total of fifty clusters were generated in the unsupervised classification. These clusters were assigned into three land-cover types: urban/transportation impervious surface, crop/pasture, and forest. The ancillary datasets that we used included 1:24,000-scale USGS Digital Elevation Model (DEM) data (<http://ned.usgs.gov/>), USGS Land Use and Land Cover (LULC) datasets and USGS National Land Cover Dataset 1992 (NLCD92) dataset (<http://edc.usgs.gov/products/landcover.html>), local transportation and hydrologic maps (<https://gis1.state.ga.us>). Classification accuracies were assessed using aerial photos of the study region. Accuracy of the 2002 land-cover map was assessed using a 2003 aerial orthophoto (Lockaby et al., 2005), while accuracy of the 1991 land-cover map was assessed using 1993 Digital Ortho Quarter Quads (DOQQs) (<http://www.usgs.gov/>; <https://gis1.state.ga.us/>). Finally, accuracy of the 1983 and 1974 land-cover maps were assessed using 17 USGS high resolution scanned aerial photos (<http://edc.usgs.gov/products/aerial/hiresscan.html>), which were orthorectified using 1:25,000 USGS DEM dataset (<http://ned.usgs.gov/>) and 1993 DOQQs orthophoto (<http://www.usgs.gov/>). Two hundred points were randomly selected on the reference aerial photos for accuracy assessment of each land-cover map.

Table C4.1 Error matrix of the land-use classification

	Land-use types	Reference Data*				total	Users Accuracy
		Water	Urban	Forest	Cropland & pasture		
1974 Classified Data Background	Water	19		3		22	86%
	Urban		7	2	1	10	70%
	Forest			105	14	119	88%
	Cropland & pasture		1	10	38	49	78%
	Total	19	8	120	53	200	
Producers Accuracy						Overall accuracy = 84%	
1983 Classified Data Background	Water	25				25	100%
	Urban		24	1	3	28	86%
	Forest		3	111	7	121	92%
	Cropland & pasture		1	4	21	26	81%
	Total	25	28	116	31	200	
Producers Accuracy						Overall accuracy = 90%	
1991 Classified Data Background	Water	14				14	100%
	Urban		20	2		22	91%
	Forest		1	127	6	134	95%
	Cropland & pasture		2	8	20	30	67%
	Total	14	23	137	26	200	
Producers Accuracy						Overall accuracy = 90%	
2002 Classified Data Background	Water	16		2		18	89%
	Urban		28	3	1	32	88%
	Forest		2	105	11	118	89%
	Cropland & pasture		2	2	28	32	88%
	Total	16	32	112	40	200	
Producers Accuracy						Overall accuracy = 88%	

* Sources of reference data for 2002: 2003 aerial photos of West GA region (Lockaby et al., 2005); Sources of reference data for 1991: 1993 DOQQs (<http://www.usgs.gov/>; <https://gis1.state.ga.us/>); Sources of reference data for 1983 and 1974: nine USGS high resolution scanned aerial photos in early 1980s and eight USGS high resolution scanned aerial photos in early 1970s (<http://edc.usgs.gov/products/aerial/hirescan.html>), which were orthorectified using 1:25,000 USGS DEM dataset (<http://ned.usgs.gov/>) and 1993 DOQQs orthophoto (<http://www.usgs.gov/>).

Table C4.1 shows the classification error matrixes and users/producers accuracies for the four land-cover maps (1974, 1983, 1991, and 2002) derived from Landsat images. The overall accuracies of the four land-cover maps range from 84% to 90%. Producer accuracy of forestland, the major land-cover type in the region, exceeded 90%. User accuracy of forestland exceeded 85%. In all the four land-cover maps, producer accuracy of the cropland/pasture was the lowest (68% ~ 77%), mainly due to the misclassification of cropland/pasture land covers into forest type. This error of input associated with land-use dataset could result in overestimation of the soil C storage (Guo and Gifford 2002), the aboveground carbon storage, and NPP. These effects, however, are not significant because of the slow vegetation and soil C accumulation rate in newly abandoned croplands. For example, if a cropland pixel in 1974 Landsat image was misclassified into forest type, forest would begin to regrow in that location sometime between 1974 and 1982 in our simulation. If this pixel was correctly classified as cropland in the 1983 land-cover map (the chances of a pixel being misclassified in the consecutive two images were very low), its land cover type would be turned back into cropland in 1983. Therefore, this misclassification caused a pseudo-forest regrowth for about 1 to 8 years. In such a short time period, the NPP, the total vegetation C, and especially the soil C accumulation rate of a newly abandoned cropland could not increase much.

The user's accuracy of cropland and pasture types in 1991 is only 67%. Of those reference plots that were incorrectly classified into cropland and pasture type, 80% were forest plots, 20% were urban plots. The consequences of misclassification of urban land-use type into cropland and pasture type will not be significant, since both types are

disturbed ecosystems that have relatively low NPP and low vegetation carbon. The misclassification of forest into cropland will cause overestimation of agricultural deforestation area, which in turn will result in overestimation of the C release due to agricultural conversion by our model simulation. Table C4.1 shows that of the 62 sample plots that were classified as cropland and pasture in 1991 and 2002 land-use maps, 11 plots were actually forest type. Our analysis further shows that, of these 11 misclassified plots, 9 were forest clear-cuts or newly established forest plantations. In the Landsat images, clear-cut plantations or forest stands in seedling stage were difficult to distinguish from the pasture land-use type. According to FIA (USDA Forest Service Forest Inventory and Analysis), about 3% of the West GA forest was clear-cut or newly established forest (<http://www.fia.fs.fed.us>). As the results of this classification error, our simulation will misattribute considerable C released due to plantation rotation to negative NCE due to agricultural deforestation. These two kinds of disturbances, both of which involve clear-cut, have similar effects on the regional ecosystem C cycle. Therefore, this classification error is not likely to affect the estimation of total carbon balance in the study region.

Since the spatial resolutions of Landsat MSS (1974) and Landsat TM (1983, 1991, and 2002) differ, bias with regard to the estimates of land-use change over the study area is possible. To reduce the error of the spatial mismatch, therefore, we further aggregated the simulation resolution to 1 km.

2.3.2. Annual time series of land cover across the study area: 1974-2002

Land cover maps were used to create an annually gridded dataset from 1974 to 2002. There are a total of 3,110 grid pixels at a resolution of 1 km for in each land-use map. To generate this dataset, we first aggregated the 30-meter (80 meter for 1974) resolution land-use maps into 1 km resolution using majority rule (Jensen, 1996), and recorded the area fraction of each land cover type in each grid pixel. Second, for those years between two adjacent remote-sensing time periods, we constructed land cover maps by linear interpolation so that in each year a fixed number of grid pixels will change their land cover types. For a grid pixel, the higher the area fraction of the destination land cover type it has, the earlier its land cover change would take place.

2.3.3 Reconstruction of historical land-cover change of the study area: 1850-1973

We reconstructed 1 km resolution historical land-use maps for each year between 1850 and 1973 in two steps: First, we estimated the cropland, urban and forest area in each year based on historical census data (Waisanen and Bliss, 2002); Then, we generated land-use maps for each year based on the total area of each land-use type and the 1974 land-use map.

We estimated the historical urban area (before 1974) by assuming that urban area per capita remained constant from 1850s to 1970s. With this assumption, we first derived the per capita urban area based on the 1974 population census data and 1974 land-use map.

Then, we estimated the total urban area in each year from 1850 to 1973 by multiplying its population size with the per capita urban area constant. For those years that have no population census data available, a linear interpolation was done based on urban areas of the nearest two census years. The database developed by Waisanen and Bliss (2002) provides historical cropland area census data back to 1850. For those years that have no cropland census data available, we used linear interpolation based on cropland areas of the nearest two census years. We assumed that the area of water land-use type did not change from 1850 to 1973. Therefore, the forest area could be estimated by subtracting water area, cropland area and urban area from the total area of each county.

Land-use maps for each year from 1850 to 1973 were reconstructed based on the recorded area fractions of different land-use types in each grid pixel of the 1 km resolution 1974 land-use map (see *Section 2.3.2*). We assigned one of the three land-use types (forest, urban, and cropland/pasture) to each non-water grid pixel based on the area fraction of different land-use types in that grid pixel, so that the higher the area fraction of a land-use type in the grid pixel the higher the probability that kind of land-use type will be assigned to the grid pixel. For each land-use map, we controlled the total number of pixels that were assigned a certain land-use type, so that the total area of each land-use type will match the historical census data of that year.

2.4 Other data sets

In this study, climate, soil, elevation, and cloudiness are assumed to be stable annually. The elevation data represent a 1 km aggregation of the 7.5 minute USGS National Elevation Dataset (<http://edcnts12.cr.usgs.gov/ned/ned.html>). We also used a 1 km resolution digital general soil association map (STATSGO map) developed by the United States Department of Agriculture (USDA) Natural Resources Conservation Service to create a soil texture map of the study area. The texture information of each map unit was estimated using the USDA soil texture triangle (Miller and White, 1998). We used a 2002 six-category (coniferous forest, deciduous forest, mixture forest, cultivated land, intensive urban and transportation, and water) land cover map (the cultivated land and urban types are substituted by the potential vegetation type of this region) as the natural vegetation map of this region to generate baseline conditions in the equilibrium portion of the simulations. For the simulation, we used five major land cover classes – urban impervious surfaces, coniferous forest, deciduous forest, mixture forest, and cropland/pasture. Lakes, streams, and other aquatic ecosystems were excluded from the simulation. We put the grassland category into the cropland/pasture category for this simulation, because natural grassland areas were small in this region.

Climate data were obtained from the National Climatic Data Center (NCDC). Monthly precipitation and average air temperature records (1970-2000) of the 25 cooperative network stations in the three counties and the counties adjacent to the research region were used. For each month of the year, a temperature and precipitation raster layer at 1

km resolution was constructed using a Trend Surface Interpolation (TSI). Mean monthly cloudiness data for this study were derived from the Climatic Research Unit (CRU) TS 2.0 climate dataset (Mitchell et al., 2003). We then constructed the cloudiness map at 1 km resolution in the research area by linear interpolation.

3. Results and discussion

3.1 Land-cover changes during 1974 – 2002

Table C4.2 Land cover changes between 1974 and 2002

		Land cover 2002 (km ²)			total of 1974 (km ²)
		forest	Cropland & Pasture	Urban & Transportation	
Land cover 1974	forest	2203	95	116	2414
	Cropland & Pasture	407	169	68	644
	Urban & Transportation	0	0	48	48
total of 2002		2610	264	232	3106

Our results indicated that, from 1974 to 2002, abandoned cropland area in the three counties was 407 km², most of which was converted to forests (Table C4.2). At the same time, the conversion of forests to cropland and urban had taken over 95 km² and 116 km² of forestland, respectively. The net effect was a slight increase in forest area from 2414 km² in 1974 to 2610 km² in 2002. Cropland area was reduced more than 59%, while the urban land use more than doubled. Forestland (including urban forest and woodlands)

covered 78%, 81%, and 82% of the West GA counties in 1989, 1997, and 2000, respectively. These estimates were higher than the FIA data of 74%, 74%, and 75% of these three years (<http://fia.fs.fed.us/rpa.htm>). This difference may have occurred since forests identified by remote sensing in our investigation included all the forest and woodland (including urban forests) that can be identified on the 30 meter resolution images (80 meter for Landsat MSS), while the FIA project estimated forest area based on a more restricted definition of forest which requires a forest plot with at least 10% tree stocks and at least 1 acre in size (USDA Forest Service, 2005).

Total forest area changed little as a result of the balance between cropland abandonment and urbanization. This is in agreement with the reports of other studies in the Southeast US (Wear, 2002, Milesi et al., 2003). Most of the new development (63%) was due to the conversion of forests, similar to the reports by the USDA Natural Resources Conservation Service (www.nrcs.usda.gov).

Rapid land-use change in this region has impacts on the age of forest stands (Hart, 1980). Our data indicate that about 63% of the forests in 1989 are less than 40 years old. This value is a little lower than FIA's reports, which indicate 75% of forests in 1 to 40 age class (<http://ncrs2.fs.fed.us/4801/fiadb/>).

The major land-use change in Muscogee County was urbanization (red and black in Figure C4.2 (b)), while the major land-use change in Meriwether County was cropland abandonment (green in Figure C4.2 (b)) accompanied by considerable agricultural conversion (*i.e.* cropland/pasture converted from forest; blue in Figure C4.2 (b)). In

Harris County, a large area of cropland abandonment was evident in the Northwest portion of the county, while urbanization is evident in the Southeast. Because of the military installation to the south, Columbus expanded in a northerly direction.

In addition, the urbanization rate changed along the gradient. The urban area of Muscogee County which had the highest urban (or impervious surface) area ratio (6.9% of total county area in mid 1970s) increased 3.31 km² annually, while the urban area of Meriwether County (which had the lowest urban ratio at 0.06% of total county area in mid 1970s) only increased 0.93 km² each year. Harris County, located in the middle, gained 1.22 km² of urban land each year. Our analysis indicates that since 1990, urbanization became more evident for all three west Georgia counties (Figure C4.3). The impervious surface coverage (ISC) in West GA increased from 1.5% in 1974 to 7.5% in 2002. Our land-cover dataset, however, may overestimate the ISC in urban regions and slightly underestimate ISC in rural regions. We selected eight West GA watersheds and compared their ISCs in our 2002 land-use map to the results of another study based on high resolution color infrared (CIR) aerial photos (Lockaby et al., 2005) in 2003. Our estimation of 0.4% ISC for the most undeveloped watershed is lower than the estimation of 0.7% ISC by Lockaby et al., while our estimation of 49% ISC for the most developed watershed is higher than the estimation of 42% ISC by Lockaby et al. (2005). For the 6 watersheds whose ISC falls between 1.5% and 7.5%, our estimations of ISCs are 1.2%, 1.5%, 1.6%, 1.8%, 2.3%, and 3.5%, respectively, generally agree with the estimations (1.5%, 1.6%, 1.8%, 1.9%, 2.5%, and 2.6%, respectively) by Lockaby et al. (2005).

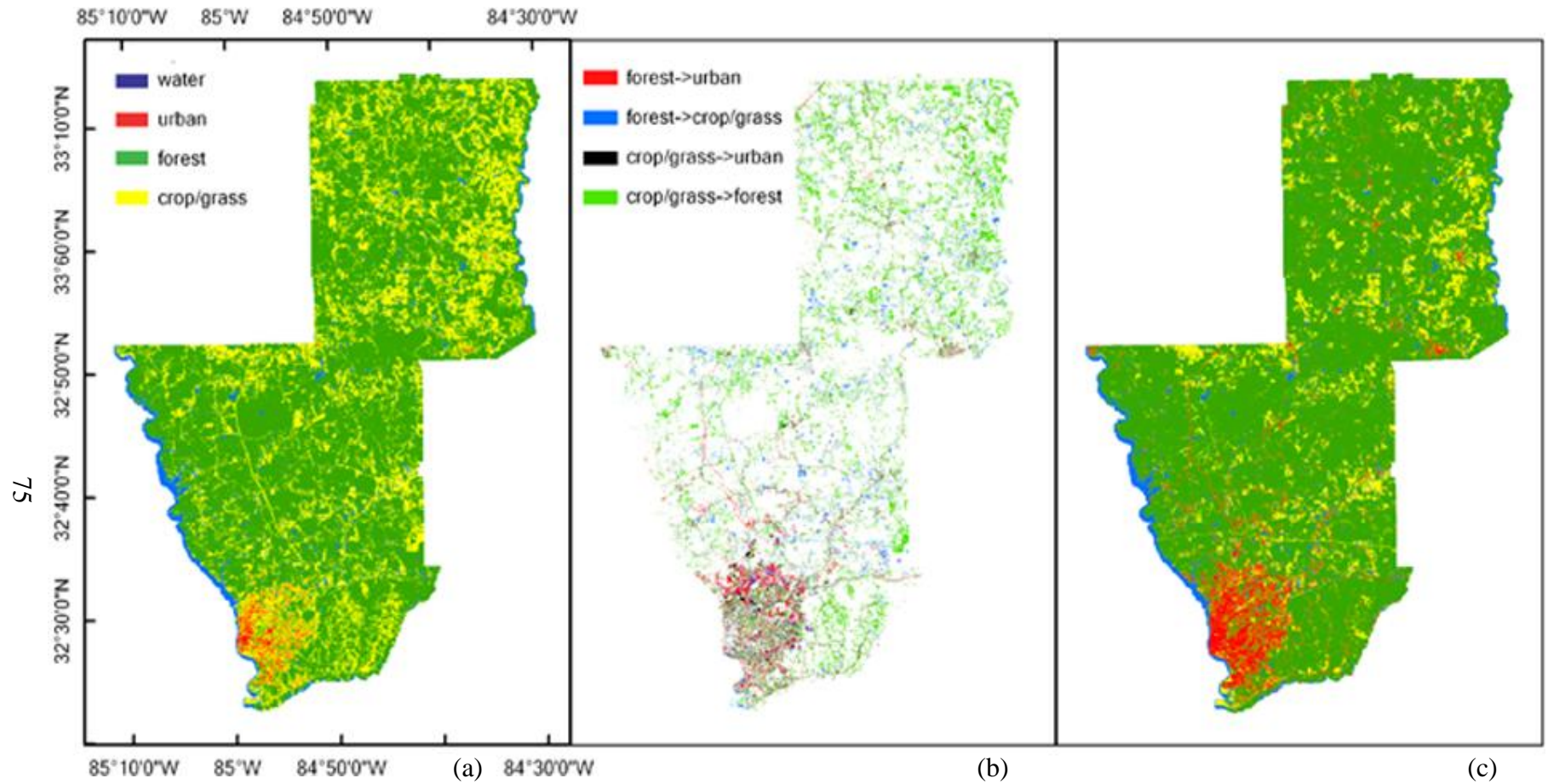


Figure C4.2 Land-cover change in the three counties of west Georgia from mid-1970s to early 2000s.
 (a) Land-cover map in 1974; (b) Land-cover change (LCC) from 1974 to 2002; (c) Land-cover map in 2002.

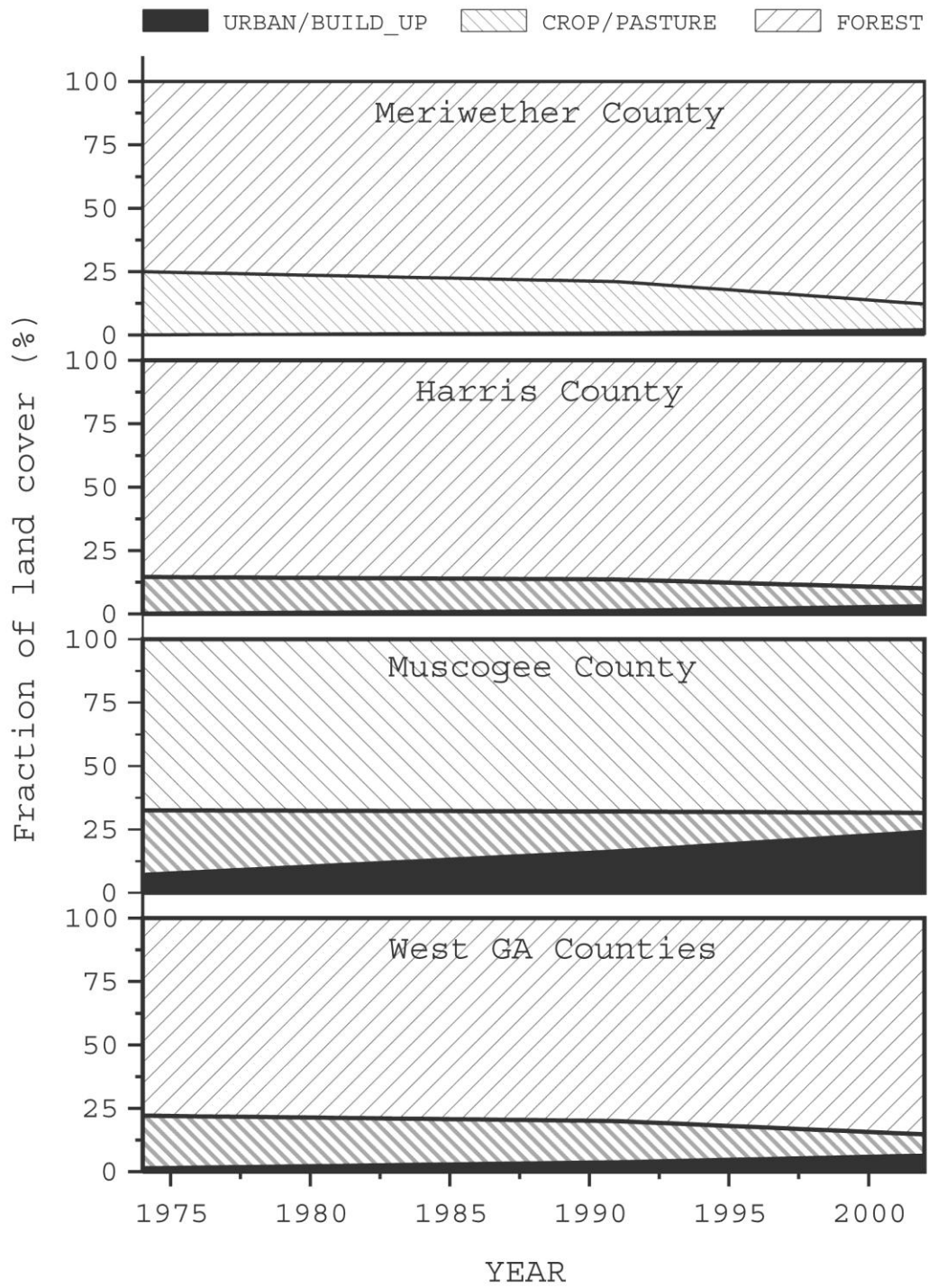


Figure C4.3 Land-cover change in the three counties of west Georgia during 29 years (1974-2002)

According to Wear (2002) the two major changes in land use that occurred in the southern US during the latter half of last century were urbanization (most converted from forest land) and reforestation on abandoned croplands. As a result of the balance between urbanization and reforestation, forest area in the region has been roughly constant. Our results showed that the pattern of land-use change at the West GA rural-urban interface matched well with the general patterns of land-use change observed in the Southeast US region as a whole.

In general, the land cover in this area has been changed significantly since the mid 1970s. Although total forest cover did not change much, the disturbed forest land over the 29 year time period is more than 27% of the total forest land. Clearly, the two counteracting land-use change processes (deforestation vs. forest regrowth on abandoned croplands) were important for the balance of carbon in the region.

3.2. Estimation of carbon storage and net primary productivity

Our simulation results indicate that, in 2002, total carbon storage in the West GA counties was 42 million ton (M t), including 27 M t stored in vegetation and 18 M t stored in soil. Vegetation carbon in the three counties of Meriwether, Harris, and Muscogee was 12 M t, 13 M t, and 2 M t respectively. Soil organic carbon in the three counties was 8 M t, 8 M t, and 2 M t respectively. The total ecosystem carbon density of the West GA region increased slightly from 13,409 g C/m² in 1974 to 13,539 g C/m² in 2002 (Table C4.3). The ecosystem storage of carbon in 1980 (13,543 g C/m²) and 2002

(13,539 g C/m²) was nearly equal. In other words, the total C storage did not change much during the study period. Changes in ecosystem C storage induced by land-use change varied spatially (Figure C4.4). Two C sink regions located in the northeast and southeast (Fort Benning) corners, reflecting areas that were less influenced by urbanization. The most intensive carbon loss was located at the periphery of urban areas at the urban/rural interface. Both Imhoff et al. (2000) and Milesi et al. (2003) observed that most of the newly developed land is located at the periphery of large urban areas. Our results also indicate that large C sources emerge at rural-urban interfaces.

Table C4.3 Carbon density in three West Georgia counties (1974 – 2002) (unit: g/m²)

YEAR	1974 (g/m ²)	1980 (g/m ²)	1990 (g/m ²)	2000 (g/m ²)	2002 (g/m ²)
Vegetation carbon density	7922	8051	8004	8117	8136
Soil carbon density	5487	5492	5518	5414	5403
Total ecosystem carbon density	13409	13543	13522	13531	13539

Model simulations show that during the 1990s, the coniferous forest C stocks averaged 6,755 g C/m². This estimate was higher than the eastern softwood average biomass of 5,500 g C/m² derived from FIA inventory data (Brown and Schroeder 1999; Brown et al., 1999). One possible explanation for our higher estimation is the inclusion of all vegetative biomass in our simulation while the estimation derived by Brown et al. (1999) included only trees greater than 2.54 cm at breast-height diameter. Our estimate of vegetation C in deciduous forests is 14,352 g C/m², falling in the range of the eastern hardwood carbon density (11,800 to 17,200 g C/m²) according to the FIA data (Brown et al., 1999). The average upper 1 meter of soil C density is about 6,500 g C/m² in the 1990s, an estimate comparable to Birdsey and Lewis's (2003) report of 7,140 g C/m² in Georgia

forest soils in 1997. The soil carbon density of deciduous forests in the area is 9,347 g C/m², which is close to Turner et al.'s (1995) estimate of 9,500 g C/m² in the Eastern US.

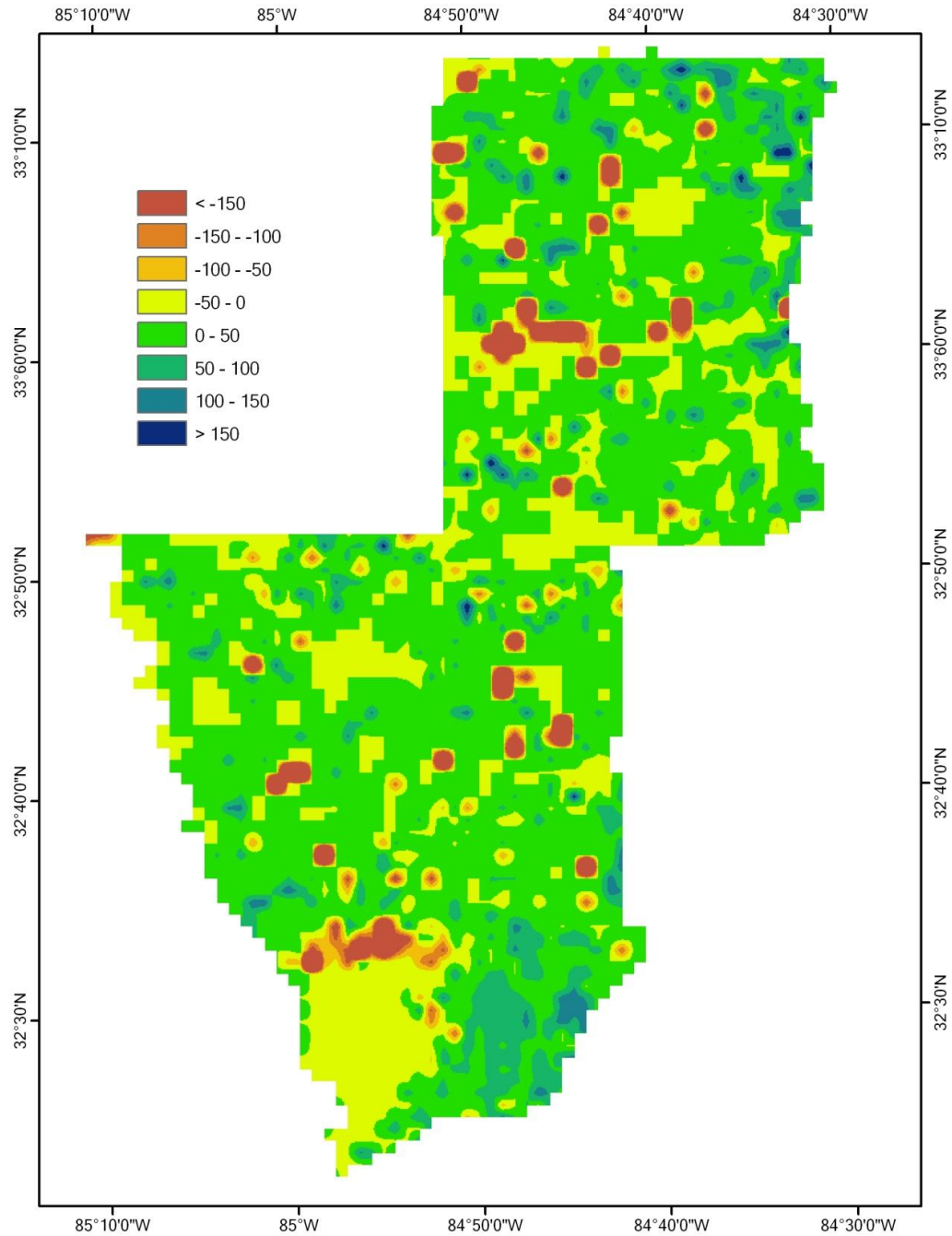


Figure C4.4 Net carbon exchange between the atmosphere and terrestrial ecosystems in the three west GA counties from 1974 to 2002 (unit: g C/m²/yr).

Our simulated average 1990s' net primary productivity (NPP) for coniferous forests was 494 g C/m²/yr. The predominant coniferous forest type in the research region was loblolly pine (*Pinus taeda L.*) (Thompson and Thompson 2002). Teskey et al. (1987) reported that above-ground NPP for loblolly pine forests ranged between 100 and 500 g C/m²/yr and averaged 300 g C/m²/yr. If below-ground production equals to 40% of above-ground NPP (Nadelhoffer et al., 1985; McNulty et al., 1994), the total NPP will be 420 g C/m²/yr. This value is very close to our estimate for total NPP (494 g C/m²/yr). Our simulated average 1990s' NPP of deciduous forest is 1,020 g C/m²/yr. This estimate was similar to the estimation of 1,081 g C/m² in Georgia (Melisi et al., 2003), and also falls in the range of 805 to 1,715 g C/m²/yr derived by Brown and Schroeder (1999).

3.3. Effects of land-use change on ecosystem carbon storage

Our simulation indicates that from 1974 to 2002 reforestation in West GA sequestered about 23.0 g C/m²/yr, which was offset by the 18.4 g C/m²/yr released by deforestation. The net carbon exchange was an uptake of about 4.6 g C/m²/yr by terrestrial ecosystems. Although the magnitude was similar, the spatial patterns of C fluxes induced by deforestation and reforestation were quite different. Figure C4.4 illustrates that C losses occurred in only a few locations in the study area. While concentrated areas resulted in large C losses, the spatial pattern of C gains was diffuse and its magnitude in each grid was relatively small. The negative NCE induced by deforestation was much more variable than the positive NCE due to forest regrowth (Figure C4.5). Our analysis showed that the release of C due to deforestation generally followed the patterns of annual

deforestation, while C sequestration due to reforestation did not match the patterns of annual reforestation (*i.e.* abandoned croplands). The differing patterns between deforestation NCE and reforestation NCE may have resulted from differences of scale for the two processes. While ecosystem C loss instantly responds to the deforestation events, the C sequestration due to forest regrowth is a relatively slow and stable process. Furthermore, newly reforested areas only compose a small portion of growing forests that are sequestering C. Therefore, reforestation, unlike deforestation, has a long lag effect. Figure C4.5 also indicates that the short-period fluctuation in total NCE was dominated by deforestation, while the long-term trend showed net accumulation of C resulted from reforestation. The combined effects of these two kinds of processes at different scales generated a complex NCE pattern.

Effects of different deforestation processes on regional C balance was further identified. During the study period agricultural deforestation was the major C release process. In the study area, agricultural deforestation released -15.6 g C/m^2 per year, 4.6 times more than the C released by urbanization. However, the relative importance of these two processes changed both along the rural-urban gradient and through time (Figure C4.5). In Meriwether County, which is furthest from Columbus, the agricultural deforestation dominated the negative NCE fluxes and the effect of urbanization was negligible. Conversely, in Muscogee County, which is within the Columbus city limits, the negative NCE generated by urbanization is 2% larger than that generated by agricultural deforestation. In Harris County, agricultural deforestation released 25 times more C each year than urbanization before 1998. In the last two years of the 1990s, C released from

agricultural deforestation declined to about $-2.7 \text{ g C/m}^2/\text{yr}$, but still was higher than the emission of urbanization ($-1.4 \text{ g C/m}^2/\text{yr}$). After 2000, the carbon emission due to agricultural deforestation was only 63% of the carbon released during urbanization.

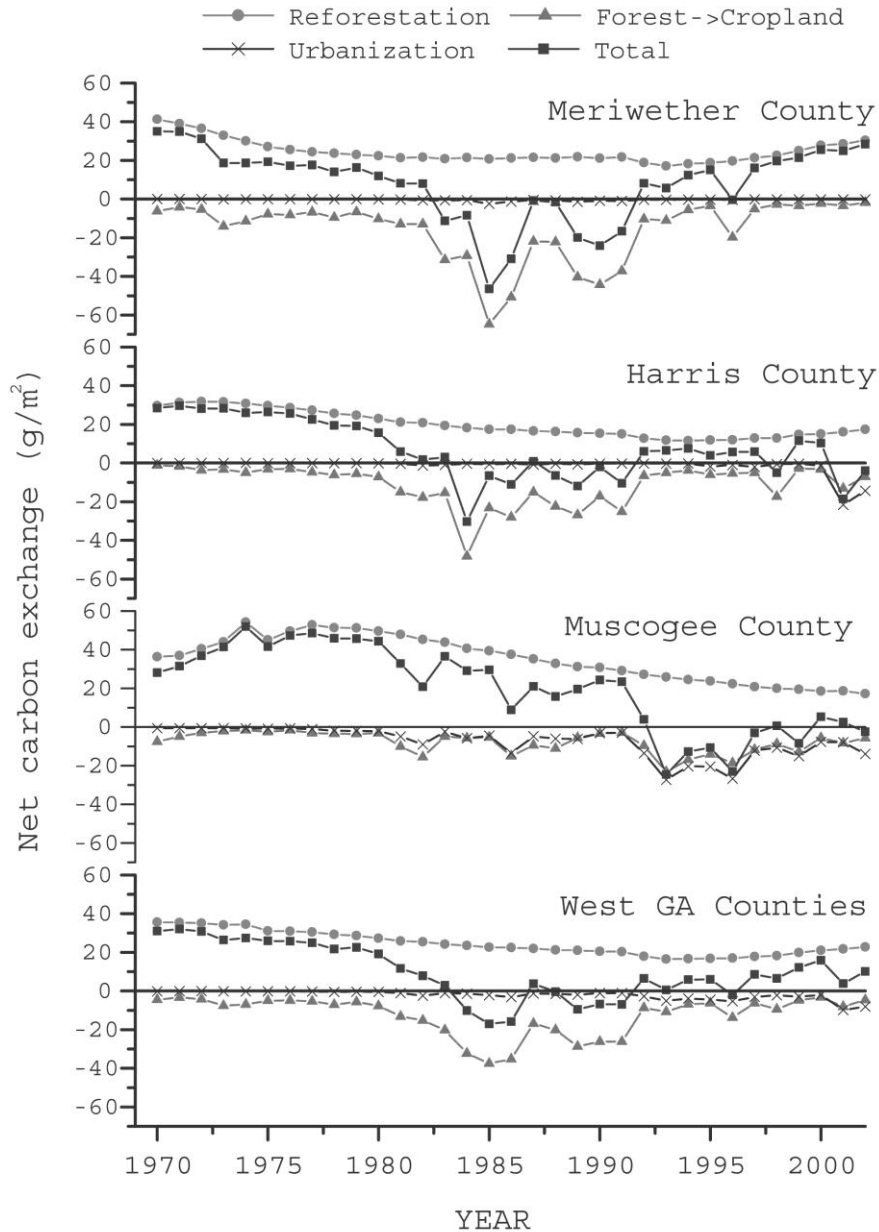


Figure C4.5 Contribution of different land conversion to net carbon exchange (g/m^2) between terrestrial ecosystems and the atmosphere in the study area as estimated by TEM.

Positive NCE means carbon sink, negative NCE means carbon source.

For the entire West Georgia research region, the importance of agricultural deforestation on ecosystem C balance also changed through time. In the 1980s, agricultural deforestation generated considerable negative NCE fluxes (about $-24 \text{ g C/m}^2/\text{yr}$), about 14 times the amount released by urbanization ($-1.7 \text{ g C/m}^2/\text{yr}$). This flux was larger than the $22 \text{ g C/m}^2/\text{yr}$ NCE sequestered by the forest regrowth, making the West GA area a net carbon source. In the 1990s, C released by urbanization increased to $-3.4 \text{ g C/m}^2/\text{yr}$, while the magnitude of negative NCE due to agricultural deforestation declined to about $-12 \text{ g C/m}^2/\text{yr}$, only 50% of the magnitude of 1980s. During this decade, following the declination of cropland area (Figure C4.2), the magnitude of C release due to agricultural deforestation has decreased by 50% (from $16 \text{ g C/m}^2/\text{yr}$ in the first half of 1990s to $8 \text{ g C/m}^2/\text{yr}$ in the late 1990s). However, agricultural deforestation still accounted for more than seventy percent of the total C released by deforestation in the 1990s, because the annual agricultural deforestation area accounted for 71% of the annual total deforestation area in the same period. As a result of the reduced deforestation and the steady forest regrowth, West GA became a net carbon sink of $3 \text{ g C/m}^2/\text{yr}$ in the 1990s. In the early 2000s, the negative NCE due to agricultural deforestation decreased to $-5 \text{ g C/m}^2/\text{yr}$, about 40% of the average NCE in 1990s, while the NCE of urbanization nearly tripled the amount in 1990s. As a result, urbanization released more C than agricultural deforestation. However, the total C released by deforestation was only 55% of the C sequestered by forest regrowth, and reforestation has dominated the West GA C balance since.

Much uncertainty associated with models and data still exists in estimating terrestrial carbon balance (Chen et al., 2006b). In this study, several valuable lessons were gained

regarding how to reduce uncertainty by improving our ability to simulate the effects of land-use change on ecosystem carbon dynamics within the Southeast US. First, our study in West GA shows that historical land-use change has strong legacy effects on ecosystem C cycles. Recognition of this effect is especially important for simulating long-term and large-scale processes such as regional forest regrowth. Therefore, reconstructing accurate historical land-use maps is very important for assessing responses of southeastern US ecosystems to land-use change. Any attempts to accurately assess the regional carbon budgets in the Southeast must await spatially-explicit reliable data sets such as land-use data for the entire region (McNulty et al., 1994; Wofsy and Harris, 2002). Secondly, the Southeast has undergone large-scale land-use change in the last several decades. Our results showed that the relative roles of major land-use change processes on carbon storage have changed over time. A similar pattern was predicted for the entire Southeast US region by other studies (Wear, 2002). Therefore, having the capacity to simulate urban ecosystem processes is important for a successful simulation of land-use related to C dynamics in this region. Finally, the important role of forest NPP on C balance of the West GA and the expanding forest plantations (Thompson and Thompson, 2002; Wear, 2002) suggest that to successfully assess the C fluxes in the Southeast, current biogeochemical models should be improved to better represent the structure and dynamics of the managed immature forests (Song and Woodcock, 2003).

CHAPTER 5
CASE STUDY III –
Impacts of urbanization on carbon balance in the Southern United States
from 1865 to 2002

Abstract

Urbanization could have important impacts on the carbon balance of the Southern United States (SUS) terrestrial ecosystems. We generated a spatially explicit historical land-use change dataset of this region based on high resolution land cover maps, historical urban coverage and population census records. We then applied the process based dynamic land ecosystem model (DLEM) over the entire region to investigate the impacts of urbanization on terrestrial ecosystem carbon balance from 1865 to 2002. Our simulation results indicate that about 505 T g C (1 T = 10^{12}) is stored in urban ecosystems of SUS. Most of this carbon is stored below-ground. Productivity and carbon storage of SUS urban ecosystem increased rapidly in the late half of the 20th century. The model predicted that from 1865 to 2002, urbanization resulted in a net carbon emission of about 204 T g C, 99% of which were released due to deforestation. The impact of urbanization on ecosystem carbon dynamics depended on the pre-urban land cover types. While significant carbon sources were created during urbanization from forests, many of the developed regions converted from shrublands and croplands became carbon sinks. The

model results further suggested that management could enhance the productivity of urban lawns by about 25% and significantly improve their carbon sequestration capacity. More field studies, especially regarding impervious surface in the urban land area, are necessary to provide parameters and calibration dataset to improve the accuracy of model assessment.

1. Introduction

Human alteration of the Earth is substantial and growing. Previous studies of impacts to the biosphere estimate that between one third and one half of the planet's land surface has been transformed by human actions (Vitousek et al., 1986). Recently, urbanization is recognized as an important human-induced disturbance as it "constitutes one of the more ecologically disturbing land transformation processes and urban areas are expanding rapidly as human populations grow in size, affluence, and technological capability" (Imhoff et al., 2000). The urbanization process is occurring at accelerated rates in the United States (US). From 1982 to 1997, for example, land devoted to urban uses grew by more than 34% (Alig et al., 2004). Developed areas currently occupy 5.2% of the conterminous US land; and it was projected to occupy 9.2% of US land in 2025 (Alig et al., 2004). A recent investigation indicated that the total area of this increase approaches the area of Ohio (Elvidge et al., 2004). The urban lawn area of conterminous US was estimated to be about 163,800 km², an area three times larger than that of any irrigated crop (Milesi et al., 2005). The population growth and urbanization rate was especially high in the Southern United States (SUS) where strong economic forces are reshaping the

landscape through urbanization (Hart, 1980). Wear (2002) suggested that urbanization represents a primary threat to the forestland of the South which is among the most productive forests of the United States.

Large amounts of carbon may be released from southern rural ecosystems due to land conversion (Houghton et al., 1999). Unlike the effect of other types of land management (e.g. silvicultural harvest or clear-cut during cropland conversion), trees that are removed due to urbanization are not normally developed into wood products for long-term carbon storage (Nowak and Crane, 2002). Removed wood is usually burned on site or mulched and then quickly decomposed. The relatively small vegetation cover in urban regions also indicates less carbon storage capacity and productivity of the urban ecosystem.

Furthermore, due to urban heat island (UHI) effect, the respiration rate of vegetation and the decomposition rate of urban soil organic matter pools may be also higher than rates in the rural ecosystem. All these factors suggest that urbanization could release significant quantities of carbon in the SUS, as indicated in an investigation of the urban-rural gradient in the west Georgia (Zhang et al., 2007).

Urban vegetation is, however, highly productive (Milesi et al., 2003). Urban trees have been reported as having higher carbon storage (9.25 kg C/m^2 cover) and gross sequestration (0.3 kg C/m^2 cover) on a per unit tree cover basis than average forest stands due to the more open canopy structure (Nowak and Crane, 2002). Furthermore, intensively managed urban lawns have high productivity, with potential to sequester 17 T g C ($1 \text{ T} = 10^{12}$) each year, a large portion of which is incorporated into soils, according

to a modeling study by Milesi et al. (2005). Urban soils as a result have the potential to sequester large amounts of soil organic carbon, especially in residential areas where management inputs and the lack of annual soil disturbance create conditions for net increases in carbon pool size (Pouyat et al., 2006).

The role of urbanization in carbon balance of the SUS was/is both important and complex, depending on several factors such as the pre-urbanization land types and their carbon density (Pouyat et al., 2006), the structure of urban ecosystem (fraction of urban impervious surface, remnant vegetation, and lawn), and the functions of urban vegetation which is controlled by many environmental factors (e.g. climate, concentration of atmospheric CO₂ and air pollutants, and soil properties). At present, most studies on urban ecosystems in the US either focus on a special component (Nowak and Crane 2002; Milesi et al., 2005; Pouyat et al., 2006) or on certain ecosystem functions, such as the net primary productivity (Imhoff et al., 2000; Milesi et al., 2003).

The majority of previous studies either ignored or highly simplified the impacts of land-use history on the current urban carbon balance. Urban carbon storage was estimated by multiplying the average carbon density of each urban land type with its total area. The carbon densities were usually based on few field measurements (e.g. Pouyat et al., 2006). This approach inevitably ignored the spatial and temporal heterogeneity inside each urban land types, which reflects the impacts of heterogeneous environmental factors and land-use histories. More process-based methodologies are required to capture the impacts of urbanization on regional ecosystem carbon dynamics in the long-term history.

In this study, we used a process based integrated dynamic land ecosystem model (DLEM) (Tian et al., 2005; Chen et al., 2006a; Ren et al., 2007; Zhang et al., 2007) to estimate the impacts of urbanization on the carbon balance of SUS from 1865 to 2002. Our overall goal is to estimate the total carbon storage of the SUS urban land area and further assess the different responses of these ecosystems to the urbanization processes.

2. Dataset and research methods

2.1. Study region and research approach

The study region included thirteen southern states (Wear, 2002): Alabama, Arkansas, Florida, Georgia, Kentucky, Louisiana, Mississippi, North Carolina, Oklahoma, South Carolina, Tennessee, Texas, and Virginia (Figure C5.1). According to the US Geological Survey (USGS) National Land Cover Database 2001 (NLCD 2001) (Homer et al., 2004), in 2000, the total urban/developed area of SUS was about 68,928 km². An integrated process-based dynamic land ecosystem model (DLEM) was used to assess the carbon storage and carbon dynamic in SUS in response to historical climate change, atmospheric change, and land-use change. The simulation time period covered the 142 years from 1865 to 2002. The spatial resolution of the simulation was 8 km.

We designed the following three experiments to investigate the impacts of urbanization and urban lawn management on the SUS carbon dynamics.

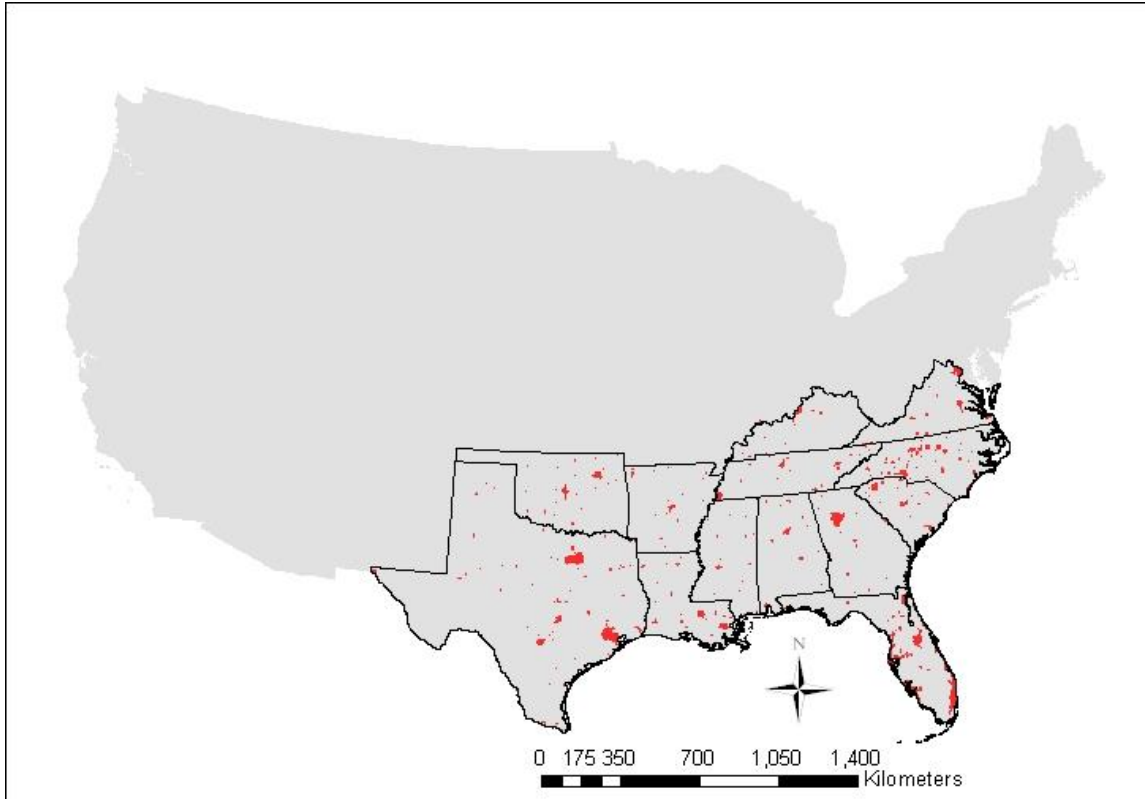


Figure C5.1 The boundary of SUS and the location of urban/developed regions (in red).

- I. ALLCOMBINE: the scenario that includes the effects of land-use change (cropland conversion, cropland abandonment, and urbanization), climate change, atmospheric change (tropospheric ozone stress, nitrogen deposition, and CO₂ fertilization effect). This scenario is used to estimate the actual carbon storage of SUS urban.

- II. URBAN: this scenario is used to estimate effects of urbanization on the ecosystem carbon dynamics. To exclude effects of other environmental factors, we only let the urban area change from year to year, all other factors were fixed to the value that were used to drive the equilibrium state (for climate

dataset these are climate normal; for the other dataset these are values of the first year, *i.e.* 1865).

III. UNMANAGED_LAWN: the design of this scenario was similar to

ALLCOMBINE except that all the urban lawn (*i.e.*, managed urban grasslands the majority of which are turf grasses) management processes (*i.e.*, N fertilization and irrigation) were turned off. We use this scenario to estimate the impacts of urban lawn management on the urban carbon dynamics.

2.2. Input datasets

Input datasets required by DLEM include transient climate, atmospheric CO₂ concentration, tropospheric ozone concentration, nitrogen deposition, nitrogen fertilization, land-use change datasets and 11 base maps (Table C5.1). All the input datasets for the SUS urban simulation were extracted from the Southern United States Database developed by the Environmental Science Research (ESRA) laboratory, School of Forestry and Wildlife Sciences, Auburn University (<http://www.sfws.auburn.edu/esra/>; also see Section 1 of Chapter 6). In the following sections approaches used to generate these environmental datasets of SUS will be discussed.

2.2.1. Base maps

(1) Elevation, slope, and aspect maps were derived from the 7.5 minute USGS National Elevation Dataset (<http://edcnts12.cr.usgs.gov/ned/ned.html>).

(2) Soil datasets (acidity, bulk density, depth to bedrock, soil texture represented as the percentage content of clay, sand, and silt) were derived from the 1 km resolution digital general soil association map (STATSGO map) developed by the United States Department of Agriculture (USDA) Natural Resources Conservation, while the texture information of each map unit was estimated using the USDA soil texture triangle (Miller and White, 1998).

(3) A potential vegetation map shows the distribution of four general plant functional groups of SUS. The concept of “potential vegetation” in this study actually refers to the natural vegetation type that had or can exist in a grid. It was derived from GLC2000 with a resolution of 1 km (Bartholomé et al., 2002). We reclassified the potential vegetation into four general plant functional groups and replaced the cropland and urban area in the GLC2000 with the potential vegetation types from Ramankutty and Foley (1998). Water bodies were excluded from the map. All of these input maps were aggregated into 8 km resolution.

2.2.2. Generating daily climate dataset

One important advantage of DLEM is that it requires relatively few input datasets. For example, a minimum climate dataset like precipitation, maximum temperature, mean temperature, and minimum temperature will be enough to drive the model. In this study we reconstructed an 8 km resolution daily climate dataset of the entire SUS from 1895 to 2005 by integrating the daily climate pattern of the North American Regional Reanalysis

(NARR) dataset (<http://wwwt.emc.ncep.noaa.gov/mmb/rreanl/>) into the monthly PRISM (Parameter-elevation Regressions on Independent Slopes Model) climate dataset (<http://prism.oregonstate.edu/>).

Table C5.1 The input dataset in the case study three

	Unit	Type	Temporal Resolution	Temporal Extend
Potential vegetation	4 categories [#]	Base map		
Soil clay content	%	Base map		
Soil sand content	%	Base map		
Soil silt content	%	Base map		
Soil depth	m	Base map		
Soil acidity	pH	Base map		
Soil bulk density	g/cm ³	Base map		
Elevation map	m	Base map		
Aspect map	Degree	Base map		
Slope map	Degree	Base map		
Irrigation map	1/0	Base map		
Precipitation	mm /year	Climate data	Daily	1865 ~ 2002
Maximum temperature	Celsius	Climate data	Daily	1865 ~ 2002
Minimum temperature	Celsius	Climate data	Daily	1865 ~ 2002
Average temperature	Celsius	Climate data	Daily	1865 ~ 2002
CO ₂	Ppmv	Atmospheric data	Annual	1865 ~ 2002
Ozone concentration, AOT40 [@]	ppb-hr	Atmospheric data	Daily	1865 ~ 2002
Nitrogen deposition ^{\$} (NH _x)	mgN/(m ² ·year)	Atmospheric data	Annual	1865 ~ 2002
Nitrogen deposition (NO _y)	mgN/(m ² ·year)	Atmospheric data	Annual	1865 ~ 2002
Nitrogen fertilization	gN/(m ² ·year)	Land-use data	Annual	1945 ~ 2002
Cropland distribution	0/1	Land-use data	Annual	1865 ~ 2002
Urban distribution	0/1	Land-use data	Annual	1865 ~ 2002

The 4 potential plant functional types are: deciduous broadleaf forest, coniferous broadleaf forest, arid shrubland, and grassland.

@ AOT40 (ppb-hr) is the accumulated dose over a threshold of 40 ppb tropospheric O₃ concentration during daylight hours.

\$ Nitrogen deposition includes NH_x (NH₃ and NH₄⁺), and NO_y (all oxidized forms of nitrogen other than N₂O).

We first extract the daily pattern of NARR dataset for each month as

$$P_T = T_d - T_m \quad \text{equation 1}$$

$$P_P = P_d / P_m \quad \text{equation 2}$$

where P_T and P_P are the daily pattern of the temperature and precipitation respectively; T_d and the P_d are the NARR daily temperature (mean, maximum, and minimum temperature), respectively; T_m and P_m are the NARR monthly average temperature and monthly total precipitation respectively. Then, for the period before 1979 when there was no NARR climate data available, we randomly selected the annual climate pattern dataset which we generated from the NARR dataset. Finally, we integrated the selected climate patterns into the PRISM monthly climate dataset and built the daily climate dataset:

$$T_d' = P_T + T_m' \quad \text{equation 3}$$

$$P_d' = P_P * P_m' \quad \text{equation 4}$$

where T_d' and the P_d' are the derived daily temperature (mean, maximum, and minimum temperature) and precipitation, respectively; P_T and P_P are the daily pattern of the temperature and precipitation respectively; T_m' and P_m' are the PRISM monthly average temperature and monthly total precipitation respectively.

We further generated a 30-year detrended climate dataset from the interpolated climate dataset between 1895 and 1924. The data-detrending approach subtracts the best-fit line

from transient climate dataset, and only retains the fluctuations about the trend. Such a dataset is required for stabilizing the simulation before entering the transient mode. These 30-year detrended data were also used as the climate input for the years from 1865 to 1894.

2.2.3. Atmospheric dataset

Atmospheric dataset include the daily tropospheric ozone dataset (AOT40, accumulated dose over a threshold of 40 ppb during daylight hours), annual nitrogen deposition dataset (including NH_x (NH_3 and NH_4^+), and NO_y (all oxidized forms of nitrogen other than N_2O), and annual CO_2 concentration.

DLEM requires daily AOT40 input as the index of tropospheric ozone stress. AOT40 is the accumulated dose over a threshold of 40 ppb during daylight hours (Felzer et al., 2004). In DLEM, we used an accumulation period of 30 days back-trajectory (For more information about the DLEM ozone input and its submodel please read Section 2 of Chapter 3). The AOT40 dataset we used was generated by Felzer et al. (2004). The original resolution is half degree and covers the entire conterminous US. We cut out the SUS region and rescaled the dataset into 8 km resolution using bilinear interpolation.

The dataset developed by Felzer et al. (2004) ended in 1995. To determine the trend of ozone stress after 1995, we analyzed the annual mean ozone concentration records from the database of Clean Air Status and Trends Network (<http://www.epa.gov/astnet/>). A total of 22 stations were included in our study region that have continuous records of

more than 5 years between 1995 and 2005. The plot (Figure C5.1.8, Chapter 6) indicates that the observed tropospheric ozone concentration in most of the SUS region generally did not vary significantly after 1995 (there are exceptions, e.g. ozone stress of the Great Smoky Mountains, NC, was observed to rise quickly until 2000. See Chapter3, Figure C5.5). We therefore used the mean AOT40 of the early 1990s as the ozone for years after 1995.

Nitrogen deposition datasets were reconstructed based on three periods (1860, 1993, and 2050) global nitrogen deposition maps generated by Dentener (2006). We removed the SUS region from the global nitrogen deposition maps, and then rescaled them into 8 km resolution using bilinear interpolation. We further created annual dataset using linear interpolation based on Dentener's maps (2006) of three time periods.

For years before 2003, standard IPCC CO₂ concentration history dataset (Enting et al., 1994) was used in this simulation. Annual CO₂ concentration for years after 2003 was calculated based on the "Global Annual Mean Growth Rate of CO₂" by Earth System Research Laboratory (ESRL, <http://www.esrl.noaa.gov/gmd/ccgg/trends/>). We did not consider the intra-annual CO₂ concentration change. The spatial pattern of atmospheric CO₂ concentration was assumed to be homogenous.

2.2.4. Land-use dataset

The land-use dataset included both the land management dataset (*i.e.* cropland nitrogen fertilization maps), and the land-use type dataset (urban/developed region maps and

cropland maps) from 1865 to 2002. We also generated the impervious maps and lawn maps based on the US Geological Survey (USGS) National Land Cover Database 2001 (NLCD 2001) (Homer et al., 2004). We then estimated the average proportions of impervious surface and urban lawn in the urban/developed regions of the SUS.

2.2.4.1. Land management – nitrogen fertilization dataset

Alexander and Smith (1990) developed county-level nitrogen fertilization tabular datasets for the conterminous US from 1945 to 1985, and Ruddy et al. (2006) developed datasets for the conterminous US from 1987 to 2001. By assuming the nitrogen fertilization of 1986 to be about the average of the amount in 1985 and 1987, we combined the two dataset together and derived a county level nitrogen fertilizer tabular dataset from 1945 to 2001. Then, based on the county-level cropland area census data (Waisanen and Bliss, 2002), we derived the nitrogen fertilization application dataset (gram N fertilizer per cropland area).

2.2.4.2. Land-use change dataset

Approaches similar to Chen et al. (2006b) and Zhang et al. (2007) were used to combine the contemporary land-use map that was derived from USGS National Land Cover Datasets (<http://edc.usgs.gov/products/landcover.html>) with the historical census datasets of cropland area, urban area, and population to reconstruct the maps of cropland and urban/developed region from 1865 to 2002.

We first aggregated the 30-m resolution the USGS National Land Cover Map into 8 km resolution and recorded the fractions of human-disturbed land-cover types (cropland and urban/developed region) in each grid. Then for cropland dataset, we conducted temporal interpolation by calculating the cropland percentage for each cell in each year based on cropland census data (Waisanen and Bliss, 2002; http://www.nass.usda.gov/Census_of_Agriculture/). We used county-level relative change of cropland area from the Census of Agriculture as controls to identify change rate of cropland so that the total area of a certain land-cover type would match the county-level data.

Urban/developed region datasets were reconstructed in the same way. During 1945–1997, the state-level urban area survey data (once every 5 year) conducted by the USDA Economic Research Service (<http://www.ers.usda.gov/>, verified 24 Jan. 2006) was used as a control to generate the annual urban area dataset using the linear interpolation method. For years before 1945 and after 1997, however, due to the lack of urban census records, we reconstructed the annual urban maps by assuming the urban area was positively correlated with population density (Waisanen and Bliss, 2002; <http://www.census.gov/>). The urban map of 2002 was used to determine the study area for this research (red region in Figure C5.1).

Figure C5.2 shows the spatial and temporal distribution of croplands and urban/developed lands during the study period. The cropland area kept increasing before the 1920s. After the 1930s, cropland area declined gradually in the SUS. The

urban/developed area was small until the end of 1900s. After 1940s, the urban/developed area in SUS increased rapidly. The mean annual urbanization rate after 1940 was 11 times the rate before 1940. In the last 30 years of the 20th century, urbanization accelerated tremendously in the SUS. The mean annual urbanization rate after 1970 was about 130% higher than the urbanization rate before 1970.

2.2.4.3. Impervious surface and urban lawn

The USGS NLCD 2001 provides 30-meter resolution national wide impervious surface fraction map of entire US (Yang et al., 2003). We derived the SUS impervious map by cut out the study region from the national impervious surface map and aggregated it into 8 km resolution. According to Milesi et al. (2005), the following equations can be used to estimate the fraction of urban lawn, *i.e.* managed urban grassland the majority of which are turf grasses:

$$\text{lawn\%} = 79.53 - 0.83 * \text{ISA\%} \quad \text{equation 5}$$

where ISA% is the percentage of urban impervious area. This equation, however, is only valid in the urban regions. The results showed that the lawn covers about 14.43% of SUS urban area.

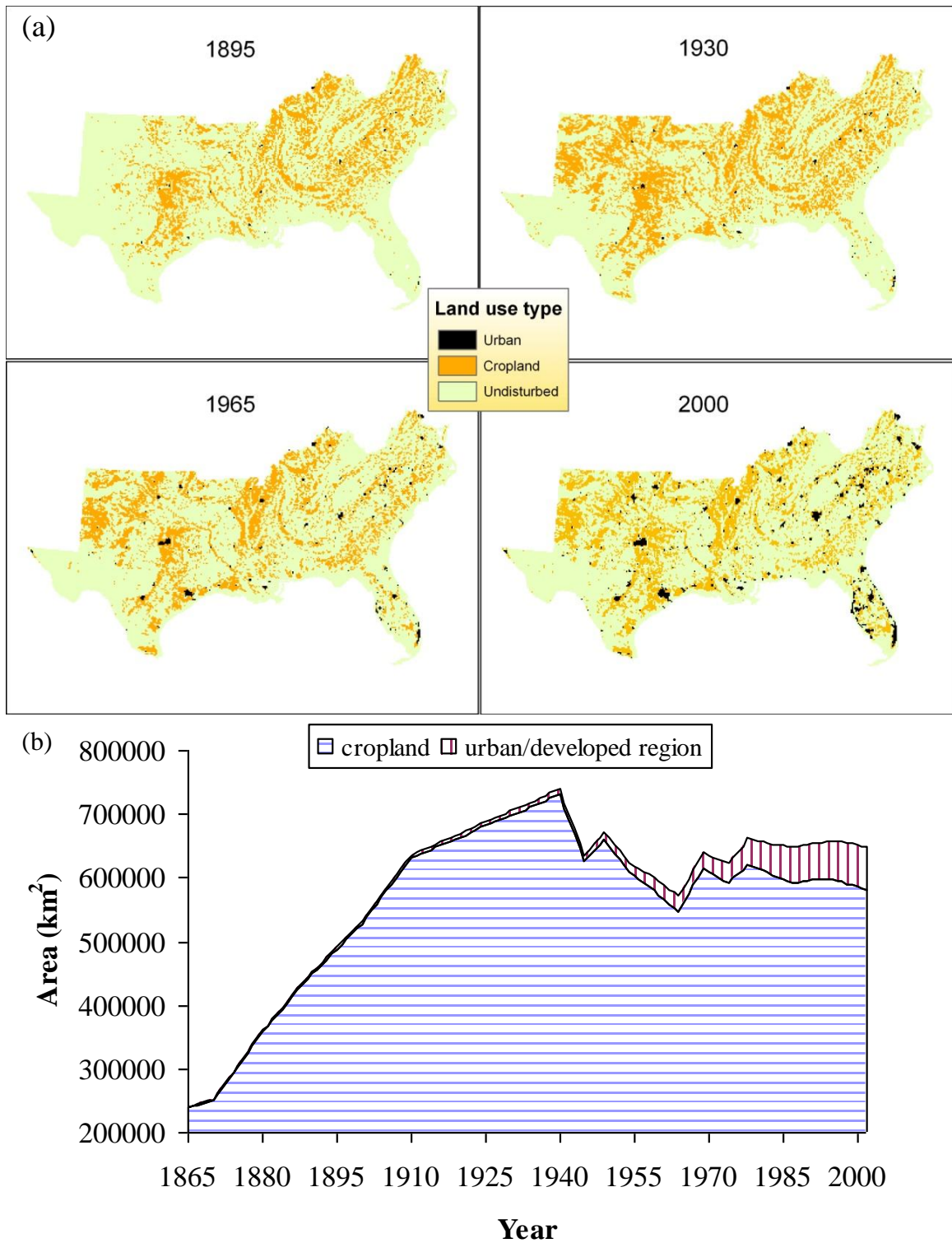


Figure C5.2 The spatial pattern (a) and temporal pattern (b) of land-use change between 1865 and 2002.

2.3. Model description

DLEM model has been well documented in other places (Tian et al., 2005; Chen et al., 2006a; Ren et al., 2007; Zhang et al., 2007) (also see Chapter 6). But our focus was on the structure and function of DLEM urban-submodel. Unlike most of current biogeochemical models that either ignore the urbanization processes or simply treat the urban ecosystem as cropland or grassland, DLEM includes a concise but effective urban submodel that can simulate the impacts of urbanization on ecosystem structure and functions (Figure C5.3). DLEM assumes that only the lands that will be converted into impervious surface and urban lawn are disturbed during urbanization; the remaining lands were unchanged after urbanization and thus called urban remnant vegetation. The model, therefore, treats the urban region as a combination of three different land-use fractions: urban impervious surface (UIS), urban lawn (ULW), and urban remnant vegetation (URV). Urbanization takes place when the land-use type of the current year is changed from non-urban types (*i.e.* the potential vegetation or cropland) into an urban type. During the urbanization, the land-conversion takes place in UIS and ULW fractions. A fraction of above-ground vegetation biomass and all below-ground vegetation biomass enters the soil organic matter (SOM) pool, another fraction of biomass both from SOM and above-ground vegetation will be released (into atmosphere or ground water) due to the disturbance of land-conversion, the largest fraction of the above-ground vegetation biomass will enter the product pools of 1 year residential time which will be released in the coming year.

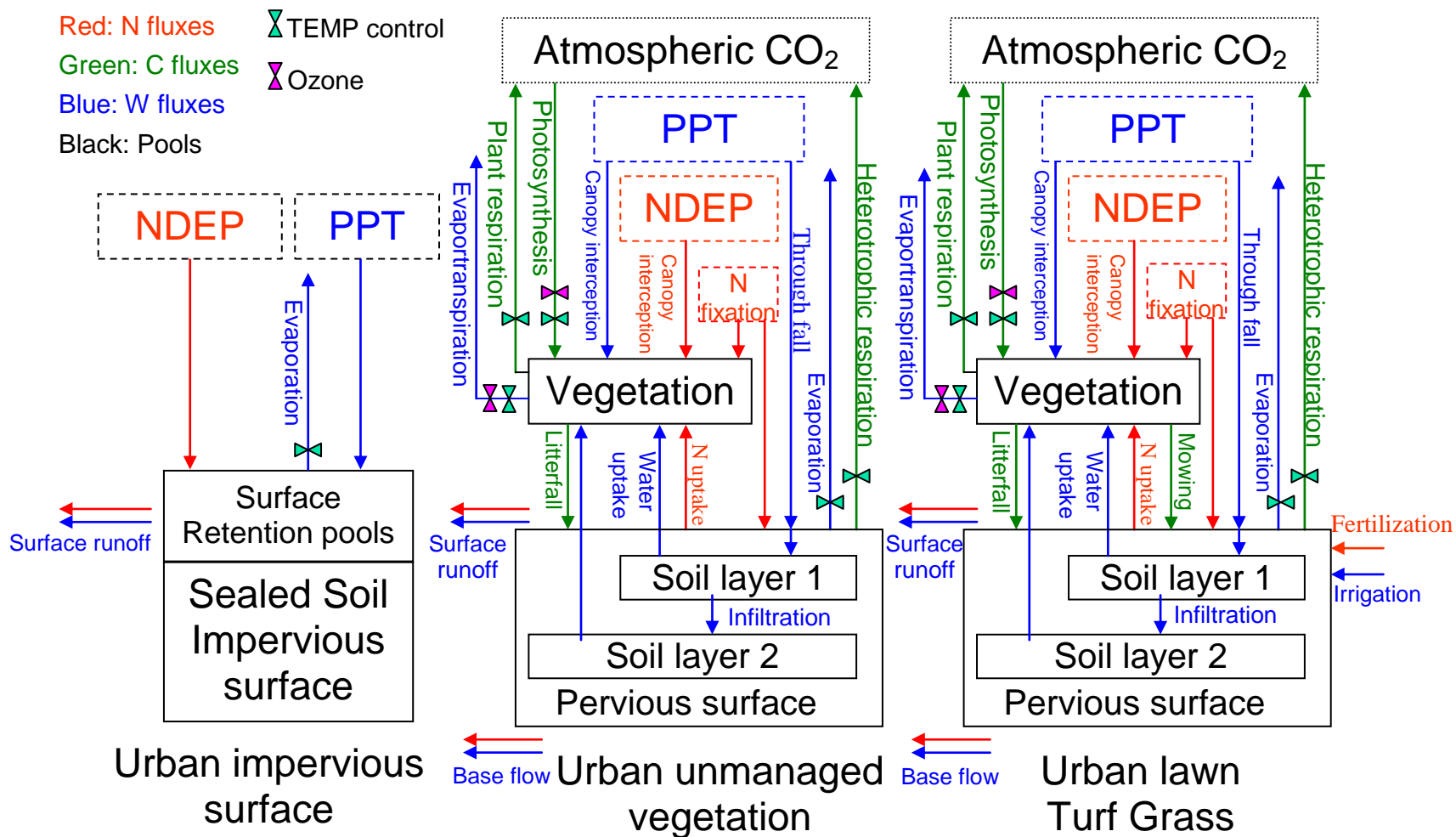


Figure C5.3 Diagram of urban-submodel. PPT: precipitation (mm); TEMP: temperature ($^{\circ}\text{C}$); NDEP: N deposition (gN/m^2)

Table C5.2 Parameters for DLEM urban processes

	Description	Unit	Woody plants	Herbaceous plants	Source
retentWMax	Maximum water retention capacity of impervious surface	mm	0.56	0.56	Brater 1968
retentNMax	Maximum nitrogen retention capacity of impervious surface	g N /m ²	0.1	0.1	Calculated based on retentWMax
lawnFert	Nitrogen fertilization rate of urban lawn	g N /m ²	10	10	Qian et al., 2003; Milesi et al., 2005
lawnMaxLai	Maximum Leaf area index of turfgrass above which the lawn will be mowed	ratio	1.5	1.5	Milesi et al., 2005
lawnIrrigation	Will lawn be irrigated?	0/1 ¹	1	1	User control
vProd	Fraction of vegetation biomass that will enter the product pool during urbanization	%	27%	0	Mcguire et al., 2001
vConv	Fraction of vegetation biomass that will enter atmosphere due to urbanization	%	40%	50%	Mcguire et al., 2001
vSlash	Fraction of vegetation biomass that will enter soil as slash during urbanization	%	33%	50%	Mcguire et al., 2001
sConv	Fraction of soil organic matter that will enter atmosphere due to urbanization	%	1%	1%	Mcguire et al., 2001
isConv	Fraction of soil organic carbon that will be lost due to construction of impervious surface	%	50%	50%	Calibrated parameter. ²

¹ If lawnIrrigation = 1, the urban lawn is irrigated. Otherwise there will be no irrigation.

² We let isConv = 50%, so that the average soil organic carbon density of SUS urban area will equal to the estimation of Pouyat et al. (2006).

The below-ground biogeochemical pools of UIS are assumed to be completely sealed by the impervious surface. That is, no water and carbon or any kind of flux exchange can take place between the above-ground UIS and below-ground UIS. Except for a small fraction of water held by the UIS fraction according to the impervious surface water retention capacity (Brater, 1968), most of the precipitation input to the UIS fraction will either enter the atmosphere as evaporation or as runoff water fluxes. The UIS has zero vegetation cover and therefore zero productivity. The URV fraction maintains the pre-urbanization vegetation types (except for cropland, which will change into the potential vegetation type for the region). The ULW is managed turfgrass, which is irrigated and fertilized and mowed periodically (Table C5.2). If the lawn is irrigated, its soil water will be refilled to field capacity whenever the soil water content is lower than 50% of the maximum soil-water-hold-capacity which is the difference between field capacity and wilt point of the soil. Whenever the leaf area index of lawn exceeds the maximum leaf area, the lawn will be “mowed”. The excessive vegetation biomass will enter the soil carbon pool, and the leaf area index will be cut back to the maximum leaf area index of lawn.

There are not interactions and horizontal fluxes among the three urban fractions in the model. The total ecosystem function of the urban grid is the area weighted summarization of the ecosystem functions of each of these three urban land types.

3. Results and analysis

3.1. Productivity and carbon storage of SUS urban ecosystems

Our simulation results indicate that about 505 T g C is stored in the urban ecosystems of SUS (Table C5.3), with about 73% of this carbon is stored below-ground. Among the different components, the remnant vegetation stores the majority (about 62%) of the urban carbon. Among the different urban vegetation types, forest is the dominant carbon pool accounting for about 87% of total carbon storage. Urban remnant vegetation also has the highest total carbon density of 12255 g C /m², with urban lawns having the second largest density of 8392 g C/m². On average, soil organic carbon accounted for about half of the total carbon storage in urban. More than 85% of carbon storage of urban lawn, however, was located in the soil. Urban impervious surface has zero vegetation carbon and litter storage, with soil organic carbon density also low (3208 g C/m²).

According to our simulation results, the Southern urban forest has relatively high annual net primary productivity (NPP) of 748 g C/m²/yr. Due to intensive management, the SUS urban lawn also has high productivity of 633 g C/m²/yr, nearly equal to the mean productivity of the remnant vegetation (642 g C/m²/yr). The urban impervious surface is assumed to have no NPP. The mean NPP (*i.e.* the area-weighted NPP of all land fractions) of SUS urban is about 331 g C/m²/yr, and the total regional productivity is estimated to be 23 T g C /yr.

Table C5.3 The productivity and carbon storage of the Southern US (SUS) urban and developed regions as simulated by the Dynamic Land Ecosystem Model.

	NPP		VEGC ¹		LTRC		SOC		TOTEC		Fraction of urban area	AREA (km ²)
	density (g/m ² /yr)	SUS total (T g/yr)	density (g/m ²)	SUS total (T g)	density (g/m ²)	SUS total (T g)	density (g/m ²)	SUS total (T g)	density (g/m ²)	SUS total (T g)		
Forest	748	13	7116	123	900	16	7754	134	15770	273	25.1%	17293
Grass and shrub	423	4	589	5	285	2	4142	35	5016	42	12.2%	8396
Remnant vegetation ²	642	16	4983	128	699	18	6573	169	12255	315	37.3%	25689
Lawn	633	6	785	8	442	4	7165	71	8392	83	14.4%	9946
Impervious surface	0	0	0	0	0	0	3208	107	3208	107	48.3%	33292
Urban average ³	331	23	1970	136	324	22	5033	347	7328	505	100%	68928

106

1 Carbon pools of SUS urban and developed regions as estimated by the model simulation. VEGC: vegetation carbon; LTRC: litter carbon; SOC: soil organic carbon; TOTEC: total ecosystem carbon.

2 Remnant vegetation includes both the urban forest and urban grass/shrub.

3 Area-weight average NPP and carbon pools of all the three urban fractions (UIS, ULW, URV).

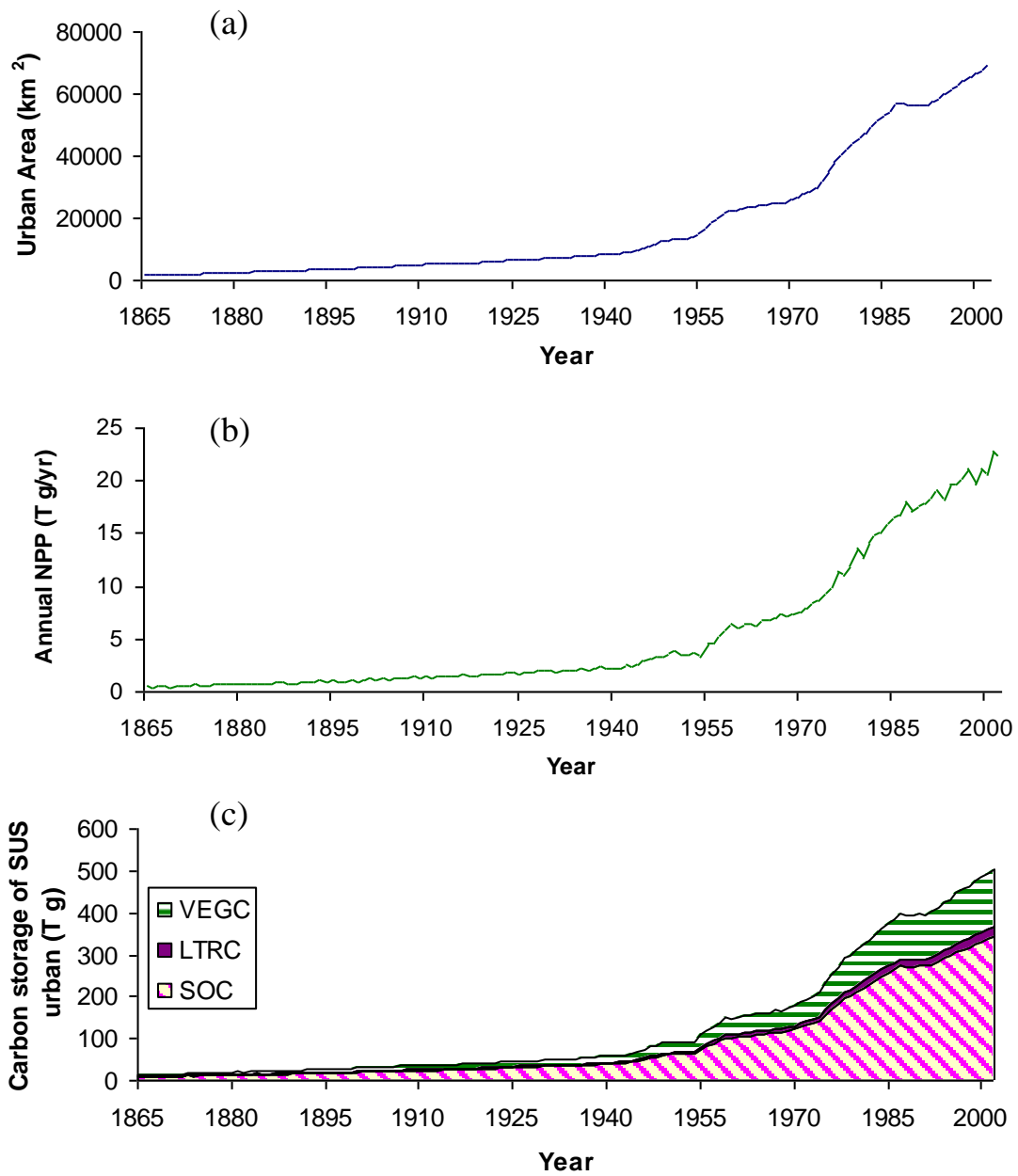


Figure C5.4 The temporal pattern (a) urban area, (b) urban ecosystem productivity, and (c) urban carbon storage from 1865 to 2002 in Southern US. VEGC: vegetation carbon; LTRC: litter carbon; SOC: soil organic carbon.

Urbanization became obvious in 1894, and accelerated after the mid-1940s in SUS (Figure C5.4 a). Accordingly, both the productivity and carbon storage of SUS urban ecosystems increased rapidly in the late half of the 20th century. The overall productivity of the SUS urban area increased from 0.04% of SUS total NPP in 1865 to 1.9% in 2002, and urban carbon storage increased from 0.06% in 1865 to 2.5% in 2002 (Figure C5.4 b).

3.2. The possibility of managing urban lawn as carbon sinks

Many studies indicate that intensively managed (irrigated, fertilized, and mowed) urban lawn have high productivity and can store large amounts of soil organic carbon (Qian and Follett 2002; Qian et al., 2003; Milesi et al., 2005; Pouyat et al., 2006). Urban lawns are therefore proposed as a tool for carbon sequestration. In this study, we compared the SUS urban carbon dynamics with and without lawn management (Table C5.4). We found that management could have enhanced the productivity of turfgrass by about 25%, and have increased total carbon storage by 14%. Most (80%) of the increased carbon storage was fixed in the soil. In SUS, about 10 T g C was sequestered in the urban ecosystem due to lawn management, equaling approximately 2% of total urban pools size. These results indicate that management could improve the productivity and carbon sequestration capacity significantly. However, unless the fraction of urban lawn area will increase dramatically in the future (current coverage is about 14.4% in SUS), the impacts on the overall SUS urban carbon balance is limited.

The effects of urban lawn management, however, are not the same in all regions. Figure C5.5 indicates that the lawn management significantly improved the productivity and carbon storage in regions where natural vegetation had low productivity due to environmental stresses (e.g. the Texas arid ecosystems or the Florida grasslands growing on sandy soils). This was possible because human management has ameliorated the environmental stresses on vegetations.

Table C5.4 Comparison of the productivity, carbon density and carbon storage of managed and unmanaged urban lawn

		Managed lawn	Unmanaged lawn	Effect of management	Percentage of change due to management
Lawn NPP ¹	density (g/m ² /yr)	633	508	125	25%
	SUS total (T g/yr)	6	5	1	25%
Lawn VEGC	density (g/m ²)	785	663	122	18%
	SUS total (T g)	8	7	1	18%
Lawn LTRC	density (g/m ²)	442	367	75	20%
	SUS total (T g)	4	4	1	20%
Lawn SOC	density (g/m ²)	7165	6350	815	13%
	SUS total (T g)	71	63	8	13%
Lawn TOTEC	density (g/m ²)	8392	7380	1012	14%
	SUS total (T g)	83	73	10	14%
Urban TOTEC	density (g/m ²)	7328	7184	144	2%
	SUS total (T g)	505	495	10	2%

¹ NPP: net primary productivity; VEGC: vegetation carbon; LTRC: litter carbon; SOC: soil organic carbon; TOTEC: total ecosystem carbon.

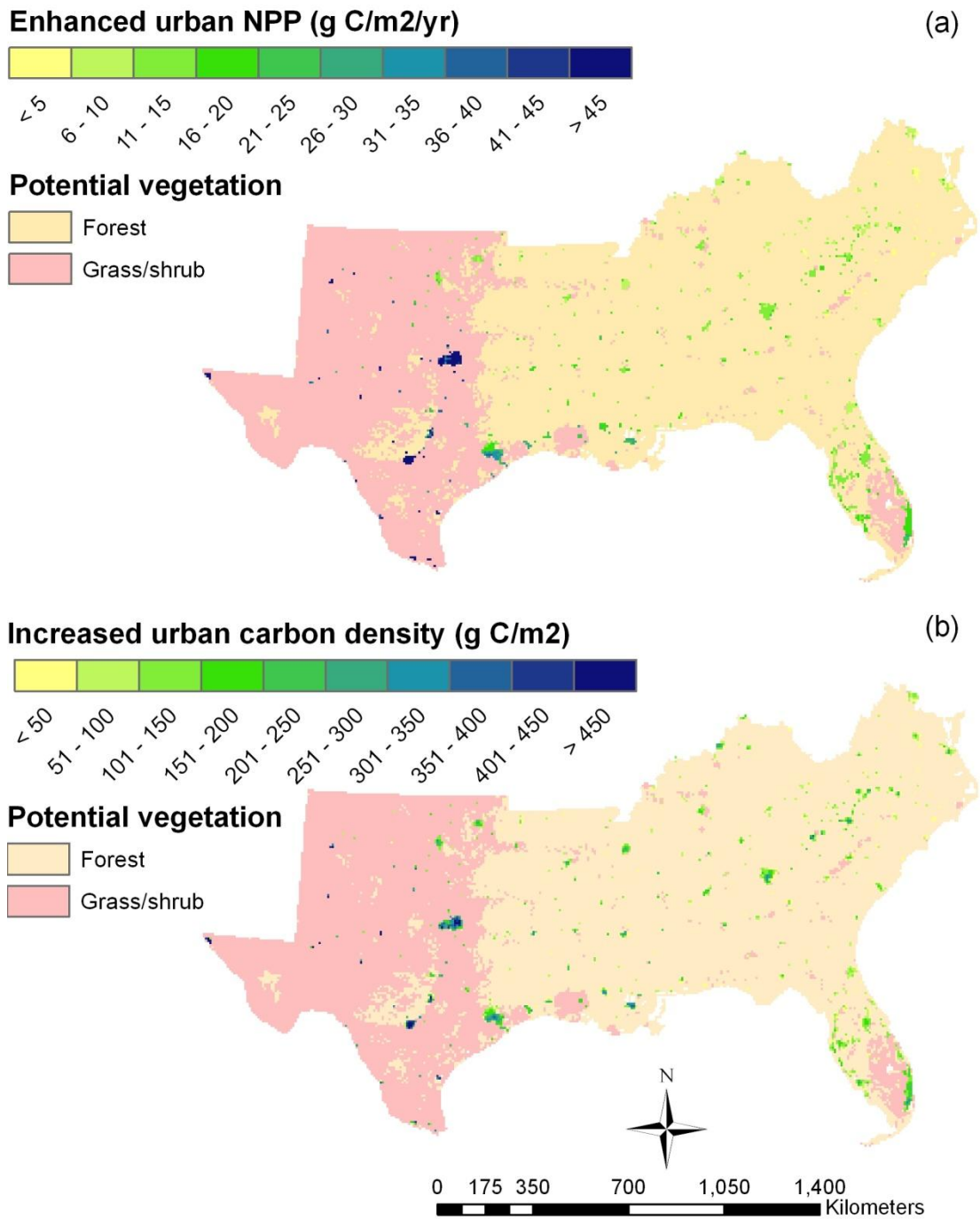


Figure C5.5 Effects of the lawn managements on the (a) productivity and (b) carbon storage of Southern urban/developed regions.

4. Discussion

4.1. Comparing our simulation outputs with results of other studies.

We compared our simulated carbon density of Atlanta, GA with results from other studies (Table C5.5). Except for the soil organic carbon of urban impervious surface of which is about 500 g C/m^2 higher than the estimation of Pouyat et al. (2006), most of our numbers are lower than the results from other studies. There are currently no measurements of SOC under impervious surface available, so Pouyat et al. (2006) assumed the value to equal to the SOC of urban landfill. They used a constant value (3300 g C/m^2), the average SOC of ten landfill samples (ranged from 1500 g C/m^2 to 4600 g C/m^2) from three US cities, as estimates. It is obvious, however, that the actual SOC of impervious surface should vary from place to place. The impervious surface can be looked at as a sealed surface that no water or carbon fluxes can pass through. It is therefore reasonable to assume that the SOC under this surface does not change. Urbanization, however, should disturb soil organic carbon drastically. Therefore, the SOC content sealed by impervious surface is determined by the pre-urban storage and the intensity of soil disturbance during urbanization we assumed that in the lands that will be converted to impervious surface 50% of SOC will be lost due to the disturbance. Based on this assumption our model estimate the average SOC of urban impervious surface in SUS to be about 3208 g C/m^2 (Table C5.3), close to the average SOC value measured in the ten urban landfills as mentioned above. The impervious surface SOC in local scale, however, varies from place to place based on the pre-urban SOC content. The general

pattern is that the urban area converted from forest land type or locations in the northeast (*i.e.* Virginia, Kentucky, North Carolina, and Tennessee) has higher SOC content than others. A more accurate estimation will depend on the future field study on the urban impervious surface.

Table C5.5 Comparison of our estimates of carbon density of the city of Atlanta against other studies (unit: g C/m²)

Urban carbon pools	This study	Other studies	Source of other studies
Lawn SOC	9614	14400 ¹	Pouyat et al., 2006
PS SOC ²	8738	10800	Pouyat et al., 2006
IS SOC	4033	3300	Pouyat et al., 2006
Urban SOC	6466	7800	Pouyat et al., 2006
Forest VEGC	8619	9700	Nowak and Crane 2002
Urban VEGC	3329	3600	Pouyat et al., 2006

1 Mean of SOC of lawns in Baltimore, MD, Moscow, Russia, and Chicago, IL.

2 PS: pervious surface; IS: impervious surface.

Our estimation of SOC of urban lawns is 9614 g C/m², much lower than the value (14400 g C/m²) used by Pouyat et al. (2006). Similar to the approaches of impervious surface SOC estimation, Pouyat et al. (2006) used a constant value which derived from 22 field measurements from three cities (Baltimore, MD (12200 g SOC/m²); Moscow, Russia (14600 g SOC/m²), and Chicago, IL (16300 g SOC/m²). The estimates from our process-based model were not constant. The SOC density of lawn generally decreased with

latitude due to the positive relations between the temperature and SOC decomposition rate. Our study region is warmer than any of the three cities that lawn soil samples were measured. It is therefore not surprising that our estimation of Atlanta lawn SOC is lower than the mean value of the three northern cities. In fact, our average estimates of the SOC of urban lawns in the Baltimore-Washington Metropolitan Area (e.g. Arlington, VA) are about 11513 g SOC/m², very close to the value measured in Baltimore, MD (Pouyat et al., 2006).

Our estimation of urban vegetation carbon density (3329 g C/m²) is similar to Pouyat et al. (2006) (3600 g C/m²). The estimation of urban forest VEGC, however, is about 1000 g C/m² lower than those of Nowak and Crane (2002). It was found that the carbon density of urban forest is double that of rural forest. This is possibly due to the old age structure, less disturbance and fertilization effects from urban pollutants (e.g. increased nitrogen and cation deposition), and more open structure of urban woodlands that allows higher incident radiation. Our model, although accounting for the effects of old age structure and decreased disturbances in urban forest, ignores the effects of atmospheric fertilization and more open urban woodland structure. These factors should be included into our model in the future for more accurate assessments.

Another possible reason for our lower estimation is because neither of the other two studies included the effects of historical land-use changes on the urban carbon balance. Many of the SUS urban regions were rapidly developed in recent decades. Although the urban vegetation was reported to have the potential to store large amounts of carbon, they

however cannot regrow in one year. Therefore, it is incorrect to estimate the productivity and carbon storage of vegetation in newly developed urban area with the regional mean value or even the value measured in mature urban ecosystems. The pre-urban land-cover type before the urbanization, as shown in Section 3.2, also has an important legacy effect on the urban soil carbon. The study of Qian and Follett (2002) in four US cities (Denver, CO; Fort Collins, CO; Loveland, CO; and Saratoga, WY) indicated that urban vegetation converted from agricultural lands exhibited 24% lower SOC than the vegetation converted from native grasslands. Their results also suggested that about 30 to 45 years are required for the urban lawn to reach its maximum soil carbon density. The static approaches adopted by the other two studies are therefore tending to overestimate the urban carbon storage.

In Table C5.6, we compared our estimates of state level carbon density against the estimation made by Pouyat et al. (2006). Our estimation of total ecosystem carbon density was generally comparable to the estimates of Pouyat et al. (2006) findings, except for the states of Florida and Texas, where our estimated total ecosystem carbon and soil organic carbon densities are about half. Our underestimation of Florida urban carbon density, especially the low soil carbon density, is caused by our omission of the urban wetland. For simplification, our model assumes that there is only one urban remnant vegetation type which is the dominant urban vegetation of the urban. Wetlands, which only occupy 20% of the Florida urban area were therefore, ignored by our model simulation. However, the extraordinary high soil organic carbon content of wetlands actually made a disproportional contribution to the Florida urban carbon storage.

Table C5.6 Comparison of the mean carbon densities for each of the 13 Southern states as estimated by Dynamic Land Ecosystem Model against the estimates of Pouyat et al. (2006)

STATE	SOC (g C/m ²)		TOTEC (g C/m ²)*	
	This study	Pouyat et al., 2006	This study	Pouyat et al., 2006
AL	6836	7200	9554	11700
AK	5637	6500	8420	8800
FL	4499	9800	6155	11500
GA	6750	8100	9128	13200
KY	6393	8200	9350	11300
LA	5580	9000	7766	11300
MS	6054	8400	8499	12000
NC	7431	7900	10586	11900
OK	4005	5000	4382	6300
SC	7185	8300	9548	12000
TN	6855	6700	9951	10800
TX	3242	6200	3975	7200
VA	7623	7700	11067	11000

* SOC: soil organic carbon; TOTEC: total ecosystem carbon

Pouyat et al. (2006) may have overestimated the SOC density of Texas urban areas (and other urban areas) due to their overestimation of the urban lawn SOC content. The value of 14400 g SOC/m² used for Texas lawns was probably too high for this warm region. First, the high temperature in Texas should result in high SOC decomposition rate and therefore less SOC pool size. Second, the soil carbon storage of pre-urban vegetation in Texas is the lowest among all 13 states due to its warm-dry climate and low natural vegetation productivity. The studies of Qian and Follett (2002) indicated that the SOC of

urban vegetation is related to the pre-urbanization SOC. Therefore, the SOC of Texas lawns can not be as high as the value of other regions. Third, as discussed above, Pouyat et al. (2006) ignored the long time period required for the disturbed soil to accumulate carbon before reaching an equilibrium state.

4.2. The impacts of urbanization on ecosystem carbon storage

We estimated the impacts of urbanization on SUS ecosystem carbon storage based on the outputs of single factor scenario LUC which excludes the effects of other changing environmental factors such as elevated CO₂. According to our estimation, from 1865 to 2002, SUS urbanization resulted in a net carbon emission of about 204 T g C, 99%, of which were released through deforestation. Urbanization, however, does not necessarily create a carbon source. Pouyat et al. (2006) suggested that the impacts of urbanization on soil carbon balance are related to the pre-urbanization soil carbon densities. They compared the dynamic of soil organic carbon pools of six US cities, and found that for those cities in the northeastern US there was 1.6-fold less SOC post- than in pre-urban development scenarios. By contrast, they found the SOC pools of cities located in warmer and or drier climates increased after urbanization. According to our simulation results, the SOC and TOTEC in the northeast part of the study region, where climate is relatively cold and wet, released large amount of carbon during urbanization, while many of the urban/developed areas located in warmer regions (e.g. Florida) or under drier climate regimes (such as the west part of the study region) were carbon sinks (Figure C5.6). This pattern is more evident in the dynamic of SOC pools (Figure C5.6a) than in

the TOTEC pools (Figure C5.6 b), indicating that the mechanisms of carbon sink due to urbanization may be related to the change of carbon sequestration process in the soil carbon pools. Both Pouyat et al. (2006) and Qian and Follett (2002) suggested that managed lawns have the potential to sequester large amount of carbon into the soil, and thus turning urban/developed area into carbon sink in regions where natural ecosystems has relatively low carbon storage.

Figure C5.6 also reveals the relationship between urban carbon balance and the spatial pattern of potential vegetation types which is determined by the bioclimatic regime. We found that the urban carbon sinks were generally developed from shrubland and grassland, while the urban/developed areas converted from forest region were usually carbon sources. There are, however, some obvious carbon sinks in the forested region, especially on the map of TOTEC (Figure C5.6 b). In these grids, both the SOC and the vegetation carbon storage (VEGC) were increased after urbanization. Most grids indicate places where urban/developed areas were converted from croplands which had much lower VEGC and SOC than the Southern forest. In Figure C5.7, we compared the impacts of urbanization on the carbon balance of different Southern terrestrial ecosystems. We found that the effects of urbanization on carbon balance depended on the land cover type it was converted from (Figure C5.6). Unlike deforestation which results in significant sources of carbon (a mean of 5176 g C was lost from each square meter of forest that was converted into urban), urbanization from grassland only caused relatively small amounts of carbon lost (about 862 g C /m²), while the urbanization on both shrub and cropland created carbon sinks (Figure C5.7).

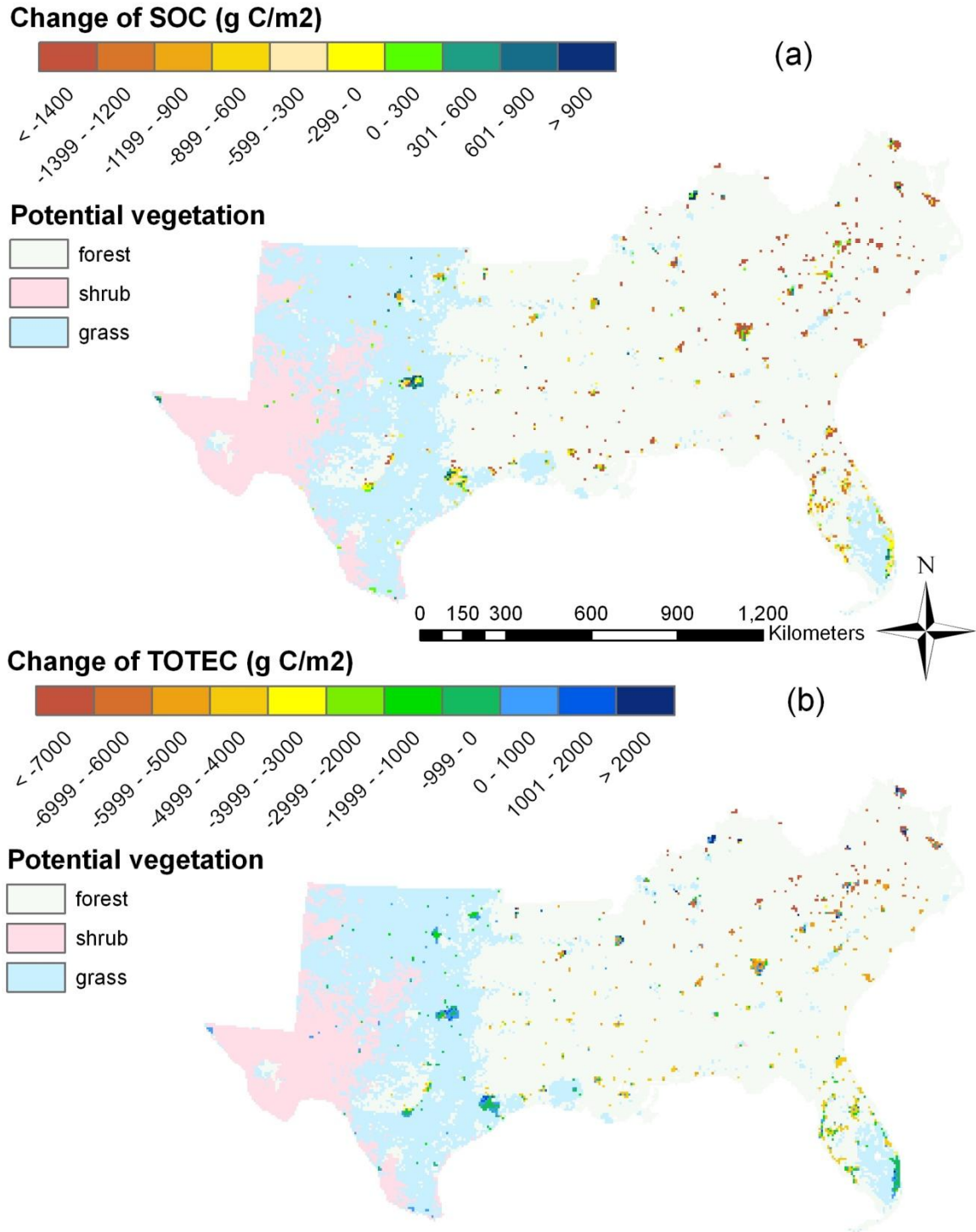


Figure C5.6 Changes in (a) soil organic carbon (SOC) and (b) total ecosystem carbon (TOTEC) due to urbanization in Southern US. The values are derived by comparing the size of contemporary urban carbon densities against pre-urbanization carbon pools.

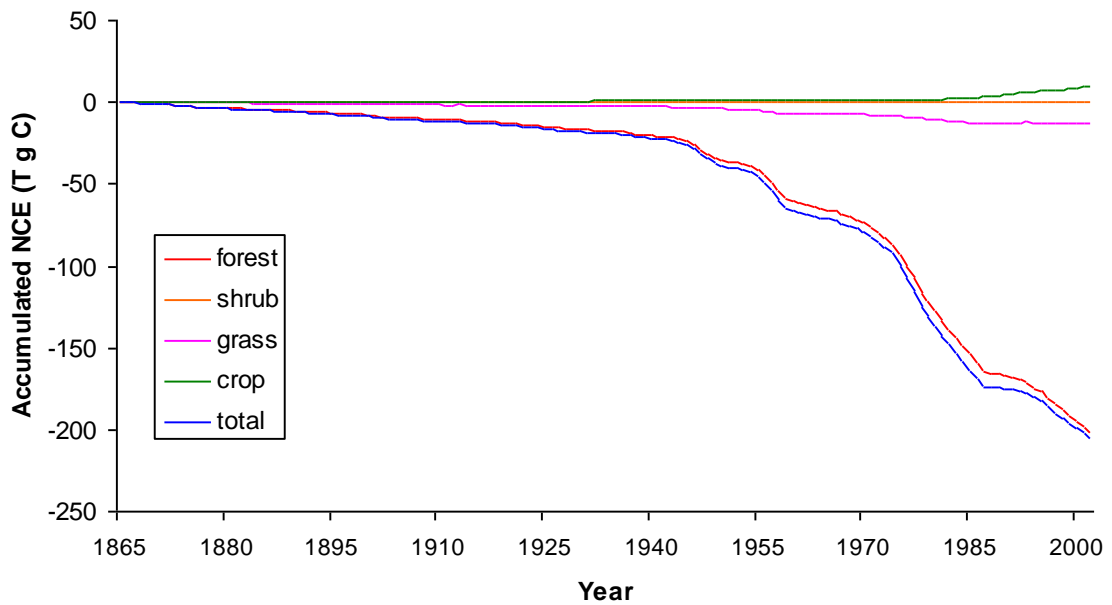
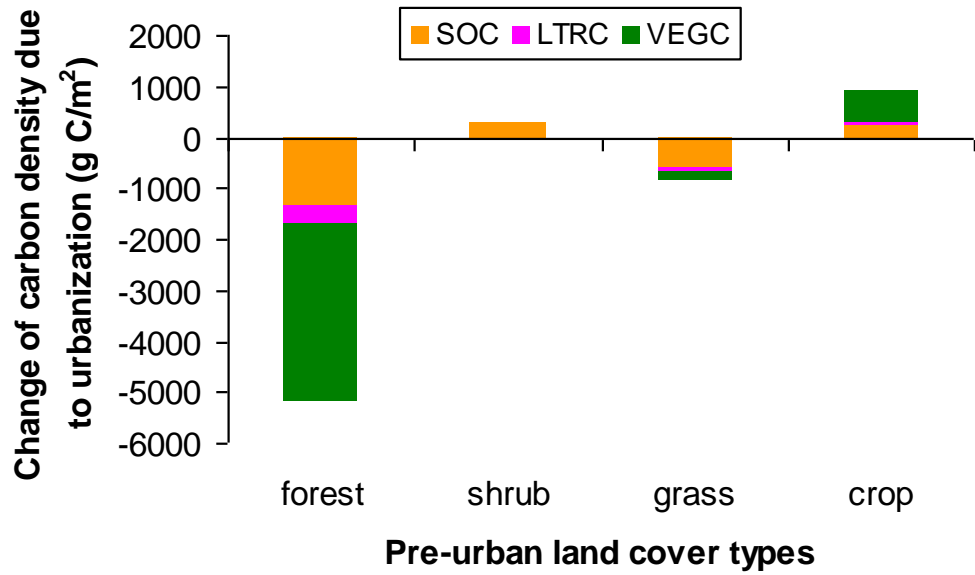


Figure C5.7 Impacts of urbanization on carbon balance of different SUS terrestrial ecosystems; (a) impacts of urbanization on the carbon density of different carbon pools. NCE is the net carbon exchange or net carbon balance of ecosystem due to urbanization, it equals to the change of total carbon storage during a certain period of time; (b) the temporal pattern of net carbon exchange due to urbanization.

The impacts on different carbon pools also varied among the different pre-urban land cover types (Figure C5.7 a). While the majority of the forest carbon emissions came from the vegetation carbon pool, grassland soil carbon was the largest source during urbanization. In the arid regions of Texas and Oklahoma where remnant urban vegetation were primarily shrubs, most of the newly sequestered carbon were stored in the soil of urban lawn, while in the Southeast, the regrowth of urban forest sequestered much more vegetation carbon than the pre-urban cropland (Figure C5.6b and Figure C5.7 a).

The regional impact of urbanization is also determined by the total urbanization area on different pre-urban land types. Our results indicate that the impacts of deforestation determined the overall effects of SUS urbanization due to the large area converted from forest to urban (Figure C5.6b). The intensity of negative NCE due to deforestation is five times larger than urbanization fluxes from any other pre-urban land cover types. Furthermore, about 58% of this area was converted from forest during the study period. This estimation agrees with the results of an urbanization study in the west Georgia region (Zhang et al., 2007) and Wear (2002) that the majority of Southern urban/developed land was converted from forest. The regional impacts of carbon sequestered by urban converted from shrubland, on the contrary, was negligible (Figure 5 b).

5 Conclusions

Our simulation results indicate that about 505 T g C is stored in urban ecosystems of SUS. Most of this carbon is stored in soil organic matter. The productivity and carbon storage capacity increased rapidly in the late half of the 20th century. According to our estimation, from 1865 to 2002, urbanization resulted in net carbon emissions of about 204 T g C, 99% of which were released through deforestation. The carbon dynamic of the urban area was related to the pre-urban land cover type. The area converted from shrub and cropland is usually a carbon sink rather than source. Our model results further suggested that human management could enhance the productivity of urban lawns by about 25% and significantly improve its carbon sequestration capacity. This study also provided evidence that process-based biogeochemical models can be a powerful tool to study the spatial and temporal dynamics of regional urbanization processes. More field studies, however, are required to provide parameters and calibration of datasets in order for the ecosystem models to make a more accurate assessment.

CHAPTER 6
REGIONAL STUDY –
Carbon Storage of the Southern United States and Its Response to Multiple
Stresses from 1895 to 2005

Abstract

North American terrestrial ecosystems, especially in the Southern United States (SUS) were suggested to be important carbon sinks. In this study we developed a high resolution spatial database throughout thirteen Southern states and used it as input to a Dynamic Land Ecosystem Model (DLEM) to assess the carbon storage of SUS terrestrial ecosystem in response to multiple stresses in the past 110 years. The model output suggests that the total terrestrial ecosystem carbon (TOTEC) storage of the SUS is about 20.26 P g C (1 P = 10^{15}), 55% of which is stored in soil, 39% in plant biomass, and about 7% in litter pools. Forests account for 84% of the ecosystem carbon storage in SUS. Our model estimation, which is comparable to the results of other studies, indicated that since 1950, the terrestrial ecosystem of SUS was a carbon sink of 46.4 T g C / year. Before 1950, however, the region had acted as a net carbon source of 1.56 P g C since 1895. Historical land-use change, elevated CO₂ and elevated atmospheric nitrogen deposition were among the most important factors controlling the carbon balance in the South US. Temporal patterns were generally controlled by the impacts of historical land-use change,

while the long-term CO₂ and nitrogen fertilization effects due to atmospheric change enhanced the carbon sequestration capacity of Southern ecosystems. All the environmental factors together resulted in a net carbon sink of about 0.9 P g C in SUS from 1895 to 2005.

1. Introduction

Human activities have profoundly changed the carbon cycle since the industrial revolution. Fossil combustion and vast deforestation have released large amounts of CO₂ into the atmosphere. Atmospheric concentration of CO₂ has increased by 31 percent (Intergovernmental Panel on Climate Change, IPCC, 2007) during the last two centuries. At the same time, the global temperature has increased in an unprecedented rate (0.2 °C per decade in the 20th century), which is generally believed mainly caused by the stronger heat insulating capability of the atmospheric CO₂, or so called “greenhouse effect” (<http://www.ipcc.ch/>).

Evidence shows that over the last 10-20 years, nearly half of the CO₂ released by burning fossil fuels has been absorbed on land and in the oceans (<http://www.ipcc.ch/>), and increasing amounts of atmospheric CO₂ appears to be being absorbed by terrestrial vegetation (IGBP Terrestrial Carbon Working Group, 1998). Both inventory dataset and model simulation results suggested that most of these carbon sinks are located in the North Hemisphere, where the terrestrial ecosystems of North America seem to uptake more carbon than the region of Eurasia-North Africa (Fan et al., 1998). It is suggested

that the mid-latitude North America, *i.e.* the coterminous US, is where the major North American carbon sinks are located. Research results indicated that approximately 30% of US fossil fuel emissions are offset by a sink of approximately 530 ± 265 million tons of carbon per year (Pacala et al., 2007).

Land-use changes were reported to be the primary mechanisms for transferring carbon between the land and the atmosphere in North America and other regions of the world (Birdsey and Lewis, 2003; Caspersen et al. 2000; Pacala et al., 2001; Tian et al., 2003). It was generally agreed that the vast forest regrowth on degraded cropland since the second World War generated the largest carbon sink in the US (Houghton et al., 1999; Schimel et al., 2000; Pacala et al., 2001, 2007). Other factors such as elevated CO₂ and nitrogen deposition could also stimulate a plant's carbon sequestration. Increased air temperature may stimulate the productivity of plants, but it can also enhance the soil respiration rate, and thus its net effect on the ecosystem carbon storage is difficult to evaluate, and could vary from region to region or change through time.

Accounting for 29% of the total forest area and 40% of the timberland area (Haynes 2003), the SUS has the most productive terrestrial ecosystems in the US (Holland et al., 1999; Birdsey and Heath, 1995). The SUS has undergone substantial land use change during the past century (Delcourt and Harris 1980) and more changes are projected in coming decades (Wear, 2002; Woodbury et al. 2006). Many study results indicate that the region was a net carbon source before the mid of 20th century due to deforestation. After the mid-20th century, the regrowth of forest on abandoned croplands resulted in a sink for

atmospheric CO₂ (Delcourt and Harris, 1980). The SUS terrestrial ecosystems were suggested to play an important role in the North American carbon sink (Woodbury et al., 2006). Compared to studies in other parts of the US, research on carbon dynamics of the SUS is still rare. At present, only a few empirical regional assessments were conducted (Chen et al., 2006b). Most of them either only cover a small part of the SUS (Liu et al., 2004), or focus on a certain vegetation type of the region (Woodbury et al., 2006), or center on a single environmental factor (Delcourt and Harris, 1980; Chen et al., 2006), or was limited to a short study period due to lack of inventory data and the empirical method applied (Han et al., 2007).

In this study we conducted a comprehensive analysis of the SUS carbon dynamics in response to multiple environmental stresses across multiple scales. Our regional study covered 13 states (Alabama, Arkansas, Florida, Georgia, Kentucky, Louisiana, Mississippi, North Carolina, Oklahoma, South Carolina, Tennessee, Texas, and Virginia) (Wear, 2002) with a high spatial resolution of 8 km × 8 km. The study period covers 110 years from 1895 to 2005. Our objectives were: (1) estimate the total carbon storage and carbon balance of the 13 Southern states; (2) study the spatial and temporal patterns of historical carbon dynamics of the SUS; (3) analyze the (individual and combined) impacts of climate change, atmospheric change (including effects of elevated CO₂, ozone, and nitrogen deposition), and land-use change (cropland conversion, cropland abandonment, and urbanization) on ecosystem productivity and carbon balance of Southern terrestrial ecosystems.

2. Research Method

2.1 Study region and research approach

The southern United States region extends roughly from 75°W to 108°W longitude and from 30°N to 38°N latitude, including the southeast (SE) and south-central (SC) subregion (Chen et al. 2006b). The SE covers Florida, Georgia, North Carolina, South Carolina, and Virginia while the SC includes Alabama, Arkansas, Kentucky, Louisiana, Mississippi, Oklahoma, Tennessee, and Texas. The SE and SC cover approximately 28 and 72% of the southern United States, respectively (Figure C6.1.1). Elevations within the region range from near sea level along the Gulf and Atlantic coasts to more than 1800 m in the Appalachian Mountains. Overall, the climate is temperate, becoming largely subtropical near the coast. The dominant forest types in this region include temperate coniferous forest and temperate deciduous forest. The four states located to the northeast of the study region (Virginia, Kentucky, Tennessee, and North Carolina, which from now on will be referred as Northeast-SUS region or NE-SUS) and Arkansas were dominated by the temperate deciduous forest. The dominant forest type in other states is coniferous forest.

Integrated process-based ecosystem models, which include the physiological responses to atmospheric and climate changes have been proved to be a powerful tool in such multiple stress studies, especially over large regions (Tian et al., 1998, 2002, 2003; Karnosky et al., 2005). The Dynamic Land Ecosystem Model (DLEM) (Tian et al., 2005; Chen et al.,

Vegetation Type

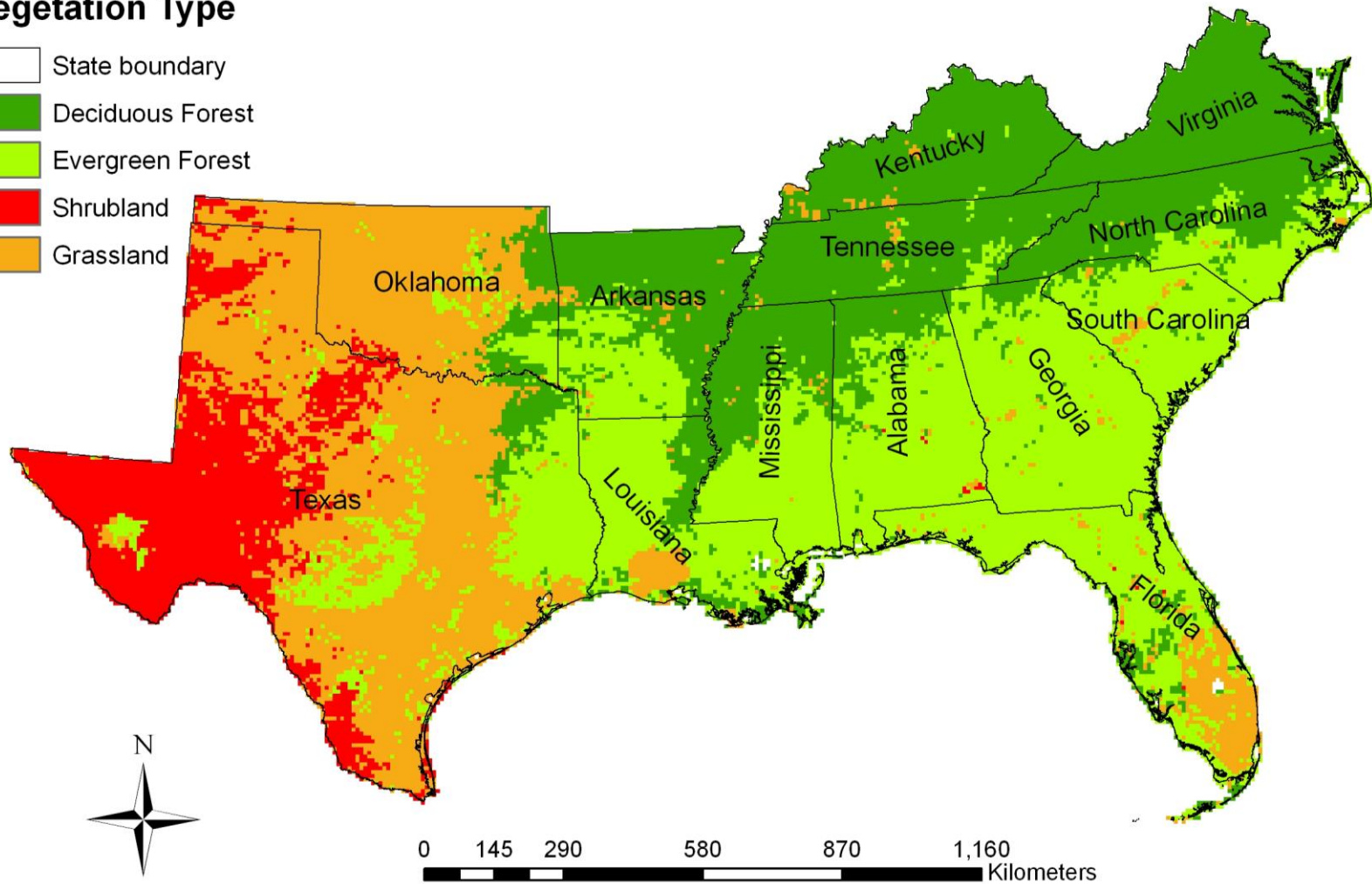
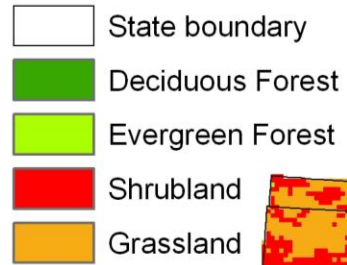


Figure C6.1.1 The boundary and potential vegetation (see Section 2.2) of the Southern US.

2006a; Ren et al., 2007; Zhang et al., 2007) was used to assess the total carbon storage and historical carbon dynamic in the SUS due to climate change, atmospheric change, and land-use change. The simulation was over a 110 year timeframe from 1895 to 2005 with a spatial resolution of 8 km. Twelve experiments were designed to investigate the impacts of multiple stresses on the SUS carbon dynamic (Table C6.1.1).

2.2. Input datasets

Input datasets required by DLEM include transient climate, atmospheric CO₂ concentration, tropospheric ozone exposures (AOT40 index), nitrogen (N) deposition, nitrogen fertilization, land-use change datasets and 11 base maps (Table C6.1.2).

2.2.1. Base maps

The 11 base maps provide unchanging information of the location, topology, soil, and natural vegetation of the study region.

(1) Elevation, slope, and aspect maps were derived from the 7.5 minute USGS National Elevation Dataset (<http://edcnts12.cr.usgs.gov/ned/ned.html>).

(2) Soil datasets (acidity, bulk density, depth to bedrock, soil texture represented as the percentage content of clay, sand, and silt) were derived from the 1 km resolution digital general soil association map (STATSGO map) developed by the United States Department of Agriculture (USDA) Natural Resources

Table C6.1.1 The simulation design to investigate the impacts of multiple stresses on the Southern US carbon dynamic from 1865 to 2005

Scenario code	Climate change	CO ₂ change	Ozone change	Nitrogen deposition change	LUC	Note
CLM	√					Single factor ¹
CO2		√				Single factor
O3			√			Single factor
NDEP				√		Single factor
LUC					√	Single factor
CLMLUC	√				√	Multi-factor ²
CLMCO2LUC	√	√			√	Multi-factor
CLMCO2O3LUC	√	√	√		√	Multi-factor
CLMCO2NDEPLUC	√	√		√	√	Multi-factor
CLMCO2O3NDEP	√	√	√	√		Multi-factor
CLMO3NDEPLUC	√		√	√	√	Multi-factor
ALLCOMBINE	√	√	√	√	√	“real” scenario ³

1 The single factor experiments revealed the theoretical effects of each environmental factors on the SUS carbon dynamic.

2 The multi-factor scenarios can be used to study the combined effects of different factors and their interactions. By comparing a multi-factor result against the result of “real scenario” which is the combination of all factors investigated in this study, we can assess the actual impacts of the “missing factor(s)” of the multi-factors scenario.

3 The real scenario considers all environmental factors. This simulation result reflects the carbon dynamic in the real world. Therefore, the ALLCOMBINE scenario is used to estimate the carbon storage and sinks of the SUS, while other scenarios were used as accessorial tools to analyze the mechanism of the controls over the SUS carbon dynamic.

Table C6.1.2 The input dataset required by Dynamic Land Ecosystem Model in the Southern US regional study

	Unit	Type	Temporal Resolution	Temporal Extend
Potential vegetation	4 categories ¹	Base map		
Soil clay content	%	Base map		
Soil sand content	%	Base map		
Soil silt content	%	Base map		
Soil depth	m	Base map		
Soil acidity	pH	Base map		
Soil bulk density	g/cm ³	Base map		
Elevation map	m	Base map		
Aspect map	Degree	Base map		
Slope map	Degree	Base map		
Irrigation map	1/0	Base map		
Precipitation	mm /year	Climatic data	Daily	1895 ~ 2005
Maximum temperature	Celsius	Climatic data	Daily	1895 ~ 2005
Minimum temperature	Celsius	Climatic data	Daily	1895 ~ 2005
Average temperature	Celsius	Climatic data	Daily	1895 ~ 2005
CO ₂	Ppmv	Atmospheric data	Annual	1895 ~ 2005
Ozone concentration, AOT40 ²	ppb-hr	Atmospheric data	Daily	1895 ~ 2005
Nitrogen deposition ³ (NH _x)	mgN/(m ² ·year)	Atmospheric data	Annual	1895 ~ 2005
Nitrogen deposition (NO _y)	mgN/(m ² ·year)	Atmospheric data	Annual	1895 ~ 2005
Nitrogen fertilization	gN/(m ² ·year)	Land-use data	Annual	1945 ~ 2002
Cropland distribution	0/1	Land-use data	Annual	1895 ~ 2003
Urban distribution	0/1	Land-use data	Annual	1895 ~ 2003

1 Four categories of potential vegetation plant functional groups are: deciduous broadleaf forest, coniferous broadleaf forest, arid shrubland, and grassland.

2 AOT40 (ppb-hr) is the accumulated dose over a threshold of 40 ppb during daylight hours.

3 Nitrogen deposition include NH_x (NH₃ and NH₄), and NO_y (all oxidized forms of nitrogen other than N₂O).

Conservation, while the texture information of each map unit was estimated using the USDA soil texture triangle (Miller and White, 1998).

(3) Our potential vegetation map shows the distribution of four natural plant functional groups (Figure C6.1.1) of SUS before human disturbances, derived from GLC2000 with a resolution of 1 km (Bartholomé et al., 2002). We reclassified the potential vegetations into four general plant functional groups and replaced the cropland and urban area in the GLC2000 with the potential vegetation types from Ramankutty and Foley (1998). Water bodies were excluded from the vegetation map. All of these input maps were aggregated into 8 km resolution.

2.2.2. Generating daily climate dataset

One important advantage of DLEM is that it requires relatively few input datasets. For example, a minimum climate dataset like precipitation, maximum temperature, mean temperature, and minimum temperature will be enough to drive the model. In this study we reconstructed a 8 km resolution daily climate dataset of the entire SUS region from 1895 to 2005 by integrating the daily climate pattern of North American Regional Reanalysis (NARR) dataset (<http://wwwt.emc.ncep.noaa.gov/mmb/rrean/>) that covers the period of 1979 to 2005, into the monthly resolution long-term (1895 to 2005) historical, climate dataset developed by PRISM (Parameter-elevation Regressions on Independent Slopes Model) Group at Oregon State University (OSU)

(<http://prism.oregonstate.edu/>). We first extracted the daily pattern of NARR dataset for each month as

$$P_T = T_d - T_m \quad \text{equation 2.1}$$

$$P_P = P_d / P_m \quad \text{equation 2.2}$$

where P_T and P_P were daily pattern of the temperature and precipitation respectively; T_d and the P_d are the NARR daily temperature (mean, maximum, and minimum temperature), respectively; T_m and P_m are the NARR monthly average temperature and monthly total precipitation respectively. Then, for the period before 1979, we randomly selected the annual climate pattern dataset which we generated from the NARR dataset. Finally, we integrated the selected climate pattern into the PRISM monthly climate dataset and then constructed the daily climate dataset:

$$T_d' = P_T + T_m' \quad \text{equation 2.3}$$

$$P_d' = P_P * P_m' \quad \text{equation 2.4}$$

where T_d' and the P_d' were the derived daily temperature (mean, maximum, and minimum temperature) and precipitation, respectively; P_T and P_P are the daily pattern of the temperature and precipitation, and T_m' and P_m' are the PRISM monthly average temperature and monthly total precipitation, respectively. Figures 1.2 and 1.3 illustrate the spatial and temporal pattern of mean daily temperature, respectively (note: Figure C6.1.2 shows the mean daily temperature averaged for the 110 years). The spatial and

temporal patterns of mean annual precipitation are shown in Figures 1.4 and 1.5, respectively.

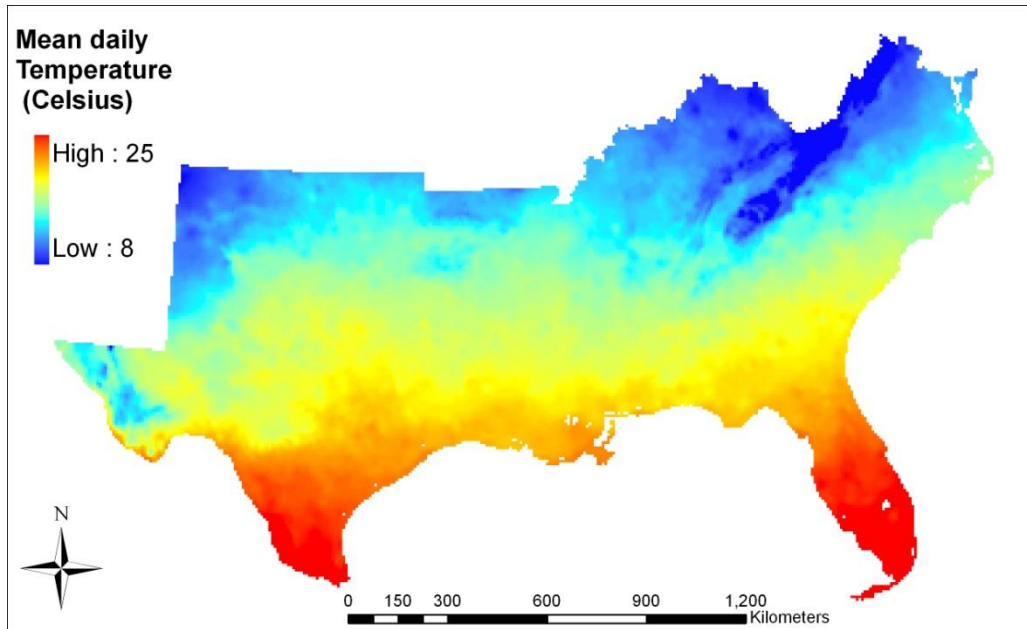


Figure C6.1.2 Spatial pattern of the mean daily temperature of Southern US from 1895 to 2005.

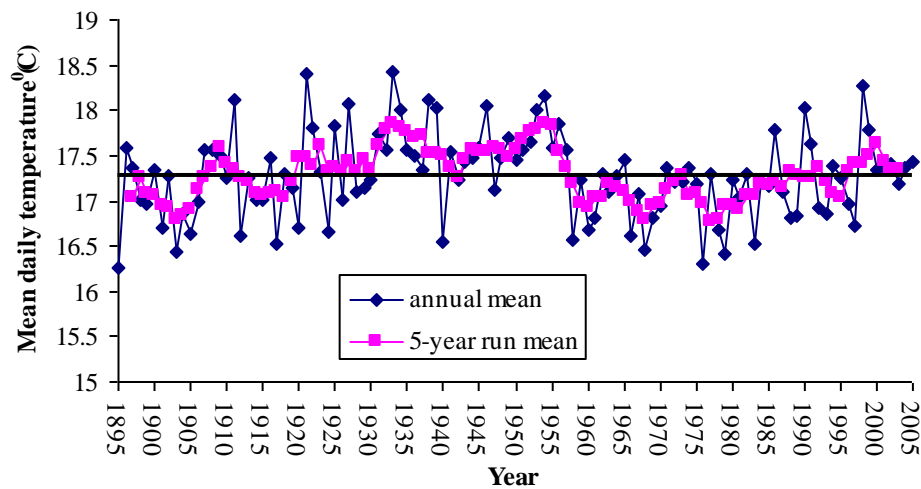


Figure C6.1.3 Temporal pattern of mean daily temperature from 1895 to 2005.

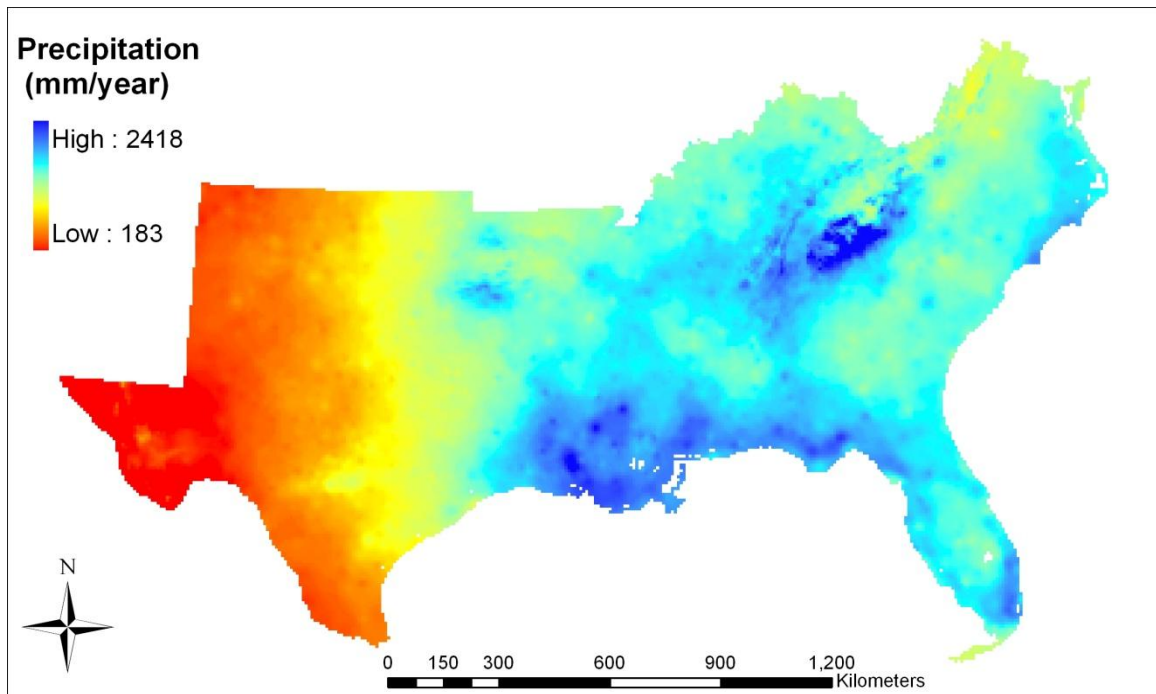


Figure C6.1.4 Spatial pattern of mean annual precipitation of Southern US from 1895 to 2005.

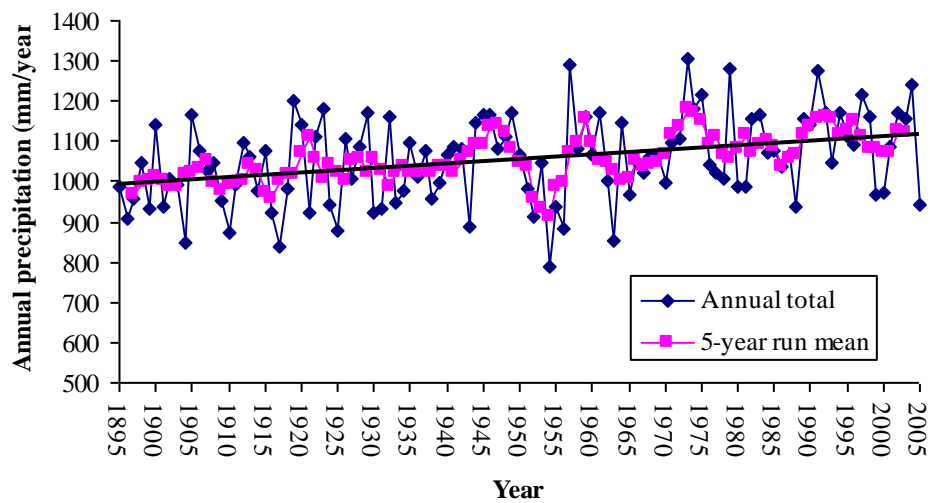


Figure C6.1.5 Temporal pattern of annual precipitation from 1895 to 2005.

Although fluctuating from year to year, the temporal pattern of SUS temperature did not show an obvious trend during the study period. After the 1950s, however, the temperature increased through time. The precipitation showed an inclination trend during the study time. We also found that the interannual variation of precipitation increased after 1940s.

We further generated a 30-year detrended climate dataset (1895-1924) from the interpolated climate dataset. The data-detrending approach subtracts the best-fit line from the transient climate dataset, only retains the fluctuations about the trend. Such a dataset is required for stabilizing the simulation before entering the transient mode.

2.2.3 Atmospheric dataset

The atmospheric dataset included the daily tropospheric ozone (AOT40, accumulated exposure over a threshold of 40 ppb during daylight hours), annual nitrogen deposition, *i.e.* NH_x (NH₃ and NH₄⁺) and NO_y (all oxidized forms of nitrogen other than N₂O), and annual CO₂ concentration.

2.2.3.1. Tropospheric ozone concentration (AOT40 index)

DLEM required a daily AOT40 input as the index of tropospheric ozone stress. AOT40 is the accumulated exposure over a threshold of 40 ppb during daylight hours (Felzer et al., 2004). In DLEM, we used an accumulation period of 30 days back-trajectory. For more information about the DLEM ozone input and its submodel please read Section 2 of Chapter 3. The AOT40 dataset we used was generated by Felzer et al. (2004). The original resolution is half degree and covers the entire conterminous US. We removed the

SUS region and rescaled the dataset into a 8 km resolution using bilinear interpolation (Figures 1.6 & 1.7). The dataset developed by Felzer et al. (2004) ended in 1995, therefore to determine the ozone trend after this time, we analyzed the annual mean ozone concentration records from the database of Clean Air Status and Trends Network (CASTNET, <http://www.epa.gov/astnet/>). There are a total of 22 stations located in our study region with continuous records of more than 5 years between 1995 and 2005. The observed tropospheric ozone concentration did not vary significantly in the SUS after 1995 (Figure C6.1.8). We therefore used the mean AOT40 of the early 1990s as the ozone for years after 1995 (Figure C6.1.7).

2.2.3.2. Nitrogen deposition dataset

Nitrogen deposition datasets (NH_x and NO_y) were reconstructed based on the three-period (1860, 1993, and 2050) global nitrogen deposition dataset developed by Dentener (2006). We removed the SUS region from the nitrogen deposition maps, and then rescaled them into a 8 km resolution using bilinear interpolation. We further created annual datasets using linear interpolation based on Dentener (2006) of three time periods (Figures 1.9, 1.10, 1.11, 1.12). The states located to the north and east received higher N deposition. In the whole SUS, the nitrogen deposition rate more than doubled during the past 110 years.

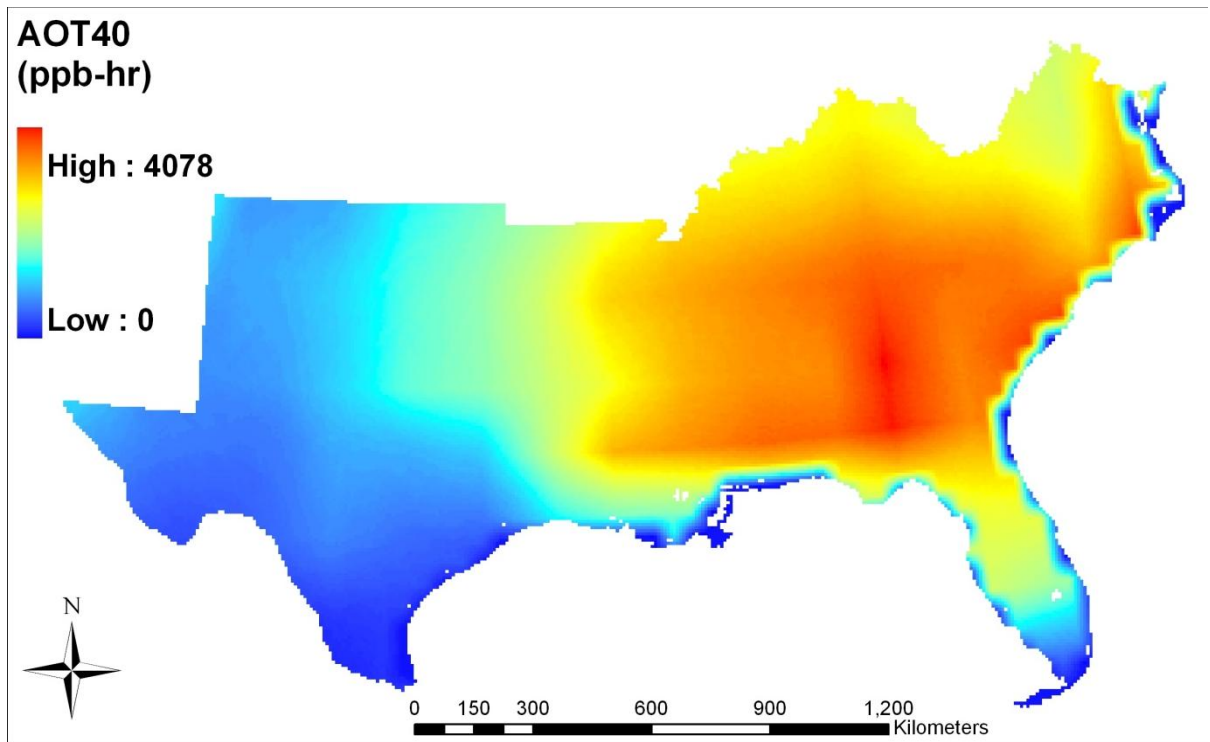


Figure C6.1.6 Spatial pattern of tropospheric ozone, using average AOT40 in 1990 as an illustration.

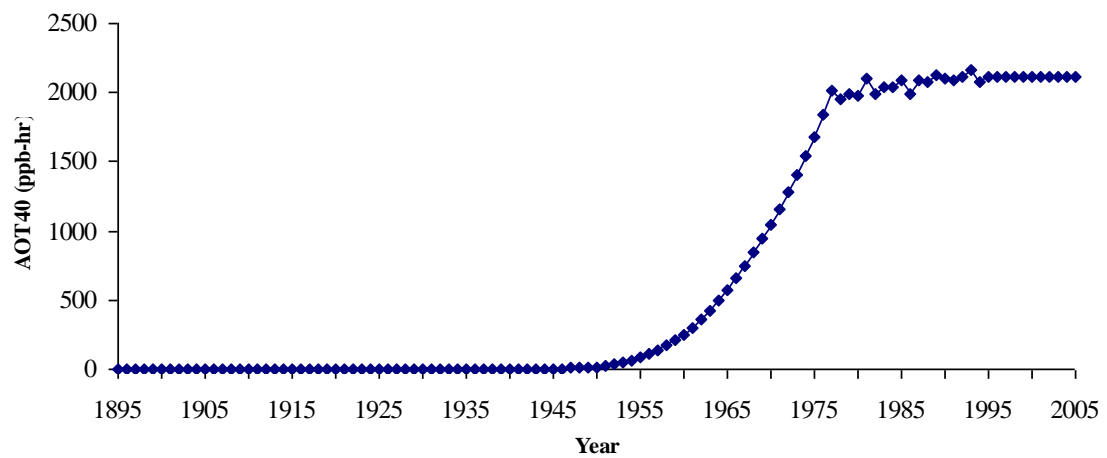


Figure C6.1.7 Temporal pattern of ozone input dataset. The AOT40 in years after 1995 are replications of the mean AOT40 of 1990 to 1995 [based on Felzer et al. (2004)].

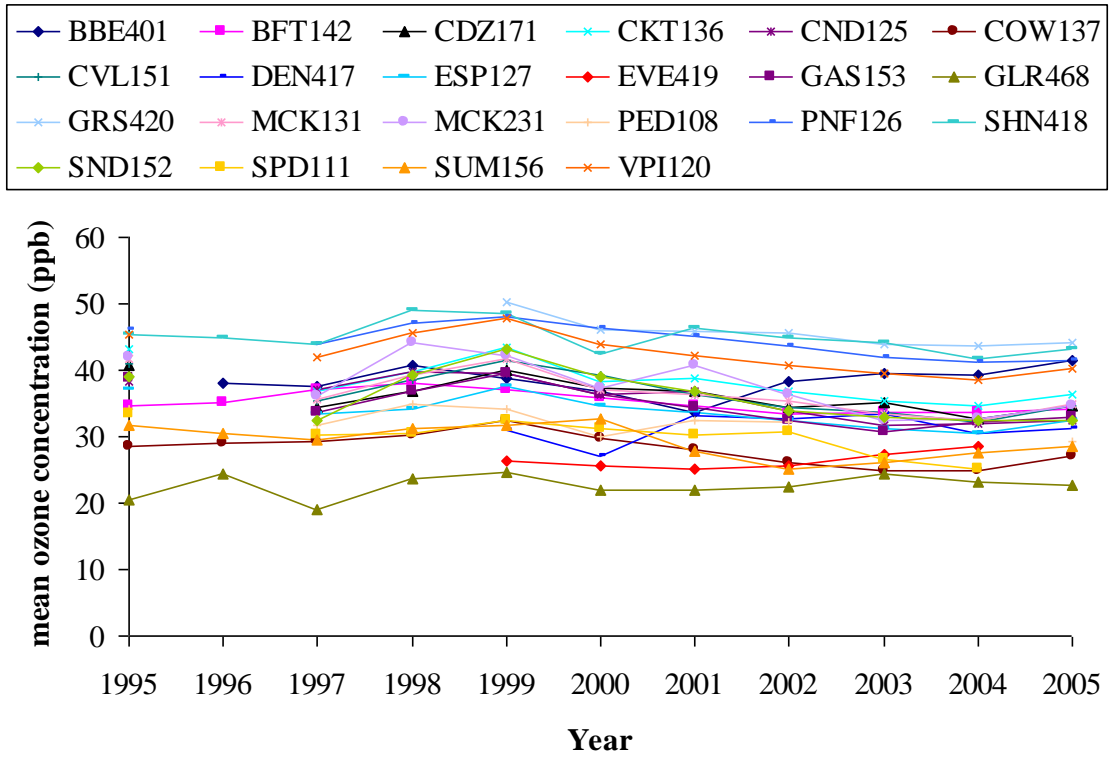


Figure C6.1.8 Annual mean ozone concentration records from 22 CASTNET stations in the study region showed that had continuous records of more than 5 years between 1995 and 2005. Legend shows the site-ids of the CASTNET stations.

2.2.3.3. Atmospheric CO₂ concentrations

For the years before 2003, a standard IPCC CO₂ concentration history dataset (Enting et al., 1994) was used in this simulation. Annual CO₂ concentrations after 2003 were calculated based on the "Global Annual Mean Growth Rate of CO₂" by Earth System Research Laboratory (ESRL, <http://www.esrl.noaa.gov/gmd/ccgg/trends/>) (Figure C6.1.13). To focus on the long-term interannual changes of atmospheric CO₂, we did not consider the intra-annual CO₂ concentration change in this study. The spatial pattern of atmospheric CO₂ concentration was assumed to be homogenous.

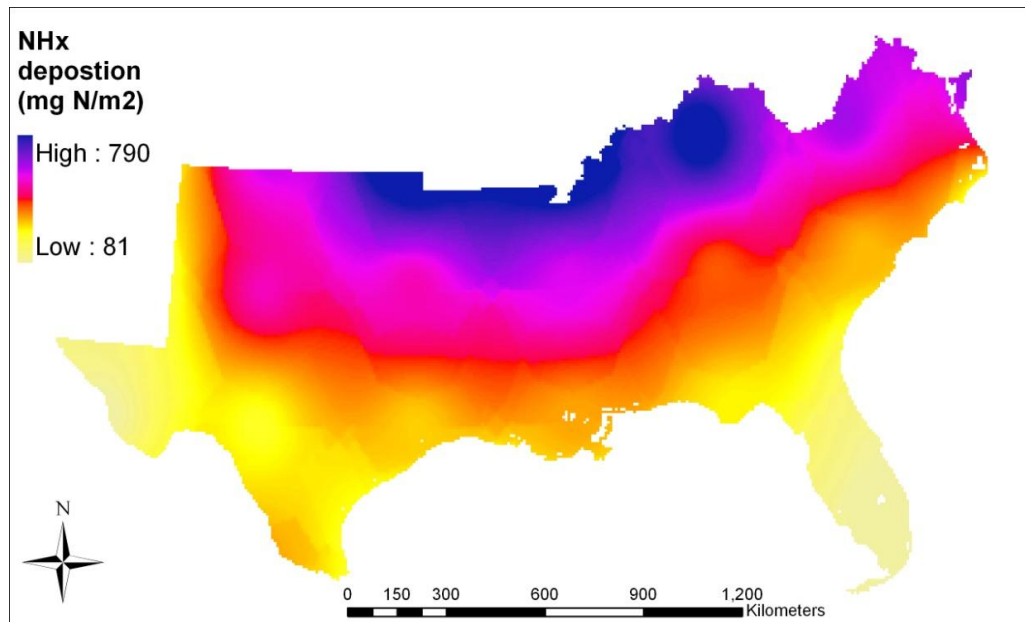


Figure C6.1.9 NH_x deposition in 2005 illustrated as an example. NH_x includes NH₃ and NH₄⁺.

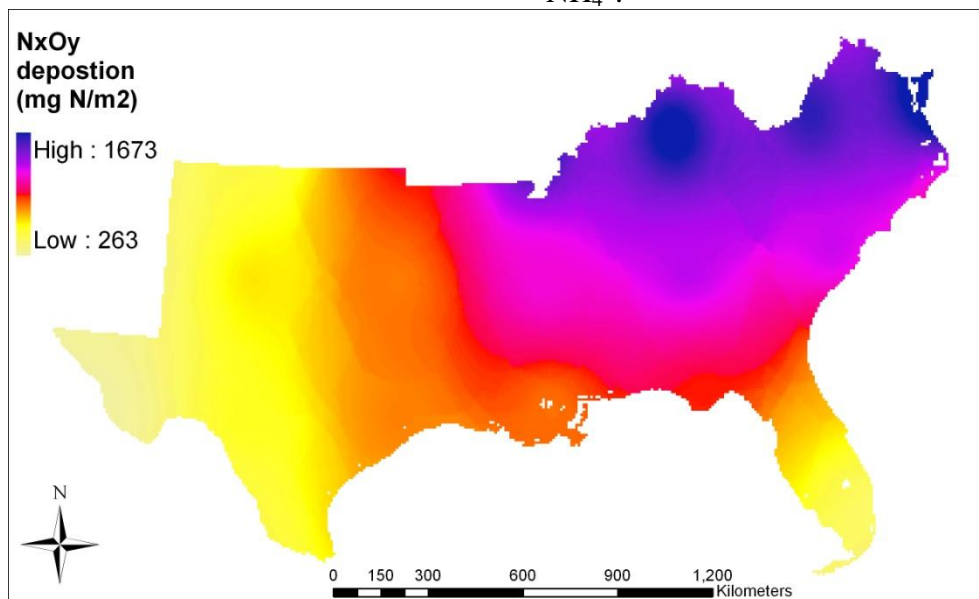


Figure C6.1.10 N_xO_y deposition in 2005 illustrated as an example. N_xO_y includes all oxidized forms of nitrogen other than N₂O.

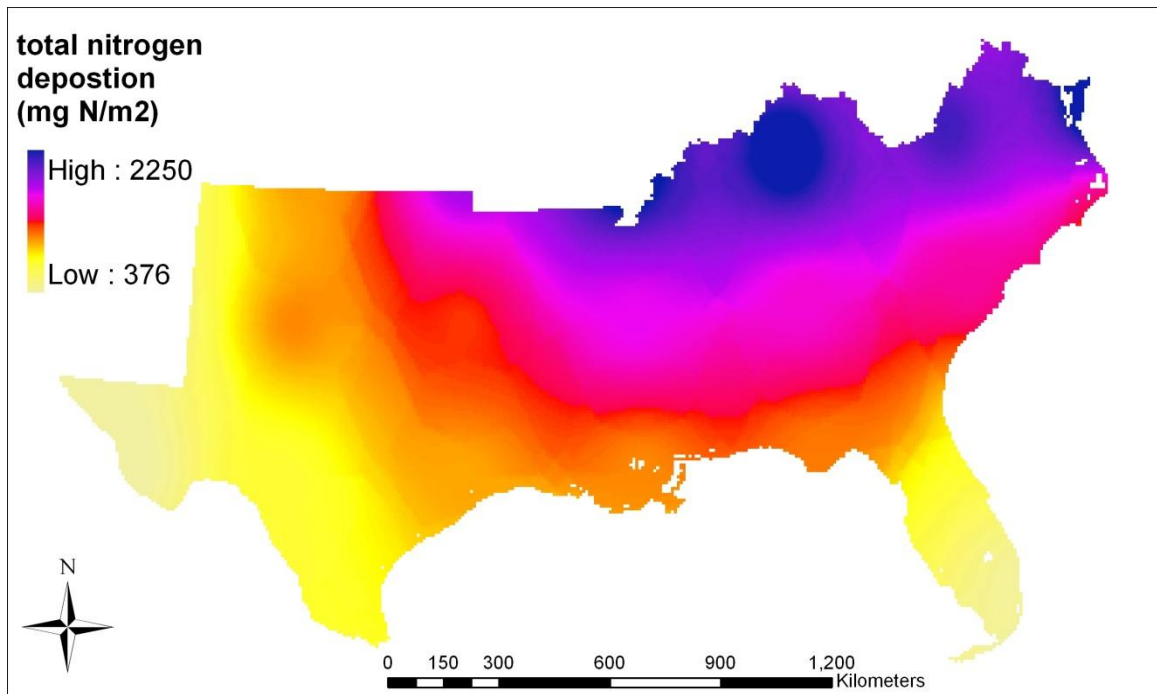


Figure C6.1.11 Total nitrogen deposition in 2005 illustrated as an example.

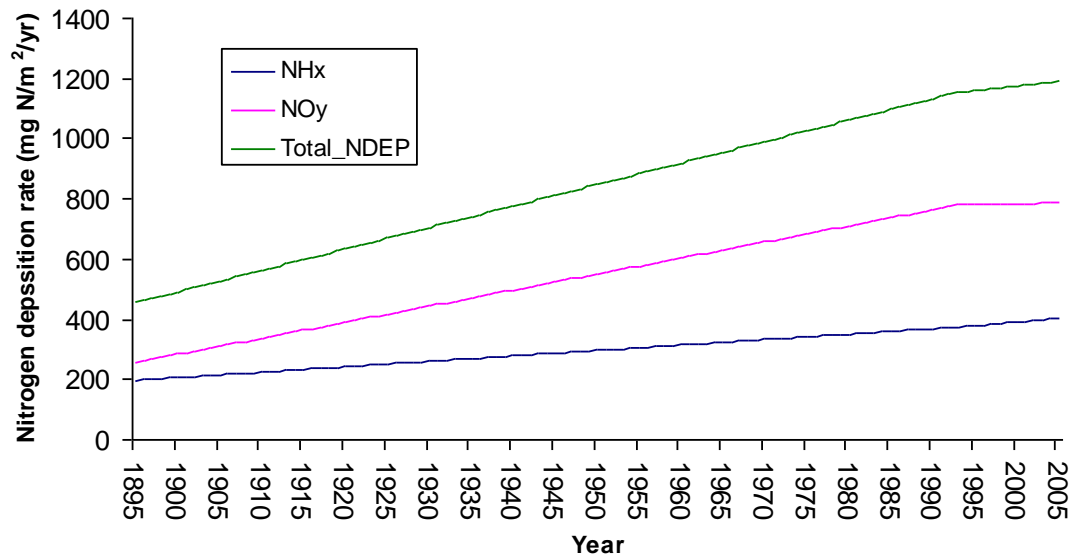


Figure C6.1.12 Temporal patterns of nitrogen deposition from 1895 to 2005 based on the three period (1860, 1993, 2050) N deposition dataset of Dentener (2006).

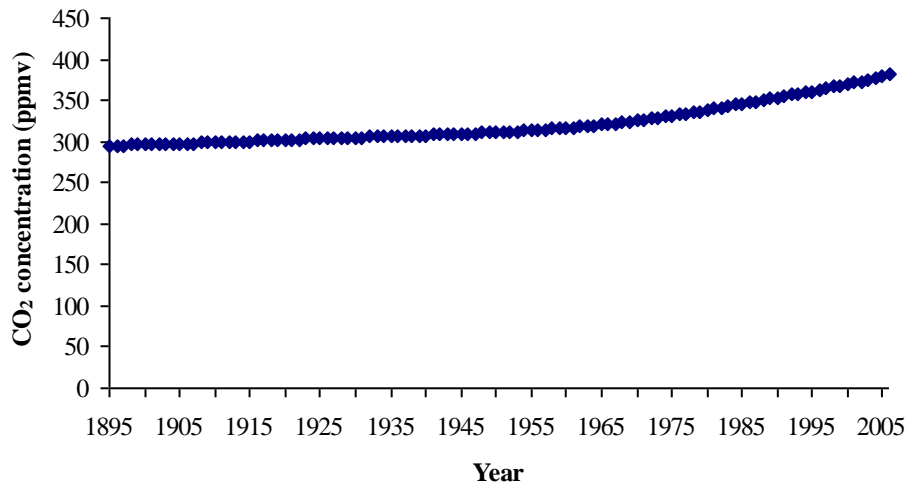


Figure C6.1.13 Changes in global mean atmospheric CO₂ from 1895 to 2005.

2.2.4 Land-use dataset

The land-use dataset included both the land management (*i.e.* cropland nitrogen fertilization maps), and land-use types (urban/developed region maps and cropland maps) from 1895 to 2005. We also generated the impervious map and urban lawn (*i.e.*, managed grasslands in urban/developed areas, the majority of which is turf grass) map based on the US Geological Survey (USGS) National Land Cover Database 2001 (NLCD 2001) (Homer et al., 2004). We then estimated the average proportions of impervious surface and urban lawn in the urban/developed regions of the SUS.

2.2.4.1. Cropland nitrogen fertilization maps

Alexander and Smith (1990) developed county-level nitrogen fertilization tabular datasets for the conterminous US from 1945 to 1985, and Ruddy et al. (2006) developed datasets

for the conterminous US from 1987 to 2001. By assuming the nitrogen fertilization of 1986 to be about the average of the amount in 1985 and 1987, we combined the two dataset together and derived a county level nitrogen fertilizer tabular dataset from 1945 to 2001. Then, based on the county-level cropland area census data (Waisanen and Bliss, 2002), we derived the nitrogen fertilization application dataset (gram N fertilizer per cropland area) (Figure C6.1.14 and 1.15).

2.2.4.2. Land-use change dataset

Approaches similar to Chen et al. (2006b) and Zhang et al. (2007) were used to combine the contemporary land-use map derived from the USGS National Land Cover Datasets (<http://edc.usgs.gov/products/landcover.html>) with the historical census datasets of croplands, urban area, and population to reconstruct maps of cropland and urban/developed regions from 1895 to 2005.

We first aggregated the 30-m resolution National Land Cover Map from USGS into 8 km resolution and recorded the fractions of human disturbed land-cover types (cropland and urban/developed region) in each grid. Then for the cropland data, we conducted temporal interpolation by calculating the cropland percentage for each cell in each year based on the cropland census data (Waisanen and Bliss, 2002) as the change trends. We used county-level relative change of cropland from the Census of Agriculture as controls to identify change rate of cropland so that the total area of a certain land-cover type would match the county-level data.

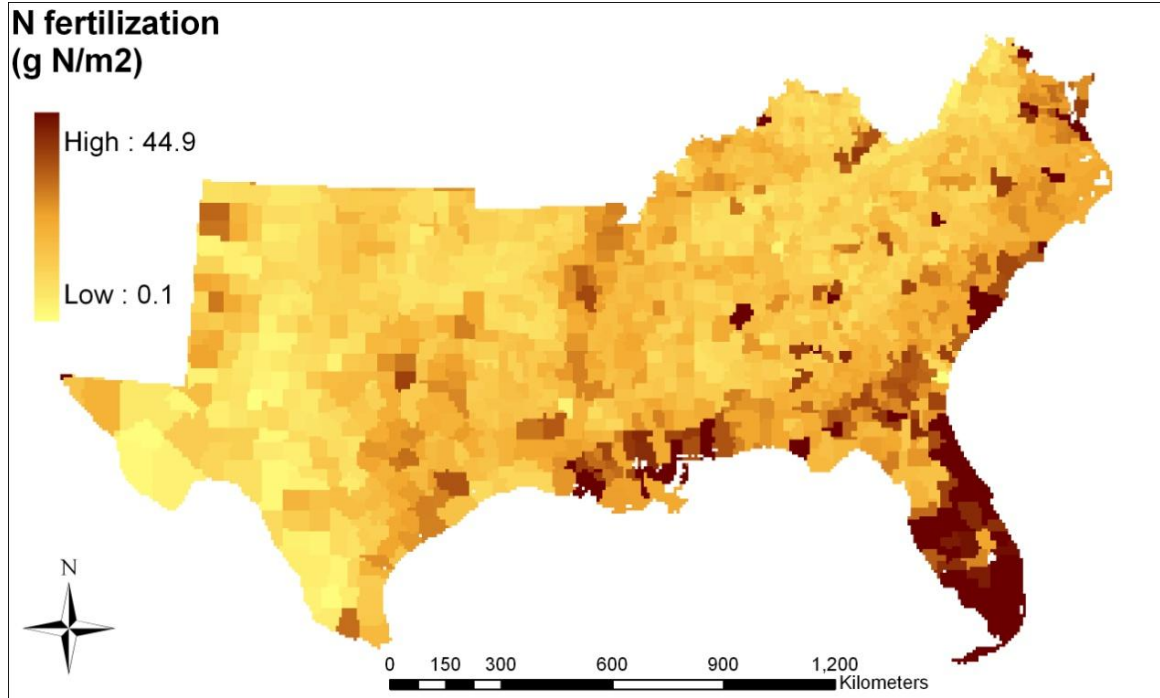


Figure C6.1.14 Spatial pattern of nitrogen fertilizer map of Southern US in 2000 as an illustration.

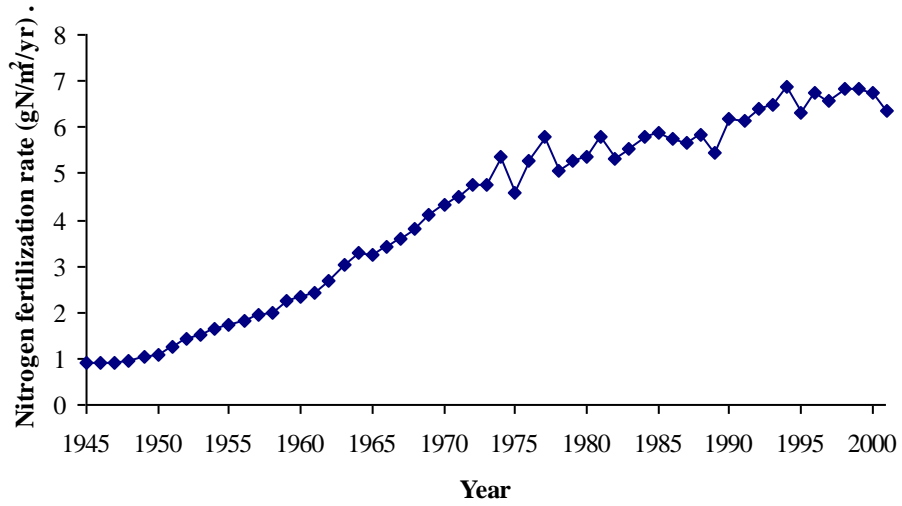


Figure C6.1.15 Temporal pattern of nitrogen fertilization in Southern US from 1945 to 2001.

Urban/developed region datasets were reconstructed in the same manner. During 1945–1997, the state-level urban area survey data (once every 5 year) conducted by the USDA Economic Research Service (<http://www.ers.usda.gov/>, verified 24 Jan. 2006) was used as a control to generate the annual urban area dataset using the linear interpolation method. For years before 1945 and after 1997, however, we reconstructed the annual urban maps by assuming the area was positively correlated with population density, due to the lack of urban census records (Waisanen and Bliss, 2002; <http://www.census.gov/>). Figures 1.16 and 1.17 illustrate the spatial and temporal patterns, respectively, of land-use change during the study period.

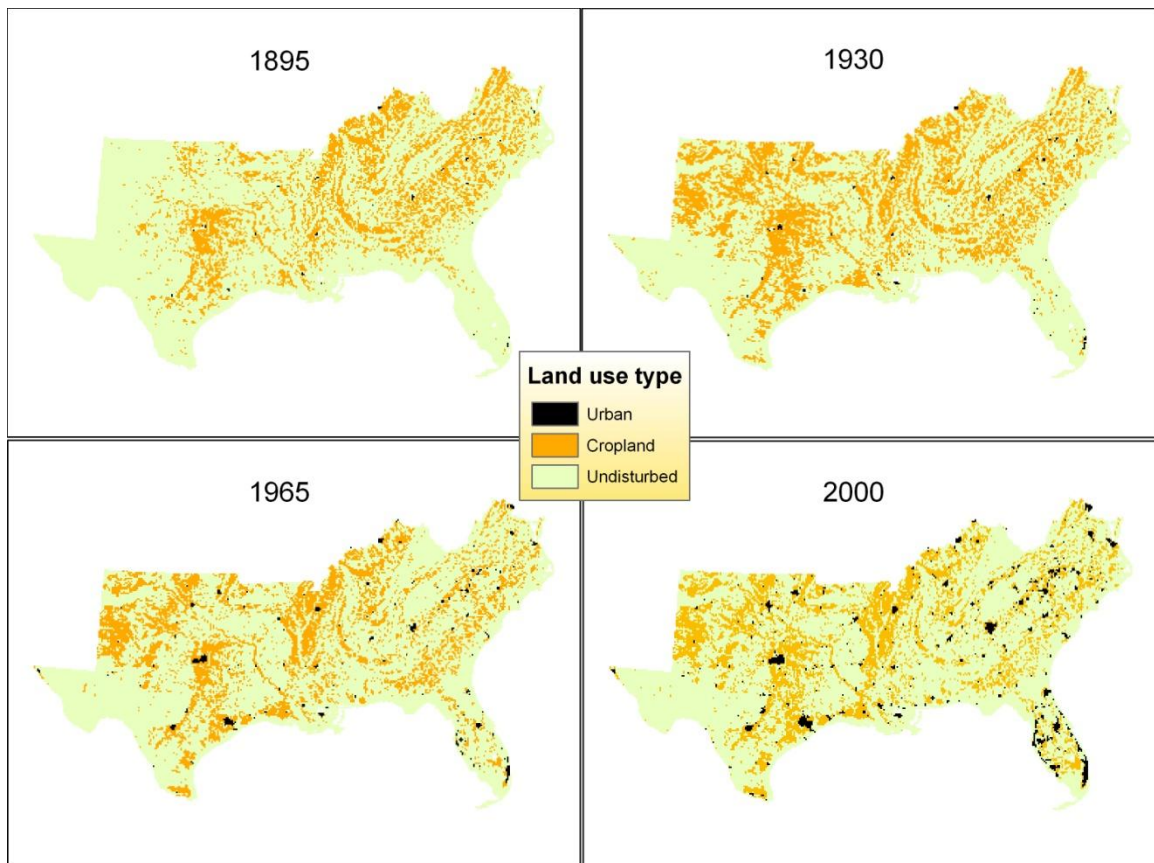


Figure C6.1.16 Spatial patterns of land-use change in Southern US during the study period (1865-2005).

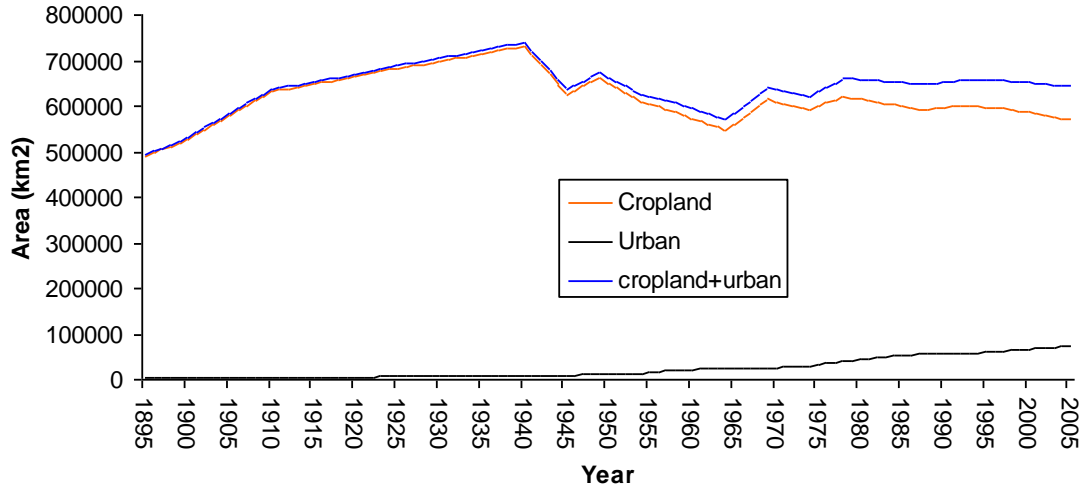


Figure C6.1.17 Temporal patterns of land-use change in Southern US from 1895 to 2005.

Cropland area kept increasing before 1920s, after the 1930s, cropland area declined gradually in the SUS. The urban/developed area was small until the end of the 1900s. After the 1940s, the urban/developed area in the SUS increased rapidly. The mean annual urbanization rate after the 1940 was 11 times the mean urbanization rate before 1940. In the last 30 years of the 20th century, urbanization processes accelerated in SUS. The mean annual urbanization rate after 1970 was about 130% higher than the urbanization rate before 1970.

2.2.4.3. Impervious surface and urban lawn

The USGS NLCD 2001 provides 30-meter resolution national wide impervious surface fraction map of entire US (Yang et al., 2003). We derived the SUS impervious map by cut out the study region from the national impervious surface map and aggregated it into

8 km resolution (Figure C6.1.18). According to Milesi et al. (2005), the following equations can be used to estimate the fraction of urban lawn, *i.e.* managed urban grassland the majority of which are turf grasses:

$$\text{lawn\%} = 79.53 - 0.83 * \text{ISA\%} \quad \text{equation 5}$$

where ISA% is the percentage of urban impervious area. This equation, however, is only valid in the urban regions. The results showed that the lawn covers about 14.43% of SUS urban area.

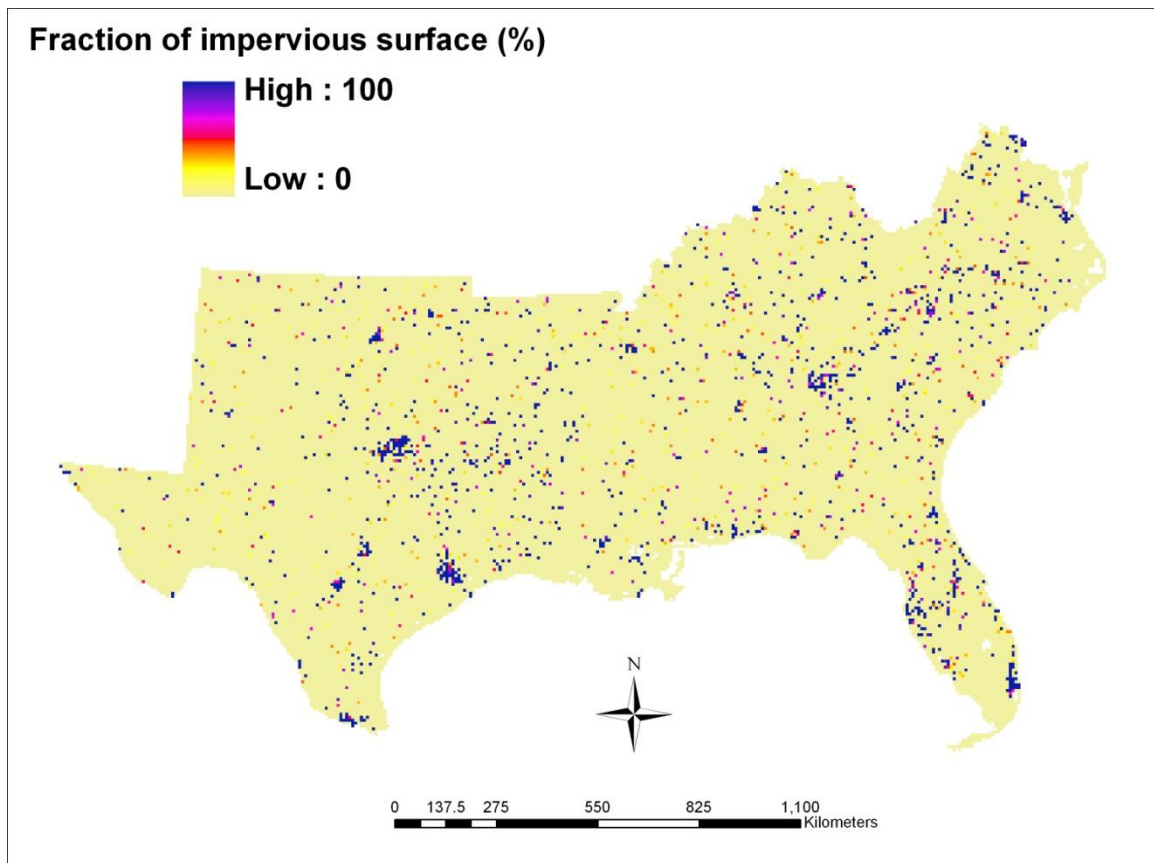


Figure C6.1.18 Impervious surface map of the Southern US in 2005.

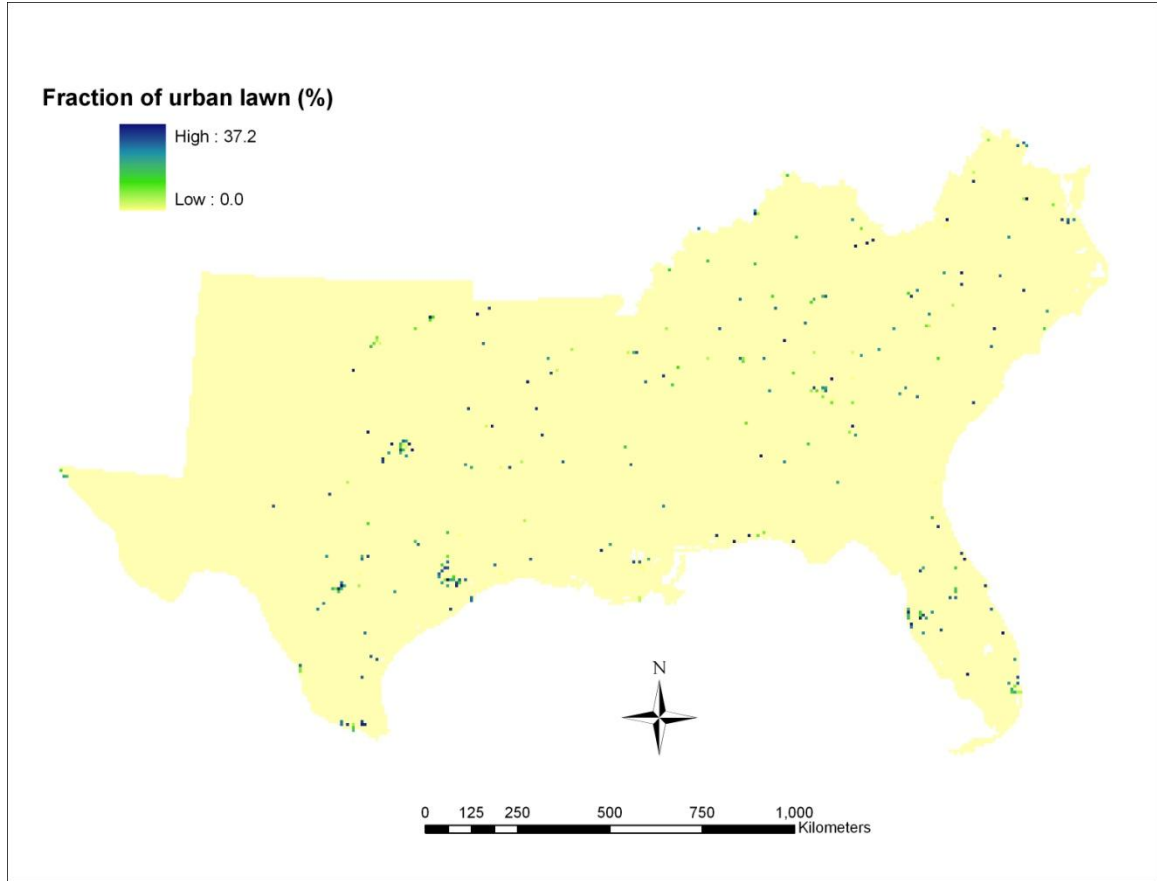


Figure C6.1.19 The distribution of urban lawn in the Southern US in 2005.

3. Results and discussion

3.1. Estimation of terrestrial carbon storage in the thirteen Southern United States

Based on our simulation results, the total terrestrial ecosystem carbon (TOTEC) storage of the thirteen southern United States is estimated to be 20.26 P g C ($1 \text{ P} = 10^{15}$) (Table C6.2.1), 55% of which is stored in soil, 39% in plant biomass, and about 7% in litter pools. Among the thirteen southern states, South Carolina has the lowest carbon storage

of 0.97 P g C, while Texas has the largest carbon pool size of 2.64 P g C, mainly due to its large area (about 31% of the total study area). Both the soil organic carbon (SOC) and litter carbon (LTRC) storage of Texas are the highest in the study region. North Carolina, however, has the largest vegetation carbon storage of 0.81 P g C among the 13 states. The two NE-SUS states in the study region, Virginia and North Carolina, together, contribute more than 20% of the total vegetation carbon storage of the southern United States, although they occupy only 10.9% of the study region.

Table C6.2.1 Estimated carbon storage of southern United States (unit: 10^{15} g C) according to our model simulation.

STATE	VEGC ¹	LTRC	SOC	TOTEC
Alabama	0.66	0.11	0.89	1.66
Arkansas	0.60	0.10	0.75	1.45
Florida	0.59	0.09	0.94	1.63
Georgia	0.66	0.12	1.01	1.79
Kentucky	0.67	0.10	0.60	1.37
Louisiana	0.55	0.08	0.75	1.39
Mississippi	0.55	0.08	0.67	1.30
North Carolina	0.81	0.13	0.97	1.90
Oklahoma	0.26	0.07	0.79	1.11
South Carolina	0.35	0.06	0.56	0.97
Tennessee	0.69	0.09	0.62	1.40
Texas	0.71	0.16	1.77	2.64
Virginia	0.80	0.12	0.74	1.65
SUS Total	7.89	1.32	11.05	20.26

1 VEGC: vegetation carbon; LTRC: carbon in litter and wood debris; SOC: soil organic carbon; TOTEC: total ecosystem carbon storage.

Although Texas has the largest carbon storage among the 13 southern states, it has the lowest total ecosystem carbon density of 3807 g C/m² (Table C6.2.2). Virginia has the highest total ecosystem carbon density of 15,138 g C/m². North Carolina, Kentucky, and Tennessee, have the second, third, and fourth highest total carbon density of the study region, respectively. These four states located in NE-SUS have a relatively high vegetation carbon density (average to 6482 g VEGC/m²) due to their large coverage of hardwood forests, while Texas and Oklahoma, the two states located in the western part of the study region, have lower vegetation densities (average to 1217 g VEGC/m²). The spatial pattern of the ecosystem carbon density is related to the land cover types (Figure C6.2.1).

Table C6.2.2 The estimated carbon density of the Southern United States (unit: g C/m²)

STATE	Vegetation carbon	Litter carbon	Soil organic carbon	Total carbon
Alabama	4861	827	6576	12263
Arkansas	4399	715	5488	10602
Florida	3582	560	5677	9819
Georgia	4275	792	6529	11597
Kentucky	6431	909	5689	13029
Louisiana	4212	637	5771	10621
Mississippi	4403	662	5337	10403
North Carolina	5904	931	7023	13858
Oklahoma	1413	372	4344	6129
South Carolina	4188	787	6793	11768
Tennessee	6296	870	5706	12872
Texas	1021	232	2553	3807
Virginia	7298	1082	6758	15138
SUS Average	3482	583	4876	8941

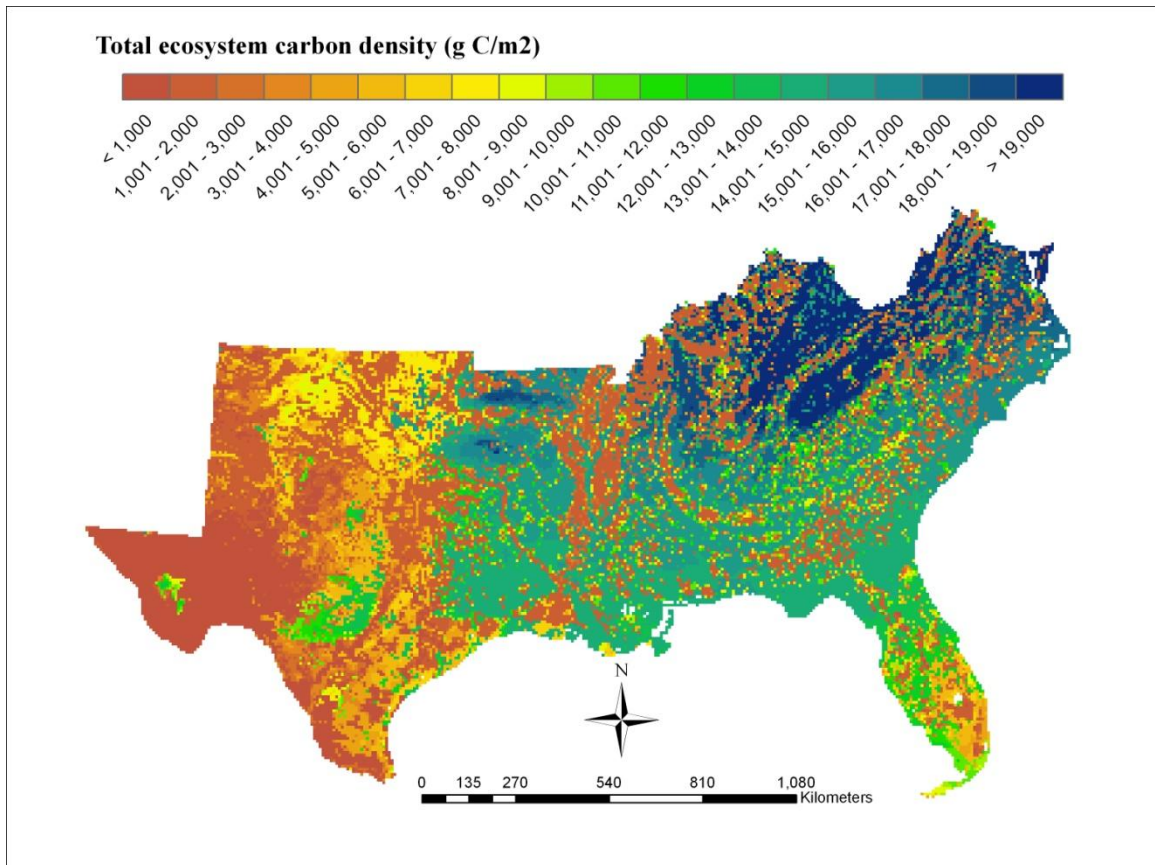


Figure C6.2.1 Total ecosystem carbon density of the Southern US in 2005 as estimated by our model.

3.2. The carbon storage and carbon density of different land-use/vegetation types

According to our model estimation, more than 46% of SUS total ecosystem carbon is stored in softwood forest (temperate evergreen coniferous forest), while about 38% is stored in hardwood forest. These forests in total account for 84% of the ecosystem carbon in the study region (Figure C6.2.2). The arid shrubland occupies more than 8% of the SUS, and stores only 0.5% of the regional ecosystem carbon due to its extremely low carbon density (596 g C/m²). Hardwood forests, in contrast, have a high carbon density of

17,097 g C/m² a value higher than the carbon density of softwood forest (14,150 g C/m²) (Figure C6.2.3). Softwood forests, however, occupy a larger area in the SUS and stores more carbon in total. Figure C6.2.3 indicates different land cover types have different carbon allocation pattern. While more than 80% of ecosystem carbon is stored in soil in grassland and cropland, more than half of the ecosystem carbon in hardwood forest is stored in vegetation biomass.

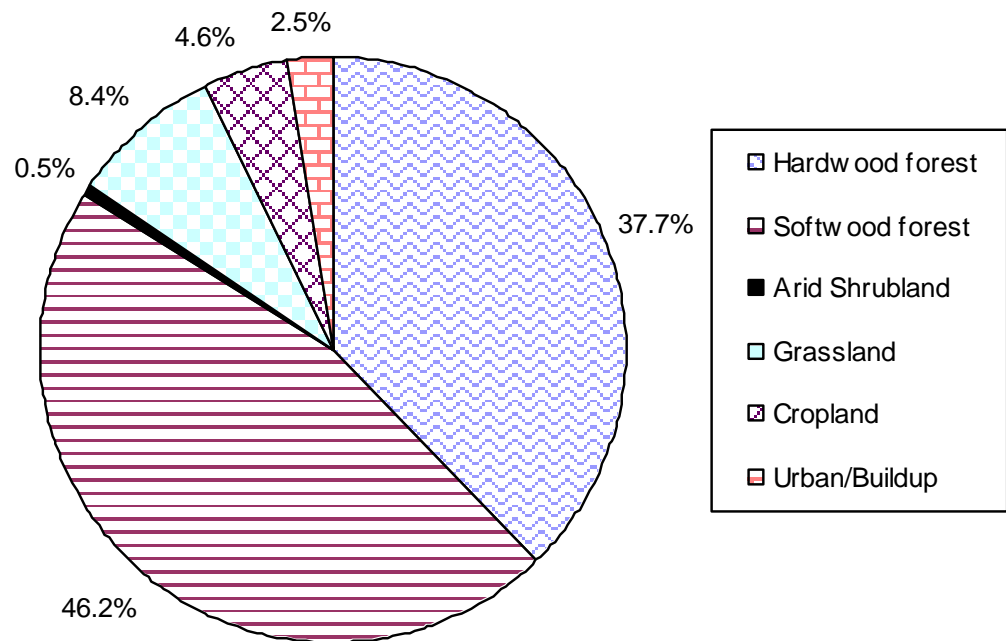


Figure C6.2.2 Ecosystem carbon storage in different land cover types of the Southern US in 2005 as estimated by our model.

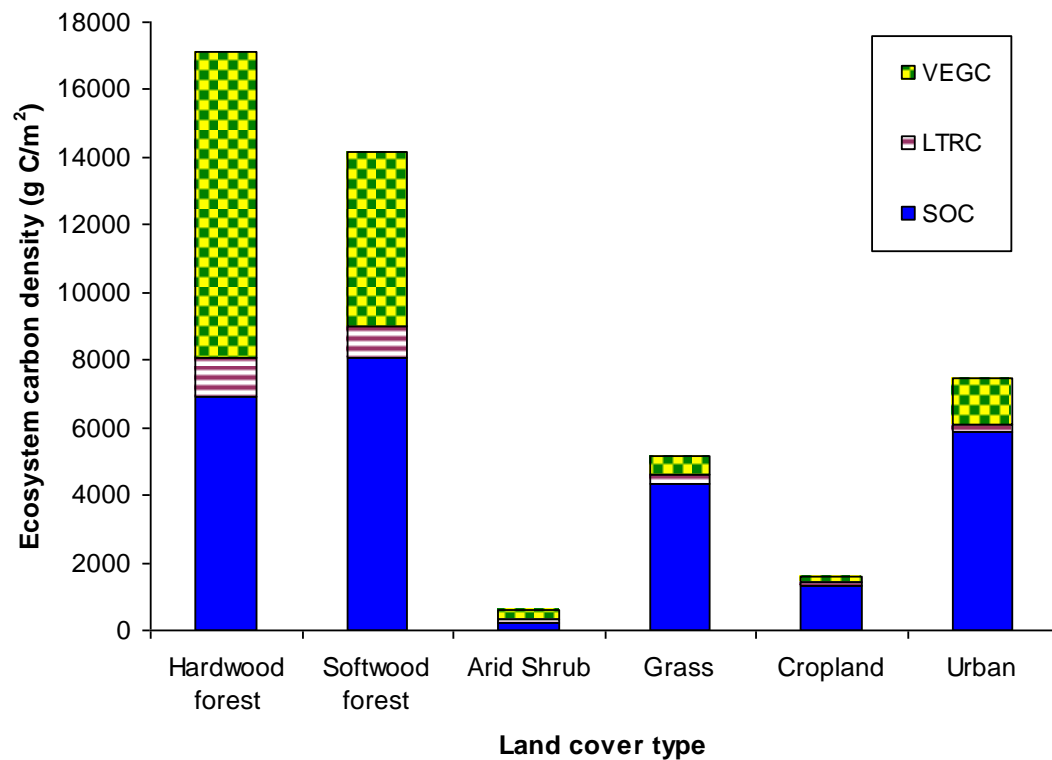


Figure C6.2.3 The ecosystem carbon density of different land cover types in the Southern US in 2005 as estimated by our model.

We further analyzed the total carbon storage of different land cover types in each of the 13 southern states (Table C6.2.3). Simulation results indicate that except for Oklahoma, where grasslands store nearly half of the total ecosystem carbon, the forest carbon pool generally composes the largest fraction of the total terrestrial ecosystem carbon storage. In the NE-SUS region most of the forest carbon is stored in hardwoods. In Arkansas, about half of the state carbon is stored in hardwoods, while 41% of terrestrial ecosystem carbon is stored in softwoods. In all other states, the majority of forest carbon is stored in softwoods. Except for forest and grassland, other land cover types store relatively small fractions of the total terrestrial ecosystem carbon. The shrubland carbon pool size in most

states can be ignored, except for Texas, where 4% of terrestrial carbon is stored in the shrubland. In average, the cropland carbon storage is about 4.6% of the total terrestrial carbon pool size of the study region. More than 38% of total cropland carbon is stored in two states, Oklahoma and Texas. In the SUS, Florida is the most intensively urbanized state (Wear, 2002). Urban and suburban regions cover more than 9% of the total state land area. Florida therefore, has the largest urban carbon pool size which equals one fourth of the total urban carbon storage in SUS.

Since the southern forest is the most important carbon pool in the study region, we further compared the simulated forest carbon density with the forest inventory datasets. We found that our simulated average hardwood vegetation carbon density in the study region is about 8381 g C/m² from late 1980s to early 1990s, 11% higher than the estimate based on the forest inventory dataset (Brown and Schroeder, 1999; Brown et al., 1999) (Table C6.2.4). Our estimation of softwood vegetation carbon density is about 5166 g C/m², slightly higher than Brown and Schroeder's (1999) estimate of 5026 g C/m². One possible explanation for our higher values is that we included all vegetative biomass in our simulation, whereas the estimate derived by Brown et al. (1999) included only trees with a diameter of more than 2.54 cm at breast height. Our estimation of forest soil carbon densities of the southern states are also comparable to the estimates based on the forest inventory analysis dataset (Birdsey and Lewis, 2002) (Table C6.2.5). The simulated average forest soil carbon density in 1987 and 1997 are 7364 g C/m² and 7540 g C/m² respectively, close to Birdsey and Lewis's (2002) estimation of 7225 g C/m² and 7245 g C/m².

Table C6.2.3 Carbon storage of different land cover types in the thirteen southern states (unit: T g C; 1 T = 10¹²) in 2005.

STATE	Hardwood forest		Softwood forest		Arid Shrubland		Grassland		Cropland		Urban / buildup	
	Carbon storage (T g)	Percent of state carbon storage	Carbon storage (T g)	Percent of state carbon storage	Carbon storage (T g)	Percent of state carbon storage	Carbon storage (T g)	Percent of state carbon storage	Carbon storage (T g)	Percent of state carbon storage	Carbon storage (T g)	Percent of state carbon storage
Alabama	347	21.0%	1255	75.8%	1	0.0%	1	0.1%	34	2.0%	18	1.1%
Arkansas	739	51.0%	604	41.7%	0	0.0%	9	0.6%	86	5.9%	11	0.8%
Florida	159	9.7%	1140	69.8%	0	0.0%	167	10.2%	56	3.4%	112	6.9%
Georgia	154	8.6%	1537	86.4%	0	0.0%	8	0.5%	41	2.3%	39	2.2%
Kentucky	1273	93.5%	11	0.8%	0	0.0%	3	0.2%	60	4.4%	15	1.1%
Louisiana	239	17.2%	1042	75.2%	0	0.0%	30	2.2%	45	3.3%	29	2.1%
Mississippi	428	33.0%	800	61.7%	0	0.0%	3	0.2%	51	3.9%	14	1.1%
North Carolina	1136	60.0%	631	33.4%	0	0.0%	2	0.1%	67	3.5%	55	2.9%
Oklahoma	203	18.3%	247	22.2%	3	0.3%	531	47.8%	112	10.1%	15	1.3%
South Carolina	88	9.1%	806	83.6%	0	0.0%	15	1.6%	24	2.5%	31	3.2%
Tennessee	1225	87.7%	84	6.0%	0	0.0%	6	0.4%	60	4.3%	23	1.6%
Texas	121	4.6%	1186	44.9%	106	4.0%	928	35.2%	243	9.2%	57	2.2%
Virginia	1533	93.4%	27	1.6%	0	0.0%	0	0.0%	47	2.9%	33	2.0%
Total SUS	7644	37.8%	9369	46.4%	109	0.5%	1704	8.4%	925	4.6%	453	2.2%

Table C6.2.4 Comparison of model-simulated vegetation carbon density (g C/m²) of each state against the estimate based on forest inventory data.

State	Time of Investigation (Year)	Estimation based on the forest inventory dataset ¹ (g C/m ²)		Model simulation result (g C/m ²)	
		Hardwood	Softwood	Hardwood	Softwood
Alabama	1990	6736	4416	8519	5030
Arkansas	1995	6556	5257	8073	5225
Florida	1995	7679	3545	7078	5075
Georgia	1989	8183	4737	9587	4913
Kentucky	1988	8086	4348	9029	5352
Louisiana	1991	8091	5468	8853	5111
Mississippi	1994	6906	4542	7969	5035
North Carolina	1990	9684	6524	9223	5318
Oklahoma	1993	4270	4136	7300	5181
South Carolina	1993	8402	5052	8453	5058
Tennessee	1989	7812	5019	8962	5662
Texas	1992	6068	5757	6574	4618
Virginia	1992	9560	6537	9334	5580
Average		7541	5026	8381	5166

¹ Forest inventory data were derived by the studies of Brown and Schroeder (1999); Brown et al. (1999).

Table C6.2.5 Comparison of model- simulated soil carbon density (g SOC/m²) from 1987 and 1997 against the state-by-state estimate based on the forest inventory analysis dataset (FIA) (Birdsey and Lewis, 2003) in the Southern US.

STATE	1987		1997	
	FIA SOC	Simulated	FIA SOC	Simulated
	(g C/m ²)	SOC (g C/m ²)	(g C/m ²)	SOC (g C/m ²)
Alabama	6718	7414	6856	7608
Arkansas	7022	7323	6932	7558
Florida	7224	7065	7345	7122
Georgia	7115	7549	7197	7740
Kentucky	8436	7169	8082	7374
Louisiana	6801	7128	7183	7220
Mississippi	6906	6887	6929	6844
North Carolina	7571	8313	7675	8494
Oklahoma	7079	7331	6816	7634
South Carolina	7209	7960	7005	8103
Tennessee	7128	7151	7061	7383
Texas	7102	6778	7281	7007
Virginia	7611	7666	7820	7927
Average	7225	7364	7245	7540

3.3. Carbon dynamics in the Southern United States from 1895 to 2005

During the study period (1895 - 2005), the carbon storage dynamic of the southern United States can be divided into two periods according to the general trend of the pool size (Figure C6.2.4). Our simulation shows that from 1895 to mid 1950, terrestrial ecosystems lost about 8% (1.56 P g) of its carbon storage (Table C6.2.6). From 1950 to 2005, however, they sequestered about 2.55 P g C, making the study region a net carbon sink of about 1 P g during the whole study period. From 1895 to 2005, the regional vegetation carbon and litter carbon storage increased by about 12% and 14% respectively, while the soil carbon storage did not change much (Figure C6.2.4). Figure C6.2.5 indicates that in the first half of the study period (1895-1950), except for Virginia which acted as a carbon sink of 1.3 T g per year, most southern states released carbon. In the second half of study period (1950-2005), all the southern states became carbon sinks. During the whole study period, except for the two SC states, Arkansas and Oklahoma, and one SE state, Florida which was nearly in carbon balance, all other states acted as a net carbon sink.

The carbon sequestration rate after 1980 was higher than any period in recorded history. From 1980 to 2005, the SUS uptake about 54.3 T g C each year, more than 6 times the mean carbon sequestration rate during the study period and 17% higher than the mean carbon sequestration rate after 1950 (Table C6.2.6). It should be noted that not all southern states became stronger carbon sinks after 1980. During the recent 25 years, the carbon sequestration rate of the four most productive states were either less than (*i.e.*

Virginia, North Carolina, and Kentucky) or equal to (*i.e.* Tennessee) the mean carbon sequestration rate since 1950, showing a trend of decreased carbon sequestration capacity in regions that already have high carbon density. Other SE states and Alabama have moderately enhanced carbon sequestration rates which were estimated to be about 9% to 14% higher than the mean carbon sequestration rate since 1950. The carbon uptake rates in most SC states were enhanced rapidly after 1980. For example, when comparing the mean carbon uptake rate between 1950 and 2005, Texas took up 2.5 T g more carbon each year after 1980, while the mean carbon uptake rate of Arkansas has increased by about 141% since 1980.

Many other studies also indicated that ecosystems of United States and the mid-latitude northern hemisphere might have acted as a net carbon sink in the last two centuries (Fan et al., 1998; Houghton et al., 1999; Caspersen et al., 2000; Pacala et al., 2003). We compared our estimation of SUS carbon sequestration rate with those of other regional studies as shown in Table C6.2.7. We found that our results are generally comparable, except that our estimation of the current (*i.e.* year 2004 to year 2005) time frame is only about two thirds of Pacala et al. (2007) estimate. Pacala et al. (2007) included in their estimation the carbon sinks due to woody encroachment (120 T g) and organic sediment accumulation (25 T g) which are not considered in our investigation. If these extra sinks were added to our results, current annual carbon sequestration rate of SUS ecosystems would be 52 g C/m², quite close to the national average of 54 g C/m². Therefore, the mechanisms of these two processes, especially the effects of woody encroachment, should be included into the DLEM model to make a more comprehensive assessment of

ecosystem carbon dynamics. Schimel et al. (2000) did not consider the effect of land-use change, the most important factor controlling the ecosystem carbon balance in the US since the 17th century. Therefore, their estimate of carbon sequestration rate could be lower than the actual value of regional total carbon sequestration capacity (Pacala et al., 2003).

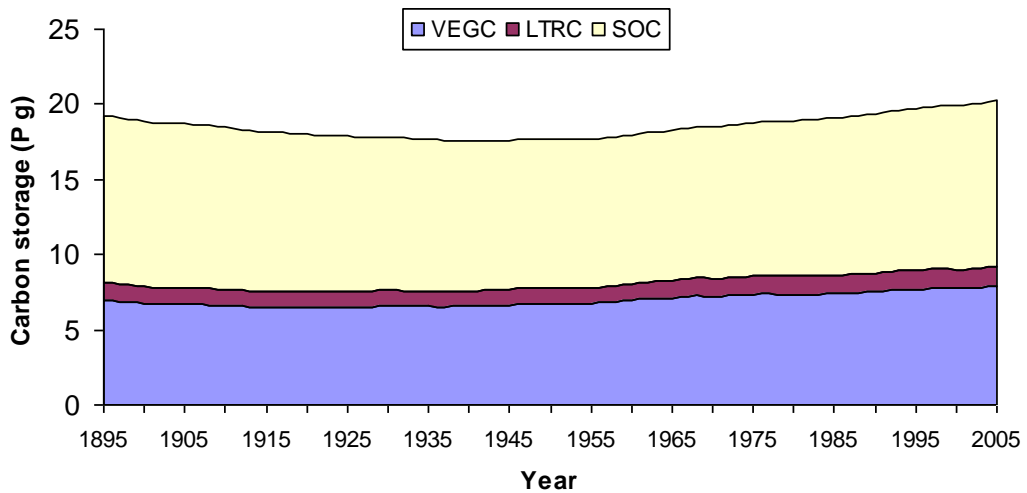


Figure C6.2.4 Trends in carbon dynamics in the southern United States from 1895-2005.

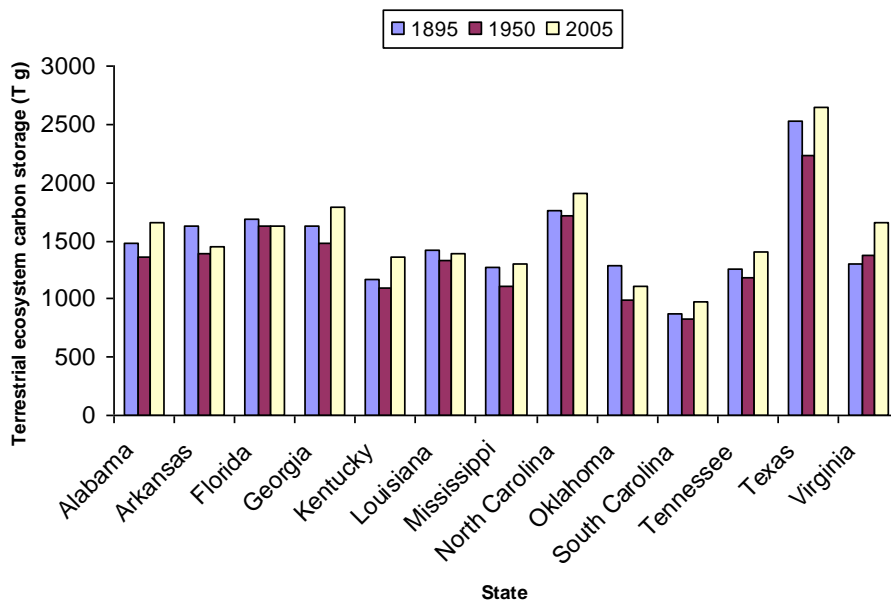


Figure C6.2.5 Carbon storage of 13 southern states in 1895, 1950, and 2005, respectively.

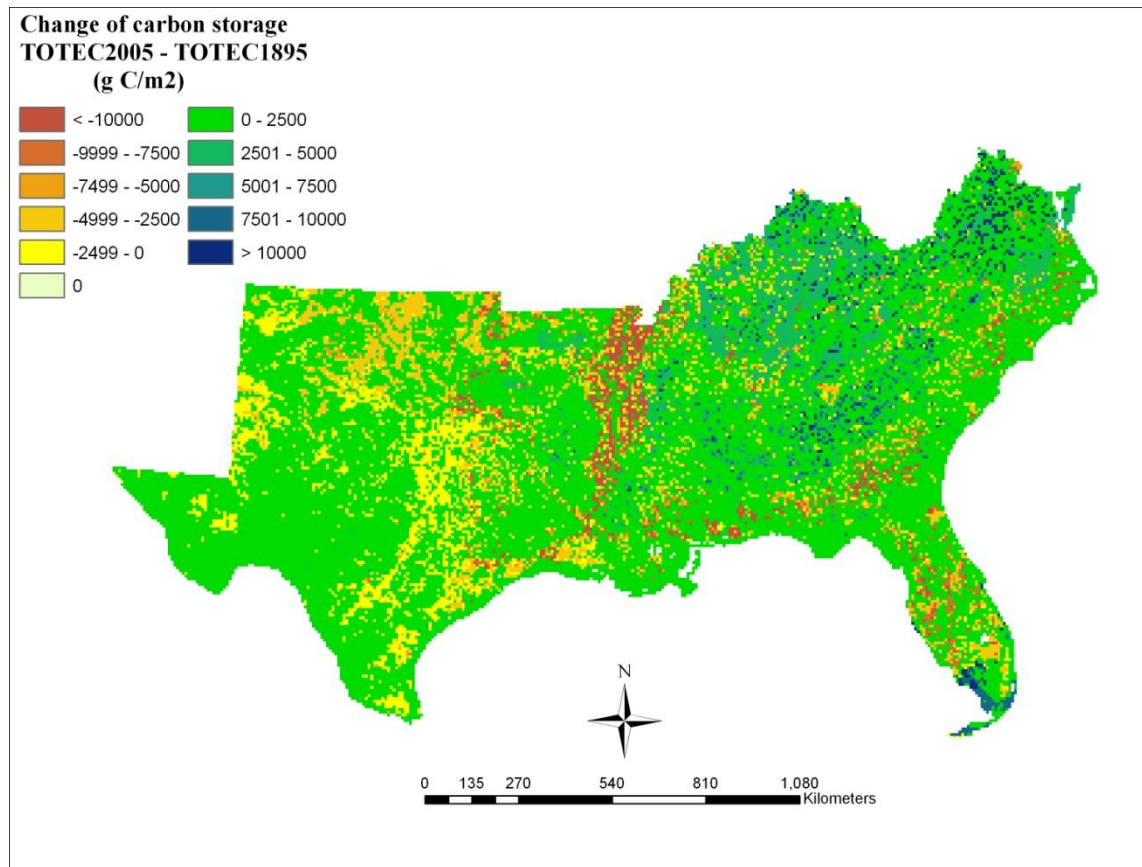


Figure C6.2.6 Spatial distribution of carbon sinks and sources in the Southern US during 1895 – 2005.

Table C6.2.6 Estimated total ecosystem carbon storage (TOTEC) of southern United States (SUS) in 1895, 1950, 1980, and 2005.

Abbreviations of State Names	AL	AK	FL	GA	KY	LA	MS	NC	OK	SC	TN	TX	VA	Total
TOTEC (T g C) of 1895 *	1482	1627	1678	1627	1167	1413	1277	1755	1292	871	1263	2525	1298	19276
TOTEC (T g C) of 1950	1366	1392	1627	1480	1093	1328	1112	1720	984	829	1182	2231	1370	17712
TOTEC (T g C) of 1980	1510	1387	1614	1634	1251	1338	1181	1832	1022	897	1303	2395	1544	18906
TOTEC (T g C) of 2005	1660	1451	1627	1787	1367	1389	1298	1904	1112	970	1405	2644	1650	20265
1950 - 1895														
ΔTOTEC (T g C)	-116	-235	-52	-146	-75	-86	-165	-35	-309	-43	-81	-294	72	-1564
change rate (T g C/year)	-2.11	-4.27	-0.94	-2.66	-1.36	-1.56	-3.00	-0.64	-5.61	-0.77	-1.48	-5.35	1.31	-28.44
2005 - 1950														
ΔTOTEC (T g C)	294	59	0	307	274	62	186	185	129	141	223	413	280	2552
change rate (T g C/year)	5.34	1.07	0.00	5.58	4.98	1.12	3.38	3.36	2.34	2.57	4.06	7.51	5.09	46.41
2005 - 1980														
ΔTOTEC (T g C)	150	64	13	153	116	51	117	72	91	73	102	250	106	1358
change rate (T g C/year)	6.01	2.58	0.51	6.13	4.63	2.04	4.69	2.90	3.62	2.94	4.08	9.98	4.23	54.33
2005 - 1895														
ΔTOTEC (T g C)	178	-176	-51	160	199	-24	21	149	-180	99	142	119	352	988
change rate (T g C/year)	1.62	-1.60	-0.47	1.46	1.81	-0.22	0.19	1.36	-1.64	0.90	1.29	1.08	3.20	8.99

* 1 T = 10¹²

Table C6.2.7 Comparison of model-derived SUS carbon sequestration rate against the estimates from other regional studies.

Source	Method	Region	Time	Regional carbon sink (T g)		Carbon sequestration rate g C/(m ² ·year)	
				low	high	Other studies	This study
Birdsey & Heath (2002)	Inventory Data	SUS	1987~1997	87		38	31
Ciais et al. (1995)	Book Keeping Model	Northern mid-latitudes	1992	2000	3500	33 ~ 55	50
Houghton et al. (1999)	δ ¹³ C measurements	US ¹	1980s	150	350	16 ~ 38	19
Pacala et al. (2007)	Literature review and synthesis	US	Current	492		54	36 ²
Schimel et al. (2000) 3	Biogeochemical Model	C. US	1980~1993	60	100	8 ~ 13	24
Schimel et al. (2001)	Inverse model	North America	1990~1994	800		32	38

1 Area of US is $9.162 \times 10^{12} \text{ m}^2$.

2 Pacala et al.'s (2007) estimate include the carbon sink due to woody encroachment (120 T g; 1 T = 10^{12}) and organic sediments accumulate in artificial lakes and in alluvium (25 T g) which are not included in our investigation. If added these sinks into the estimation of our study, current annual carbon sequestration rate of SUS ecosystems would be 52 g C/m^2 , quite close to the national average of 54 g C/m^2 estimated by Pacala et al. (2007).

3 Area of the terrestrial ecosystem of conterminous United States (C. US) is about $7.66 \times 10^{12} \text{ m}^2$ (Pacala et al., 2001). Schimel et al. (2000) did not consider the effect of land-use change, the most important factor that controls the ecosystem carbon balance in the US since the 17th century. Therefore, their estimate of carbon sequestration rate could be lower than the actual value of regional total carbon sequestration capacity (Pacala et al., 2003).

Figure C6.2.6 shows the spatial distribution of the net carbon balance of the study region from 1895 to 2050. The NE-SUS, where large areas of temperate deciduous forests have been maintained through time, were strong carbon sinks, while large areas of eastern Arkansas where many forestlands have been converted into cropland were carbon sources. Since the pattern of carbon balance seems to be related with the land-cover pattern, we compared the carbon dynamic of different land-cover types through the time (Figure C6.2.7). The carbon storage of forests increased significantly during the study period, although their carbon storage once decreased by about 1% during the first half of the study period. Cropland carbon storage decreased, while the carbon storage of urban areas increased during the study period.

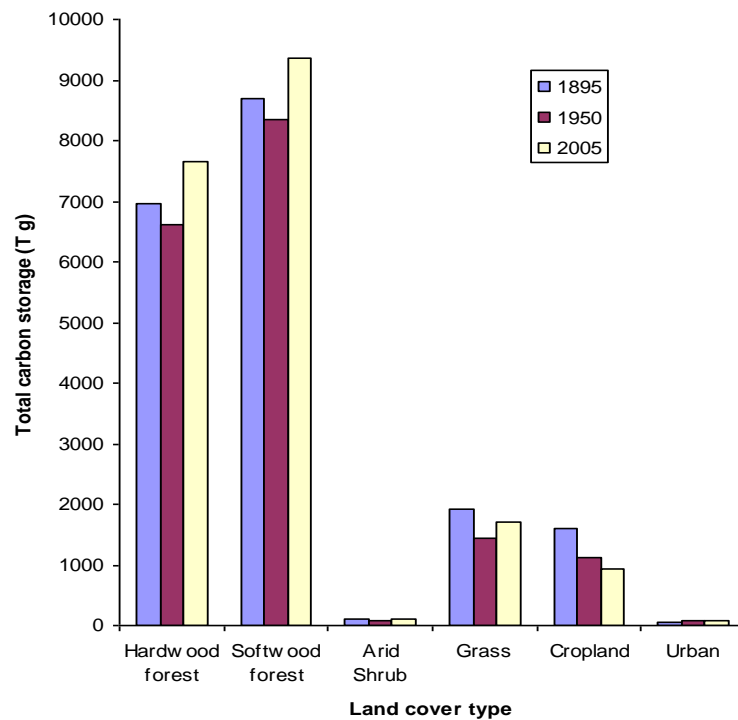


Figure C6.2.7 Comparisons of carbon storages of different land-cover types in the Southern US in 1895, 1950, and 2005.

3.4. Controls over SUS carbon dynamics

The carbon dynamics of terrestrial ecosystems are controlled by many factors including: climate (e.g. temperature, precipitation, and radiation), atmospheric chemical composition (e.g. CO₂ concentration, air pollutants such as ozone and nitrogen oxides), and land-use type (natural ecosystems, cultivated land, and urban area). One of the major advantages of DLEM, a highly integrated mechanistic ecosystem model, is that it can assess the impacts of individual factors that are usually highly spatially and temporally heterogeneous as well as assess the interactions among environmental factors and these combination effects on the ecosystem carbon balance. In this section we will analyze the spatial and temporal pattern of these environmental factors and their contribution to the carbon dynamic of the study region. First, we will discuss the impacts of climate factors. Since the potential incident radiation is decided by location and time, and net incident radiation is found to be highly correlated with precipitation and temperature variables (Thornton et al., 1997, 2000; Thornton and Running 1999), we will focus on the effects of temperature and precipitation. Second, we will discuss the effects of atmospheric changes. The atmospheric factors investigated in this research include CO₂, tropospheric ozone, and nitrogen deposition. The concentrations of these chemicals increased dramatically due to human activities in the last century. Third, we will discuss the impacts of land-use changes. A previous case study in west Georgia (Chapter 4) identified two counter-balanced land-use change processes in our study region: (1) deforestation for cultivation or urbanization and (2) the abandonment of cultivated land followed by reforestation. Finally, we will put all the factors together, and analyze their

combination effects. We will also try to assess the major control over the SUS carbon balance during the study period.

To discuss the mechanisms of how these environmental factors affect the ecosystem carbon balance, we will first analyze the dynamics of net primary productivity which controls the ecosystem carbon input and is sensitive to the environmental change.

Knowledge of spatial-temporal patterns of driven factors and their impacts on the ecosystem functions (e.g. productivity) can help us to identify critical time periods that control the carbon dynamic pattern. We will then discuss how the regional carbon balance varied through time in response to these environmental changes.

3.4.1. Effects of climate change

Climate factors, especially precipitation, are one of the major controls over ecosystem productivity and carbon balance (Tian et al., 2003). Nemani et al. (2003), for example, estimated that the global NPP increased by about 6% from 1982 to 1999 due to lengthened growing season. Another study indicated that global warming may enhance the productivity of boreal ecosystems (Peng and Apps, 1999). Ecosystem productivity, however, was found to be more sensitive to soil moisture in low latitudes or even some part of southern boreal ecosystems and therefore may be inhibited due to the dryness attributed to global warming (Melillo et al., 1993; Lüdeke et al., 1995).

Our simulation on the warm, temperate ecosystems in the SUS region indicated that the ecosystem productivity is generally controlled by the fluctuations of annual precipitation, while temperature seems negatively correlated with regional NPP (Figure C6.3.1). The average annual precipitation in SUS increased slightly from 1895 to 2005 (Figure C6.1.5). As the result, the mean annual NPP increased from 409 g C/m² in the first half of the study period (*i.e.* 1895 to 1950) to 418 g C/m² in the second half of the study period (1950 to 2005).

Since the climate and ecosystem productivity did not change dramatically in the study region, the ecosystem carbon storage did not vary significantly through time (Figure C6.3.2). Even the drought in the mid-1950s only resulted in 3% decrease in total ecosystem carbon storage (by comparing the decadal mean of 1950s against the mean of 1940s).

The patterns of carbon storage dynamics among states were highly variable. In Figure C6.3.3 we compared the change of carbon storage of the 13 southern states in 1895, 1955, and 2005. Texas has the largest variation in the three years possibly due to the sensitivities of its dry shrub-land and grassland ecosystems to the variation of precipitation. The variation of carbon storage in Oklahoma, another region whose grassland ecosystem is generally limited by soil moisture was also relatively high when considering its small carbon pool size.

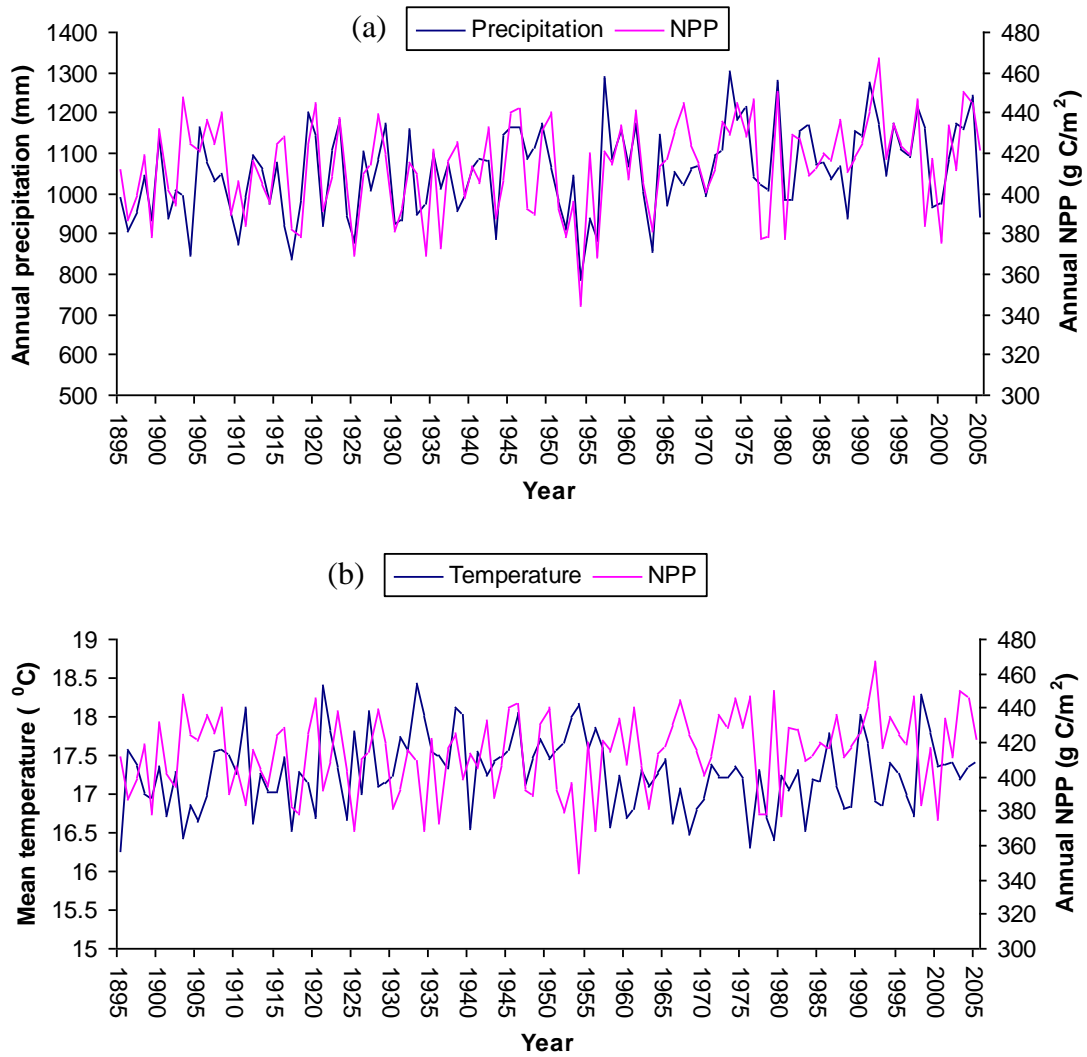


Figure C6.3.1 The effects of air temperature (a) and precipitation (b) on ecosystem productivity in Southern US estimated by model simulation. (a) The pattern of NPP generally follows the fluctuation of annual precipitation. (b) The temperature seems negatively correlated with the pattern of NPP; implying global warming may have a negative impact on warm temperate ecosystems like the Southern US.

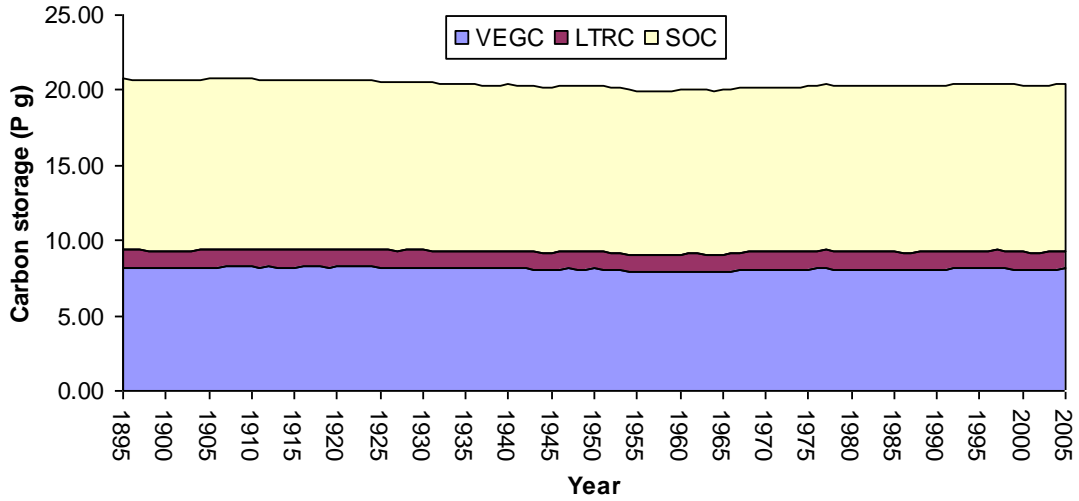


Figure C6.3.2 Changes in Southern US carbon storage in response to climate change during the study period (1895-2005).

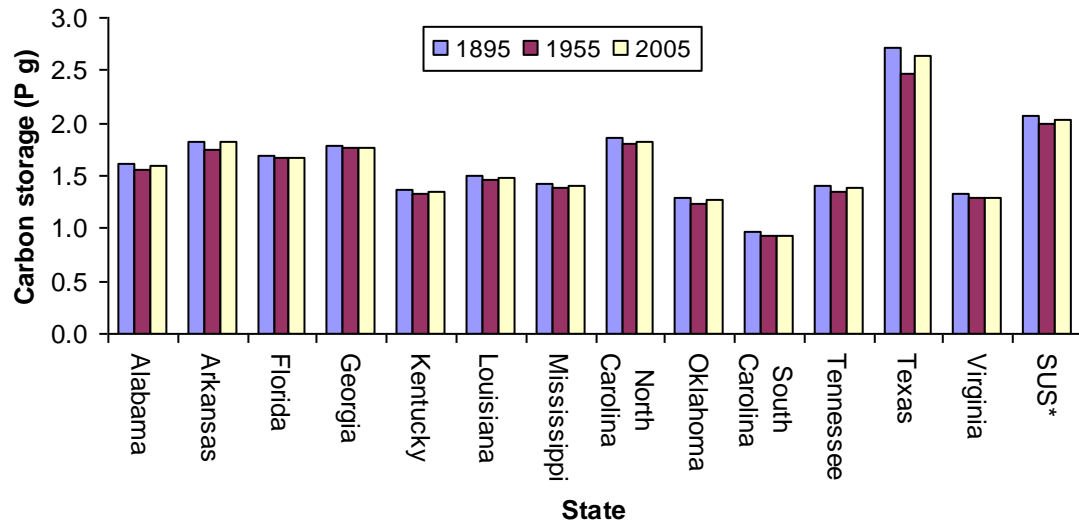


Figure C6.3.3 Comparison of the carbon storage of the 13 southern states in 1895, 1955, and 2005. * Note: The unit of total Southern US ecosystem carbon storage is 10 P g C.

In general, climate in the SUS did not change significantly from 1895 to 2005. As a result, there was no obvious impact on the regional carbon balance. The productivity of SUS ecosystems responded promptly to the variation of precipitation, especially in Texas and Oklahoma the two SC states whose vegetation types are dry-shrubland and grasslands.

3.4.3. Effect of atmospheric change

3.4.3.1. CO₂ fertilization effect

Atmospheric CO₂ concentration has risen quickly since the industrial revolution. The CO₂ concentration increased from 295 ppmv (1 ppm = 10⁻⁶) in 1895 to 380 ppmv in 2005. Accordingly, results of the single factor scenario, CO₂ (Table C6.4.1), suggests that the annual NPP of the study region may have changed from 425 g C/m² in 1895 to 496 g C/m² in 2005, increased by about 17% (Figure C6.3.4). The accumulation of atmospheric CO₂ and its effect on the NPP accelerated since mid-1950. Our results suggest that the NPP could have increased by about 12% from 1950 to 2005. Since plant response to CO₂ fertilization is nearly linear with respect to CO₂ concentration over a range of a few hundred ppmv around the ambient CO₂ concentration, as indicated by Robinson et al.'s review paper (1998), it is possible to normalize experimental measurements at different levels of CO₂ enrichment. Based on these results Robinson et al. (2007) estimated that, as the result of the atmospheric increase of about 80 ppmv from 1800s to 1990s, the production of hardwood trees could have been enhanced by 29%. Robinson et al. (2007) may have overestimated the CO₂ fertilization effect, however, since their analysis was

based on the response of young trees, and they also recognized that “The relative growth enhancement of trees by CO₂ diminishes with age”. As a comparison, Boisvenue and Running (2006), based on the results of Free Air Enrichment (FACE) studies (Norby et al., 2005), estimated that the CO₂ fertilization effect from 1950s to 1990s could have only increased global forest productivity by about 4%. Such a low value, however, may underestimate the forest response to CO₂ fertilization effect (Zhang et al., 2007). According to our estimation, the productivity of hardwoods may have increased by 13% since 1895, and 8% between 1950 and 1995. These values fall between the estimations of Robinson et al. (2007) and Boisvenue and Running (2006).

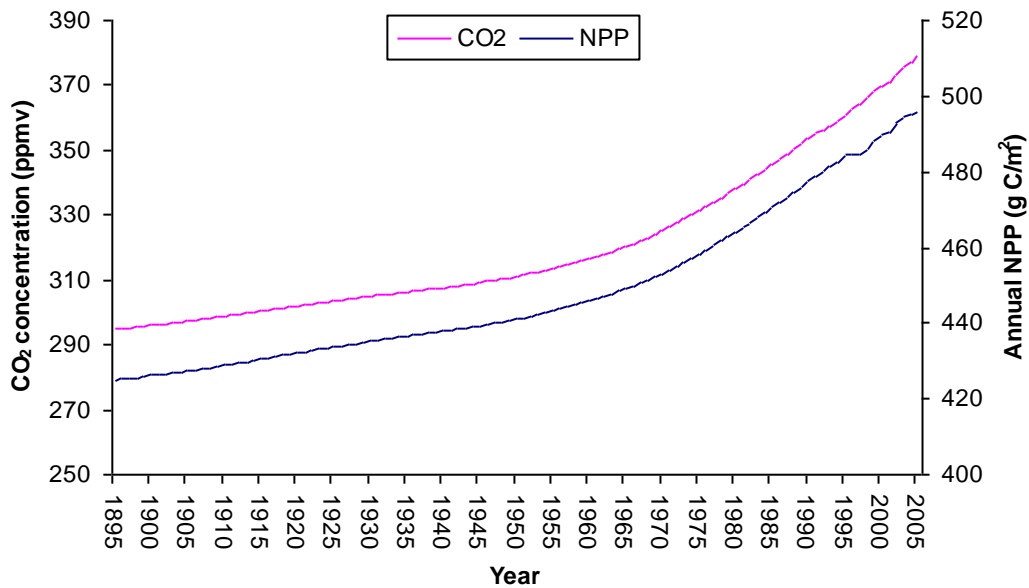


Figure C6.3.4 CO₂ fertilization effect on the annual NPP of the Southern US based on single factor scenario.

According to the results of the single-factor scenario, CO₂, SUS ecosystems constantly sequestered carbon from the atmosphere in response to the CO₂ fertilization effect. The whole study region sequestered about 1.72 P g C during the study period if all other

factors were not changed (Figure C6.3.5). Ecosystem response to elevated CO₂, however, is affected by other environmental factors, such as global warming (Oechel et al., 1994), nitrogen (Reich et al., 2006), phosphorus (Robinson et al., 2007), and water limitation (Volk et al., 2000). To estimate the actual impacts of atmospheric CO₂ concentration change on the ecosystem carbon dynamic, a better strategy is to compare the differences of ALLCOMBINE scenario against CLMO3NDEPLUC scenario (Table C6.4.1). We estimate the actual carbon sequestration due to CO₂ fertilization effect based on the following equation:

$$\text{CO}_2\text{_Effect} = \text{ALLCOMBINE} - \text{CLMO3NDEPLUC} \quad \text{equation 2.5}$$

Our analysis indicates that about 7% (1.47 P g C) of SUS carbon storage was fixed due to the CO₂ fertilization effect from 1895 to 2005. About 10% of this carbon was sequestered in the litter pool, the rest were evenly distributed in vegetation and soil pools (Figure C6.3.6). The study by the Vegetation/Ecosystem Modeling and Analysis Project (VEMAP) estimated that from 1980 to 1993 the climate/CO₂ change together resulted in a carbon sequestration rate of about 14.5 g C/m²/year in the SUS, where “the bulk of the increase is due to CO₂ fertilization” (Schimel et al., 2000). Our estimation of the CO₂-induced carbon sequestration rate in this period is about 10.8 g C/m²/ year, quite close to the estimation by VEMAP (Schimel et al., 2000). Due to its large area, Texas acted as the largest regional carbon sink of in response to the elevated CO₂. From 1895 to 2005, Texas terrestrial ecosystems sequestered about 346 T g C, more than 68% of which was accumulated in soil (Figure C6.3.6). The carbon sequestration rate of Texas, however,

was only 4.53 g C/m²/yr, the lowest among all the southern states (Figure C6.3.7). Due to the prompt response of hardwood forest to carbon fertilization (Robinson et al., 2007) (Figure C6.3.8), Virginia has the highest carbon sequestration rate of 8.37 g C/m²/yr, and more than half of the flux entered the vegetation carbon pool. Forests generally had higher carbon sequestration rate in response to rising CO₂ than shrub and croplands (Figure C6.3.8).

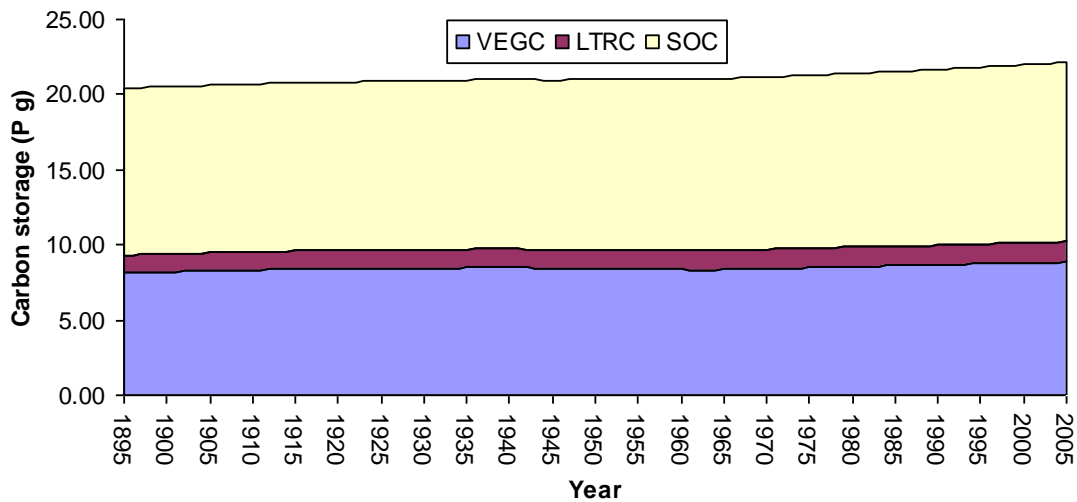


Figure C6.3.5 Dynamics of SUS carbon storage in response to elevated CO₂ concentration as indicated by the single factor scenario.

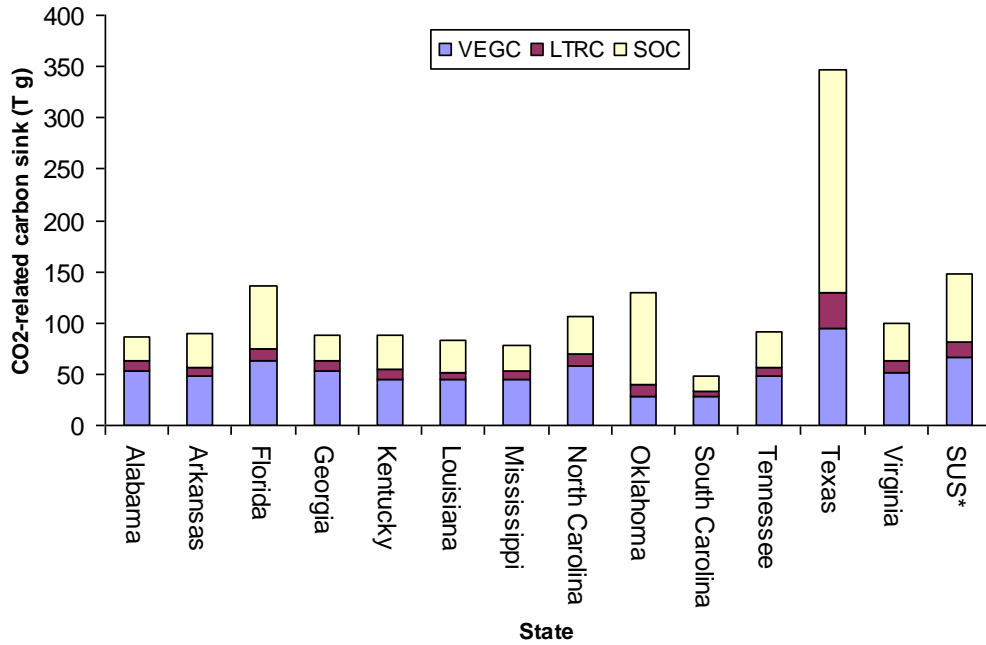


Figure C6.3.6 Carbon accumulation in ecosystems of the 13 southern states in response to the CO₂ fertilization effect during the study period. (The unit for SUS is 10 T g)

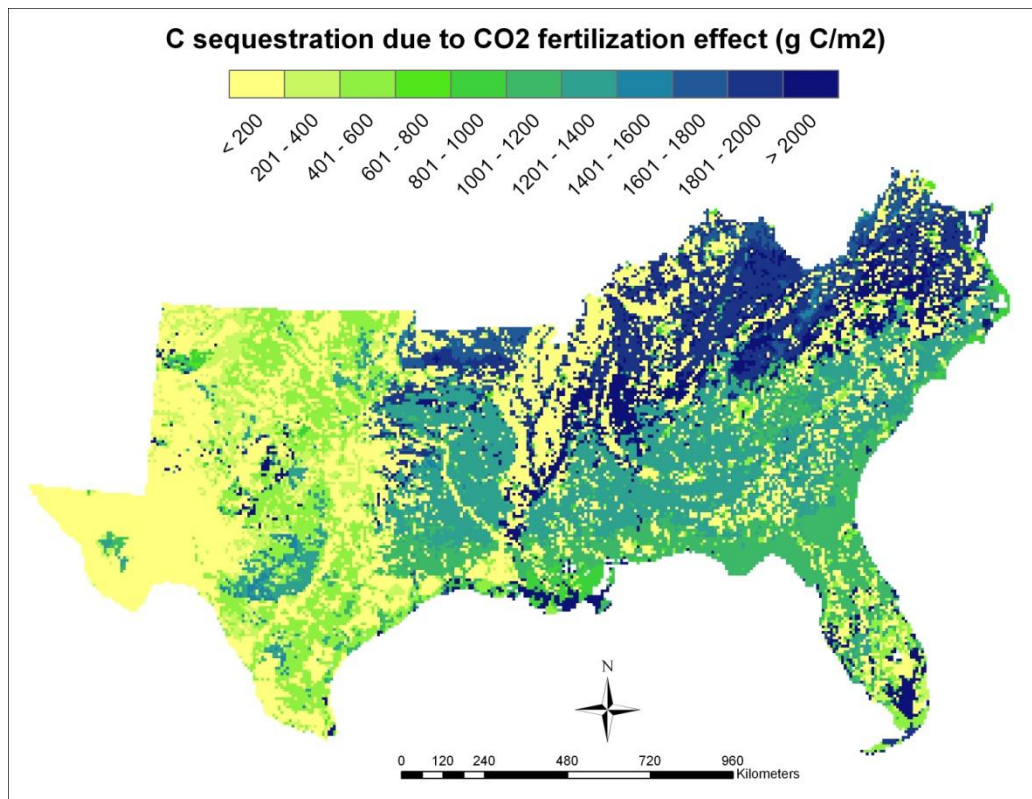


Figure C6.3.7 The CO₂-induced carbon sequestration map of the study region.

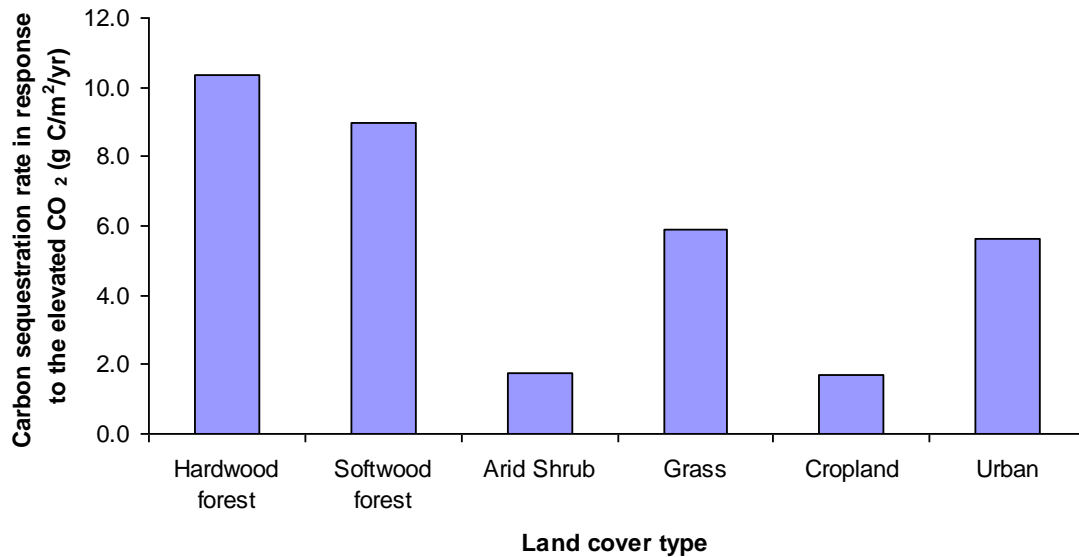


Figure C6.3.8 The response of land cover types to the elevated CO₂ concentration in the Southern US from 1895 - 2005.

3.4.3.2. Effect of tropospheric ozone

Increases in ozone exposures, AOT40, indicate that the ozone stress in SUS has increased dramatically since the mid-20th century. The results of the single factor scenario O3 suggest that this factor could reduce terrestrial ecosystem productivity by about 2.7%. This effect is only slightly higher than the impact of climate change (climate change from 1895 to 2005 increased NPP by about 2.2%; see Section 2.4.1). Our estimation of the ozone effect generally falls on the lower boundary of former studies. Based on a 6-year uncontrolled field study of mature loblolly pine growing in eastern Tennessee, McLaughlin and Downing (1995, 1996) reported that forest productivity could be reduced by 0~15% (average 5%) due to the ambient ozone stress. Teskey (1995)

reviewed the literature for southern coniferous forests, concluding that ambient ozone could reduce forest productivity by 2-5%. Chappelka and Samuelson (1998) reviewed the ambient ozone effects on forest trees of the eastern United States and suggested that ozone may reduce the growth of mature trees by about 2-9%.

Our study in the Great Smoky Mountains, as well as many other studies (e.g. Ollinger et al., 1997, 2002; Martin et al., 2001; Felzer et al., 2004; Hanson et al., 2005; Karnosky et al., 2005), showed that ozone stress could compromise carbon sequestration capacity of terrestrial ecosystems. We analyzed the impacts of ozone stress on carbon storage using the following equation:

$$O3_Effect = ALLCOMBINE - CLMCO2NDEPLUC \quad \text{equation 2.6}$$

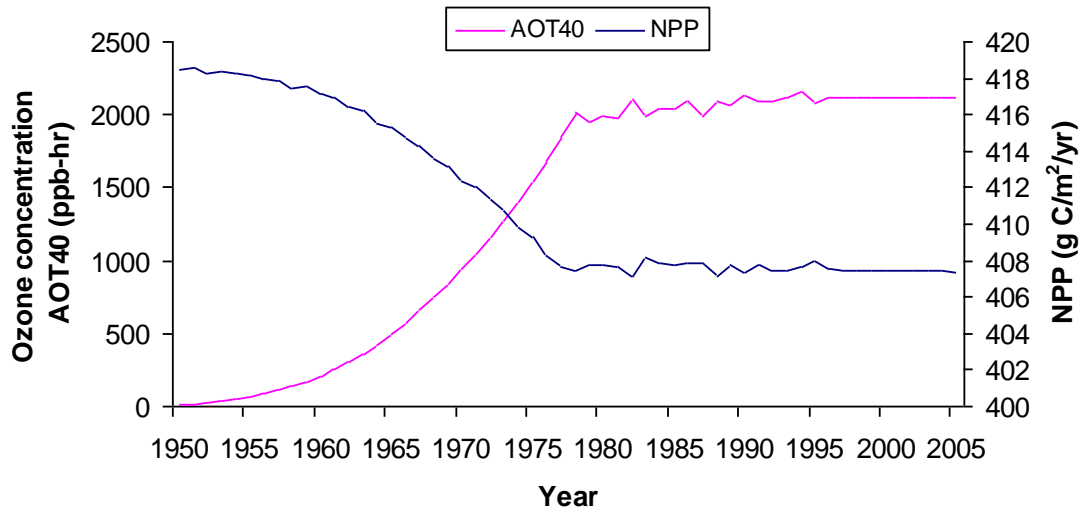


Figure C6.3.9 Effects of ozone stress on the ecosystem NPP estimated by a single factor scenario.

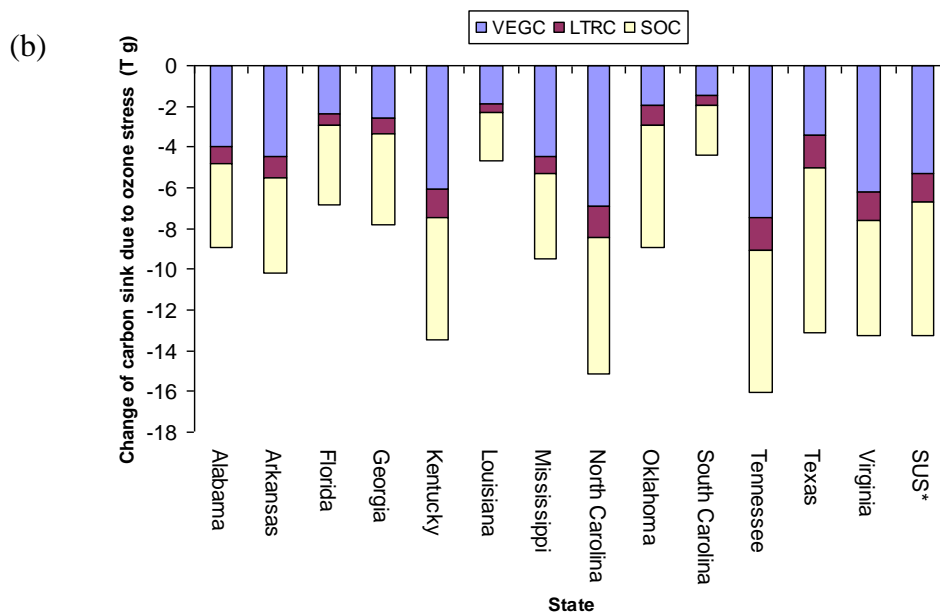
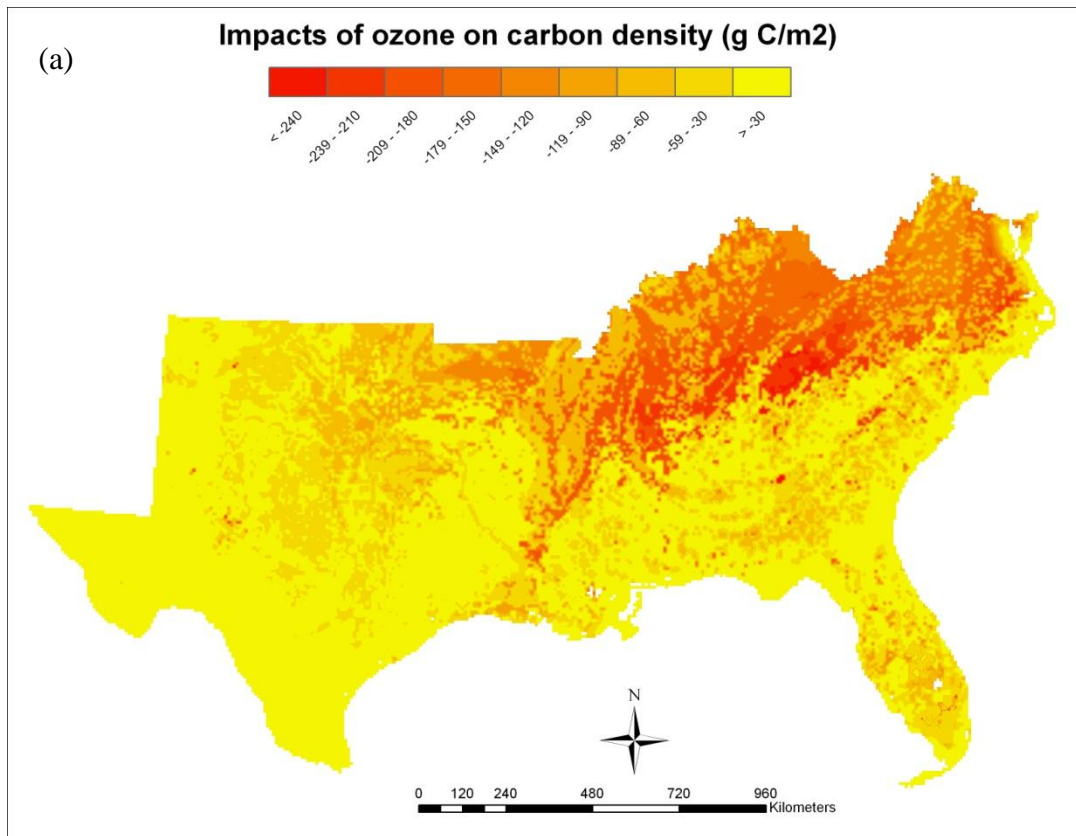


Figure C6.3.10 Impact of ozone stress on the terrestrial carbon storage in SUS. (a) Spatial patterns of the ozone impact. (b) The impact on carbon storage of each state. (* The unit of total SUS ecosystem carbon storage is 10 T g C.)

We estimate that the SUS terrestrial ecosystem could store 132.23 T g more carbon if there were no ozone stress. The SUS has relatively high tropospheric ozone pollution (Figure C6.1.6) and high carbon density (Figure C6.2.1). Therefore, ozone stress resulted in relatively high carbon loss in Tennessee, North Carolina, and Kentucky (Figure C6.3.10).

3.4.3.3. Effects of elevated nitrogen deposition

Because N supply often limits primary production and other ecosystem processes in the temperate and subtropical regions (Vitousek and Howarth, 1991; Vitousek et al., 1998; Galloway and Cowling, 2002), anthropogenic changes to the global N cycle are important to the ecosystem carbon balance (Högberg, 2007). According to the nitrogen deposition dataset compiled by Dentener (2006), the nitrogen deposition rate of the SUS might increase by 160% from 1895 to 2005. Based on the output of NDEP scenario, we estimated that the NPP would have increased by about 12% in response. A chronic N fertilization experiment in a mature North American temperate forest reported that the productivity of hardwood trees and softwood trees were enhanced by 12% and 10% respectively in response to the annual fertilization rate of 5 g N/m² (Aber et al., 1993). We compared the NPP of ALLCOMBINE scenario and CLMCO2O3LUC scenario, and found that during the study period the NPP of hardwood and softwood in SUS could have been enhanced by 12% and 6%, respectively, due to rising nitrogen deposition (Figure

C6.3.12). The lower increase of softwood NPP may be related to the relatively low N deposition it received (Figure C6.1.11 and Figure C6.3.12).

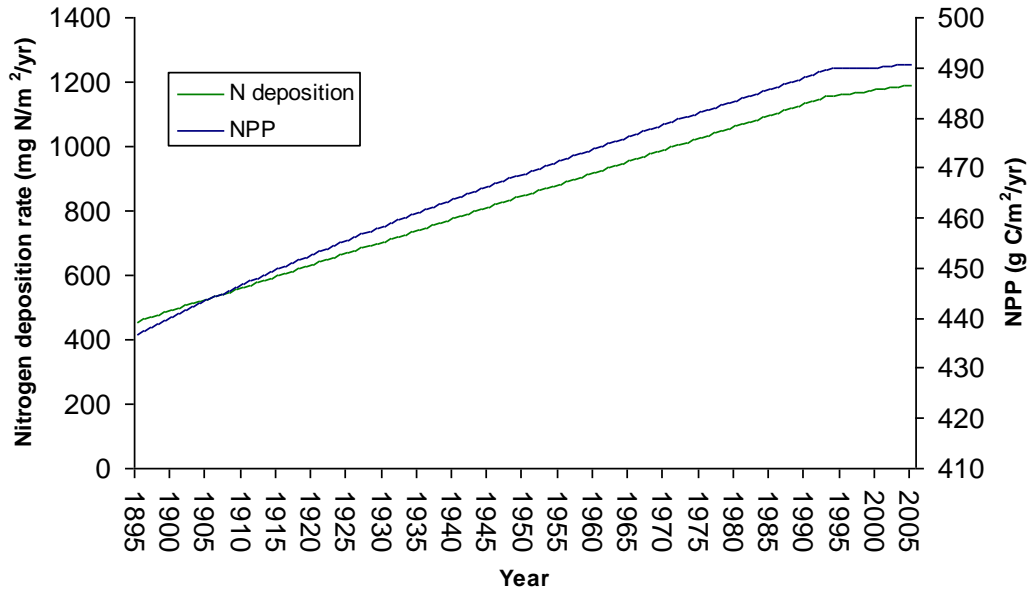


Figure C6.3.11 Impacts of elevated atmospheric N deposition on ecosystem productivity.

$$N_Deposition_Effect = ALLCOMBINE - CLMCO2O3LUC \quad \text{equation 2.7}$$

Based on equation 2.7, we estimate that from 1895 to 2005 the SUS terrestrial ecosystems sequestered about 1.97 P g C due to the elevated N deposition. The annual N deposition stimulated carbon sequestration rate is about 7.9 g C/m²/yr in SUS. Holland et al. (1997) estimated that anthropogenic N deposition stimulates C uptake in North America by 0.29 to 0.35 Pg C/yr. Dividing these values by the total area of North America, *i.e.* 25×10^{12} m² (Schimel et al., 2001), their estimation equals to a carbon sequestration flux of 12 to 14 g C/m²/yr. Nadelhoffer et al. (1999), however, suggested that Holland et al. (1997) overestimated the ecosystem response. They pointed out that Holland et al.'s (1997) estimation was based on the assumption that trees are the primary

sinks for nitrogen deposition while a ^{15}N -tracer study in nine forests indicated that the soil was the primary sink. Gifford et al. (1996) explored the assumptions about the partitioning of N deposition between different ecosystem pools. Their work suggested that the strength of N deposition stimulated carbon sink could decline by 83% if N deposition entered soil first. The actual N deposition stimulated carbon uptake in North America, therefore, could range from 2 to 14 g C/m²/yr.

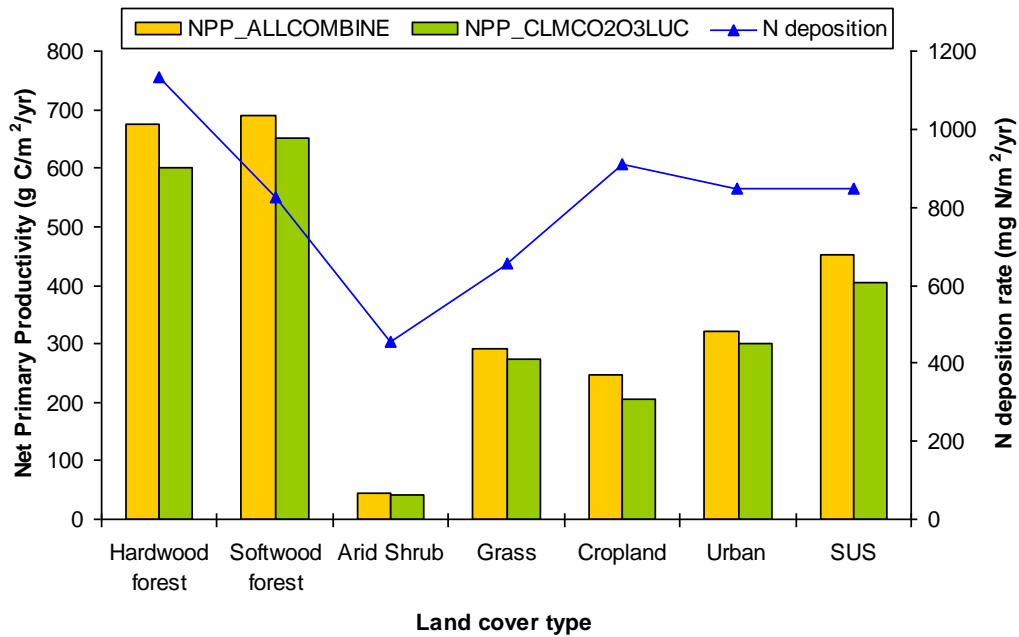


Figure C6.3.12 Responses of different land cover types to the elevated atmospheric N deposition.

Our results indicated that about 48% of the sequestered carbon accumulated in the soil carbon pool, 42% in vegetation carbon pool, and 10% in litter carbon pool (Figure C6.3.13). Texas, although the largest carbon sink, had the smallest carbon sequestration rate of 3 g/m²/yr. Virginia has the highest N deposition stimulated carbon uptake rate (15

g C/m²/yr). The different vegetation types could explain the different carbon uptake rate among southern states (Figure C6.3.14). Our simulation results, like other studies (Vitousek and Howarth 1991; Vitousek et al., 1998), indicated that forest ecosystems are more sensitive to the N fertilization effect (Figure C6.3.14). We normalized the C uptake response rate for each vegetation type by the average N deposition they received. We found that the forest response to N fertilization was about 14.5 g C/ g N, more than 2 times larger than the response of other vegetation types (Figure C6.3.14).

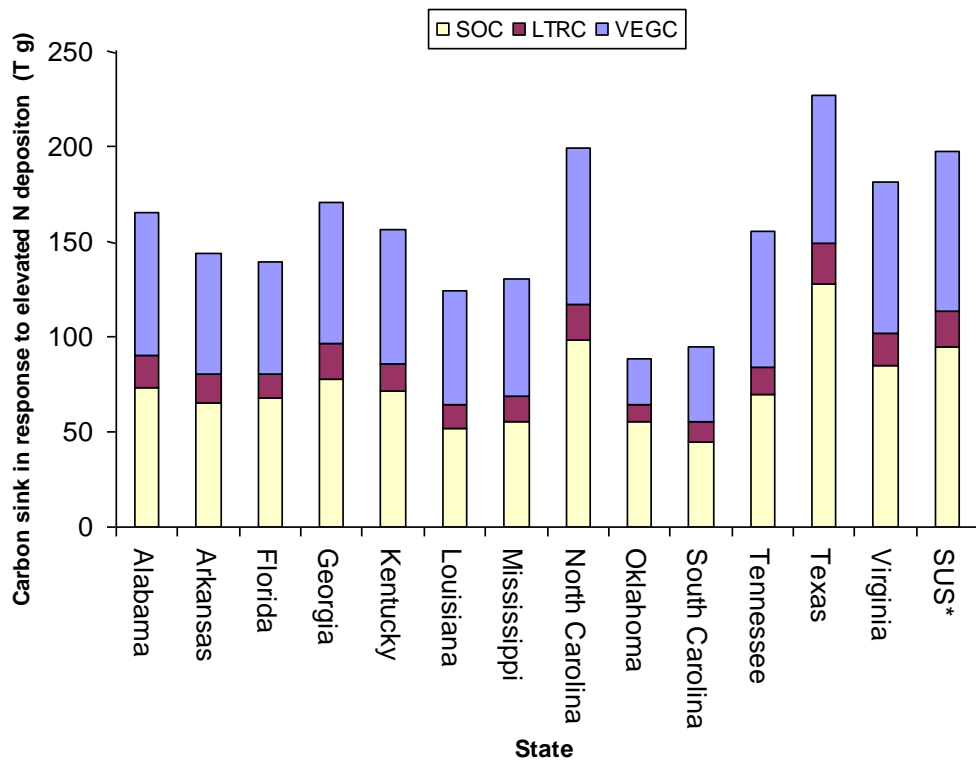


Figure C6.3.13 The carbon sinks generated by elevated atmospheric nitrogen deposition in the 13 southern states.

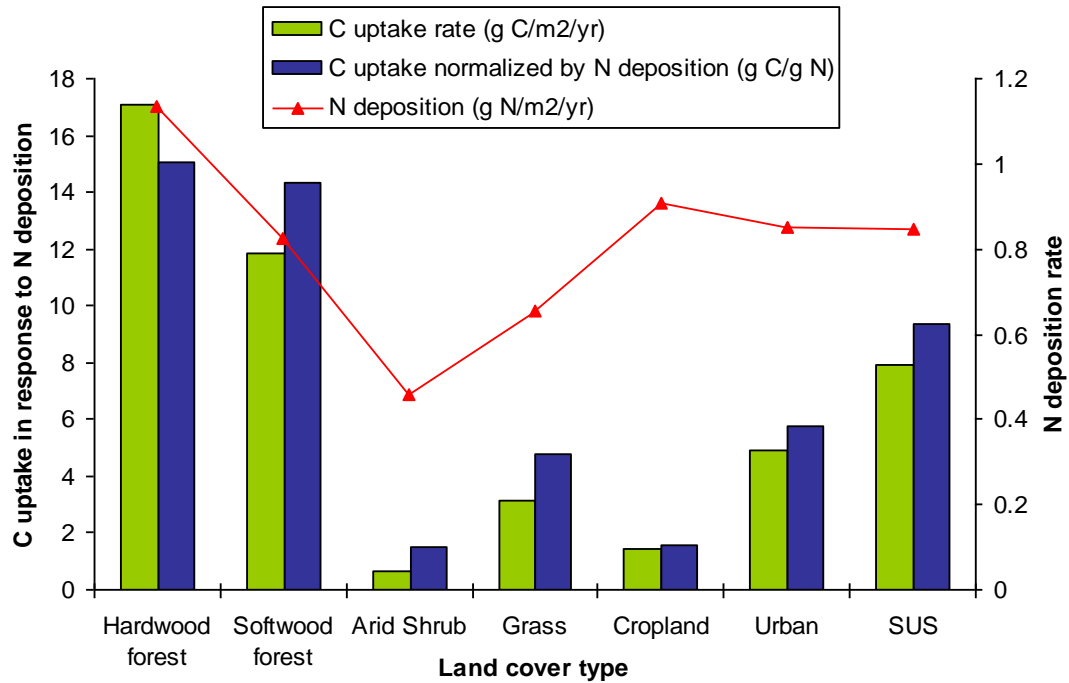


Figure C6.3.14 Responses of different land cover types to N deposition in Southern US in 2005

The spatial pattern (Figure C6.3.15) of N deposition effect shows that SUS can be divided into three regions according to their N deposition stimulated carbon sinks. The large carbon sink region located at the NE-SUS, where the growth of N sensitive hardwood forest was stimulated by the highest N deposition rate in SUS. The western part of study region (Texas and Oklahoma) where both the wet deposition and the ecosystem productivity are generally limited by water stress, acted as small carbon sink in response to N deposition. The rest of the study region, which was dominated by softwood forests, had middle carbon sink strength.

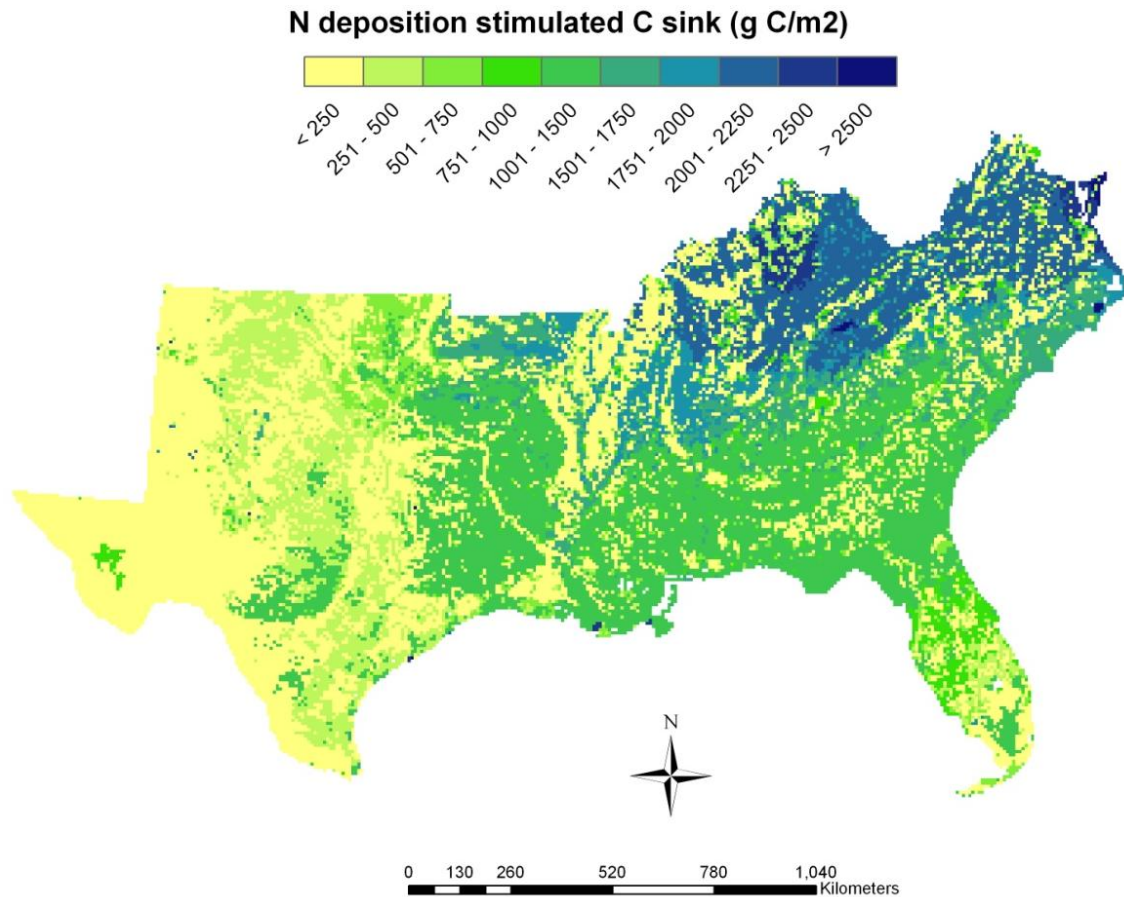


Figure C6.3.15 The spatial pattern of N deposition induced C sink in the Southern US from 1895 - 2005.

3.4.3. Land-use change

Land-use changes were reported to be the primary mechanisms for transferring carbon between the land and the atmosphere in North America and other regions of the world (Caspersen et al., 2000; Pacala et al., 2001; Tian et al., 2003; Birdsey and Lewis, 2003). The forest regrowth in the US was suggested to have fixed large amounts of carbon into terrestrial ecosystems since the mid of last century (Houghton et al., 1999; Caspersen et al., 2000; Schimel et al., 2000).

3.4.3.1. Land use change history of SUS

We constructed a land use dataset based on the 30 meter resolution USGS National Land Cover Dataset 1992 (NLCD92) dataset (See Section 2.1.4.2). By aggregating the NLCD92 map into 8 km resolution, we developed the land cover map of 1990. Then we estimated the annual land-use change pattern (the percentage of one land cover type that changed into another each year) using historical census data as described in Section 2.1.1. Land-use change patterns with the 1990 land-use map were then combined and a land-use history dataset was developed for each year between 1895 and 2005. Therefore, the area of each land cover in our dataset is actually remote sensing derived (since NLCD92 map was generated from Landsat TM imageries) although the annual land-use change pattern was based on a census dataset. When comparing against the forest inventory (FIA) dataset, our estimates of forest area were constantly higher than the reports of FIA (Figure C6.3.16). This difference, like the case study in West Georgia (Chapter 4), may be due to the fact that areas identified as forest by remote sensing included all forests and woodland (including urban forests) that can be identified on the 30-m resolution images, whereas the FIA project estimates are based on a more restricted definition that requires a plot to have at least 10% tree stocks and to be at least 1 acre in size before it can be classified as forestland (USDA Forest Service, 2005). Holden et al. (2005) compared the NLCD92 forest coverage against the FIA-Plot derived forest coverage in North-central US and found that the NLCD92's estimates are generally 11% higher than the FIA estimates.

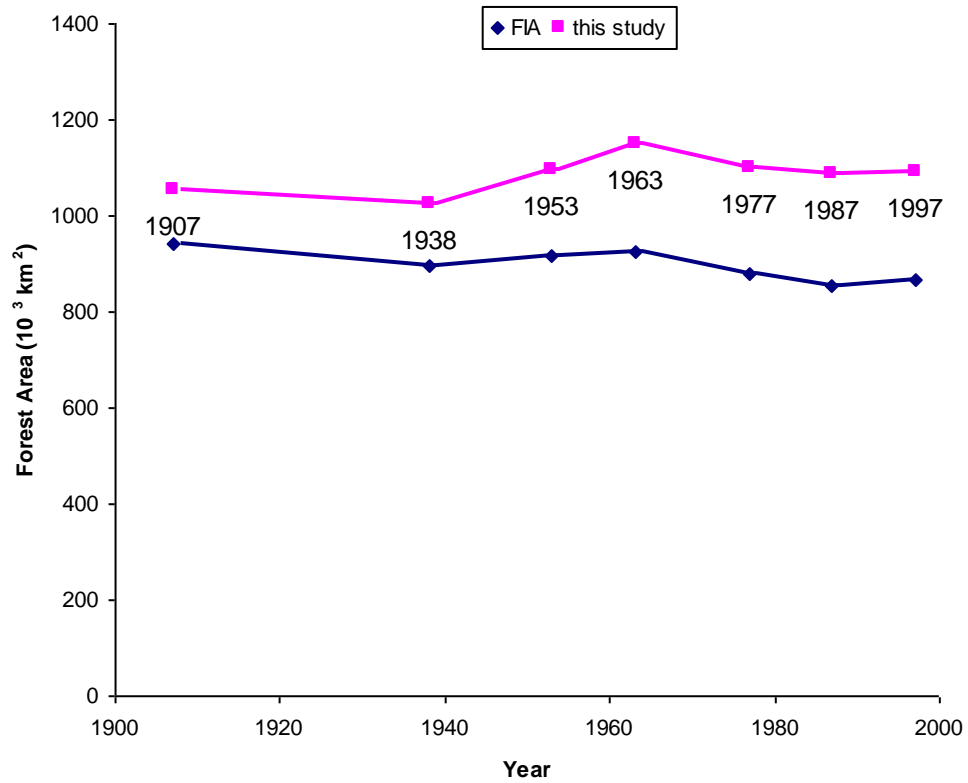


Figure C6.3.16 Comparison of forest area between this study and Forest Inventory and Analysis (FIA)–derived data (Woodbury et al. 2006).

Our dataset shows that the forest area in 1895 ($1112.6 \times 10^3 \text{ km}^2$) nearly equal to the forest area in 2005 ($1116.5 \times 10^3 \text{ km}^2$). This fact may imply that the carbon emission due to land-use change may be limited in SUS, because the 18.6% increase of cropland area from 1895 to 2005 was at the expense of 24% loss of grass/shrublands which, in contrast to forest, have similar carbon density to cropland. However, both historical records (Delcourt and Harris, 1980; Wear, 2002) and our dataset indicate that a large amount of southern forests were converted into croplands before the mid 20th century. These croplands were abandoned lately and forest regrowth dominated the second half of the 20th century. The information of temporal and spatial pattern of land-use change,

therefore, is important for accurate assessment of regional carbon dynamic due to historical land-use change.

Our spatially explicit long-term historical land-use change dataset, like forest survey records (Delcourt and Harris, 1980; Woodbury et al., 2006), indicates that the land-use history of SUS from 1895 to 2005 can be divided into two periods (Figure C6.1.17). From 1895 to the end of the Great Depression, the cropland conversion (*i.e.* natural ecosystems were converted into cultivated lands) dominated the land-use change pattern in the SUS (Wear, 2002). Since the beginning of World War II, significant amounts of degraded croplands in the SUS were abandoned, and large areas of forest regrowth took place (Wear, 2002). From 1895 to 1940, cropland increased by about 50%, while forests decreased by about 9% (Table C6.2.4.1). The urban area gradually increased from 3600 km² to 8300 km². From 1940 to 2005, forests increased by 9%, while cropland declined by about 21%. The urban area in this period increased dramatically from 8300 km² to 68900 km². The spatial pattern of land use changes during the two periods (Figure C6.3.17) also show that in the first period, the cropland conversion dominated the study region, while in the second period, except for Florida, east Arkansas and Louisiana, and west Texas, cropland abandonment dominated most of the SUS. Forest regrowth was the most significant land-use change event in the east and central-South (Figure C6.3.17, b).

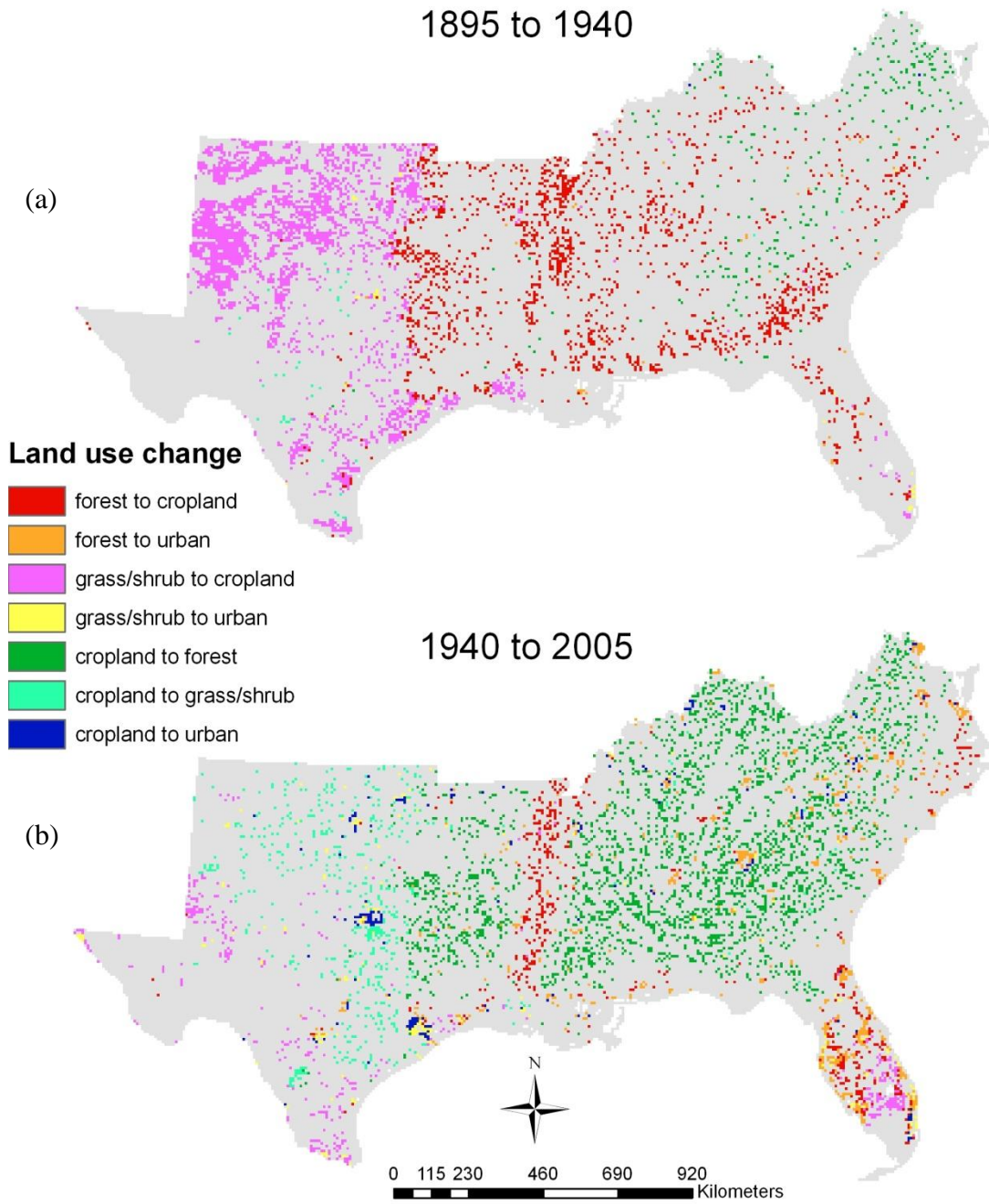


Figure C6.3.17 Land-use change of the Southern US in two periods: 1894 to 1940; 1940 to 2005.

3.4.3.2. Impacts of land-use change on SUS carbon balance

The land-use change together with its interactions with other changing environmental factors such as discussed above appear to create a significant carbon sink in temperate ecosystems of the US (Birdsey and Heath, 1995; Pacala et al., 2001). Caspersen et al. (2000) reported that land use is the dominant factor governing the rate of carbon accumulation in five states that span a latitudinal gradient in the eastern United States, with growth enhancement contributing far less than land use change effect. Our simulation results show that if we do not consider other environmental factors (*i.e.* scenario LUC), the land-use change could have resulted in a net carbon loss of about 18.5 T g C (10% of total ecosystem carbon storage) from 1895 to 2005 in the SUS. Agreeing with the conclusion of former studies (Chen et al., 2006b; Woodbury et al., 2006), our study shows that the period between late-1940s and early-1950s was the turning point of SUS carbon dynamic in response to land-use change (Figure C6.3.18). Before this period, the SUS was a carbon source due to land-use change. Until 1950, the region lost about 2.5 P g C. That is, 13% of total terrestrial carbon storage in SUS was released into atmosphere. After 1950, the study region gradually became a carbon sink due to cropland abandonment. About 0.65 P g C have been sequestered by the SUS terrestrial ecosystem since 1950s.

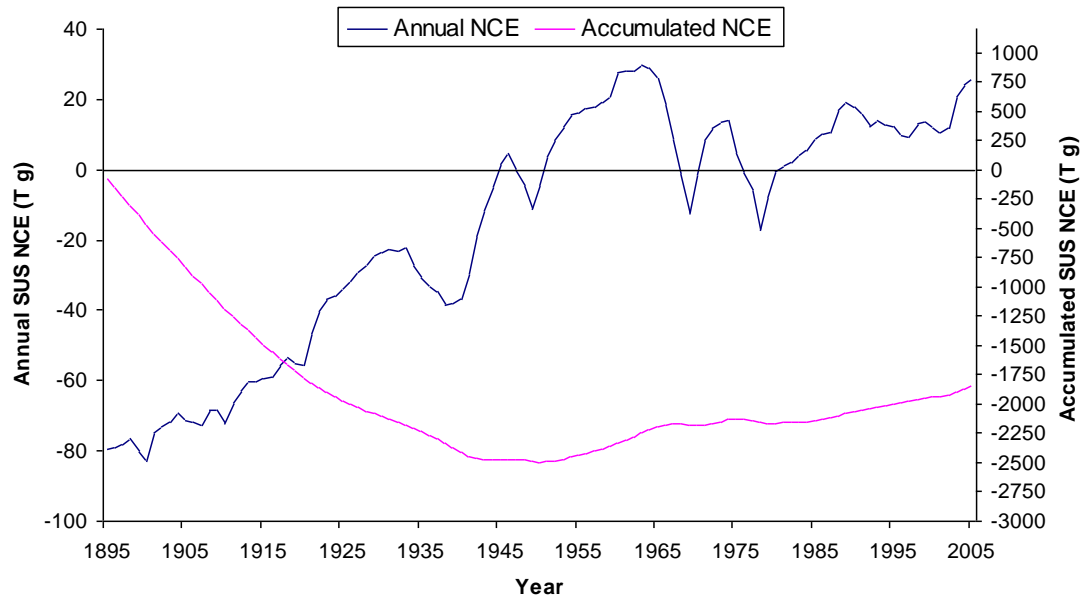


Figure C6.3.18 Net carbon exchange (NCE, see Chapter 4, Section 2.2 for detail explanation) of the Southern US ecosystems due to land-use change from 1895 to 2005 (based on the results of single factor scenario).

3.4.3.3. Individual impacts of urbanization, cropland conversion, and cropland abandonment on regional carbon balance

Since the single factor scenario LUC does not consider the effects of climate or atmospheric changes, the carbon dynamics of all cropland and urban grids can be treated as responses to human disturbances (including cropland conversion and urbanization). Similarly, the carbon dynamics of natural ecosystems, such as forest, shrubland, and grassland, reflect the impacts of reforestation or cropland abandonment (to shrubland/grassland).

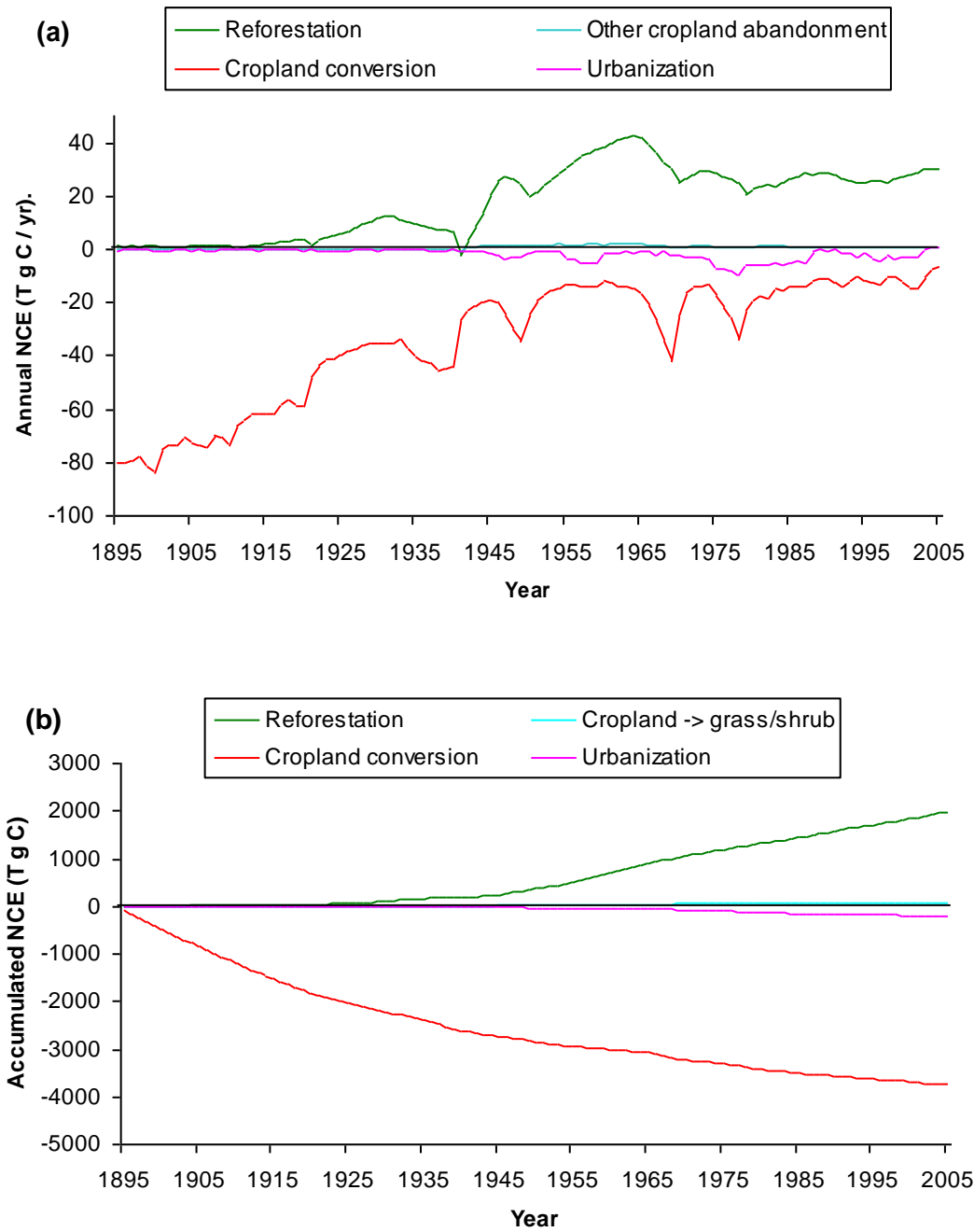


Figure C6.3.19 Impacts of urbanization, cropland conversion, and cropland abandonment on the regional carbon balance from 1895 to 2005 presented as (a) annual carbon dynamic and (b) accumulated net carbon exchange. (Based on the results of single factor scenario LUC).

The first half of the study period was dominated by carbon release processes (cropland conversion and urbanization) (Figure C6.2.3.19). Cropland conversion was the major carbon release process, especially before the 1950s. Urbanization also became important carbon source in the late 20th century. Since the 1910s, the impacts of reforestation gradually increased. During the late-1940s, carbon sequestered by reforestation nearly counterbalanced the carbon released due to cropland conversion (Figure C6.3.19 (a)). After the 1950s, the carbon sequestration rate of reforestation rose quickly. Between 1950 and 1970, the SUS sequestered about 33.5 T g C each year due to reforestation. The average annual carbon sequestration rate of reforestation was about 29 T g C per year since 1950. Much less carbon was sequestered when cropland was changed into other land types. The recovery of grassland and shrubland from abandoned cropland only sequestered 1.2 T g C per year during the same period. The trend of accumulated carbon fluxes (Figure C6.3.19b) implied that the accumulated impacts of cropland conversion and urbanization will level off gradually through time, while regrowing forests may keep accumulating carbon. Although the net carbon balance was negative during the study period, the SUS has the potential to sequester more carbon in the future to balance carbon emissions in the past. The magnitudes of the net carbon exchange (Figure C6.3.20) of the ecosystem restoration processes (*i.e.* reforestation or other vegetation recovery from abandoned cropland) were relatively smaller but more stable than the NCE intensity of human disturbances (cropland conversion and urbanization), even in the second half of the 20th century. This pattern agrees with our observation in the West Georgia rural-urban gradient (Chapter 4).

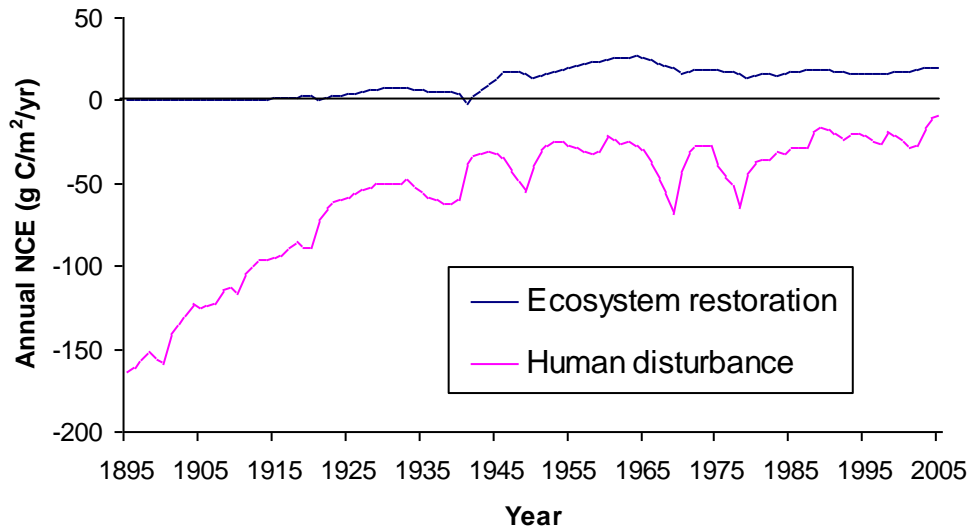


Figure C6.3.20 Comparisons of the intensity of carbon sequestration due to ecosystem restoration (cropland abandonment) and carbon emission due to human disturbances (cropland conversion and urbanization) in the Southern US from 1895 - 2005. (Based on the single factor scenario).

3.4.3.4. The land-use change effect under changed climate and atmosphere

To assess the impacts of land-use change on regional carbon dynamics under changed climate and atmosphere, we estimated the effects of land-use change by comparing the outputs of the ALLCOMBINE scenario with the outputs of the CLMCO2O3NDEP scenario:

$$\text{Land-use change effect} = \text{ALLCOMBINE} - \text{CLMCO2O3NDEP} \quad \text{equation 2.8}$$

The result suggested that the land-use change, interacting with climate change and atmospheric change, might have resulted in a net carbon loss of 2.4 P g C in the SUS

from 1895 to 2005. Due to land-use change, the SUS terrestrial ecosystem released about 27.2 P g C from 1895 to 1950, then sequestered about 0.3 P g C after 1950.

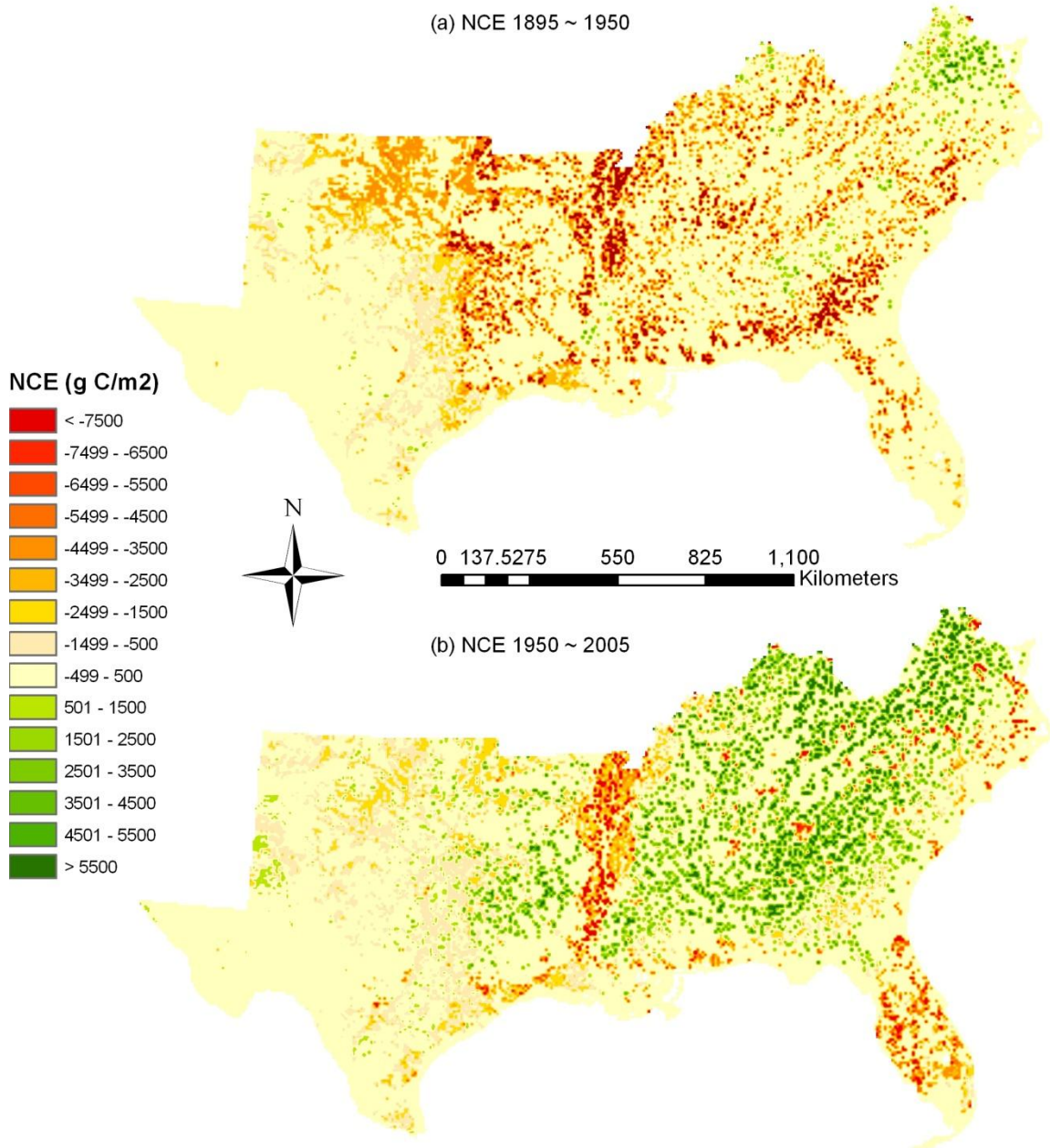


Figure C6.3.21 The spatial distribution of carbon pools and sinks during two time periods: (a) the land-use change resulted in large carbon loss from 1895 to 1950 and (b) the cropland abandonment created carbon sinks in the Southern US from 1950-2005.

Figure C6.3.21 presents the spatial distribution of carbon sources and carbon sinks created by land-use changes. The agriculture region in the center of the study area was the major carbon source through time. Florida, due to cropland conversion before 1950s and urbanization in late-20th century (Figure C6.3.21 b) was another important carbon source. Other places were generally carbon sources in the first half of the 20th century (Figure C6.3.21 (a)), and became carbon sinks in the second half of the century (Figure C6.3.21 (b)). Significant carbon sinks even exist before 1950s in the NE-SUS (Figure C6.3.21 (a)). Texas, due to its limited terrestrial ecosystem biomass, only has small contributions to the variation of regional carbon dynamics.

It should be noted that, because the above land-use change effects are estimated by comparing the scenario considering land-use change (ALLCOMBINE) against the scenario omitting land-use change (CLMCO2O3NDEP) (equation 2.8), the net results include interactions between the land-use change and the other environmental changes such as atmospheric change. For example, forests were generally more sensitive than cropland to CO₂/nitrogen fertilization effect (see Section 2.4.2). After a forest was changed into a cropland, impacts of elevated CO₂ and nitrogen deposition were reduced. The interaction with other environmental factors magnified the impacts of the land-use change on ecosystem carbon balance.

3.5. The impacts of multiple stresses on SUS carbon dynamic

The impacts of each environmental factor and their combined effects on the productivity of the SUS were compared (Figure C6.3.22). According to our model outputs, the mean

annual productivity of SUS terrestrial ecosystems increased from 396 g C/m²/yr in 1890s to 533 g C/m²/yr in the 2000s. Before the 1950s, there was no obvious trend in the NPP. After 1950s, the SUS NPP rose quickly. The inclination of NPP after the 1950s was primarily due to the combined effects of elevated CO₂, increased nitrogen deposition, and cropland abandonment (see Section 2.4). Before the 1950s, the positive effects of CO₂ and nitrogen deposition was counterbalanced by the negative effect of land-use change (mainly due to cropland conversion, see Section 2.4). Although climate change seemed to control the inter-annual variation of the regional NPP (compare the CLM and ALLCOMBINE), the long-term temporal pattern of the SUS was actually controlled by the land-use change effect.

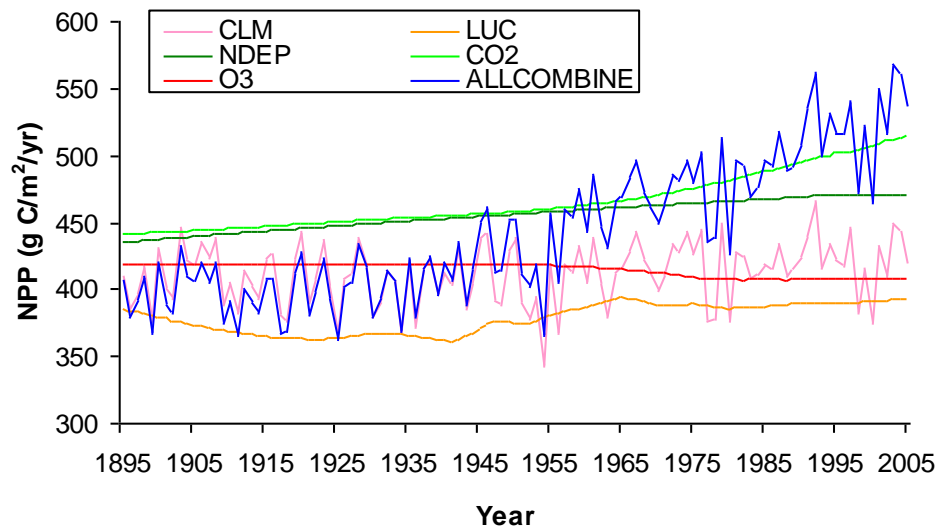


Figure C6.3.22 Comparing the model simulated responses of ecosystem productivity to multiple environmental stresses in the Southern US from 1895 – 2005.

We further analyzed the impacts of different environmental stresses on carbon storage of the SUS by comparing their NCE in Figure C6.3.22. Again, the 1950s seemed to be the

threshold of the regional carbon balance. The temporal pattern of SUS carbon dynamics generally followed the accumulated effects of land-use change. It is also quite obvious that the constant positive (*i.e.* stimulated carbon sequestration) effects of CO₂ and nitrogen deposition accumulated through time. These effects, combined with the impacts of reforestation in the late-20th century, not only compensated for the total carbon loss due to historical land-use change in the 1980s, but also have turned the SUS terrestrial ecosystems into a net carbon sink since the 1990s. However, former studies showed that large amounts of carbon were already lost from the terrestrial ecosystems due to overwhelming deforestation in the SUS before 1895 (Delcourt and Harris, 1980; Chen et al., 2006b). It is unlikely that the carbon accumulated after the 1980s can counterbalance the carbon emission due to the land conversion before the 20th century. Delcourt and Harris (1980) were probably correct by suggesting that “because of the difference in biomass between virgin and secondary forests, managed reforestation can never completely offset the losses incurred by initial deforestation.” This prediction also means that the SUS terrestrial ecosystems have a large potential to sequester more carbon in the future. According to our study results, due to the increased CO₂ and nitrogen fertilization effect, and by appropriate management of the forest product pools, productivity of the SUS terrestrial ecosystems could be enhanced in the future. The SUS could act as a stable carbon sink at least in the first half of the 21st century.

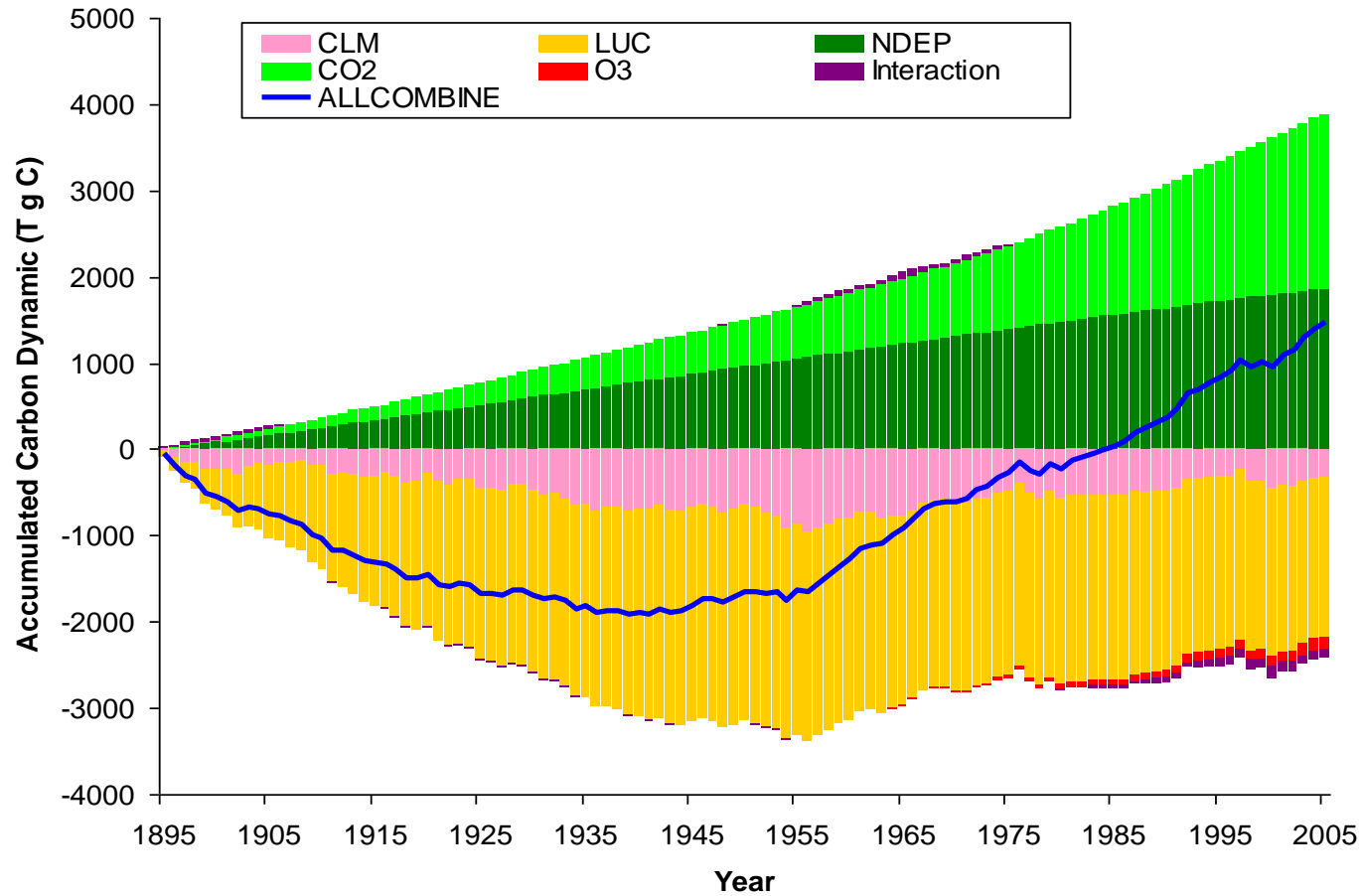


Figure C6.3.23 Comparison of the accumulated impacts of multiple stresses on the Southern US carbon storage. Interaction = ALLCOMBINE – CLM – LUC – NDEP – CO₂ – O₃. ALLCOMBINE: multiple stress scenario; CLM, LUC, NDEP, CO₂, O₃ were single factor scenarios for climate, land-use/land cover, N deposition, CO₂, and tropospheric ozone respectively.

4. Uncertainties and future research needs

This study suggests important impacts of land-use change and cropland management on the carbon storage of SUS terrestrial ecosystems. Our simulation, however, did not consider the effects of forest management, an important human effect that has the potential to modify the SUS forest carbon storage. Houghton et al. (1999) estimated the harvest of wood alone was responsible for 16% of the net land-use flux on average after studying a global level land-use change. In particular, timber production on forest plantations is very important in the southern United States. In recent decades, there has been a decided shift in timber production from the west to the east. The southern region now produces over 50% of commercial timber harvests for the nation (Mickler et al., 2002). Most of timber harvests occur in forest plantations, which have adopted intensive forest management practices, including site preparation, utilization of pesticides and fertilization, and short-term rotation. However, how harvest of wood on these intensively managed plantations influences carbon dynamics in the southern United States remains unclear. Better spatial and temporal data sets of timber harvest and plantation establishment are needed to assess the exact impact of wood harvest and plantations on carbon dynamics. These data sets should include better spatial and temporal information such as locations of timber harvest and plantations, harvested timber volume, plantation area, type of forest product, and changes over time.

Furthermore, not only intensively managed forest plantations are controlled by human activities, many natural regenerated forests in the South are also fertilized. Due to the

lack of field data, in our study we did not consider the effects of nitrogen fertilization on forest productivity in the South. Therefore, our simulation could have underestimated the productivity and carbon storage of Southern terrestrial ecosystem due to our overlook of the nitrogen fertilization effect due to forest management.

The lack of a transient ozone dataset after 1995 generated another source of uncertainty in our analysis. Although the records from 22 ozone monitoring sites indicated that the ozone concentration of 2005 was not significantly different from the value of 1995 in the SUS (Figure C6.1.8), there were still considerable inter-annual variations. The case study in the Great Smoky Mountains (see Chapter 3) also indicated that in some regions of the SUS, the O₃ stress increased rapidly during the 1995-2005 period. A transient O₃ datasets will be required to investigate how ecosystems in the SUS respond to the fluctuation of tropospheric ozone from year to year.

For simplification, our urban assume constant landscape composition through out the study period (1895 – 2005). The fraction of urban lawn, however, actually changed through time. The turf grass was introduced into US urban/developed areas around 1950s. Before that time, the backyards of residential areas were either impervious surface or covered with natural vegetation. For a more accurate estimation of the carbon dynamics of Southern urban/developed areas in the history, we need to develop a more dynamic landscape submodel which account for the changes of urban lawn area from 1895 to 2005 in the Southern US.

5. Conclusion

The carbon dynamics of the SUS were controlled by the interaction of multiple stresses including climate, atmospheric, and land-use change. A comprehensive analysis of the regional carbon balance in the last 110 years based on an integrated dynamic land ecosystem model, DLEM, suggested that the total terrestrial ecosystem carbon (TOTEC) storage of the thirteen southern United States is about 20.26 P g C ($1 \text{ P} = 10^{15}$), 55% of which is stored in soil, 39% in plant biomass, and about 7% in litter pools. The forests account for 84% of the ecosystem carbon storage in the SUS. Among the 13 states, Texas has the largest carbon storage due to its large area. This model assessment which is comparable to the results of other studies indicates that since 1950, the terrestrial ecosystem of the SUS is a net carbon sink of 46.4 T g C per year. Before 1950, however, the region was a net carbon source which was estimated to have lost about 1.56 P g C from 1895 to 1950. Among the many factors that could affect the regional carbon dynamic, historical land-use change, CO₂ fertilization effect, and the elevated atmospheric nitrogen deposition were among the most important factors that control the Southern carbon balance. The temporal patterns of Southern carbon balance were generally controlled by the impacts of historical land-use change. It was, however, the gradually but constantly accumulated positive effects (enhanced carbon sequestration) due to elevated atmospheric CO₂ and nitrogen deposition that turned the SUS into a net carbon sink of about 0.9 P g C during the study period.

CHAPTER 7

GENERAL CONCLUSIONS

Through this multi-scale integrative study (Figure C7.1), we found that:

1. The undisturbed Southern forest ecosystem has the potential to store large amounts of carbon (as high as 15.9 kg m^{-2} in GRSM). Its carbon storage, however, is very sensitive to disturbances, especially land-use changes.
2. Historical cropland conversion had resulted in significant carbon emission in the SUS. Recently, urbanization became a more and more important carbon source, while the vast cropland abandonment made many regions in the SUS net carbon sinks since the late 20th century.
3. The carbon storage of urban/developed area in the SUS is estimated to be 505 T g C according to model simulation. Since 1864, the SUS lost about 204 T g C due to urbanization, 99% of which were released through deforestation. When converted from shrubland or cropland, however, the Southern urban/developed area could be net carbon sinks. The urban lawn has high soil carbon density, and thus has the potential to sequester carbon into the soil by appropriate lawn management.
4. The total terrestrial ecosystem carbon (TOTEC) storage of the thirteen southern United States is estimated to be 20.26 P g C (1 P = 10^{15}), 55% of which is stored in soil, 39% in plant biomass, and about 7% in litter pools. The forests account for

5. 84% of the ecosystem carbon storage in the SUS. Among the 13 states, Texas has the largest carbon storage due to its large area.
6. The terrestrial ecosystem of the SUS is a net carbon sink of 46.4 T g C per year. Before 1950, however, the region was a net carbon source which was estimated to have lost about 1.56 P g C from 1895 to 1950.
7. The temporal patterns of the Southern carbon balance were generally controlled by the impacts of historical land-use change. Before the 1940s, the SUS region was a carbon source due to agricultural deforestation. Since the mid-20th century it has become a carbon sink due to the large scale forest regrowth. The positive effects of elevated CO₂ and nitrogen deposition further accelerated the carbon sequestration rate in SUS, and turned it into a net carbon sink of about 0.9 P g C during the study period.

Improvements and future research needs:

1. Improvement of the model so that it can address the impacts of plantation managements on the forest carbon storage.
2. Development of land management datasets that include the information of historical forest managements in the SUS.
3. Reconstruction of the daily ozone maps for the 1995-2005 periods.

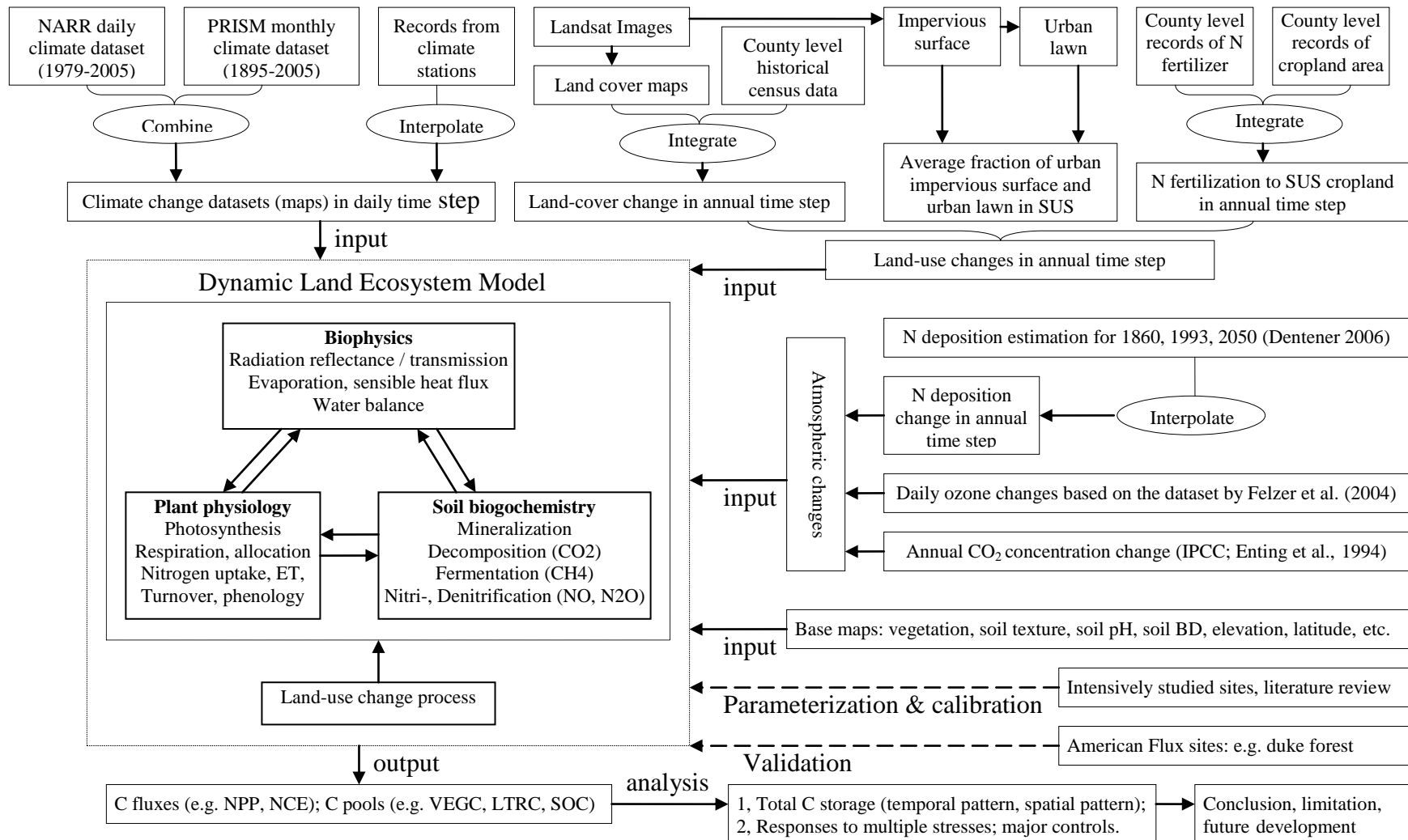


Figure C7.1 Application of the integrative approach in Southern US to study the impacts of multiple stresses on regional C dynamics.

REFERENCES

- Aber, J.D., Magill, A., Boone, R., Melillo, J.M., Steudler, P. (1993) Plant and Soil Responses to Chronic Nitrogen Additions at the Harvard Forest, Massachusetts. *Ecological Applications*, 3, 156-166.
- Adams, R.M., Hamilton, S.A., McCarl, B.A. (1986) The benefits of pollution control: the case of ozone and U.S. Agriculture. *American Journal of Agricultural Economics* 68, 886–893.
- Alexander, R.B., Smith, R.A. (1990) County-level estimates of nitrogen and phosphorus fertilizer use in the United States, 1945 to 1985: U.S. Geological Survey Open-File Report 90-130, 12 p.
- Alig, R.J., Kline, J.D., Lichtenstein, M. (2004) Urbanization on the US landscape: looking ahead in the 21st century. *Landscape and Urban Planning* 69, 219-234.
- Allen, A.H. (1990) Plant responses to rising carbon dioxide and potential interactions with air pollutants. *Journal of Environmental Quality* 19, 15–34.
- Arnold, C.L., Gibbons, C.J. (1996) Impervious surface coverage: the emergence of a key environmental indicator. *Journal of the American Planning Association* 62: 243-258
- Bartholomé, E., Belward, A.S., Achard, F. (2002) GLC2000—Global landcover mapping for the year 2000. Project status, November 2002. EUR 20524 EN. European Commission, JRC, Ispra, Italy.

- Becker, A., Bugmann, H. (2001) Global change and mountain regions: The Mountain Research Initiative. IGBP Report #49, IGBP Secretariat, Stockholm, Sweden.
- Birdsey, R.A., Lewis, B.M. (2003) Carbon in U.S. Forests and Wood Products, 1987-1997: State-by-state Estimates. Gen. Tech. Rep. NE-310, Washington (DC): U.S. Department of Agriculture, Forest Service, 47p
- Birdsey, R.A., Heath, L.S. (1995) in Productivity of America's Forests and Climatic Change, General Technical Report RM-GTR-271, L. A. Joyce, Ed. (U.S. Department of Agriculture (USDA), Forest Service, Rocky Mountain Forest and Range Experiment Station, Fort Collins, CO), pp. 56-70.
- Boisvenue, C., Running, S.W. (2006) Impacts of climate change on natural forest productivity - evidence since the middle of the 20th century. *Global Change Biology* 12, 1-21.
- Bousquet, P., Peylin, P., Ciais, P., Le Quere, C., Friedlingstein, P., Tans, P.P. (2000) Regional changes in carbon dioxide fluxes of land and oceans since 1980. *Science* 290,1342–1346.
- Brater, E.F. (1968) Steps toward a better understanding of urban runoff processes, *Water Resour. Res.*, 4, 335-347.
- Brown, S.L., Schroeder, P.E., Kern, J.S. (1999) Spatial distribution of biomass in forests of the eastern USA. *Forest Ecology and Management* 123, 81-90.
- Brown S.L., Schroeder, P.E. (1999) Spatial patterns of aboveground production and mortality of woody biomass for eastern US forests. *Ecological Application* 9, 968-980.

- Busing, R.T., Clebsch, E.E.C., White, P.S. (1993) Biomass and production of southern Appalachian cove forests reexamined. *Canadian Journal of Forest Research* 23, 760-765.
- Busing, R.T., Stephens, L.A., Clebsch, E.E.C. (2005) Climate data by elevation in the Great Smoky Mountains: a database and graphical displays for 1947 – 1950 with comparison to long-term data. U.S. Geological Survey Data Series Report DS 115, (Online only: <http://pubs.usgs.gov/ds/2005/115/>).
- Cao, M., Woodward, F.I. (1998). Dynamic responses of terrestrial ecosystem carbon cycling to global climate change. *Nature* 393, 249–252.
- Caspersen, J.P., Pacala, S.W., Jenkins, J.C., Hurtt, G.C., Moorcroft, P.R., Birdsey, R.A. (2000) Contributions of Land-Use History to Carbon Accumulation in U.S. Forests. *Science* 290, 1148-1151.
- Chapin III, F.S., Matson, P.A., Mooney, H.A. (2002) Principles of terrestrial ecosystem ecology, Springer-Verlag New York, Inc.
- Chappelka, A., Skelly, J., Somers, G., Renfro, J., Hildebrand, E. (1999) Mature black cherry used as a bioindicator of ozone injury. *Water, Air and Soil Pollution* 116, 261-266.
- Chappelka, A.H., Chevone, B.I. (1992) Tree responses to ozone, in: Lefohn, A.S. (Eds.), Surface level ozone exposures and their effects on vegetation. Lewis Publishers, Chelsea, MI. pp. 271–324.
- Chappelka, A.H., Chevone, B.I., Seiler, J.R. (1988) Growth and physiological responses of yellow-poplar seedlings exposed to ozone and simulated acidic rain. *Environ. Pollut.* 49, 1–18.

- Chappelka, A.H., Renfro, J.R., Somers, G.L., Nash, B. (1997) Evaluation of ozone injury on foliage of black cherry (*Prunus serotina*) and tall milkweed (*Asclepias exaltata*) in Great Smoky Mountains National Park. *Environmental Pollution* 95, 13-18.
- Chappelka, A.H., Samuelson, L.S. (1998). Ambient ozone effects on forest trees of the eastern United States: A review. *New Phytol.* 139, 91–108.
- Chen, G., Tian, H., Liu, M., Ren, W., Zhang, C., Pan, S. (2006a) Climate Impacts on China's Terrestrial Carbon Cycle: An Assessment with the Dynamic Land Ecosystem Model, in: Tian, H.Q. (Eds.), *Environmental Modeling and Simulation – 2006*. ACTA Press, St. Thomas, USVI, USA, pp56-70.
- Chen, H., Tian, H., Liu, M., Melillo, J., Pan, S., Zhang, C. (2006b) [Effect of land-cover change on terrestrial carbon dynamics in the southern USA](#), *Journal of Environmental Quality* 35, 1533-1547.
- Christine, L.S., Kathy A.T., Tonnie G.M. (1994) Clearing the air at Great Smoky Mountains National Park. *Ecological Applications* 4, 690-701.
- Ciais, P., Tans, P.P., Trolier, M., White, J.W.C., Francey, R.J. (1995) A large northern hemisphere terrestrial CO₂ sink indicated by the ¹³C/¹²C ratio of atmospheric CO₂. *Science* 269, 1098–1102.
- Cleveland, C.J., Costanza, R., Hall, C.A.S., Kaufmann, R. (2006) Energy and the U.S. economy: a biophysical perspective. *Science* 225, 890-897.
- Cramer, W., Bondeau, A., Woodward, F.I., Prentice, I.C., Betts, R.A., Brovkin, V., Cox, P.M., Fisher, V., Foley, J., Friend, A.D., Kucharik, C., Lomas, M.R., Ramankutty, N., Sitch, S., Smith, B., White, A., Young-Molling C. (2001). Global response of

- terrestrial ecosystem structure and function to CO₂ and climate change: results from six dynamic global vegetation models. *Global Change Biology* 7, 357-373.
- Daniels, W.L., Everett, C.J., Zelazny, L.W. (1987) Virgin hardwood forest soils of the southern Appalachian Mountains: I. Soil morphology and geomorphology. *Soil Science Society of America Journal* 51, 722–729.
- de Graaff, M., van Groenigen, K., Six, J., van Kessel, C. (2006) Interactions between plant growth and soil nutrient cycling under elevated CO₂: a meta-analysis. *Global Change Biology* 12, 2077-2091.
- Delcourt, H.R., Harris, W.F. (1980) Carbon budget of the southeastern United States: analysis of historic change in trend from source to sink. *Science* 210, 321-323.
- Dentener, F.J. (2006) Global Maps of Atmospheric Nitrogen Deposition, 1860, 1993, and 2050. Data set. Available on-line [<http://daac.ornl.gov/>; http://mercury.ornl.gov/metadata/ornl/daac/html/daac/daacsti.ornl.gov_SMM_MERCURY_harvest21_771.html] from Oak Ridge National Laboratory Distributed Active Archive Center, Oak Ridge, Tennessee, U.S.A.
- Department of the Interior, National Park Service. (1982) Preliminary certification of no adverse impact on Theodore Roosevelt National Park and Lostwood National Wildlife Refuge under Section 165(d)(2)(C)iii of the Clean Air Act, Fed. Regs. 47, 3022-24.
- Department of the Interior, National Park Service. (2002) Air Quality in the National Parks (2nd edition). D-2266, US DOI, Washington, DC.

- Drake, B.G., Gonzalez-Meler, M.A., Long, S.P. (1997) More efficient plants: a consequence of rising atmospheric CO₂? *Annual Review of Plant Physiology and Plant Molecular biology* 48, 609-639.
- El Maayar, M., Ramankutty, N., Kucharik, C.J. (2006) Modeling global and regional net primary production under elevated atmospheric CO₂: On a potential source of uncertainty. *Earth Interactions* 10, 1-20.
- Ellsworth, D.S. (1999) CO₂ enrichment in a maturing pine forest: are CO₂ exchange and water status in the canopy affected? *Plant, Cell and Environment* 22, 461-472.
- Elvidge, C.D., Milesi, C., Dietz, J.B., Tuttle, B.T., Sutton, P.C., Nemani, R., Vogelmann, J.E. (2004) U.S. Constructed Area Approaches the Size of Ohio, *Eos Trans. AGU*, 85, 233.
- Enting, I.G., Wigley, T.M.L., Heimann, M. (1994) Future emissions and concentrations of carbon dioxide: key ocean/atmosphere/land analyses. CSIRO Division of Atmospheric Research Tech Paper No. 31, Melbourne.
- Fan, S., Gloor, M., Mahlman, J., Pacala, S., Sarmiento, J., Takahashi, T., Tans P. (1998) A Large Terrestrial Carbon Sink in North America Implied by Atmospheric and Oceanic Carbon Dioxide Data and Models. *Science* 282, 442 – 446.
- Felzer, B., Kicklighter, D.W., Melillo, J.M., Wang, C., Zhuang, Q., Prinn, R. (2004) Effects of Ozone on Net Primary Production and Carbon Sequestration in the Conterminous United States using a Biogeochemistry Model. *Tellus* 56B, 230-248.
- Field, C.B. (2001) Plant Physiology of the “Missing” Carbon Sink. *Plant Physiology* 125, 25–28.

- Galloway, J.N. Cowling, E.B. (2002) Nitrogen and the world. *Ambio* 31, 64–71.
- Gifford, R.M., Lutze, J.L., Barrett, D. (1996) Global atmospheric change effects on terrestrial carbon sequestration: Exploration with a global C- and N-cycle model (CQUESTN). *Plant and Soil* 187, 369-387.
- Gilliam, F.S., Sigmon, J.T., Reiter, M.A., Krovetz, D.O. (1989) Elevational and spatial variation in daytime ozone concentrations in the Virginia Blue Ridge Mountains: implications for forest exposure. *Canadian Journal Forest Research* 19, 422-426.
- Gilliam, F.S., Turrill, N.T. (1995) Temporal patterns of ozone pollution in West Virginia: implications for high-elevation hardwood forests. *Journal of the Air and Waste Management Association* 45, 621-626.
- Goodale, C.L., M.J. Apps, R.A. Birdsey, C.B. Field, L.S. Heath, R.A. Houghton, J.C. Jenkins, G. H. Kohlmaier, W. Kurz, S. Liu, G.-J. Nabuurs, S. Nilsson and A.Z. Shvidenko. (2002) Forest carbon sinks in the northern hemisphere. *Ecological Applications* 12, 891-899.
- Grulke, N.E., Neufeld, H.S., Davison, A.W., Roberts, M., Chappelka, A.H. (2007) Stomatal behavior of ozone-sensitive and –insensitive coneflowers (*Rudbeckia laciniata* var. *digitata*) in Great Smoky Mountains National Park. *New Phytologist* 173, 100–109.
- Guo, L.B., Gifford, R.M. (2002) Soil carbon stocks and land use change: a meta analysis. *Global Change Biology* 8, 345-360.
- Haefner, J.W. (2005) Modeling biological systems. Springer Science+Business Media Inc. New York, NY, USA.

- Han, F.X., Plodinec, M.J., Su, Y., Monts, D.L., Li, Z. (2007) Terrestrial carbon pools in southeast and south-central United States. *Climatic Change* DOI 10.1007/s10584-007-9244-5
- Hansen, J., Sato, M., Ruedy, R., Lo, K., Lea, D.W., Medina_Elizade, M. (2006) Globale temperature change. *PNAS* 103, 14288-14293.
- Hanson, P.J., Wullshleger, S.D., Norby, R.J., Tschaplinski, T.J., Gunderson, C.A. (2005) Importance of changing CO_2 , temperature, precipitation, and ozone on carbon and water cycles of an upland-oak forest: incorporating experimental results into model simulations. *Global Change Biology* 11, 1402–1423.
- Hart, J.F. (1980) Land use change in a piedmont county. *Annals of the association of American geographers* 70, 492-525
- Haynes, R.W. (2003) An analysis of the timber situation in the United States: 1952-2050. Gen. Tech. Rep. PNW-560. USDA For. Serv., Pacific Northwest Res. Stn., Portland, OR.
- Hobbie, S.E. Chapin, F.S. (1998) The response of tundra plant biomass, aboveground production, nitrogen, and CO_2 flux to experimental warming. *Ecology* 79, 1526-1544.
- Högberg, P. (2007) Nitrogen impacts on forest carbon. *Nature* 447, 781-782.
- Holden, G.R., Nelson, M.D., McRoberts, R.E. (2005) Accuracy Assessment of FIA's Nationwide Biomass Mapping Products: Results From the North Central FIA Region. In: Proceedings of the fifth annual forest inventory and analysis symposium; 2003 November 18-20; New Orleans, LA. Gen. Tech. Rep. WO-69. Washington, DC: U.S. Department of Agriculture Forest Service. 222p.

- Holland, E.A., Brown, S., Potter, C.S., Klooster, S.A., Fan, S., Gloor, M., Mahlman, J., Pacala, S., Sarmiento, J., Takahashi, T., Tans, P. (1999) North American Carbon Sink. *Science* 283, 1815-1815.
- Holland, E.A., Braswell, B.H., Lamarque, J.F., Townsend, A., Sulzman, J., Muller, J.F., Dentener, F., Brasseur, G., Penner, J.E., Roelofs, G.J. (1997) Variations in the predicted spatial distribution of atmospheric nitrogen deposition and their impact on carbon uptake by terrestrial ecosystems, *J. Geophys.Res.* 102, 15849-15866.
- Homer, C. Huang, C., Yang, L., Wylie, B., Coan, M. (2004) Development of a 2001 National Landcover Database for the United States. *Photogrammetric Engineering and Remote Sensing*, Vol. 70, No. 7, July 2004, pp. 829-840.
- Houghton, R.A., Hackler, J.L., Lawrence, K.T. (1999) The U.S. Carbon Budget: Contributions from Land-Use Change. *Science* 285, 574–578.
- Houghton, R.A., Hackler, J.L. (2002) Carbon Flux to the Atmosphere from Land-Use Changes. In *Trends: A Compendium of Data on Global Change. Carbon Dioxide Information Analysis Center, Oak Ridge National Laboratory, U.S. Department of Energy, Oak Ridge, Tenn., U.S.A.*
- IGBP Terrestrial Carbon Working Group (1998) The Terrestrial Carbon Cycle - Implications for the Kyoto Protocol. *Science* 280,1393-1394.
- Imhoff, M.L., Tucker, C.J., Lawrence, W.T., Stutzer, D.C. (2000) The use of multisource satellite and geospatial data to study the effect of urbanization on primary productivity in the United States. *IEEE Transactions on Geoscience and Remote Sensing* 38, 2549- 2556.

Intergovernmental Panel on Climate Change (2001) IPCC Third Assessment Report –
Climate Change 2001: Summary for Policy Makers. Available online:
www.ipcc.ch.

Intergovernmental Panel on Climate Change (2007) IPCC Fourth Assessment Report.
Available online: www.ipcc.ch

Jensen, J.R. (1996) Introductory Digital Image Processing, 2nd Ed.. Prentice-Hall, Inc.

Karnosky, D.F., Pregitzer, K.S., Zak, D.R., Kubiske, M.E., Hendrey, G.R., Weinstein, D.,
Nosal, M., Percy, K.E. (2005) Scaling ozone responses of forest trees to the
ecosystem level in a changing climate. *Plant, Cell and Environment* 28, 965-981.

Kimball, J. S., White, M.A., Running, S.W. (1997) BIOME-BGC simulations of stand
hydrologic processes for BOREAS. *Journal of Geophysical Research* 102, 29043-
29051.

Kutzbach, J., Bonan, G., Foley, J., Harrison, S.P. (1996) Vegetation and soil feedbacks
on the response of the African monsoon to orbital forcing in the early to middle
Holocene. *Nature* 384, 623-626.

Liu, S., Loveland, T.R., Kurtz, R.M. (2004) Contemporary Carbon Dynamics in
Terrestrial Ecosystems in the Southeastern Plains of the United States.
Environmental Management 33, S442–S456.

Lockaby, B.G., Zhang, D., McDaniel, J., Tian, H., Pan, S. (2005). Interdisciplinary
research at the urban – rural interface: the Westga Project. *Urban Ecosystems* 8,
7-21.

Long, S.P., Ainsworth, E.A., Rogers, A., Ort, D.R. (2004) Rising atmospheric carbon
dioxide: Plants FACE the future. *Annual Review of Plant Biology* 55, 591-628.

- Lorius, C., Jouzel, J., Raynaud, D., Hansen, J., Treut, H.L. (1990) The ice-core record: climate sensitivity and future greenhouse warming. *Nature* 347, 139–45.
- Loya, W.M., Pregitzer, K.S., Karberg, N.J., King, J.S., Giardina, C.P. (2003) Reduction of soil carbon formation by tropospheric ozone under elevated carbon dioxide. *Nature* 425, 705-707.
- Lüdeke, M.K.B., Dongers, S., Otto, R.D., Kindermann, J., Badeck, F.W., Ramage, P., Jakel, U., Klaudius, A. and Kohlmaier, G.H. (1995) Response in NPP and carbon storage of the northern biomes to a CO₂ induced climate change, as evaluated by the Frankfurt Biosphere Model (FBM). *Tellus* 47B, 191–205.
- MacKenzie, M. D. (1993) The vegetation of Great Smoky Mountains National Park: Past, present, and future. Ph.D. dissertation, University of Tennessee, Knoxville. 154 pp.
- Malhi, Y. (2002) Carbon in the atmosphere and terrestrial biosphere in the 21st century. *Phil. Trans. R. Soc. Lond. A* 360, 2925–2945.
- Marland, G., Boden, T. A., Andres, R. J. (2002) Global, regional and national fossil fuel CO₂ emissions. In *Trends: a compendium of data on global change*. Carbon Dioxide Information Analysis Center, Oak Ridge National Laboratory, US Department of Energy, Oak Ridge, TN.
- Martin, M.J., Host, G.E., Lenz, K.E., Isebrands, J.G. (2001) Simulating the growth response of aspen to elevated ozone: a mechanistic approach to scaling a leaf-level model of ozone effects on photosynthesis to a complex canopy architecture. *Environmental Pollution* 115, 425-436.

- McGuire A.D., Melillo, J.M., Joyce, L.A., Kicklighter, D.W., Grace, A.L., Moore III, B., Vorosmarty, C.J. (1992) Interactions between carbon and nitrogen dynamics in estimating net primary productivity for potential vegetation in North America. *Global Biogeochemical Cycles* 6,101-124.
- McGuire, A.D., Sitch, S., Clein, J.S., Dargaville, R., Esser, G., Foley, J., Heimann, M., Joos, F., Kaplan, J., Kicklighter, D.W., Meier, R.A., Melillo, J.M., Moore III, B., Prentice, I.C., Ramankutty, N., Reichenau, T., Schloss, A., Tian, H., Williams, L.J., Witterberg, U. (2001) Carbon balance of the terrestrial biosphere in the twentieth century: Analyses of CO₂, climate and land use effects with four process-based ecosystem models. *Global Biogeochemical Cycles* 15, 183-206.
- McGuire, A.D., Melillo, J.M., Kicklighter, D.W., Pan, Y., Xiao, X., Helfrich, J., Moore III, B., Vorosmarty, C.J., Schloss, A.L. (1997). Equilibrium responses of global primary production and carbon storage to doubled atmospheric carbon dioxide: Sensitivity to changes in vegetation nitrogen concentration. *Global Biogeochem.Cycles* 11, 173–189.
- McLaughlin, S.B., Downing, D.J. (1995) Interactive effects of ambient ozone and climate measured on growth of mature forest trees. *Nature* 374, 252-254.
- McLaughlin, S.B., Downing, D.J. (1996) Interactive effects of ambient ozone and climate measured on growth of mature loblolly pine trees. *Canadian Journal of Forest Research* 26, 670-681.
- McNulty, S.G., Vose, J.M., Swank, W.T., Aber, J.D., Federer, C.A. (1994) Regional-scale forest ecosystem modeling: database development, model predictions and validation using a Geographic Information System. *Climate Research* 4, 223-231.

- Melillo, J.M., Steudler, P.A., Aber, J.D., Newkirk K., Lux, H., Bowles, F.P., Catricala, C., Magill, A., Ahrens, T., Morrisseau, S. (2002) Soil warming and carbon-cycle feedbacks to the climate system. *Science* 298, 2173-2176.
- Melillo, J.M., McGuire, A.D., Kicklighter, D.W., Moore, B., Vörösmarty, C.J., Schloss, A.L. (1993) Global climate change and terrestrial net primary production. *Nature* 363, 234-40.
- Mickler, R.A., Earnhardt, T.S., Moore, J.A. (2002) Regional estimation of current and future forest biomass. *Environ. Pollut.* 116, S7–S16.
- Milesi, C., Running, S.W, Elvidge, C.D., Dietz, J.B., Tuttle, B.T., Nemani, R.R. (2005) Mapping and Modeling the Biogeochemical Cycling of Turf Grasses in the United States. *Environmental Management* 36, 426.
- Milesi, C., Elvidge, C.D., Nemani, R.R., Ruuning, S.W. (2003) Assessing the impact of urban land development on net primary productivity in the southeastern United States. *Remote Sensing of Environment*, 86, 401-410.
- Miller, D.A., White, R.A. (1998) A Conterminous United States Multi-Layer Soil Characteristics Data Set for Regional Climate and Hydrology Modeling. *Earth Interactions*, 2: [Online] URL: <http://EarthInteractions.org>
- Miller, J.O., Galbraith, J.M, Daniels, W.L. (2004) Soil Organic Carbon Content in Frigid Southern Appalachian Mountain Soils. *Soil Science Society of America Journal*. 68, 194-203.
- Mitchell, T.D., Carter, T.R., Jones, P.D., Hulme, M., New, M. (2003) A comprehensive set of high-resolution grids of monthly climate for Europe and the globe: the

- observed record (1901-2000) and 16 scenarios (2001-2100). *Journal of Climate*, in press.
- Moore, B.D., Cheng, S.H., Sims, D., Seemann, J.R. (1999) The biochemical and molecular basis for photosynthetic acclimation to elevated atmospheric CO₂. *Plant Cell Environment* 22, 567–582.
- Mott, K.A. (1988) Do stomata respond to CO₂ concentrations other than intercellular? *Plant Physiology* 86, 200–203.
- Mueller, S.F. (1994) Characterization of ambient ozone levels in the Great Smoky Mountains National Park. *Journal of Applied Meteorology* 33, 465–472.
- Nadelhoffer, K., Aber, J.D., Melillo, J.M. (1985) Fine roots, net primary production, and soil nitrogen availability: a new hypothesis. *Ecology* 66, 1377-1390.
- Nadelhoffer, K.J., Emmett, B.A., Gundersen, P., Kjonass, O.J., Koopmans, C.J., Schleppi, P., Tietema, A., Wright, R.F. (1999) Nitrogen deposition makes a minor contribution to carbon sequestration in temperate forests. *Nature* 389, 415-417.
- Nemani, R.R., Keeling, C.D., Hashimoto, H., Jolly, W.M., Piper, S.C., Tucker, C.J., Myneni, R.B., Running, S.W. (2003) Climate-Driven Increases in Global Terrestrial Net Primary Production from 1982 to 1999. *Science* 300, 1560-1563.
- Neufeld, H.S., Renfro, J.R., Hacker, W.D., Silsbee, D. (1992) Ozone in Great Smoky Mountains National Park: Dynamics and effects on plants, in: Berglund, R.L, (Eds.), *Tropospheric Ozone and the Environment II*. Air and Waste Management Association, Pittsburgh, PA, pp. 594-617.
- Norby, R.J., Luo, Y.Q. (2004) Evaluating ecosystem responses to rising atmospheric CO₂ and global warming in a multi-factor world. *New Phytol.* 162, 281–293.

- Norby, R.J., DeLucia, E.H., Gielen, B., Calfapietra, C., Giardina, C.P., King, J.S., Ledford, J., McCarthy, H.R., Moore, D.J.P., Ceulemans, R., De Angelis, P., Finzi, A.C., Karnosky, D.F., Kubiske, M.E., Lukac, M., Pregitzer, K.S., Scarascia-Mugnozza, G.E., Schlesinger, W.H., Oren, R. (2005) Forest response to elevated CO₂ is conserved across a broad range of productivity. *Proceedings of the National Academy of Sciences* 102, 18052-18056.
- Nowak, D.J., Crane, D.E. (2002) Carbon storage and sequestration by urban trees in the USA. *Environmental Pollution* 116, 381-389.
- Oechel, W.C., Cowles, S., Grulke, N., Hastings, S.J., Lawrence, B., Prudhomme, T., Riechers, G., Strain, B., Tissue, D., Vourlitis, G. (1994) Transient nature of CO₂ fertilization in arctic tundra. *Nature* 371, 500-503.
- Ollinger, S.V., Aber, J.D., Reich, P.B., Freuder, R.J. (2002) Interactive effects of nitrogen deposition, tropospheric ozone, elevated CO₂ and land use history on the carbon dynamics of northern hardwood forests. *Global Change Biology* 8, 545-562.
- Ollinger, S.V., Aber, J., Reich, P. (1997) Simulating ozone effects on forest productivity: interactions among leaf-, canopy- and stand-level processes. *Ecological Applications* 7, 1237-1251.
- Oren, R., Ellsworth, D.E., Johnsen, K.H., Phillips, N., Ewers, B.E., Maier, C., Schäfer, K.V.R., McCarthy, H., Hendrey, G., McNulty, S.G., Katul, G.G. (2001) Soil fertility limits carbon sequestration by forest ecosystems in a CO₂-enriched atmosphere. *Nature* 411, 469-472.
- Pacala, S.W., Hurtt, G.C., Baker, D., Peylin, P., Houghton, R.A., Birdsey, R.A., Heath, L., Sundquist, E.T., Stallard, R.F., Ciais, P., Moorcroft, P., Caspersen, J.P.,

- Shevliakova, E., Moore, B., Kohlmaier, G., Holland, E., Gloor, M., Harmon, M.E., Fan, S.M., Sarmiento, J.L., Goodale, C.L., Schimel, D., Field, C.B. (2001) Consistent land- and atmosphere-based U.S. carbon sink estimates. *Science* 292, 2316-1320.
- Pacala, S., Birdsey, R., Bridgham, S., Conant, R.T., Davis, K., Hales, B., Houghton, R.A., Jenkins, J.C., Johnston, M., Marland, G., Paustian, K. (2007) The North American Carbon Budget Past and Present. p 3-1 ~ 3-21. In W.J. Brennan et al. (ed.) *The First State of the Carbon Cycle Report (SOCCR) North American Carbon Budget and Implications for the Global Carbon Cycle*. U.S. Climate Change Science Program. Synthesis and Assessment Product 2.2. Available online: <http://www.climate-science.gov/Library/sap/sap2-2/final-report/default.htm>
- Paoletti, E., Grulke, N.E. (2005) Does living in elevated CO₂ ameliorate tree response to ozone? A review on stomatal responses. *Environmental Pollution* 137, 483–93.
- Peng, C., Apps, M.J. (1999) Modeling the response of net primary productivity (NPP) of boreal forest ecosystems to changes in climate and fire disturbance regimes. *Ecological Modeling* 20,175-193.
- Perlack, R.D., Wright, L.L., Turhollow, A.F., Graham, R.L., Stokes, B.J. Erbach, D.C. (2005) Biomass as feedstock for a bioenergy and bioproducts industry: the technical feasibility of a billion-ton annual supply. U.S. Department of Energy Document No: DOE/GO-1-2995-2135.
http://feedstockreview.ornl.gov/pdf/billion_ton_vision.pdf
- Petit, J.R., Jouzel, J., Raynaud, D., Barkov, N.I., Barnola, J.-M., Basile, I., Bender, M., Chappellaz, J., Davis, M., Delaygue, G., Delmotte, M., Kotlyakov, V.M., Legrand,

- M., Lipenkov, V.Y., Lorius, C., Pepin, L., Ritz, C., Saltzman, E., and Stievenard, M. (1999) Climate and atmospheric history of the past 420,000 years from the Vostok ice core, Antarctica. *Nature* 399, 429-436.
- Post, W.M., Emanuel, W.R., Zinke, P.J., Stangenberger, A.G. (1982) Soil carbon pools and world life zones. *Nature* 298, 156–159.
- Potter, S.K., Nemni, R., Genoves, V., Hiatt, S., Fladeland, M., Gross, P. (2006) Estimating carbon budgets for U.S. ecosystems. *EOS, Transactions American Geophysical Union*, 87, 85-90.
- Pouyat, R.V., Yesilonis, I.D., Nowak, D.J. (2006) Carbon storage by urban soils in the United States. *J. Environ. Qual.* 35, 1566-1575.
- Prentice, I.C. Farquhar, G.D., Fasham, M.J.R., Goulden, M.L., Heimann, M., Jaramillo, V.J., Kheshgi, H.S., Le Quéré, C., Scholes, R.J., Wallace, D.W.R. (2001) The carbon cycle and atmospheric carbon dioxide. In *Climate Change 2001: the scientific basis* (ed. IPCC), pp. 183–237. Cambridge University Press.
- Pye, J.M. (1988) Impact of ozone on the growth and yield of trees: a review. *Journal of Environmental Quality* 17, 347–360.
- Qian, Y.L., Bandaranayake, W., Parton, W.J., Meham, B., Harivandi, M.A., Mosier, A.R. (2003) Long-Term Effects of Clipping and Nitrogen Management in Turfgrass on Soil Organic Carbon and Nitrogen Dynamics: The CENTURY Model Simulation, *J. Environ. Qual.* 32, 1694–1700.
- Qian, Y.L., Follett, R.F. (2002) Assessing soil carbon sequestration in turfgrass systems using long-term soil testing data, *Agronomy Journal* 94, 930–935.

- Ramankutty, N., Foley J.A. (1998) Characterizing patterns of global land use: An analysis of global croplands data. *Global Biogeochem. Cycles* 12:667–685.
- Rayner, P.J., Enting, I.G., Francey, R.J., Langenfelds, R. (1999) Reconstructing the recent carbon cycle from atmospheric CO₂, δ¹³C and O₂/N₂ observations. *Tellus* 51B, 213–232.
- Reich, P.B., Hobbie, S., Lee, T.D., Ellsworth, D., West, J.B., Tilman, D., Knops, J., Naeem, S., Trost, J. (2006) Nitrogen limitation constrains sustainability of ecosystem response to CO₂. *Nature* 440, 922-925.
- Reich, P.B. (1987) Quantifying plant response to ozone: a unifying theory. *Tree Physiology* 3, 63-91.
- Ren, W., Tian, H., Chen, G., Liu, M., Zhang, C., Chappelka, A., Pan, S. (2007) Influence of ozone pollution and climate variability on grassland ecosystem productivity across China. *Environmental Pollution* 149, 327-335.
- Robinson, A.B., Robinson, N.E., Soon, W. (2007) Environmental effects of increased atmospheric Carbon dioxide. *Journal of American Physicians and Surgeons* 12, 79-90.
- Ruddy, B.C., Lorenz, D.L., and Mueller, D.K. (2006) County-level estimates of nutrient inputs to the land surface of the conterminous United States, 1982-2001. U.S. Geological Survey Scientific Investigations Report 2006-5012, accessed at <http://pubs.usgs.gov/sir/2006/5012/>.
- Schimel, D., Melillo, J.M., Tian, H., McGuire, A.D., Kicklighter, D.W., Kittel, T., Rosenbloom, N., Running, S.W., Thornton, P., Ojima, D., Parton, W., Kelly, R., Sykes, M., Neilson, R., Rizzo, B. (2000) Contribution of increasing CO₂ and

climate to carbon storage by ecosystems in the United States. *Science* 287, 2004-2006

Schlesinger, W.H. (1997) *Biogeochemistry*. Academic Press.

Shafer, S.R., Heagle, A.S. (1989) Growth response of old-grown loblolly pine to chronic doses of ozone during multiple growing seasons. *Canadian Journal of Forest Research* 19, 821-231.

Shanks, R.E. (1954) Climate of the Great Smoky Mountains. *Ecology* 35, 353-361.

Shaw, M.R., Zavaleta, E.S., Chiariello, N.R., Cleland, E.E., Mooney, H.A. (2002) Grassland responses to global environmental changes suppressed by elevated CO₂. *Science* 298,1987–1990.

Somers, G.L., Chappelka, A.H., Rosseau, P., Renfro, J.R. (1998) Empirical evidence of growth decline related to visible ozone injury. *Forest Ecology and Management* 104, 129-137.

Song, C., Woodcock, C.E. (2003) A regional forest ecosystem carbon budget model: impacts of forest age structure and land-use history. *Ecological Modeling* 164, 33-47.

Strahan, D. (2007) *The last oil shock - A Survival Guide to the Imminent Extinction of Petroleum Man*. John Murray. UK. Pp304

Teskey, R.O., Bongarten, B.C., Cregg, B.M., Dougherty, P.M., Hennessey, T.C. (1987) Physiology and genetics of tree growth response to moisture and temperature stress: an examination of the characteristics of loblolly pine (*Pinus taeda* L.). *Tree Physiology* 3, 41-61.

- Teskey, R.O. (1995) Synthesis and conclusions from studies of southern commercial pines, in: Fox, S., Mickler, R.A. (Eds.), *Impacts of Air Pollutants on Southern Pine Forests*. Springer Verlag, New York, USA, pp. 467-490.
- Thompson, M.T., Thompson, L.W. (2002) *Georgia's Forests, 1997*, Resource Bulletin SRS-72, Southern Research Station, United States Department of Agriculture, Forest Service: [Online] URL: <http://www.treesearch.fs.fed.us/pubs/srs/>
- Thornthwaite, C.W. (1948) An approach toward a rational classification of climate. *Geographic Review* 38, 55-94.
- Thornton, P.E., Running, S.W. (1999) An improved algorithm for estimating incident daily solar radiation from measurements of temperature, humidity, and precipitation. *Agriculture and Forest Meteorology*. 93, 211-228.
- Thornton, P.E., Hasenauer, H., White, M.A. (2000) Simultaneous estimation of daily solar radiation and humidity from observed temperature and precipitation: An application over complex terrain in Austria. *Agricultural and Forest Meteorology* 104, 255-271.
- Thornton, P.E., Law, B.E., Gholz, H.L., Clark, K.L., Falge, E., Ellsworth, D.S., Goldstein, A.H., Monson, R.K., Hollinger, D., Falk, M., Chen, J., Sparks, J.P. (2002) Modeling and measuring the effects of disturbance history and climate on carbon and water budgets in evergreen needleleaf forests. *Agricultural and Forest Meteorology* 113, 185-222.
- Thornton, P.E., Running, S.W., White, M.A. (1997) Generating surfaces of daily meteorological variables over large regions of complex terrain. *Journal of Hydrology* 190, 214-251.

- Tian, H., Melillo, J.M., Kicklighter, D.W., McGuire, A.D., Helfrich III, J.V.K., Moore III, B., Vörösmarty, C.J. (1998) Effect of interannual climate variability on carbon storage in Amazonian ecosystems. *Nature* 396, 664-667.
- Tian, H., Melillo, J.M., Kicklighter, D.W., Pan, S., Liu, J., McGuire, A.D., Moore III, B. (2003) Regional carbon dynamics in monsoon Asia and its implications for the global carbon cycle. *Global and Planetary Change* 37, 201-217.
- Tian, H., Melillo, J.M., Kicklighter, D.W., McGuire, A.D., Helfrich, J. (1999) The sensitivity of terrestrial carbon storage to historical atmospheric CO₂ and climate variability in the United States. *Tellus* 51B, 414-452.
- Tian, H.Q. (2002). Modeling dynamics of the terrestrial biosphere in changing global environments: models, data, and validation. *J. of Geographical Science* 57, 378-388.
- Tian, H.Q., Liu, M.L., Zhang, C., Ren, W., Chen, G.S., Xu, X.F. (2005) DLEM – The Dynamic Land Ecosystem Model, User Manual. The ESRA Laboratory, Auburn University, Auburn, AL, pp 65.
- Tian, H.Q., Melillo, J.M., Kicklighter, D.W., McGuire, A.D., Helfrich, J., Moore III, B., Vörösmarty, C.J. (2000) Climatic and biotic controls on annual carbon storage in Amazonian ecosystems. *Global Ecology and Biogeography* 9, 315-336.
- Tian, H., Xu, X., Zhang, C., Ren, W., Chen, G., Liu, M., Lu, D., and Pan, S. (2008) Forecasting and Assessing the Large-scale and Long-term Impacts of Global Environmental Change on Terrestrial Ecosystems in the United States and China. In Miao, S., Carstenn, S., and Nungesser, M. (Eds.) *Real World Ecology: large-scale and long-term case studies and methods*. Springer, New York. (In Press)

- Turner, D.P., Koerper, G.J., Harmon, M.E., Lee, J.J. (1995) A carbon budget for forests of the conterminous United States. *Ecological Applications* 5, 421-436.
- USDA Forest Service. (2005) Forest Inventory and Analysis National Core Field Guide, version 3, Volume we :[Online] URL: <http://www.fia.fs.fed.us/library/field-guides-methods-proc/>
- VEMAP Members (1995) Vegetation/ecosystem modeling and analysis project: Comparing biogeography and biogeochemistry models in a continental-scale study of terrestrial ecosystem responses to climate change and CO₂ doubling. *Global Biogeochemical Cycles*, 9, 407-437.
- Vitousek, P., Edin, L.O., Matson, P.A., Fownes, J.H., Neff, J. (1998) Within-system element cycles, input-output budgets, and nutrient limitations. In *Success, Limitations, and Frontiers in Ecosystem Science* Edited by: Pace M and Groffman P. New York, Springer-Verlag; Pp 432-451.
- Vitousek, P.M., Howarth, R.W. (1991). Nitrogen limitation on land and in the sea: How can it occur? *Biogeochemistry* 13, 87-115.
- Vitousek, P.M., Ehrlich, P, Ehrlich, A., Matson, P.M. (1986) Human appropriation of the products of photosynthesis, *BioScience* 36, 368.
- Volk, M., Niklaus, P.A. Korner, C. (2000) Soil moisture effects determine CO₂ responses of grassland species. *Oecologia* 125, 380-388.
- Waisanen, P.J., Bliss, N.B. (2002) Changes in population and agricultural land in conterminous United States counties, 1790 to 1997. *Global Biogeochemical Cycles* 16, 1137.

- Wear, D.N. (2002) Land use. p. 153–174. In D.N. Wear, and J.G. Greis (ed.) Southern forest resource assessment. Tech. Rep. GTR SRS-53. USDA, For. Serv., Washington, DC. :[Online] URL: <http://www.srs.fs.usda.gov/sustain/report/>.
- Weinstein, D.A., Gollands, B., Retzlaff, W.A. (2001) The effects of ozone on a lower slope forest of the Great Smoky Mountain national park: simulations linking an individual tree model to a stand model. *Forest Science* 47, 29-42.
- Welch, R., Madden, M., Jordan, T. (2002) Photogrammetric and GIS techniques for the development of databases of mountainous areas: Great Smoky Mountains National Park. *ISPRS Journal of Photogrammetry and Remote Sensing* 57, 53-68.
- Whittaker R.H. (1966) Forest dimensions and production in the Great Smoky Mountains. *Ecology* 47, 103-121.
- Whittaker, R.H., Bormann, F.H., Likens, G.E., Siccama, T.G. (1974) The Hubbard Brook Ecosystem Study: forest biomass and production. *Ecological Monographs* 44, 233-254.
- Wofsy, S.C., Harris, R.C. (2002) The North American Carbon Program (NACP). Report of the NACP Committee of the U.S. Interagency Carbon Cycle Science Program. Washington (DC): US Global Change Research Program
- Woodbury, P.B., Heath, L.S., Smith, J.E. (2006) Land use change effects on forest carbon cycling throughout the Southern United States. *J. Environ. Qual.* 35, 1348–1363.
- Yang, L., Huang, C., Homer, C., Wylie, B., Coan, M. (2003) An approach for mapping large-area impervious surfaces: Synergistic use of Landsat 7 ETM+ and high spatial resolution imagery. *Canadian Journal of Remote Sensing*, 29, 230-240.

- Zhang, C., Tian, H.Q., Pan, S., Liu, M, Lockaby, G., Schilling, E.B. Stanturf, J. (2007) Effects of Forest Regrowth and Urbanization on Ecosystem Carbon Storage in a Rural-Urban Gradient in the Southeast US. *Ecosystems* DOI: 10.1007/s10021-006-0126-x.
- Zhang, C., Tian, H., Chappelka, A., Ren, W., Chen, H., Pan, S., Liu, M., Styers, D.M., Chen, G., Wang, Y. (2007) Impacts of climatic and atmospheric changes on carbon dynamics in the Great Smoky Mountain. *Environmental Pollution* 149, 336-347.

APPENDIX I
MODEL VALIDATION

1. Compare model outputs against measured daily carbon fluxes

Forest composes the largest fraction of Southern US carbon pools. The accurate simulation of forest carbon dynamics is very important in assessment of regional carbon balance. We use site measured dataset from two intensively studied Southern forests: the Duke loblolly pine Forest in North Carolina (latitude: 35° 58'; Longitude: 79° 5') (http://public.ornl.gov/ameriflux/Site_Info/siteInfo.cfm?KEYID=us.duke_loblolly.01), and the deciduous broadleaf forest locates in Walker Branch Watershed, Tennessee (Latitude: 35° 57'; Longitude: 84° 17') (http://public.ornl.gov/ameriflux/Site_Info/siteInfo.cfm?KEYID=us.walker_branch.01) to drive DLEM model. Then we compare our model output to the measure daily carbon flux rate (<http://public.ornl.gov/ameriflux>). Figure A2.1 shows that the simulated carbon flux generally matched the site measured flux data.

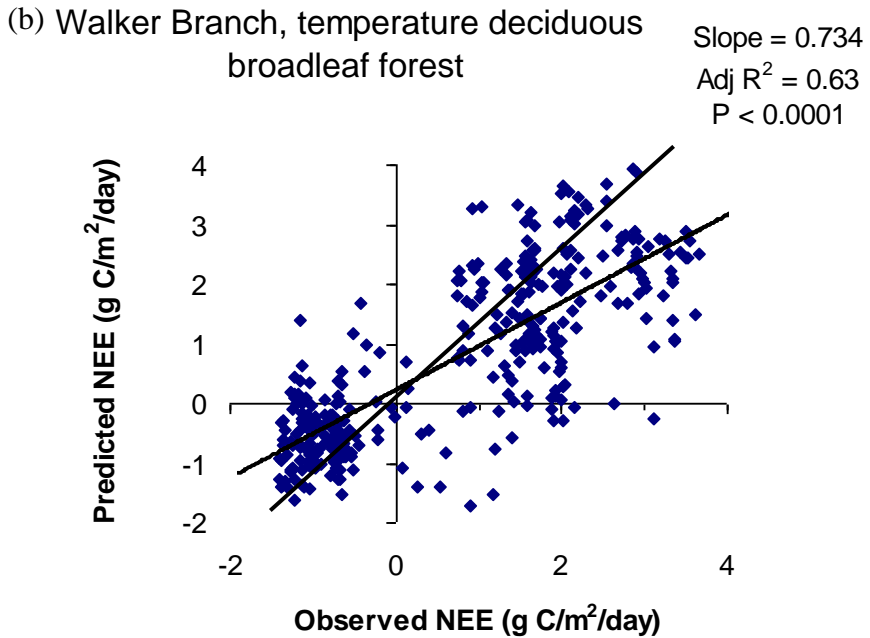
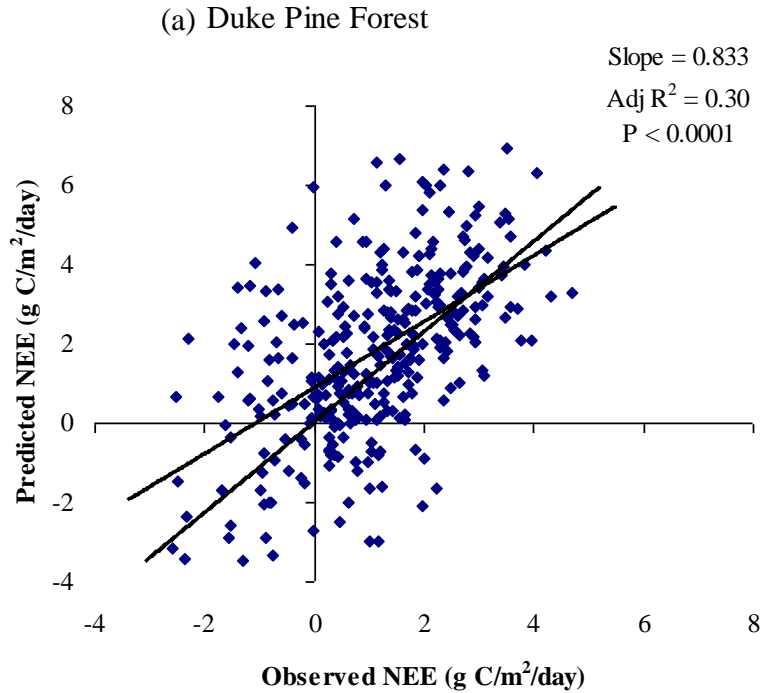


Figure A2.1 Comparison of the model simulated net ecosystem exchange (NEE) against measured site flux dataset in the (a) Duke forest and the (b) Walker Branch watershed.

2. Compare model outputs against field measured NPP

We compared the estimated Southern US NPP against the NPP database from the Oak Ridge National Laboratory Distributed Active Archive Center, Oak Ridge, Tennessee, U.S.A (<http://daacsti.ornl.gov>). We only include the studies that were in the Southern US region and have the land cover type same to our vegetation map. There are total 138 measurements used in this comparison (Figure A2.2).

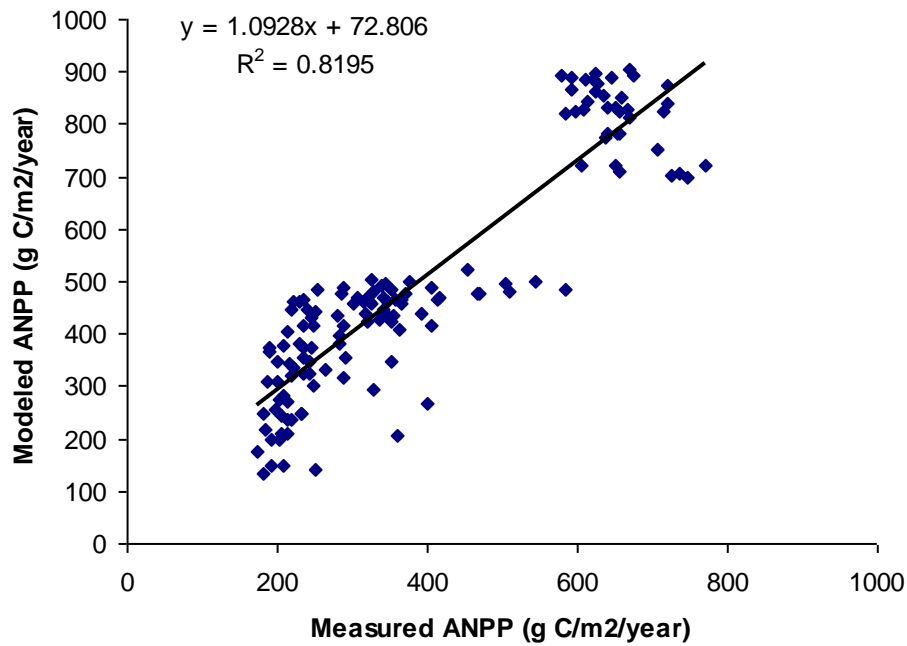


Figure A2.2 Comparisons of the modeled annual NPP against 138 field measurements in the Southern US region.

3. Compare model outputs against regional inventory data

We finally compared the carbon density of terrestrial ecosystem in 13 Southern states against the estimation based on forest inventory data (Figure A2.3). The results show

that our model estimation was similar ($R^2 = 0.72$) to the state level assessment made by Birdsey and Leis (2003) based on forest inventory dataset.

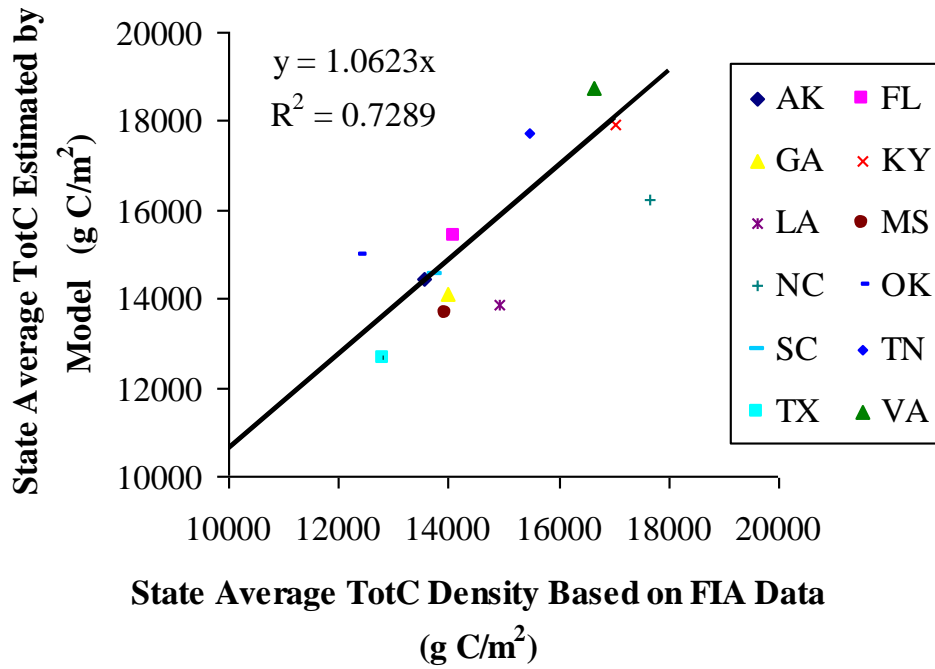


Figure A2.3 Comparisons of the model estimated carbon density of thirteen Southern states against estimation based on forest inventory analysis (FIA) dataset (Birdsey and Lewis, 2003).